UNIVERSITY OF CALIFORNIA, SAN DIEGO

Phenotypic Characterization of Estrogen-related Receptor Gamma Mutant Mice

A Dissertation submitted in partial satisfaction of the requirements for the degree

Doctor of Philosophy

in

Biomedical Sciences

by

William Arthur Alaynick

Committee in charge:

Professor Ronald M. Evans, Chair
Professor Lawrence S.B. Goldstein, Co-Chair
Professor Bruce A. Hamilton
Professor Samuel L. Pfaff
Professor Nicholas Spitzer
Professor Anthony Wynshaw-Boris

2006

The dissertation of William Arthur Alaynick is approved, and it is acceptable in quality and form for publication on microfilm:

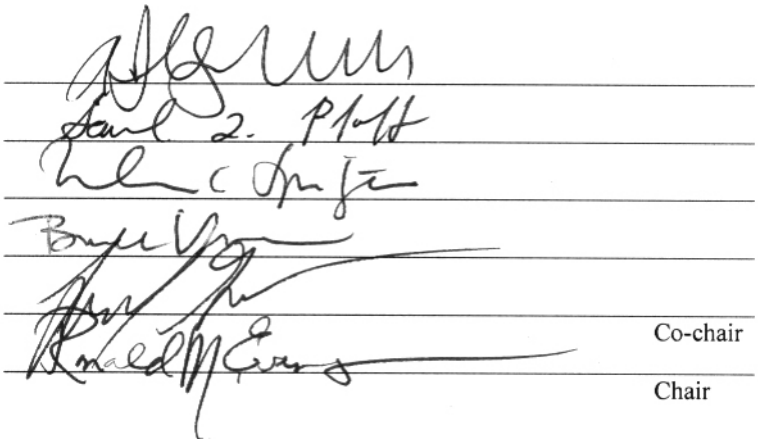

University of California, San Diego

2006

"No one can be a great thinker who does not recognize, that as a thinker it is his first duty to follow his intellect to whatever conclusions it may lead. Truth gains more even by the errors of one who, with due study and preparation, thinks for himself, than by the true opinions of those who only hold them because they do not suffer themselves to think."

John Stuart Mill

This dissertation is dedicated to my parents, Susan and Michael, who have lent me their finest qualities.

TABLE OF CONTENTS

LIST OF FIGURES

Chapter 1

Chapter 2

Chapter 3

ACKNOWLEDGEMENTS

My first question of physiology was asking my mother, “If one were in water up to their nose, would their stuffy nose clear to allow breathing?” I don’t recall her answer, but I would like to think she enjoyed the question. I was aware of my own physiology prior to this. My father’s asking why his three-year-old son did not want to join him in the pool was answered by, “Because I can’t swim and I can’t breathe under water.” Why all this concern over breathing around water? Over the years I have asked my (nearly) tireless mother countless questions about physiology and medicine. I poured over my parents’ medical texts and have been keenly aware of Guinea Worm, Grave’s Syndrome, and the down-sides of a penetrating wound—all brought to life by the Technicolor hand of Frank Netter.

When I finally gained the courage to attempt academics in 1995, I spent a formative six weeks with my father at his Emergency Medicine practice. This culminated with my suggesting that the monocularly blind patient before us might have had a penetrating wound to the optic nerve. This fortunately (?) turned out to be the case. I continued this clinical exposure by the invitation of Mickey Eisenberg to follow him in his Emergency Medicine practice at the University of Washington. Mickey’s quiet sense of confidence remains a goal I aspire to. After a two-year preceptorship with Mickey, I joined Richard Palmiter’s lab as a technician. On the first day, Richard told me he wanted me to be like a graduate student. Because he treated me like a graduate student, I was able to attend a lunch with David Mangelsdorf and came to learn about nuclear receptors and Davo’s post-doctoral mentor, Ron Evans.

When I first met with Ron, he asked me if I had any research experience. When I told him about my experience in Richard’s lab, he sprung to action and grabbed the Nature article on the first transgenic mouse from 1982 that they co-authored. Over the last five years, Ron’s has provided a limitless opportunity to learn and explore the art and practice of science. He has been there when I need him, but has fostered a sense of independence by defining what a good answer should be, and then allowing me to pursue it. While this has been frustrating at times, I am heartened that this training appears to be respected by his peers.

Ron has provided support outside the lab as well. By giving me the key to his house and allowing me a getaway from the day-to-day of graduate work while looking after The Beast (Migsy), I was able to remain energetic and engaged in the lab. Ron has provided advice on love, life, and career along the way

and provided mentorship that will last a lifetime. Ron's family—Ellen, Lena, and Bill—have been warm friends and made my move to La Jolla an easy one.

My thesis committee has been very supportive, offered me a lot of candid advice, and generally treated me as a young colleague. Sam Pfaff has been very patient and endured countless episodes of my coffee-inspired ideas and questions—which are likely continue. Bruce Hamilton has given me hours of his time and critical advice, temporally manifested as egregiously obfuscating didacticism. Larry Goldstein asked the tough questions that made me face my blind spots and invested a lot of time and confidence in my development. Tony Wynshaw-Boris offered me encouragement and critical thinking about my project which kept me going. Nick Spitzer provided time and thought about the details of my thesis. And my unofficial committee member, Wayne Giles, offered many hours of encouragement and thought, a computerized ECG system, a post-doc, lunches, an undergraduate student...

Thanks to all of my family, friends, collaborators and mentors without whom I could not have accomplished anything. And of course, Sara.

Collaborators subject to authorship deriving from this work include:

Matthew Bloch	Michael Downes, Ph.D.
Catherine Dufour , M.S.	Ronald M. Evans, Ph.D.
Benjamin W. Gallarda	Vincent Giguere, Ph.D.
Wayne R. Giles, Ph.D.	Johann W. Jonker, Ph.D.
Richard Kondo, Ph.D.	Alexander Lehrman, M.S.
Christopher P Myers, M.D. Ph.D.	Robert K. Naviaux, M.D. Ph.D.
Jordan Nevo	Samuel L. Pfaff, Ph.D.
Wen Xie, M.D. Ph.D.	Ruth T. Yu, M.D. Ph.D.

Alaynick WA; Myers CP; Gallarda BW; Pfaff SL, Evans RM. "Locomotor Defects in Estrogen-related Receptor Gamma Mutant Mice" In Preparation.

Alaynick WA; Kondo R; Xie W; Downes M; Dufour C; Jonker JW; Yu RT; Lehrman A; Nevo J; Bloch M; Naviaux RK; Giles WR; Giguere V; Evans RM. “Cardiac conduction Defects in Estrogen-related Receptor Gamma Mutant Mice”. In Preparation

VITA

2000	BA, History and Science, University of Washington
2006	Ph.D, Biomedical Sciences, University of California, San Diego

Publications

Lee CH, Kang K, Mehl IR, Nofsinger R, **Alaynick WA**, Chong LW, Rosenfeld JM, Evans RM. Peroxisome proliferator-activated receptor delta promotes very low-density lipoprotein-derived fatty acid catabolism in the macrophage. Proceedings of The National Academy of Sciences U S A Feb 14;103(7):2434-9 (2006)

Mizutani A, Wang L, Rajan H, Vig PJ, **Alaynick WA**, Thaler JP, Tsai CC. Boat, an AXH domain protein, suppresses the cytotoxicity of mutant ataxin-1. Boat, an AXH domain protein, suppresses the cytotoxicity of mutant ataxin-1. EMBO Journal. Sep 21;24(18):3339-51. (2005)

Barish GD, Downes M, **Alaynick WA**, Yu RT, Ocampo CB, Bookout AL, Mangelsdorf DJ, Evans RM. A Nuclear Receptor Atlas: Macrophage Activation. Molecular Endocrinolology Oct;19(10):2466-77. (2005)

Hnasko TS, Szczypka MS, **Alaynick WA**, During MJ, Palmiter RD. A role for dopamine in feeding responses produced by orexigenic agents. Brain Research 1023(2):309-18 (2004)

Szczypka MS, Rainey MA, Kim DS, **Alaynick WA**, Marck BT, Matsumoto AM, Palmiter RD. Feeding behavior in dopamine-deficient mice. Proceedings of The National Academy of Sciences U S A 96(21):12138-43 (1999)

Awards

2005	Best Poster, UCSD Biomedical Sciences
2002-2004	NIH Genetics Training Grant recipient, UCSD

ABSTRACT OF THE DISSERTATION

Phenotypic Characterization of Estrogen-related Receptor Gamma Mutant Mice

by

William Arthur Alaynick

Doctor of Philosophy in Biomedical Sciences

University of California, San Diego, 2006

Professor Ronald M. Evans, Chair

Professor Lawrence S.B. Goldstein, Co-Chair

Nuclear hormone receptors influence transcription in reproduction, development, and adult physiology by associating with hormones and metabolic intermediates, or in the case of orphan receptors, by acting independently of endocrine or metabolic ligands. A critical role for the orphan receptor, Estrogen-Related Receptor γ (ERRγ) is indicated by a lack of feeding and neonatal death (>72 hours after birth) of mice deficient in this transcription factor. Analysis of motor function in whole animal or in reduced preparations reveals a significant defect in ERRγ-null animals. Electrophysiologic analysis of isolated lumbar spinal cords has demonstrated an increase in spontaneous activity and a defect in the central pattern generating circuits. ERRγ is robustly expressed in the heart from early development (E8.5) through adulthood. Electrocardiographic analysis of ERRγ-null and heterozygous animals reveals a prolongation of

the QRS complex, ST and QT intervals. Isolated primary cardiomyocytes from E18.5 animals display a significant reduction in sodium current, consistent with observed ECG abnormalities. Several ion channels are dysregulated in E18.5 heart, by QPCR. Additionally, derangements of mitochondrial genes have been detected by expression and chromatin IP (ChIP) array analyses. Mitochondrial DNA is increased, per ventricular heart cell, in the ERRγ-nulls and ERRγ-nulls are prone to fasting-induced lactic acidosis. These signs of mitochondrial dysfunction occur despite normal substrate utilization, electron transport chain protein levels, and electron micrographic morphology. ERRγ appears to define the metabolic state of these excitable tissues—loss of which results in subtle, yet lethal alterations in the firing properties of these neurons. Ongoing studies are to define the characteristics of ERRγ-positive cells in the spinal cord, and to determine the contribution of ERRγ to the normal function of excitable cells in the heart and lumbar spinal cord.

Chapter 1

Introduction

Nuclear Hormone Receptors

Nuclear hormone receptors generally function as ligand-activated transcription factors that regulate the expression of specific genes related to processes as diverse as reproduction, development, and metabolism. Functionally conserved regions among nuclear receptors, such as the DNA binding domain (DBD), ligand binding domain (LBD), N- and C-terminal activation domains (AF-1 and AF-2, respectively) define this class of proteins (Evans, 1989). Functionally diverse roles are determined by variations in both ligand and DNA binding specificities, as well as in specific interactions with co-activator and co-repressor molecules that combinatorially mediate transcription (Glass, 2000; Kressler, 2002). Models of transcriptional activity are dominated by conformational changes in chromatin that alter access of permissive factors to promoter regions and subsequently nucleate transcriptional machinery (Chen, 2001). NRs affect these processes as *cis*-acting hormone-responsive switches to facilitate nucleation of factors enhancing or repressing a transcriptionally competent assemblage. However, evidence suggests that in the absence of ligand, transcriptionally inactive NRs are not passive (Lee, 2003) and may act in *trans* to sequester factors involved in other transcriptional pathways—expanding the physiologic role of NRs beyond either chromatin or ligand binding.

To date, 48 and 49 members of the nuclear hormone receptor superfamily have been identified in mouse and human, respectively. The first receptors to be cloned, the endocrine nuclear hormone receptors, were discovered in an effort to define the mechanism of action for known hormones, such as: the amino-acid-derived thyroid hormone; the cholesterol-derived glucocorticoid, mineralocorticoid, sex hormones and Vitamin D; and the retinol, Vitamin A. Although these receptors are effecter molecules for vital hormones and vitamins and contribute to nearly all aspects of health and disease, other nuclear receptors were sought. Subsequent to the molecular identification of classical endocrine receptors, another class of nuclear hormone receptors, the adopted orphan receptors, was discovered to respond with low-affinity to physiologic ligands derived from dietary and metabolic sources, such as bile salts and fatty acids, present in concentrations (micromolar) orders of magnitude higher than the hormones (nanomolar). Both the endocrine and adopted orphan receptors may have evolved from a phylogenetically ancient transcriptional

regulator that has since undergone multiple duplications and divergences. As a result, the nuclear hormone superfamily is divided into two broad groups: 1) the transcription factors that have specific ligand dependent activities; and 2) other factors that are phylogenetically more primitive and do not respond to ligands: the orphan nuclear receptors.

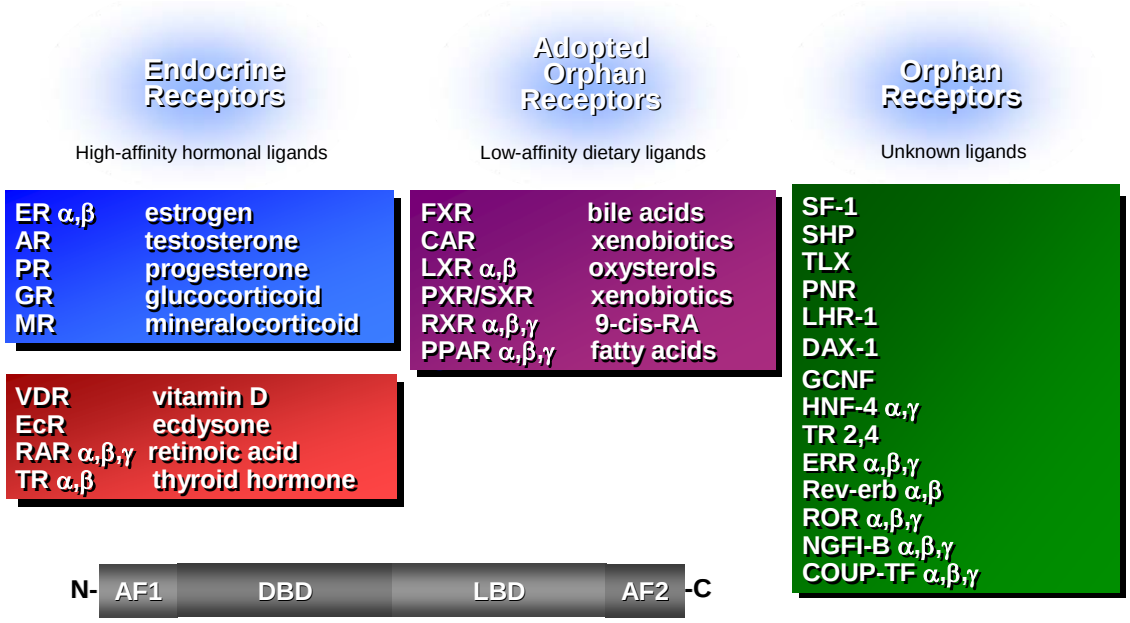

Figure 1.1: The Nuclear Hormone Receptor Superfamily

Orphan nuclear receptors comprise a subclass of nuclear hormone receptors for which no physiological ligands have been identified. The first identified members of this class, the estrogen-related receptors 1 (ERR1, ERRα, NR3B1) and 2 (ERR2, ERRβ, NR3B2), were identified by sequence homology to the estrogen receptor α (ERα, NR3A1) in a low stringency screen (Giguere, 1988). A decade later a third member was identified, estrogen-related receptor γ (ERR3, ERRγ, NR3B3) (Eudy, 1998; Hong, 1999). However none of the ERRs bind estrogen, due to presence of amino acid side-chains within the ligand binding pocket (LBD) that, firstly, sterically prohibit ligand binding; and secondly, stabilize an *apo*-LBD conformation like that of *holo* receptors. Selective estrogen receptor modulators (SERMS) such as diethylstilbestrol (DES), tamoxifen and its more active metabolite, 4-hydroxytamoxifen, have been demonstrated to bind one or more of the ERRs and act as inverse agonists. In the absence of ligand (*apo*

form), the ERRs maintain a LBD conformation like that of active, liganded ER (*holo* form), and are constitutively active. This activity is due to the conformation of the C-terminal helix 12, also known as the activation function 2 (AF2), loss of which abrogates the constitutive activity of ERRs and results in a dominant-negative protein.

Despite the structural similarities of the ERRs, compensation appears to be limited. Targeted disruption of the widely-expressed ERRα gene in mice produces a relatively subtle phenotype characterized by reduced adiposity (Luo, 2003). However, targeted disruption of ERRβ in mice results in embryonic lethality at embryonic day 10.5 (E10.5) phenotypically resembling the effects of DES on placental trophoblast formation (Luo, 1998). In the adult mouse**,** ERRβ is only significantly expressed in the retina and sparingly expressed in kidney and heart, but ERRβ-null animals rescued by tetraploid aggregation display a poorly characterized global motor deficit (Mitsunaga, In Submission). Targeted disruption of the widely-expressed ERRγ gene by insertion of neomycin resistance and beta-galactosidase genes, produces a lethal phenotype around postnatal day 1, in unpublished observations by both the Evans laboratory (Alaynick, in preparation) and groups at the pharmaceutical firms Tularik and GlaxoSmithKline (Peter Coward and Andrew Billin, personal communications).

Nuclear Hormone Receptor Structure and Function

Nuclear hormone receptors are characterized by two key features. Firstly, receptors bind to DNA in a sequence–specific manner as directed by the: 1) DNA binding domain (DBD) and, 2) dimerization characteristics of each receptor. Secondly, the receptor can influence transcription. The regulation of transcription is primarily mediated by the conformation of a structure consisting of twelve alpha helices called the Ligand Binding Domain (LBD). In the case of the endocrine and adopted receptors, these twelve alpha helices are capable of forming a pocket with ligand specificity conferred by the specific residue side-chains of that receptor. When a receptor without ligand (the *apo* form) binds its cognate ligand (the *holo* form), a conformational shift is induced which is transmitted to the external surface of the LBD and results in alterations in binding sites for associated proteins containing the amino acid motif, LXXLL, or receptor interacting domains (RIDs). It is this exchange of associated proteins that acts to subsequently influence the state of transcriptional activity. In the case of the ERR orphan receptors, the *apo*-LBD is in an active

conformation like that of the *holo*-LBD of the classical endocrine receptors (Hong, 1999; Xie, 2000; Greschik, 2002). For orphan receptors, in the absence of any identified physiologic ligand, variations in transcriptional activity result from changes in post-translational modification of the receptor and/or binding partner exchange (Kressler, 2002; Kamei, 2003; Hentchke, 2003).

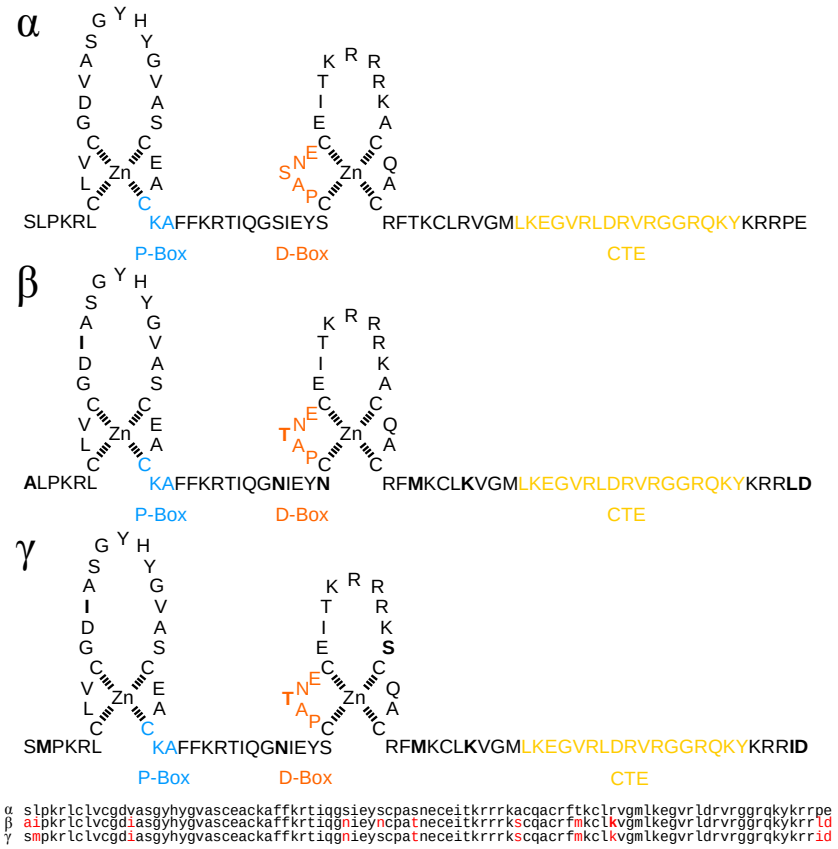

Figure 1.2: Structural Differences in ERRs

Nuclear Hormone Receptor Dependent Transcription

The canonical pathway for hormone dependent transcription is that of the glucocorticoid receptor. In this case, lipophilic glucocorticoid is carried in the blood on a serum protein, such as albumin, until diffusion results in dissociation. Responsive cells express glucocorticoid receptor which resides in the cytosol in an 8S complex with a sequestering protein, such as heat-shock protein 90 (HSP90). Binding of glucocorticoid results in dissociation of the receptor and transport into the nucleus. Upon dimeric binding to specific DNA encoded motifs, activated receptor produces changes in chromatin structure and recruits

factors which contribute to the recruitment and activation of RNA polymerase II. These actions then result in transcription of responsive genes. However, significant variations of this theme exist.

In the case of the retinoic acid receptor (RAR), the receptor is constitutively bound to chromatin in association with a heterodimer partner, RXR. This receptor pair actively represses gene expression in the absence of ligand by recruiting co-repressor molecules NCoR or SMRT with transcriptional repression properties mediated by histone deacetylase (HDAC) activity (Glass, 2000). Upon binding of retinoic acid, an exchange of transcriptional cofactors occurs to favor the dissociation of transcriptional co-repressors and recruitment of transcriptional coactivators containing histone acetylase (HAT) activities.

In the case of orphan receptors, these are also constitutively nuclear, and in the case of the ERRs, have a constitutive *apo*-LBD conformation like that of activated endocrine *holo*-receptors (Greschik, 2002). The DNA binding site motifs of the ERRs are more divergent and the binding is less specific than for ERα or β (Razzaque, 2005). Binding to response elements may occur as homodimers, heterodimers, or as monomers with ERRs proposed to bind as monomers or heterodimers. Among the ERRs, transcriptional activity has been suggested to be dependent on the recruitment of additional cofactors. These additional factors, such as PGC-1α and β and calmodulin may serve as what have been termed *protein ligands* (Kamei, 2003; Hentschke, 2003). In the absence of an identified ligand, ERRs may be more greatly dependent on protein-protein interactions and post-translational modification than other nuclear receptors. The MAP kinase pathway has been reported to confer constitutive activity on ERα (Kim, 2006). Additionally, charcoal treatment of serum may reduce the constitutive activity of the ERRs in culture, suggesting a signaling mechanism independent of ligand binding, although these results are contentious (Vanacker, 1999).

Nuclear receptors have been demonstrated to play an indirect role in transcription by interacting with other signaling cascades without binding DNA. Loss of glucocorticoid receptor results in neonatal death which can be rescued by the introduction a mutant form of the glucocorticoid receptor with reduced DNA binding activity (Reichardt, 1998). In this, and a more recent example (Lee, 2003) nuclear hormone receptors mediate inflammatory (AP1-and Bcl6-dependent) processes independent of DNA-binding. Recently, non-traditional multimerization has been proposed to regulate transcription of PNMT, an enzyme

important in monoaminergic signaling (Adams, 2003). These more recently proposed mechanisms will likely prove to be crucial for orphan receptors such as ERRγ.

Hormone Response Elements

Hormone response elements (HREs) are short sequence motifs found in the promoters of responsive genes. HREs are of two types, paired and unpaired. Of the paired types there are palindromic repeats, direct repeats and everted and inverted repeats (Forman, 1995). In addition to the variability conferred by DNA sequence, further variability can be generated by spacing between the paired repeats of

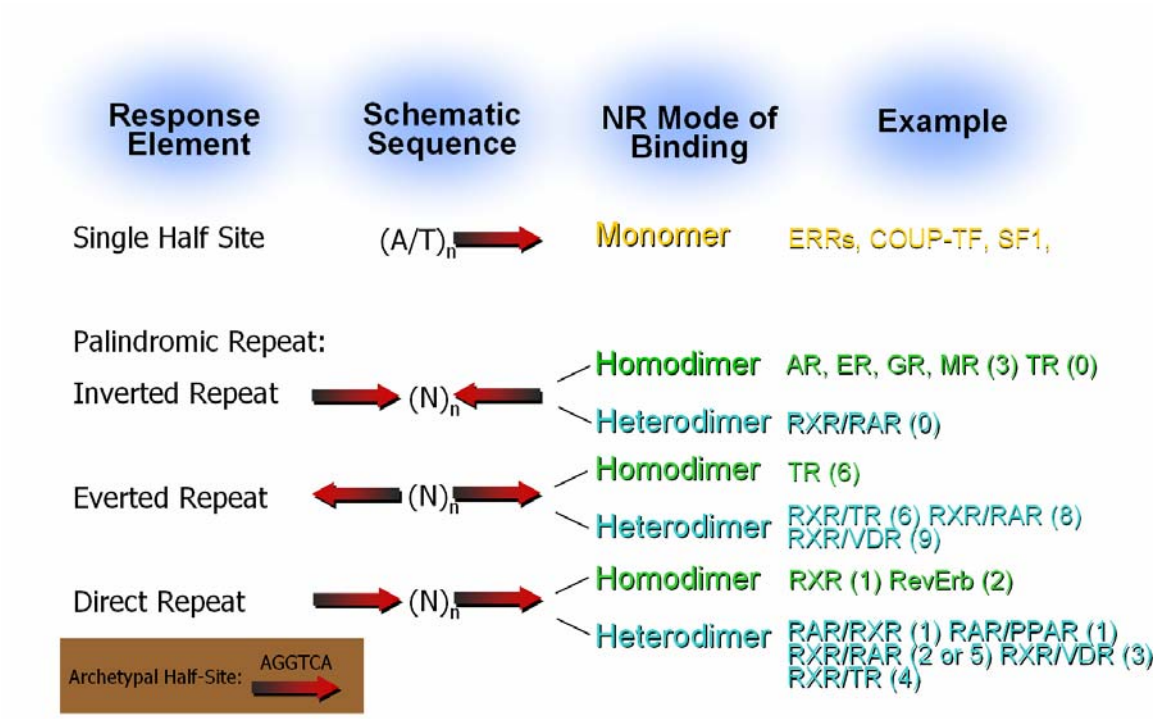

Figure 1.3: Nuclear Receptor Response Elements

zero to five (or more) nucleotides. However, degeneracy in the coding of NR half-sites reduces the predictability of these elements. These elements are typical of the endocrine and adopted receptors. The estrogen-related receptors utilize half sites with a 5' extension of three nucleotides. However, multimerized examples of the ERRs have been described, and this multimerization may confer variable responsiveness among promoters (Razzaque, 2005).

Specificity

The broad range of tissue and cell specific activity of nuclear hormone receptors is thought to be due to a combinatorial mechanism. An intersection of multiple overlapping regions of expression of transcriptionally active components acts to define temporal and spatial specificity. ERRγ has been reported to interact with several modifiers of transcriptional activity: the p160 class of co-activators (SRC-1, GRIP1/TIF2 and ACTR/p/CIP) and other classes of factors such as, PGC-1α, PERC, and calmodulin (Hong, 1999; Xie, 1999; Kamei, 2003; Hentchke, 2003). In principle, to greater or lesser degrees the ERs and ERRs are capable of 1) interacting either directly, or 2) by competing for binding on promoter elements, or 3) by competing for limited co-activating partners. The complexity of this potential for interaction is only beginning to be appreciated more completely and has important implications in cardiovascular, endocrine and cancer treatment.

Estrogen-Related Receptors (ERRs)

The estrogen-related receptors are orphan receptors that have gained increasing appreciation as regulators of metabolism, the estrogen signaling axis and the PPAR signaling axis via interactions with the PGCs. Although no natural ligands have been identified, these receptors tend to be constitutively active in the absence of ligands, depending on their coactivator and promoter interactions. New understanding of the roles of these receptors will be greatly advanced with the imminent completion of preliminary characterizations of knockout mice and the actions of selective ligands for these receptors.

ERRs are phylogenetically ancient receptors (Devine, 2002). A PCR-based strategy was used to detect the presence of nuclear receptors in the ascidian Herdmania and identified eight NRs. Sequence comparisons and phylogenetic analyses reveal that these ascidian nuclear receptors are representative of five of the six previously defined nuclear receptor subfamilies and are apparent homologues of retinoic acid [NR1B], retinoid X [NR2B], peroxisome proliferator-activated [NR1C], estrogen related [NR3B], neuron-derived orphan (NOR) [NR4A3], nuclear orphan [NR4A], TR2 orphan [NR2C1] and COUP orphan [NR2F3] receptors. Phylogenetic analyses that include the ascidian genes produce topologically distinct trees that suggest a redefinition of some nuclear receptor subfamilies. These trees also suggest that extensive gene duplication occurred after the vertebrates split from invertebrate chordates. These ascidian

nuclear receptor genes are expressed, like the vertebrates, differentially during embryogenesis and metamorphosis.

The presence of ERRs in other phyla followed the identification of the 482 amino acid Drosophila estrogen-related receptor (dERR) belonging to the NR3 subfamily (previously thought to be limited to deuterostomes), indicating the existence of an ancestor before the evolutionary split of deuterostomes and protostomes (Ostberg, 2003). Close resemblance is observed with dERR relative the human and mouse ERRs in the DBD (approximately 85% identical) and the LBD (approximately 35% identical) and dERR can bind mammalian ERREs and EREs by EMSA. The dERR demonstrated constitutive activity in CaCo-2 cells on a mammalian ERRE, but is dependent on GRIP-1 co-expression for activity on EREs. Mutation of three critical amino acids in the LBD enables ligand-dependent suppression of transcriptional activity. The Y295A/T333I/Y365L triple mutant is suppressed by 4-OHT and DES, but the WT dERR is only moderately suppressed. GRIP-1 increased the activity of the triple mutant in transfection experiments, and the addition of 4-OHT resulted in an efficient suppression of the activity. Accordingly, the ability to functionally interact with a coactivator is still maintained by the Y295A/T333I/Y365L mutant. In silico modeling suggests that the dERR LBD pocket is too small to accommodate tamoxifen, unlike the murine and human receptors (Greshik, 2002).

Several reviews suggest that the ERRs may play important, yet unappreciated roles in estrogen signaling in tissues such as bone, breast and endometrium (Horard and Vanaker 2003; Giguere, 2003). The potential for adverse, ERR-mediated, reactions to estrogen antagonists is highlighted by the observation that high-dose ‘salvage therapy’ during cancer chemotherapy is limited by neurologic and cardiac and side effects: tissues not typically associated with classic estrogen endocrine function (Chang, 1998; Decaudin, 2004). Furthermore, as discussed in following chapters, these estrogen antagonist side effects resemble aspects of the ERRγ-mutant mice: cardiac conduction defects and motor disturbances.

Emerging evidence suggests that several nuclear receptor transcription factors act to coordinate the activity of mitochondria to the needs of the cell as a whole (Scarpulla, 2006). PPARs, ERRs, SHP and CoupTFs act to alter various components of mitochondrial physiology in addition to NRF1 ad NRF2/GABPAα. These proteins act on the nuclear genome to coordinate production mitochondrial proteins

encoded by the nuclear genome and to regulate mitochondrial transcription and translation such that the respiratory complex stoichiometry of mitochondrial and nuclear encoded proteins is maintained. The expression levels and coordinated activities of these gene products summate to meet the cell-specific energy demands imposed by physiologic stimuli.

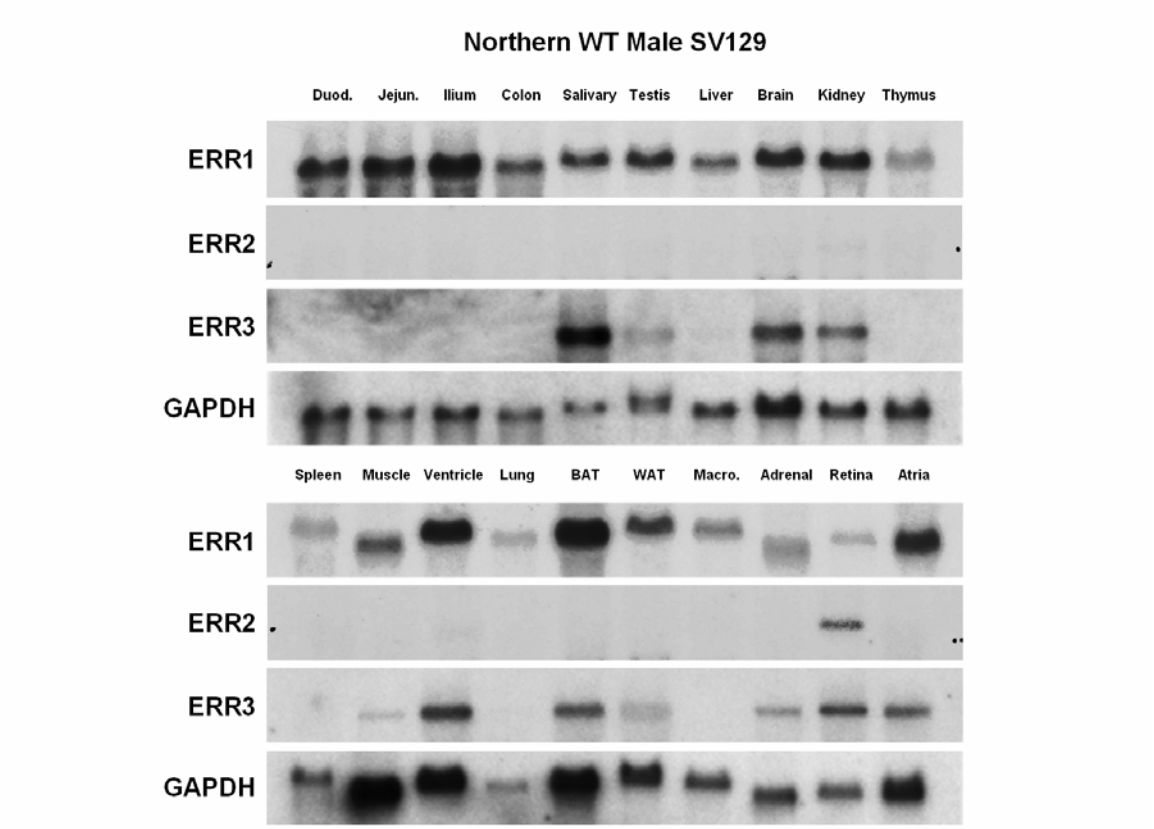

Figure 1.4: Northern Analysis of ERR Expression in Mouse

Estrogen-related Receptor α: Gene Structure, Expression and Regulation

Vincent Giguere in the Evans lab identified two cDNAs that bore similarity to the estrogen receptor by low-stringency hybridization (Giguere, 1988). He termed these estrogen-related receptor alpha (ERRα, ERR1, NR3B1) and estrogen-related receptor beta (ERRβ, ERR2, NR3B2) due to the amino acid sequence similarities to estrogen receptor α. These proteins were unable to bind any known physiologic ligand and were termed 'orphan nuclear hormone receptors'—a classification that has come to encompass over forty receptors in humans. Despite significant advances in the orphan nuclear hormone receptor field generally over the next eight years, little was advanced with regard to estrogen-related receptors in

particular. The predicted length of the ERRα protein was 521 amino acids (63-kD), but later studies (Johnston, 1997) suggest that this protein is not formed and a protein lacking the first 97 amino acids of this structure is the major form present in cells. Later studies demonstrate that the human sequence reported here is from rat (Chen, 1999).

The chromosomal location of ERRα was identified in the laboratory of Giguere (Sladek, 1997). Having demonstrated that there is an embryonic lethality in ERRβ mice, a chromosomal mapping for human and mouse was performed. F1 C57BL/6J x *mus spretus* females were crossed with male C57BL/6J. It was determined that the murine ERRα (Estrra) locus maps to chromosome 19 and Estrrb to mouse chromosome 12. Using fluorescence *in situ* hybridization, the human ESRRA mapped gene to chromosome 11q12-q13 and the human ESRRB gene to chromosome 14q24.3. In addition, a processed human ERRα pseudogene mapped to chromosome 13q12.1: this was the first report of a nuclear receptor superfamily pseudogene

A consistent tissue studied in the field of ERRs is bone due to the variable effects of estrogens and their antagonists on bone density. The effect of ERα and ERβ antisense treatment of MG63 osteosarcoma cell line revealed a potential role of ERRs in this cell type (Cao, 2003). Affymetrix expression array analysis showed that ERRα and BCAR3 are highly expressed in these cells and may contribute the functional responses to estrogens. The authors concluded that, in the MG63 cell line, estrogen increases synthesis of matrix proteins via ERβ and that in the absence of additional stimuli, these cells are not major mediators of estrogen effects on osteoclast differentiation. ERα is probably much more important in earlier stages of skeletal development, such as growth plate response, than in osteoblasts. The role of ERα is bone development is dramatically revealed in a clinical case of an ERα-deficient man who failed to undergo epiphyseal closure after puberty (Smith, 1994).

Estrogen mediated expression of ERRα was demonstrated in vivo in mouse uterus, heart (following injections of DES), and in vitro in endometrial and breast cell lines (Liu, 2003). The human ERRα promoter has multiple Sp1 sites, and Sp1 is required for activity. The estrogen response is primarily due to a 34-bp element that contains multiple steroid hormone response element (MHRE) half-sites that are conserved between the human and mouse ERRα gene promoters. Chromatin immunoprecipitation (ChIP)

revealed the presence of ERα on the ERRα promoter in MCF-7 cells that is increased with estrogen treatment. The authors conclude that ERRα is a downstream target of ERα, although the presence of widely spaced half-site potentially allows for promiscuous activation by multiple NRs. ChIP against ERRγ has revealed the presence of ERRγ on the ERRα promoter (Alaynick, Evans, Giguere, unpublished observation).

In order to better study the phylogeny of ERRs, a PCR screen was utilized to identify five ERR-like cDNAs from zebrafish (Bardet, 2004). Three of these, ERRα, ERRγ and ERRδ, were identified as having similar properties as their mammalian counterparts by transient transfection. Expression of zebrafish ERRs during development was noted in the in the hindbrain, pronephric tubes and in presumptive mesoderm. Slow-twitch muscles express ERRα in fish as well as mammals suggesting a conserved role for ERRs in certain tissue functions (Huss, 2002).

Additional descriptions of fish ERRs appear in the cloning of four ERR cDNAs from the Atlantic killifish, Fundulus heteroclitus, along with adult tissue expression and estrogen responsiveness (Tarrant, 2006). F. heteroclitus (Fh)ERRα is an ortholog of ERRα identified in mammals, and fish, according to phylogenetic analysis. Mammalian ERRβ has two orthologs: FhERRβa and FhERRβb. Identification of the mammalian ortholog of ERRγ is less certain but may be FhERRγb. Distinct, partially overlapping mRNA expression patterns for the four ERRs in adult tissues were observed. As in mammals, FhERRα was expressed broadly. Again consistent with mammalian expression, FhERRβa was expressed at low levels in eye, brain, and ovary. Perhaps sharing similarities to mammalian ERRγ expression, FhERRβb was more broadly expressed in kidney, gonad, eye, brain, and liver. Expression of FhERRγb was detected in multiple tissues including gill, heart, kidney, and eye. Estrogen was administered to elicit ERR upregulation. The authors refer to “slight upregulation” of three- to five-fold, which would be quite high for *in vivo* induction in heart had their results reached significance. While these receptors are grossly similar in their expression patterns to their mammalian orthologs, their physiologic roles in fish may, not surprisingly, be quite different.

ERRα Gene Products

Earlier studies described ERRα as hESRL1a and placed it within the Class IV monomeric NRs such as Nurr1, a classification and naming scheme that has lost favor (Shi, 1997). In addition to defining the exon and intron characteristics, with canonical GT and AG splice donors and acceptors, this study importantly defined message isoforms in different cell lines and tissues. Different isoforms were analyzed in λ-clones of a HUVEC library and subsequently detected in human uterine (HeLa, HEC and RL95-2) cell lines. The promoter region lacks typical TATA and CAAT boxes, but is rich in GC and has 10 consensus Sp-1 sites and two E-boxes. In cells lines, however, only one promoter region was detected by RNase protection assay. This promoter region was analyzed by reporter assay in RL92-2 cell lines. The majority of activity lies within the first 500 bp of the promoter; however enhancer regions were detected 1.3 kb upstream. The high number of Sp-1 sites and CpG islands has been suggested to play a role in the skeletal muscle expression of ERRα.

Ligand binding characteristics are a key aspect of nuclear receptor function. A virtual ligand *in silico* screening was performed on ERRα that predicted flavone and isoflavone phytoestrogens would be ligands (Suetsugi, 2003). Mammalian cell transfection and mammalian two-hybrid assays found three isoflavones (genistein, daidzein, and biochanin A) and one flavone (6,3',4'-trihydroxyflavone) act as agonists of ERRs. These ligands were found to induce activity of ERRα at concentrations comparable for activation of ERα and ERβ. LBD pocket volumes were predicted for ERα (450 $Å^3$), ERβ (390$Å^3$), ERRα (295$Å^3$), and ERRγ (220$Å^3$). This study also provided in depth discussion of LBD pocket side groups that confer constitutive activity and specific characteristics of the NR3A and B proteins. These ligands are non-specific, however, and can activate the PPARs as well.

ERRα Interactions with Co-regulatory Proteins

Coregulatory proteins may interact with ERRs at a protein-protein level or may compete for binding to limiting permissive factors or may compete for binding to promoter regions. In the latter case, COUP-TF was identified as a low abundance protein in bovine uterus that co-purified with estrogen receptor (ER) in a ligand-independent manner and was separated from the ER by its lower retention on estrogen response element (ERE)-Sepharose, suggesting possible interaction with the ERRs (Klinge, 1997). By EMSA, COUP-TF bound as an apparent dimer to ERE and ERE half-sites. COUP-TF bound to an ERE

half-site with high affinity, Kd = 1.24 nM. In contrast, ER did not bind a single ERE half-site. Nor were RAR, RXR, TR, PPARs or VDR detected as constituents of the COUP-TF:DNA binding complex. A direct interaction of COUP-TF with ER was indicated by GST "pull-down" and co-IP. This ER-COUP-TF interaction is estrogen dependent and blocked by tamoxifen. Co-expression of ER-expressing MCF-7 human breast cancer cells with COUP-TFI resulted in a dose-dependent inhibition of estrogen-induced expression of a luciferase reporter gene under the control of three tandem copies of EREc38. It appears that COUP-TF may inhibit ER by ERE-site binding or ER-protein binding.

The co-regulatory characterization of ERRα and ERRβ was extended in demonstrating that the p160 coactivators GRIP1, SRC1, and ACTR can functionally interact with EREs and TREpal, but not GREs (Xie, 1999). Chimeric ERRα-LBD/GR-DBD receptors were used to demonstrate that the ERRα N-terminal AF-1 does not contribute significantly to the constitutive activity of the ERRs. Reciprocal chimeric proteins demonstrated that the AF-2, from either ERRα or β is constitutively active. All p160s physically interact with ERRα and β, by GST pull-down assay, with GRIP1 inducing the greatest transcriptional activity. Chimeric ERRα and β containing the herpes simplex virus VP16 activation domain have increased transcriptional activation—suggesting utility in overexpression or transgenic animal experiments.

The interaction between NRs was demonstrated in the interaction of the aryl-hydrocarbon receptor with COUP-TF, ERα and ERRα (Klinge, 2000). However these results are limited and only modest transcriptional effects are seen (less than two-fold). Conclusions are largely drawn from EMSA binding and competition data. This report attempts to characterize combinatorial control on a CYP1A1 promoter, but fails to provide robust or compelling transcriptional effects.

A model promoter for estrogen and ERR functions is the aromatase promoter due to the role it plays in breast cancers. Continued studies of the aromatase promoter and the silencing region within it that bind SF1 and ERRα, utilized a Y2H assay to identify proteins that interact with SF1 (Zhou, 2000). PNRC (proline-rich nuclear receptor coregulatory protein) is a smaller nuclear coregulatory protein of 35 kDa, and is proline rich. In addition to its interaction with SF1, it also interacts in an AF2-dependent manner with ERRα, ER, AR, GR, PR, TR RAR and RXR. Functionally, PNRC coactivates transcription by SF1, ERRα,

PR, and TR. A 23aa sequence in the carboxy-terminal region, aa 278-300, was shown to be critical for these interactions. Addtionally, a second protein with this motif was identified in this screen. PNRC was shown to interact and activate ERRγ and that mutations in, or deletion of the AF-2 eliminated the activity.

An extension of previous work that ERRα1 can both bind and activate the lactoferrin promoter was performed by demonstrating that ERRα1 and ERα may compete for binding and coactivator recruitment (Zhang, 2001). Transient transfection of a VP16-ERRα1 chimera into HEC-1B cells activated lactoferrin gene estrogen response element (ERE) reporter constructs. Therefore, ERRα1 can compete with ERα for binding to EREs. Activity of ERRα1 can be enhanced by coactivator (SRC-1a of GRIP1) and suppressed by estrogen-bound-ERα, suggesting that SRC-1a is required by both receptors for their activity. The repression of ERRα1 activation function by estrogen-bound-ERα, however, could not be reversed by increasing concentration of SRC-1a in the cell due to squelching.

Previous findings demonstrated the interaction of ERRα with a small co-regulatory protein, PNRC (Zhou, 2001). This was followed by a description of PNRC2 (proline-rich nuclear receptor co-regulatory protein 2) a small (16kd) protein identified by its Y2H interaction with SF-1 and ERRα, and by GST-pulldown with ER, GR, PR, TR, RAR, and RXR. PNRC has an SH3 and NR interaction domain in the critical Y2H interaction region. This work extended the PNRC findings to a second protein PNRC2 that has very similar properties. This suggests the existence of a coregulatory family of proteins in addition to the p160s.

The retinoid receptor-related testis-associated receptor (RTR)/germ cell nuclear factor (NR6A1) is an orphan receptor important in early embryonic development and gametogenesis (Yan and Jetten, 2000). RTR binds as a monomer or dimer to TCAAGGTCA and to direct repeats of AGGTCA, DO motifs, and is a transcriptional repressor via an interaction with NCoR, but not SMRT or RIP140. This repressor can interfere with ERRα activity by binding to the same response element. Nr6a1-nulll animals die at day 10.5-11.5 with failure to close the neural tube and a lack of chorioallantoic fusion. Although the authors do not mention this, if RTR can interfere with ERRα, it may also repress the activity of ERs, other ERRs and SF-1, all of which can bind to the ERRE/SFRE as well as the TRE_{pal} (Xie, 1999).

Possible crosstalk between RTR and ERRα and ERRβ was suggested in placental development, although RTR is essential for neural tube closure and cardiovascular development, with RTR-nulls lost at E10.5 (Mehta, 2002). ERRs can compete with RTR for binding to the RTRE: AGGTCAAGGTCA. RTR function was studied in murine placenta and several human placental choriocarcinoma cell lines. Immunohistochemistry localized RTR to nuclei of giant trophoblasts and spongiotrophoblasts. RTR mRNA was detected in rat choriocarcinoma Rcho-1 cells and human placental choriocarcinoma cell lines BeWo, JAR, and JEG-3. In trophoblasts, RTR was co-expressed with ERRα and ERRβ. Giant trophoblast differentiation in Rcho-1 cells, decreased in the expression of RTR mRNA and down-regulation of ERRβ but not ERRα. RTR inhibits VP16-ERRα transactivation through the RTRE, potentially by competition for DNA binding.

The PGCs are a well studied group of coactivators that interact with the ERRs. PGC-1α was shown to interact with ERRα and ERRγ through an alternate interaction region distinct from the LXXLL domain that interacts with ERα, PPARα, and HNF-4 (Huss, 2002). ERRα was found to interact with PGC-1α, in a yeast-two-hybrid assay screening of an adult human cardiac cDNA library, and is co-expressed in neonatal heart, along with MCAD and PGC-1α. A functional relationship was suggested by adenoviral-mediated ERRα overexpression in primary neonatal cardiac myocytes which induced MCAD expression. PGC-1α enhanced both ERRα (22-fold) and ERRγ (6-fold) transcription from vitellogenin-derived ERE promoter and ERRα (8-fold) from the MCAD promoter. The ERRα AF-2 interacts with PGC-1α in an alternative Leu-rich region at amino acids 209-213 termed, Leu-3, and appears to utilize additional LXXLL-containing domains as accessory binding sites. Gal4 fusion experiments indicate that PGC-1α activation involves, in part, displacement of co-repressor proteins. PGC-1α may regulate mitochondrial energy metabolism through interactions with ERRα and ERRγ that utilize alternative interaction domains. The authors provide a detailed discussion of LXXLL motifs and coactivator interactions. They report an unpublished observation that ERRα and ERRγ expression follows FAO capacity in skeletal muscle Type II/slow-twitch, and is nearly undetectable in Type I/fast-twitch muscle. This and the observation that ERRα is highly expressed during the transition from glycolysis to FAO in the neonatal heart suggest that ERRs may play a role in FAO oxidation and fiber type, a hypothesis reported elsewhere (Bardet, 2004).

A third member of the PGC-1 family of coactivators was cloned that preferentially activates ERα: PERC (PGC-1 related Estrogen Receptor Coactivator) with two isoforms, a 1023 aa isoform and a shorter version lacking aa 156-194 (exon 4) that codes for one of two NR domains (Kressler, 2002). It is expressed in a tissue specific manner with highest levels in heart and skeletal muscle. The coactivation function of PERC relies on a bipartite transcriptional activation domain and two LXXLL motifs that interact with the AF2 domain of ERα in an estrogen-dependent manner. PERC differs from PGC-1 in three important ways: Firstly, PERC acts selectively on ERα and not on ERβ, whereas PGC-1 coactivates both ERs. Secondly, PERC and PGC-1 have distinct promoter contexts for ERα activation. Thirdly, PERC enhances the ERα-mediated response to the partial agonist tamoxifen, while PGC-1 modestly represses it. These coactivator differences may contribute to the tissue and SERM variations in ERα activity. Other coactivators with preferential activation include NRIF3 (TR^+, RXR^+, GR^-, ER^-, VDR^-), and the three ER-specific PELP1, CAPER, and CITED. The mouse homolog of PERC (PGC-1β) has a third NR domain that may have altered coactivator properties.

To expand the regulatory complexity of ERRα, it may act as a negative regulator of PGC-1α activity, as opposed to the co-activating properties of PGC-1α on ERRα (Ichida, 2002; Huss, 2002). Using a yeast-two-hybrid screen for interactors of a previously identified inhibitory domain from PGC-1α, ERRα was identified. ERRα binding to PGC-1α requires the AF-2. Fasting coordinately induces PGC-1α and ERRα transcription in mice. Under normal conditions PGC-1α is located within nuclear speckles, but expression of ERRα results in uniform PGC-1α nucleoplasm distribution. ERRα can dramatically and specifically repress PGC-1α transcriptional activity on the PGC-1α sensitive PEPCK promoter; however these effects may be due to squelching of limiting PGC-1α (Herzog, 2006). An experiment to evaluate the effects of increasing both ERRα and PGC-1α needs to be carried out to evaluate this possibility. Or alternatively, if ERRα can eliminate ChIP of PGC-1α it would be consistent with the speckle observations.

Further studies of ERRs and PGCs demonstrated that PGC-1 regulates ERRα at two levels (Schreiber, 2003). Firstly, PGC-1 induces the expression of ERRα, as indicated by tissue- and stimulus-specific (cold, starvation, exercise) upregulation. Secondly, PGC-1 binds ERRα and facilitates transcriptional activation. PGC-1 converts the modest ERRα basal transcriptional activity to a more robust

one. PGC-1 effectively acts as a protein ligand for ERRα (Kamei, 2003). Energy metabolism may be regulated by the coordinated interaction of these two proteins. Adenovirus-mediated delivery of either siRNA for ERRα, or PGC-1 mutants that interact selectively with different types of nuclear receptors show that PGC-1 can induce the FAO enzyme MCAD in an ERRα-dependent manner. This study is in agreement with the investigation of LXXLL interactions between PGC-1 and ERRα that use L2 and L3, not just L2 as seen with other NRs (Huss, 2002).

A related study to the work of Schreiber and coworkers showed that PGC-1β functions as ERRL1 (for ERR ligand 1), which can bind and activate orphan ERRs in vitro (Kamei, 2003; Schreiber, 2003). Consistent with the developing paradigm, PGC-1β/ERRL1 transgenic mice exhibit increased expression of the MCAD, a known ERR target and a pivotal enzyme of mitochondrial β-oxidation in skeletal muscle. Also, the PGC-1β/ERRL1 mice are hyperphagic, have elevated energy expenditure, and are resistant to diet-induced or genetic obesity. This suggests that pharmacologic increase of PGC-1β protein or agonism of ERRs, of which ERRγ is the most responsive by their assays, might reduce obesity.

In addition to sharing PGC co-regulatory interactions between ERRs and PPARs, evidence for competitive interactions, or combinatorial control, between ERRs and PPARs in binding to promoter elements is described in work on the promoter of the carnitine palmitoyltransferase (CPT) gene (Barrero, 2003). The 5'-flanking region is transcriptionally active and binds PPARα in vivo as detected by ChIP. The promoter also contains a novel PPRE. Other NRs bind this site, such as ERRα and COUP-TF, suggesting a strong interplay between the ERRs and PPARs in mediating the control of processes mediated by these receptors, such as mitochondrial biogenesis and energy utilization.

Further evidence of combinatorial control between ERRs, PPARs and COUP-TF was studied using the MCAD promoter (Maehara, 2003). Three hexameric elements in the NRRE-1 of the MCAD promoter can bind ERRα, COUP-TF, and PPARα/RXRα. The PPARα/RXRα heterodimer complex can bind two hexamer repeat sequences (between site 1 and site 3) arranged as an everted imperfect repeat separated by 14 bp (ER14), an unprecedented distance; however the authors are not able to discern if ERRα binds as a dimer or two monomers at this region. Mutations of the putative core elements have shown that these three sites are differentially involved in ERRα and PPARα/RXRα binding. The authors propose that

homodimeric ERRα binds an ER14 between sites 1 and 3; a previously unreported distance. Site 1 is required for ERRα binding while site 3 is facilitative for site 1. PPARα/RXRα may compete with ERRα for binding—and overexpression of ERRα in HeLa cells counteracted the action of PPARα/RXRα on MCAD. The mechanism of this reduced PPARα/RXRα transcriptional activity is not described and could be due to ERRα sequestering limiting coactivators in *trans*.

Specific combinatorial control interactions of the ERRs, ERRα and ERRβ, with GR was studied in cell culture (CV-1, monkey kidney; COS-1, monkey kidney; SK-N-MC, human neuroblastoma;, HeLa, human cervix carcinoma) grown in DMEM plus 10% charcoal-stripped steroid-free fetal calf serum (FCS) (Trapp and Holsboer 1996). In CV-1 cells, five-times more DEX had to be added to see the effects of GR on an MTV-Luc construct when ERRβ was co-expressed. These effects were not seen in HeLa cells. This result was not seen on the PR reporter, nor was GR expression affected by ERRβ expression. GR continues to bind the GRE in the presence of ERRβ, and ERRβ does not bind the GRE, nor do ERRβ and GR form a complex that alters DNA binding—as seen with c-jun, calreticulin, and the p65 subunit of NF-κB. It was concluded that this inhibition is the *trans* sequestration of a factor that is in a limiting concentration in some cell types.

The relationship of ERRα to cancer biology was explored by examining the transcriptional activity of human Erg (one of the Ets family-transcription factors) which was repressed by several nuclear receptors, including ERα, ERβ, ERRα, TRα1, TRβ1, RARα and RXRα, but not RevErbα1 or COUP-TFII (Vlaeminck-Guillem, 2003). Conversely, Erg inhibited ERα, TR, RAR and Fli1 dependent transcription. The antagonism between ERG and ERα did not depend on DNA binding inhibition or direct protein-protein interactions. Repression of ERα-dependent transcription required the carboxy-terminal and amino-terminal transactivation domains of Erg whereas only the carboxy-terminal AF-2 domain of ERα was necessary for repression of Erg activity. Reciprocal inhibition between Erg and ERα is not due to typical squelching as it was not alleviated by overexpressing CBP, SRC-1 or RIP 140. This atypical mechanism of mutual inhibition may be important in endothelial, urogenital and cartilaginous tissues where both factors are expressed.

The action of ERRα on eNOS expression was investigated in light of the observation that ERα can regulate eNOS expression (Sumi and Ignarro, 2003). ERRα1 activates the estrogen response element (ERE) and eNOS promoter-dependent luciferase activity in COS-7 cells and bovine pulmonary artery endothelial cells in a serum dependent manner. Transcription of eNOS by ERRα1 is mediated by three regions: basepairs -1001 to -743, basepairs -743 to -265, and downstream from basepair -265 on the eNOS promoter. These results suggest that some of the protective effects of estrogen against atherosclerotic lesions observed may be mediated by ERRα, as well as the other ERRs.

In addition to the coactivator interactions that have been described, ERRα has been described to interact with the transcriptional corepressor RIP140. ERRα was identified as a key regulator of hexose uptake and regulation of mitochondrial proteins SDHB and Cox5b secondarily to an siRNA screen which detected RIP140 (Powelka, 2006). In the screen for siRNAs that alter insulin responsiveness in 3T3L-1 adipocytes, siRNA knock-down of RIP 140 was found to improve insulin responsiveness. Expression array analysis showed that RIP140 knock-down upregulates clusters of genes in the pathways of glucose uptake, glycolysis, TCA cycle, fatty acid oxidation, mitochondrial biogenesis, and oxidative phosphorylation. Consistent with these findings, reintroduction of RIP140 to RIP140-null MEFs downregulates expression of many of these same genes. Additionally, RIP140 knockdown in cultured adipocytes increased conversion of [^{14}C]glucose to $^{14}CO_2$ and mitochondrial oxygen consumption. Re-examination of the lean, RIP140-null mice, showed increased glucose tolerance and enhanced insulin responsiveness after high-fat feeding. RIP140 requires ERRα to regulate hexose uptake and mitochondrial proteins SDHB and CoxVb, but likely requires other nuclear receptors to fully manifest the phenotype.

The characterization of RIP140 in adipogenesis was continued (Nichol, 2006). In this study an adipocyte-specific P2 promoter for RIP140 was identified that is subject to regulation by ERRα. This promoter binding is reported to occur via two distinct mechanisms: 1) direct binding to an ERE/ERRE at -650/-633 and 2) indirect binding to Sp1 sites in the proximal promoter. While the RIP140 gene contains a single exon, it is subject to alternative expression of 5' non-coding exons that may exert regulatory functions. This regulation of the transcriptional repressor RIP140 by ERRα may allow the repression of alternate NR mediated transcriptional pathways during adipogenesis.

The interaction of RIP140 and ERRα was extended to other ERRs (Castet, 2006) On natural or artificial reporter genes containing varying response elements, RIP140 can inhibit or stimulate transactivation by ERRα, β and γ. RIP140 inhibits transactivation of the TRα gene by ERRβ, it increases ERRα and ERRγ activity on this promoter—which contains Sp1 sites. Sp1 sites are also found in the p21 gene which is subject to regulation by RIP140. The DNA elements may determine the specificity of coactivator interactions.

DNA-element determination of coactivator/corepressor interactions with nuclear receptors was examined for ERRα (Barry, 2005). The ERRE for ERRα is a nine nucleotide extended half-site sequence TNAAGGTCA, which can bind ERRα as a monomer or dimer. The base at the N position of the TNAAGGTCA sequence dictates ERRα binding preference as a monomer or dimer. Dimerization is determined by a threonine residue at position 124. A cytosine (instead of thymidine) at the N position in the ERRE of the ERRα target promoter trefoil factor 1 (TFF1,also known as pS2) diminished the transcriptional response of the ERRα/PGC-1α complex. This provides another example of DNA-based influence of receptor conformation determining its binding partners, such as PGC-1α.

ERRα Target Genes and Functional Significance

The first functional demonstration of an ERR was in the observation that COUP-TFs can form multiple molecular weight bands by electrophoresis representing interactions with other proteins, such as ERRα (Wang, 1991). Another study showed that a number of proteins from 45-55kd that interact with the SV40 major late promoter (initiator binding proteins, IBPs) (Wiley, (1993). Of the many members of the NR family found to interact with these viral proteins, a major one was shown to be ERRα. It was also shown that the SV-40 MLP is regulated by members of the NR family, including ERRα (Zuo and Mertz 1995). And it was suggested that the ability of ERRα to block the activity of the large tumor antigen to effect late transcription and may be important in the regulation of primate DNA viruses.

In another viral system, the interactions ERRs on the transcriptional control of the Epstein-Barr virus (EBV) was investigated (Igarishi, 2003) The EBV nuclear antigen leader protein (EBNA-LP) (consisting of W1W2 repeats and a unique C-terminal Y1Y2 domain) plays a critical role in EBV-induced transformation. A yeast-two-hybrid was employed using EBNA-LP cDNA (containing a single W1W2

domain) as bait to screen an EBV-transformed human peripheral blood lymphocyte cDNA library. ERRα was identified by Y2H to bind various EBNA-LPs with one, two or four W1W2 repeats, and by GST pull-down in COS-7 cells. The Y2 domain of the EBNA-LP mediates the interaction with hERRA through two conserved leucines in the Y2 domain (Leu-78 and -82). This result suggests that ERRα may play a role in EBV-mediated transformation.

Expanding the actions for ERRs from protein to DNA, is was proposed that orphan receptors might bind as monomers to define a third paradigm of receptor binding (Wilson, 1993). From consensus sequence analysis, ERRα was predicted to bind as a monomer to the 5'-TCAAGGTCA-3' half-site recognized by SF-1.

The regulation of ERRs was addressed in a report that ERRα and hERRβ can be activated by different ligand-independent pathways (Lydon, (1992). hERRα and hERRβ exhibited constitutive activity in the absence of exogenously added ligands. Furthermore, this constitutive activity is localized in the carboxy terminal domain of both receptors and can be transferred to other members of this superfamily using domain switching strategies. Additionally, hERRα was shown to be active in Saccharomyces cerevisiae.

The first putative ERR-regulated gene was identified by the observation that ERRα could modulate the estrogen receptor's actions on the lactoferrin gene promoter in a RL95-2 endometrial carcinoma cell line (Yang, 1996). Lactoferrin is a protein found in milk, tears, saliva and is greatly up-regulated by estrogen in the murine uterus. Using nuclear extracts from endometrial carcinoma (RL95-2) and mammary cell (HB100) lines and footprinting, factors were identified that could protect an upstream region (-418 to -378, FP1) from DNase I digestion. This region contains an extended nuclear receptor half-site, TCAAGGTCATC, which matches the consensus site of the transcription factor SF-1/ELP that binds as a monomer (Wilson, 1993). In this cell type, RL95-2, this extended half site binds ERRα. Furthermore, ERRα can directly interact with ERα at a protein level as demonstrated by Far Western analysis. This suggests that given the distance between sites, three helical turns could allow the ERRα and ERα to interact on the DNA. This spacing hypothesis has been suggested for other transcription factors (AP-1 binding proteins: Jun, Fos, and SP-1) that interact with the promoters of estrogen-responsive genes that do

not contain EREs. Three factors were identified that modulate the activity of the lactoferrin promoter: COUP-TF (which can suppress estrogen induction), ERRα, and a third uncharacterized protein. ERRα was shown to directly bind oligonucleotides containing regulatory motifs and was supershifted with immune, but not pre-immune sera. Excess vitellogenin A2 ERE oligonucleotide was used to exclude possible ERα binding, as ERα would be competed away by this more ideal consensus sequence. Interestingly, the ERRα protein identified has a few mutations that may effect its function. Western blot with anti-hERRα showed a major band at 42-kD and a minor band at 53-kD that may be due to post-translational modifications, or possibly other reported interactions such as with COUP-TF (Wang, 1991) or with SV40 late promoter factors (Wiley, 1993; Zuo and Mertz 1995).

An extension of the finding that ERRα enhances lactoferrin expression in human endometrial carcinoma cells was undertaken and showed the transcriptional regulation of ERRα by diethylstilbestrol (DES) (Shigeta, 1997). Isolation of a mouse cDNA that encodes a protein which binds to the human ERRE was demonstrated. A mouse uterine nuclear extract also interacted with the human ERRE and produced three complexes in the mobility shift assay, one of which was supershifted by the hERRα1 antiserum. A 2.2 kb transcript was detected by Northern analysis in all adult mouse tissues tested; however, large variations in the amount of ERRα1 mRNA were found among them, a finding supported by the NURSA results (www.nursa.org). Multiple immunoreactive forms of mouse ERRα1 were detected by Western analysis in non-reproductive tissues, whereas a major 53 kDa protein was found in reproductive tissues such as uterus, cervix and vagina. Diethylstilbestrol (DES) stimulated the expression of ERRα1 mRNA in the uterus of 19-day-old mouse. DES and estradiol, but not progesterone or dexamethasone, enhanced the level of immunoreactive ERRα1 in the mouse uterus. ERRα1 is an estrogen-responsive gene in the mouse uterus.

The previously reported study of ERRα binding to the SV40 major late promoter was expanded to identify two ERRα biding sites (Johnston, 1996; Wiley, 1993). It was demonstrated that ERRα binds as a monomer to an extended half site that may include an ERE. ERRα acts as a repressor of transcriptional activity on the SV40 MLP and can physically interact with both ERα and TFIIB. The major isoform of the NR3B1 gene was proposed to be ERRα1.

An attempt to define the role of ERRα by identifying target genes was undertaken (Sladek, 1997). This study first identified the ERRα target, MCAD, as a potential target, and by DNase footprinting defined 6 regions of the promoter that bind transcription factors. Sp1 was detected as well as three nuclear receptor response elements (NRREs). COUP, PPARs, RXR/RAR ARP-1 and HNF-4 were proposed to regulate MCAD. The MCAD nuclear receptor response element 1 (NRRE-1) interacts in vitro with ERRα expressed in COS-7 cells. Two isoforms of ERRα were detected in COS-7 cells at 48 and 62-65kD; however the higher band disappeared following phosphatase treatment supporting evidence that post-translational modification occurs (Yang, 1996). The translation was determined to start at 171 of the mRNA and was not preceded by an in-frame stop codon. The promoter was described as conserved between human and mouse. Supershift experiments show that endogenous ERRα present in nuclear extracts obtained from a brown fat tumor cell line (HIB) interacts with NRRE-1. In the absence of its putative ligand, ERRα does not activate the MCAD promoter in transient transfection studies; however, a VP16-ERRα chimera activates natural and synthetic promoters containing NRRE-1. In addition, ERRα efficiently represses retinoic acid induction mediated by NRRE-1. It was hypothesized that ERRα plays a role in fatty acid metabolism in metabolic tissues, such as BAT, cardiac and skeletal muscle; a contention that has held sway.

A developmental study of ERRα expression in mouse, including in situ studies in E17.5 mouse bone was performed (Bonnelye, (1997). This work described the detection of ERRα, but not ERRβ, in osteoblastic osteosarcoma cell line as well and in primary human osteoblasts. ERRα was shown to bind to a SF-1 consensus half-site and direct ERRα-dependent expression in ROS 17.2/8 as well as in HeLa, NB-E, and FREJ4 cells but not in COS1 and HepG2 cells. Furthermore they describe the second putative target gene of ERRα: osteopontin. ERRα is found in membranous (direct differentiation from mesenchyme to osteoblast) and endochondrial bone formation, where an intervening cartilage is ossified. ERRα expression was limited to the diaphyses and not the epiphyses. By molecular analysis, Bonnelye reiterate the work of Yang and coworkers and demonstrate that ERRα binds to a consensus site: TCAAGGTCA (Yang 1996). They also confirm the work of Johnston and coworkers in showing that ERRα binds as a monomer (Johnston, 1996).

This initial expression report was followed with a more general developmental study in mouse (Bonnelye, 1997). ERRα is expressed at very early stages in ES cells and at E8.5 in the mesodermal cells of the visceral yolk sac. Expression continues later in mesodermal tissues such as cardiac and skeletal muscles which persist through adulthood. Detection of ERRα during muscle differentiation led to study of expression in C2C12 myoblasts and demonstrated increased expression during the myoblast-myotube transition. In the CNS, at E10.5, a high level of ERRα transcripts can be observed in differentiated cells of the intermediate zone of the spinal cord and in the telencephalon vesicles at E13.5. Later, at E15.5 and E17.5, expression persists in the spinal cord but decreases dramatically in the central nervous system. Moreover, ERRα expression increases during skin formation and is detected in the stratum spinosum which contains differentiated Malpighian cells. ERRα was also observed in endodermal derivatives such as the epithelium of intestine and urogenital system. It was suggested that ERRα may play a role in the differentiation process due to its spatio-temporal occurrence. In HeLa cells, a multimerized SFRE upstream of the HSV-tk minimal promoter is capable of being upregulated in the presence of either ERRα or SF-1/FTZ-F1 24- to 4-fold, respectively. In the presence of both factors transcription is about 15-fold, suggesting competition between the two factors. However, this paper does not provide compelling evidence of developmental necessity or of competent molecular biologic techniques. The RT-PCR results have spurious bands; the Northern blot lacks internal controls, and the EMSA has poor resolution and some signal in the negative control.

Following on their initial observations, Bonnelye and coworkers explored the expression of ERRα in ossification zones and osteoblastic cells where it regulates osteopontin (Bonnelye, (2001). Osteopontin is an extracellular matrix protein thought to be involved in bone remodeling. ERRα mRNA was detected in rat calvaria (RC) cells where mRNA and protein were observed at all developmental stages from early osteoprogenitors to bone-forming osteoblasts, but protein was most abundant in mature cuboidal osteoblasts. ERRα antisense oligonucleotides blocked cell growth and a proliferation-independent inhibition of differentiation. ERRα overexpression in RC cells increased differentiation and maturation of progenitors to mature bone-forming cells. ERRα is highly expressed and appears to play a physiological

role throughout the osteoblast developmental sequence; and in differentiation and bone formation at both proliferation and differentiation stages.

Because menopause and concomitant estrogen reduction and hormone replacement therapy are critical in the treatment of disturbances to bone density (osteoporosis, osteopenia) the effects of estradiol on ERRα both *in vitro* and *in vivo* as relates to osteogenesis were explored as an extension on previous findings (Bonnelye, 2002; Bonnelye, 2001). Chronic treatment of fetal rat calvaria cultures with estradiol stimulated bone nodule formation and up-regulated ERRα at early (10 h and d 8) but not later times. ERRα expression was lower in bones form ovariectomized rats (1 d and 1 wk) post surgery, but returned to control levels thereafter. ERRα is also expressed in osteoclasts (tartrate-resistant acid phosphatase + multinucleated cells) in vivo and in vitro (RAW 264.7 cells) and ovariectomization lowered the OPG/receptor activator of NFκB ligand expression ratio. ERRα antisense treatment of rat calvaria cells inhibited osteogenesis, increased adipocyte colony formation and changed the OPG/receptor activator of NFκB ligand ratio. Estradiol dependent expression of ERRα may play a role at several levels (osteoblasts, adipocytes, and osteoclasts) in osteoporosis.

Given the identification of a target gene and suggested roles of ERRs in tissues that use oxidative metabolism, studies to identify factors involved in the differentiation of BAT were performed (Vega, 1999). The study employed the previously identified ERRα target, MCAD, which has a NRRE-1, as a CAT reporter during and after differentiation (Sladek, 1997). EMSA and antibody-retention studies identified differentiation stage-specific, NRRE-1 complexes: COUP-TFI and II, are major NRRE-1 binding proteins in the pre-adipocyte, and ERRα bound NRRE-1 in differentiated BAT nuclear extracts. NRRE-1 mutant probes indicated that ERRα was capable of binding two known ERRα monomeric binding sites within NRRE-1. ERRα paralleled NRRE-1 binding activities and MCAD expression during brown adipocyte differentiation, cardiac development, and in among a variety of adult mouse tissues. COUP-TFs and ERRα are important in BAT differentiation.

With the shared consensus sites between ERRs (ERRE) and SF-1 (SFRE), which has been shown to regulate TRα, the role of ERRα on TRα was studied (Vanaker, 1998). TRα has multiple transcribed products, only one of which is transcriptionally active (the others being dominant negative regulators)—the

ratio of which is high in brain. ERRα stimulates the expression of TRα in an SFRE-dependent manner; and because SF-1 has a limited expression pattern, ERRα may be dominant in most tissues. An SFRE in the upstream promoter suggests that ERRs may bind to the promoter and regulate tissue-specific alternate regulation of TRα isoforms. Cell lines such as HeLa or NB-E support ERRα-induced SFRE-dependent transcriptional regulation, but HepG2 or COS1 do not. Both TRα and ERRα are coexpressed in embryonic intestine, brown fat and heart as well as in the adult gonads. In the testis, expression of both receptors can be found in the seminiferous tubes where it is totally restricted to spermatocytes I.

Expanding on the demonstrated ERRα /SF-1 crosstalk in mammalian cell lines, Vanacker and coworkers also dissected differences between consensus sites for ERRα and SF-1 on these SF-1 –like sites in mammals and fish (Vanaker, 1999a). Various species (mouse, human, zebrafish) were tested for their transcriptional activities, and all ERRα orthologs are activators on SFREs. This activity is dependent on the AF2 domain and is lost when serum is charcoal stripped. Further studies of the ERR/SF-1 crosstalk/combinatorial control, investigated the cross talk of ERα, ERβ, ERRα and ERRβ (Vanacker, 1999b). On ERE reporter constructs, all four receptors could bind and activate; the ERs being ligand dependent. On the SFRE, ERβ did not bind, but the others did. The osteopontin promoter was shown to retain these binding and activation characteristics. This study demonstrated the novel action of ERα on the SFRE, and the strong potential for cross talk between the ERs and ERRs on both EREs and SFREs. Notably, ERRγ was not investigated.

Because ERRα is expressed in a variety of adult and embryonic tissues (in particular, at the onset of ossification), and several osteoblastic cell lines, studies were undertaken to study bone-related genes (Vanaker, 1998). ERRα acts as a site- and cell-specific transcriptional activator. ERRα transactivates the promoter of the mouse osteopontin (OPN) gene, a marker of the late stages of osteoblastic differentiation. Regulation is cell-specific via derivatives of the ERRα response element. Overexpression of ERRα in three different osteoblast-like cell lines resulted in elevation of OPN message. ERRα may play a role in osteoblast differentiation.

A previously identified a silencer element (S1) between promoters I.3 and II of human aromatase gene that down-regulates transcription was suspected to be regulated by ERRα (Yang, 1998). A yeast one-

hybrid approach was used to screen a human breast tissue hybrid cDNA expression library for genes encoding proteins binding to the silencer region. Half of the clones detected encode for ERRα-1. Other positive clones include EAR-2 (COUP-TF, NR2F6), EAR-3 (COUP-TF1, NR3F1), RARγ, and p120E4F. ERRα-1 was examined in S1 regulatory action on the promoter I.3 of the human aromatase gene. ERRα-1 upregulated promoter I.3 and S1 reporter plasmids in breast cancer SK-BR-3 cells. EMSA and DNase I footprinting confirmed ERRα-1 binding to S1 between 96 and 107 bp relative to the transcriptional start site: 5'-AAGGTCAGAAAT-3'. SF1 has been shown to bind this site with similar affinity as ERRα-1 and mediate a cAMP response in ovary, however no SF-1 clones were found by this assay or by RT-PCR in breast cancer tissue or SK-BR-3 cells, which contradicts the work by Vanaker and coworkers (Vanaker, 1998; Vanaker, 1999a; Vanaker, 1999b). RT-PCR did detect the presence of two isoforms of ERRα-1, the shorter appearing in 28 of 32 (as well as SK-BR-3 and WS3TF cells), and the longer in 1 of 32 breast cancer specimens. The authors conclude that ERRα may interact with the aromatase promoter in breast cancer cells.

This work was followed with a review and characterization of the aromatase gene promoter in normal or cancerous breast tissue (Chen, 1999). Aromatase is expressed at a higher level in human breast cancer tissue than normal breast tissue. In situ estrogen production is more important than circulating estrogens in breast tumor promotion by autocrine and paracrine pathways. In normal tissue, aromatase is regulated by glucocorticoid to utilize exon I.4 and to incorporate exons I.3 and II by cAMP in cancerous tissue. Using a three-dimensional growth assay, they co-cultured MCF-7 cells with cells expressing high levels of aromatase (MCF7aro or T-47Daro). An additional cAMP responsive site CREaro, can overcome the inhibitory action of the S1 silencer site (Yang, 1998). The S1 interacts with ERRα-1, where ERRα-1 is a positive regulator, and suggests that ERRα-1 may contribute to the upregulation of aromatase in breast cancer tissue, where cAMP levels are increased. However, ERRα-1 is thought to interact with EAR3 which in turn may have suppressive effects through NCoR and SMRT corepressors.

The variation in aromatase promoter usage was studied in breast tumors (i.e. cAMP-stimulated promoters I.3 and II) and normal breast tissue (i.e. glucocorticoid-stimulated promoter I.4) (Chen, 2001). In normal breast tissue, the function of promoters I.3 and II is suppressed through the binding of EAR-2,

COUP-TFI, and EARγ to S1, and through the binding of Snail/Slug proteins to their binding site that quenches the CREaro activity. In cancer tissue, the expression levels of EAR-2, COUP-TFI, EARγ, Snail, and Slug decrease, and aromatase expression is then up regulated through the binding of ERRα-1 to S1 and the binding of CREB or related factors to CREaro. The modulation of aromatase expression by endocrine disrupting chemicals is exemplified by two organochlorine pesticides (i.e. toxaphene and chlordane) that have been found to be antagonists of ERRα-1 orphan receptor (Yang and Chen 1999).

Further extension and integration of studies on the regulation of the aromatase gene promoter were continued (Yang, 2002). A yeast-two-hybrid screen of human breast tissue hybrid cDNA library identified four orphan/nuclear receptors, ERRα-1, EAR-2, COUP-TFI (EAR-3), and RARγ that bind to the silencer (S1) region of the human aromatase gene. The S1 region down regulates promoters I.3 and II of the human aromatase gene. The interaction of EAR-2, COUP-TFI, and RARγ with S1 was confirmed by EMSA. ERRα-1 is a positive, but subordinate, regulatory factor: the other three NRs have negative regulatory effects that override the positive effects of ERRα. RT-PCR analysis of eleven cell lines and fifty-five human breast tumor specimens detected these nuclear receptors in human breast tissue. Since EAR-2, COUP-TFI, and RARγ are expressed at high levels, it is likely that S1 acts as a negative regulatory element that suppresses aromatase promoters I.3 and II in normal breast tissue. However, in cancer tissue, S1 may function as a positive transcriptional element since ERRα-1 is expressed, while EAR-2 and RARγ are detected in only a small number of tumor specimens. There is a weak inverse correlation between the expression of COUP-TFI and that of aromatase in breast tumor tissue. ERα can bind to S1, in a ligand-dependent manner and down-regulates the aromatase promoter activity. These studies suggest that aromatase expression is under complex combinatorial control that is significantly altered in cancer tissues.

A study to analyze the expression of known clinicopathological prognostic indicators from a pool of thirty-eight tumors and nine normal enriched mammary epithelial cells was undertaken despite the limits imposed by a small sample size and multiple statistical tests that increase the false positive findings (Ariazi, 2002). Using QPCR assays to detect transcripts within cDNA generated from tissue samples or cell lines, levels of ERα, ERβ, epidermal growth factor receptor, ErbB2, ErbB3, ErbB4, ERRα, ERRβ, and ERRγ were determined. ERRα showed potential as a biomarker of unfavorable clinical outcome and, possibly,

hormonal insensitivity. ERRα mRNA was expressed at levels greater than or similar to ERα mRNA in 24% of unselected breast tumors, and generally at higher levels than ERα in the progesterone receptor (PR)-negative tumors. Increased ERRα levels associated with ER-negative and PR-negative tumor status. ERRα levels also correlated with expression of ErbB2, an indicator of aggressive tumor behavior. Thus, ERRα was the most abundant nuclear receptor in a subset of tumors that tended to lack functional ERα and expressed ErbB2 at high levels. Consequently, ERRα may potentiate constitutive transcription of estrogen response element-containing genes independently of ERα and antiestrogens in ErbB2-positive tumors. ERRγ may be a biomarker of favorable clinical course and, possibly, hormonal sensitivity. ERRγ was overexpressed in 75% of the tumors, resulting in the median ERRγ level being elevated in breast tumors compared with normal mammary epithelial cells. ERRγ overexpression associated with hormonally responsive ER- and PR-positive status. Additionally, ERRγ expression correlated with levels of ErbB4, a likely indicator of preferred clinical course, and associated with diploid-typed tumors. Hence, ERRα and ERRγ status may be predictive of sensitivity to hormonal blockade therapy, and ERRα status may also be predictive of ErbB2-based therapy such as Herceptin.

The expression of ERRα in human breast carcinoma tissues using immunohistochemistry (n = 102) and real-time reverse transcription-PCR (n = 30) has also been examined (Suzuki, (2004). ERRα immunoreactivity was detected in the nuclei of carcinoma cells in 55% of breast cancers examined, and relative immunoreactivity of ERRα was significantly ($P = 0.0041$) associated with the mRNA level. Significant associations were detected between ERα and ERE-containing estrogen-responsive genes, such as pS2 ($P < 0.0001$) and EBAG9/RCAS1 ($P = 0.0214$), in breast carcinoma tissues. However, no significant association was detected between ERα and pS2 ($P = 0.1415$) in the ERRα-positive cases (n = 56) or between ERα and EBAG9/RCAS1 ($P = 0.8271$) in the ERRα-negative group (n = 46). ERRα immunoreactivity was significantly associated with an increased risk of recurrence and adverse clinical outcome by both uni- ($P = 0.0097$ and $P = 0.0053$, respectively) and multi- ($P = 0.0215$ and $P = 0.0118$, respectively) variate analyses. A similar tendency was also detected in the group of breast cancer patients who received tamoxifen therapy after surgery. These results suggest that ERRα possibly modulates the

expression of ERE-containing estrogen-responsive genes, and ERRα immunoreactivity is a potent prognostic factor in human breast carcinoma.

The interaction of ERRα with ERα on EREs was further explored in the context of the known interaction in ER-positive breast cancer MCF-7 cells by looking in endometrial cell lines (Wantanabe, 2006) ERRα is expressed in 4 endometrial cancer cell lines (Ishikawa, Hec1a, KLE, SNGII) and detected in 11 human endometrial tissue samples. Overexpression of ERRα repressed estrogen-induced ERE-dependent transcriptional activity in Ishikawa cells. That could be reversed by siRNA against ERRα. Overexpression of ERRα slowed the growth of endometrial cell lines exposed to estradiol, suggesting that ERRα may be a therapeutic target for anticancer therapy.

A trio of papers from Gao et al appearing in Chinese and English journals focus on the role of ERRs in endometrial carcinoma (Gao, 2006, Gao, 2005a, Gao, 2005b). ERR expression was examined in endometrial adenocarcinoma and normal endometrium control using RT-PCR and immunohistochemistry. Expression results were then correlated with clinicopathologic measures such as: FIGO stage, myometrial invasiveness, histologic grading, and metastasis to lymph nodes. After demonstrating concordance between RT-PCR results and immunostaining values, they showed a downregulation of ERRα and downregulation of ERRγ message in ERα-positive endometrial adenocarcinomas, relative to control tissue. ERRα positively correlated with FIGO and myometrial invasion, while ERRγ was negatively correlated with metastasis to lymph nodes. The statistical weight of these findings is modest with P-values of 0.049 to 0.014 and the results are only correlative with no mechanistic evidence. However, several lines of evidence have implicated ERRs in neoplastic diseases.

The mechanism of combinatorial control at the level of DNA binding was studied by measuring direct competition of ERRα1 and ERα (Krause, 2002). This study demonstrated that ERRα1 can sequence-specifically bind a consensus palindromic ERE and compete with ERα for binding. ERRα1 activates or represses ERE-regulated transcription in a cell type-dependent manner: repressing in ER-positive MCF-7 cells while activating in ER-negative HeLa cells. Thus, ERRα1 can function both as a modulator of estrogen/ERα responsiveness and as an estrogen-independent activator. Mutational analysis revealed that repression is not simply the result of competition between ERα and ERRα1 for binding to the DNA.

Rather, it also requires the presence of sequences within the carboxyl-terminal E/F domain of ERRα1. Because of these observed effects, ERRα1 can function as either an active repressor or a constitutive activator of ERE-dependent transcription. In principle, this allows ERRα1 (and ERRs generally) to interact in any estrogen-regulated process, such as the etiology of some breast cancers, reasserting the therapeutic potential of the ERRs.

Concerns of environmental effects of potentially estrogen-modulating pesticides prompted the study of the interaction of ERRα with two organochlorine pesticides, toxaphene and chlordane (with estrogen-like activities) (Yang and Chen 1999). Toxaphene and chlordane antagonize ERRα activity in mammalian SK-BR-3 cells, but had a positive effect on ERRα-Gal4-AD fusion protein in yeast. These effects were not ERRα-specific, as ERα dependent transcription was slightly increased by these compounds as well. Toxaphene suppressed the 3-fold GRIP1 induced ERRα-1 activity observed in SK-BR-3 cells. Toxaphene (10μM x 24h) also suppressed two-fold increased aromatase activity observed in a HepG2 line stably expressing ERRα. Toxaphene is not an antagonist of aromatase and these effects are thought be directly mediated by ERRα. In a computer model the investigators suggest that ERRα may have bulky LBD pocket side chains sterically hindering ligand binding, a finding later supported by structural determination (Greschik, 2002). ERRα and ERα have been shown to physically interact and this may be one target of endocrine disruption by these insecticides. Toxaphene and chlordane are among the 12 persistent organic pollutants identified by the United Nations Environment Programme as requiring urgent attention.

On a side note, a study performed on the promoter properties of LH in two placental cell lines determined that an ERE is mediating transcriptional repression, but this repression is not mediated by ERα or ERRα (Geng, (1999).

Extending the combined works of Vanaker, Yang and their respective coworkers, Zhang and others show that ERRα1 (NR3B1a) binds the SFRE, TCAAGGTCATC, 26 base pairs upstream from the ERE of the human lactoferrin promoter (Zhang, 2000; Yang, 1996; Vanaker, 1998, 1999a, 1999b). Lactoferrin is found in milk, tears and secondary granules of neutrophils. Mutation of an SFRE in the lactoferrin gene promoter reduced estrogen-dependent transcription from the lactoferrin ERE in human endometrial cells. ERRα1 binds both SFRE and ERE elements and constitutively transactivates the

lactoferrin promoter. ERRα1 binding was argued to be homodimeric as shown by M2H and DNase footprinting. The p160 coactivators, SRC1a or GRIP1, further enhance ERRα1 activity on this promoter. Both ERα and ERRα can bind ERE and SFRE promoter sequences and activate them; however ERRα does this in a ligand-independent and constitutive manner.

The molecular basis of the constitutive activity of ERRα was investigated by site directed mutagenesis (Chen, (2001). Nine of nineteen residues in the LBD of ERRα are identical in to those in ERα. Seven of these residues are conserved; however one is critically different: Phe-329 in ERRα-1 and Ala-350 in ERα. Site-directed mutagenesis experiments have revealed that Phe-329 is responsible for the constitutive activity of ERRα-1. ERRα-1 mutant F329A lost activity and was dominant negative. ERRα-1 mutant F329A, like wild-type ERα, recognized toxaphene as an agonist. Complimentary mutagenesis in ERα (A350F) was found to confer constitutive activity. Phe-329 in ERRα-1 and Ala-350 in ERα are critical to both ligand binding and transactivation functions. This space-filling aromatic ring seems to act critically as both an apo-LBD stabilizing structure which mimics ligand binding and as a steric hindrance to the binding of endogenous ligands.

Because of the importance of estrogens and antiestrogen therapy in the development and treatment of breast cancer, the possible crosstalk/combinatorial control of ERs and ERRs was explored using the estrogen-inducible pS2 gene (a human breast cancer prognostic marker) (Lu, 2001) All of the ERR isoforms can activate the pS2 promoter in a variety of cell types, including breast cancer cell lines. An extended half-site within the pS2 promoter is required for response to both ERs and ERRs. All p160 coactivators are activating, and DES antagonizes the activity. ERRα is the major isoform expressed in human breast cancer cell lines and DES can inhibit the growth of both ER-positive and -negative cell lines. ERRs may represent unappreciated pharmacological targets that can alter the expression of diagnostic markers of breast cancer and may be of therapeutic utility. By better understanding the interactions of SERMs and SERRMs upon their constituent receptors, better therapies will be achieved.

A study to address the actions of SERM/SERRMs, such as 4-hydroxytamoxifen (4-OHT, the active metabolite of tamoxifen) on the activities of ERRβ and ERRγ was undertaken by Trembley and others much like the work of Coward and coworkers (Trembley, 2001; Coward, 2001). FRET studies used

a fluorescently labeled LLXXLL motif from GRIP-1 instead of SRC-1, as used elsewhere (Coward, 2001). Half inhibition by 4-hydroxytamoxifen was 500nM for ERRβ and 90 nM for ERRγ, with no effect observed on ERRα. 4-OHT also disrupted the interaction of ERRγ, but not ERRα, with SRC-1 in a mammalian two-hybrid experiment. 4-OHT) is a first generation SERM that functions as an antagonist in breast cancer cells but displays estrogen-like activities in the uterus and bone. 4-OHT disrupts the interaction of ERRs β and γ with coactivators for which their constitutive activity is dependent. 4-OHT has been shown to act as an estrogen agonist to maintain bone density, reduce circulating cholesterol, increase uterine growth, while acting as an estrogen antagonist in breast.

A critical experimental system to study the physiologic role of ERRα was undertaken by the generation and analysis ERRα-/- mutant mice (Luo, 2003). ERRα-/- mice are viable, fertile and display no gross anatomical alterations, with the exception of reduced body weight and peripheral fat deposits. No significant changes in food consumption or energy expenditure or serum biochemistry parameters were observed. However, ERRα-nulls are resistant to a high-fat diet-induced obesity. DNA microarray analysis of gene expression in adipose tissue demonstrates altered regulation of several enzymes involved in lipid, eicosanoid, and steroid synthesis, suggesting that the loss of ERRα might interfere with other nuclear receptor signaling pathways by disrupting the metabolic of biosynthetic processes that generate ligands or their precursors. Microarray analysis also shows alteration in the expression of genes regulating adipogenesis as well as energy metabolism. ERRα-nulls had greater elimination of tritiated fats. Loss of ERRα may allow endogenous ERα signaling to be effectively higher and promote a lean phenotype. Mention of ERRγ is conspicuously absent, despite the high expression of ERRγ in metabolic tissues.

An additional level of complexity and mechanistic explanation of cross-talk/combinatorial control between PGC-1α and ERRα was identified: expression of PGC-1α upregulates the expression of ERRα, and both can regulate each other's transcriptional activities (Laganiere, 2004). This study identified a twenty-three base-pair sequence (ESRRA23) with two NR half-site motifs present in one to four copies within the promoter of human ERRα. The ESRRA23 contains an ERRE that is specifically bound by ERRα in vivo by ChIP assay (and apparently also binds ERRβ and ERRγ but not ERα, according to the study's unpublished data). ERRα reporter activity on the ESRRA promoter or ESRRA23 element is low when

assayed by transient transfections in HeLa cells. PGC-1a activates the ESRRA promoter in proportion to the ESRRA23 copy number. ERRα and PGC-1α synergistically activate the ESRRA promoter, in an ERRα binding site dependent manner. This effect is reduced in ERRα-null MEFs. ERRα and PGC-1α confer variable responses on this polymorphic ESRRA23 element that may underlie mixed responses to estrogen-related endocrine issues. This study appears to reveal a novel regulatory element and potential genetic diversity: polymorphic response element multimerization.

Further refinement of the functional interrelation of ERRα as an effecter of the PGC-1α that regulates the expression of genes involved in oxidative phosphorylation and mitochondrial biogenesis was in demonstrated in SaOs cells (which do not express ERRγ) (Schreiber, 2004). Inhibition of ERRα by siRNA compromises the ability of PGC-1α to induce the expression of genes encoding mitochondrial proteins and to increase mitochondrial DNA content. In a complimentary experiment, constitutively active VP16-ERRα can elicit both responses. ERRα binding sites (ERREs) were found in the first 1kb of most of the ERRα/PGC-1α-induced genes. NRF-1 and NRF-2/Gabpaα and now ERRα mediate the effects of PGC-1α on nuclear genes encoding mitochondrial proteins. The combination of these factors may fine tune the mitochondrial characteristics for each cellular environment (muscle, neural, BAT). It is of note that many of the ERRα-regulated genes they describe have been reported to be expressed at reduced levels in humans that are insulin-resistant.

To follow this theory, the regulation of genes by PGC-1α involved in oxidative phosphorylation (OXPHOS) that are reduced in skeletal muscle of diabetic and prediabetic humans was explored (Mootha, (2004). By overexpressing PGC-1α in C2C12 and subsequently analyzing expression changes by array, followed by a *cis*-regulatory motif identifying MotifADEalgorithm, ERRα and a GA repeat binding protein, Gabpa, were detected as key regulators of OXPHOS. ERRα and Gabpa interact with PGC-1α in muscle to form a double-positive-feedback loop that drives the expression of many OXPHOS genes. Using an ERRα inverse agonist produced by Xceptor Therapeutics (subsequently acquired by Excelexis) (XCT790, IC50: 583nM) the role of ERRα in PGC-1α-mediated effects on gene regulation and cellular respiration was demonstrated. This ambitious identification and manipulation of a complex regulatory

pathway implicated in the treatment of diabetes has securely paved the way toward greater appreciation of ERRs in metabolic and endocrine disease.

High-throughput screening and gene-expression studies have also been attempted to understand the role of ERRα in PGC-1α signaling (Willy, 2004). The same experimental compound as used by Mootha and coworkers, XCT790, decreases the activity of ERRα and PGC-1α/ERRα-dependent signaling. This study identified MAO-B as a target gene of ERRα which raises the possibility of oxidative deamination as a metabolic cue. ERRα may mediate a subset of the actions of PGC-1 and may play a role in metabolic syndrome and Type II diabetes. One aspect of metabolic syndrome is high blood pressure, a sign modified by monoamine oxidases.

Due to the established circadian patterns of gene expression in many tissues and the known cycling of estrogens, with which ERRs have been shown to interact, the circadian expression of ERRα was investigated (Horard, 2004). ERRα expression was examined in estrogen-responsive tissues such as liver, uterus and bone where ERRα has been suggested to be regulated by estrogen. The expression of ERRα displays a circadian rhythmicity in liver, bone and uterus, in contrast to other uterine estrogen-regulated genes. The circadian activity is clock dependent and Bmal1 and Rev-erbα also diurnally cycle in the uterus, but not in bone. In bone, Per2 controls rhythmicity suggesting a complex regulation of ERRα in various tissues.

The structural analysis of the constitutive activity of ERRα was deduced by the crystal structure of the LBD of ERRα complexed with a coactivator peptide from PGC-1α (Kallen, 2004). This 2.5Å resolution x-ray structure of the ERRα LBD, was the first structure of a PGC-1α complex. The ligand binding pocket (LBP) of ERRα is nearly filled by amino acid side chains, particularly. Phe328 (corresponding to Ala272 in ERRγ and Ala350 in ERα). Due to the small LBP, a ligand of greater than four carbon atoms is likely to alter the LBP and displace helix 12 from the transcriptionally active position. This study also shows how inverted LXXLL motifs (namely a LLXYL motif) bind to LBDs. The PGC-1α NR box motif from the L3 site binds the ERRα LBD with a higher affinity than a SRC-1 motif particularly when all three leucine-rich regions of PGC-1α are present.

As study to identify PCG-1α-dependent ERRα target genes was undertaken due to the importance of this signaling pathway for energy production in cardiac and skeletal muscle by overexpressing ERRα in primary neonatal cardiac myocytes (Huss, 2004). A subset of PGC-1α target genes involved in cellular fatty acid transport, mitochondrial and peroxisomal fatty acid oxidation, and mitochondrial respiration were upregulated by ERRα overexpression. These results were confirmed in cardiac myocytes, C2C12 myotubes, and cardiac and skeletal muscle of ERRα-/- mice. ERRα increased lipid accumulation and the rate of fatty acid oxidation. Because many of the genes detected by altering ERRα are PPARα targets, regulation of PPARα was explored and found to be a target of ERRα which binds directly to the PPARα promoter. ERRα could not alter several PPARα targets or increase FAO in $ERR^{-/-}$ $PPAR^{-/-}$ double null fibroblasts. The expression of ERRα is dependent on PGC-1α. ERRα acts a key player in PPARα and PGC-1α mediated mitochondrial biology.

The ability of ERRα—previously thought to act as a constitutively positive modulator of transcription—to act in either a positive or negative manner was described in the modulation of metabolic substrate preference (Herzog, 2005). It had been recognized that ERRα and PGC-1α are members of a common regulatory network controlling mitochondrial biogenesis and substrate utilization. A key node of this metabolic network is the gluconeogenic enzyme PEPCK. The promoter for PEPCK can bind ERRα and PGC1α, but unlike the positive effect of ERRα on many mitochondrial genes, this promoter is inhibited by ERRα. Repression by ERRα can be blocked by siRNA against ERRα which also allows increased occupancy by PGC-1α. This observation helps explain why ERRα-null animals have increases in the gluconeogenic genes PEPCK and glycerol kinase, with reduced of expression of mitochondrial genes, such as ATP synthase subunit beta and cytochrome c-1. These dual actions on gluconeogenesis and mitochondrial biogenesis suggest that diabetic patients might benefit from ERRα agonists. ERRα-agonists might improve metabolic parameters by suppressing hepatic glucose production and increasing mitochondrial oxidative capacity in skeletal muscle, fat and liver.

Because of the known interactions of ERRα and AhR with ER's signaling pathways and the wide use industrial products that interact with AhR, the effect of these industrial products on estrogen responsive tissues was undertaken (Schlect, 2004). Organic chemicals with structural relationships to steroid

hormones, such as the UV-screens benzophenone-2 and benzophenone-3 (BP2, BP3), are used in cosmetics and plastics to improve product stability and durability. Both BP2 and BP3 were shown to exert uterotrophic effects and BP2 was shown to bind to the estrogen receptors. The effects of BP2 and BP3 on gene-expression of the ERRα, ERα and AhR receptors in the pituitary, the uterus and the thyroid after a five-day treatment in comparison to estradiol were evaluated. It was found that BP2 has an estrogen-like effect while BP3 does not. Additionally, both substances alter receptor expression that may not be appreciated by standard assays of estrogen responsiveness.

Because ERRα-null mice display a paradoxical reduced body weight, and ERRα is expressed in epithelial cells of the small intestine, the ability of ERRα-null mice to absorb nutrients was investigated (Carrier, 2004). Intestinal gene expression revealed a subset of genes involved in oxidative phosphorylation that were down-regulated in ERRα-nulls. Isolated enterocytes from ERRα-null mice have reduced beta-oxidation. Genes involved in intestinal lipid digestion and absorption, such as pancreatic lipase-related protein 2 (PLRP2), fatty acid-binding protein 1 and 2 (L-FABP and I-FABP), and apolipoprotein A-IV (apoA-IV) were dysregulated and ERRα-null pups have malabsorption of lipid. ERRα is required to maintain basal expression, but not feeding-induced expression, of the apoA-IV gene. The apoC-III enhancer of the apoA-IV gene is regulated by ERRα in cooperation with PGC-1α. This study shows that ERRα is a global regulator of lipid metabolism from absorption through mitochondrial fatty acid oxidation.

A high throughput screen of compounds that disrupt interaction of an SRC1-derived peptide to ERRα as detected by fluorescence identified a thiadiazolopyrimidinone as an ERRα inverse agonist (Busch, 2004). This scaffold was used to derivatize a pool of compounds resulting in an inverse agonist with an IC_{50} of 370nM named XCT790.

While the homodimerization of ERRs has been shown to effect transcriptional activity, the formation of heterodimers was investigated (Horard, 2004b). Transcriptional activity can occur by the formation of ERR heterodimers. This study also identified a long isoform of the amphioxus ERR ortholog that has atypical properties: it binds as a monomer and does not activate transcription through the SF1 response element, yet does bind and a homodimer to EREs to effect transcriptional activity.

The capacity for ERRs to interact with ERs in normal and prostatic sells lines was investigated (Cheung, 2005).Message RNA and protein expression patterns of three ERR members in normal human prostate epithelial cells, established cell lines, cancer xenografts, and prostatic tissues, as well as transient transfection studies were examined. RT-PCR showed that ERRα and ERRγ transcripts were detected in most cell lines and xenografts, whereas ERRβ was detected in normal epithelial cells and few immortalized cell lines but not in most cancer lines. Western blots and immunohistochemistry detected ERRs as nuclear proteins in epithelial cells, but expression was reduced or undetected in neoplastic prostatic cells. Overexpression of ERRs inhibited cell proliferation and repressed ERα transcription in PC-3 cells. This study shows that there is potential interaction of ERRs with prostate cancer biology and that a selective agonist might be beneficial.

The interaction of ERRα with another transcription factor, Sp1, was undertaken (Sumi and Ignarro, 2005). ERRα transfection produced Sp1-DNA complex formation and was detected by EMSA analysis. A 3X-Sp1-Luc reporter was activated by ERRα. Additionally, Sp1 expression is upregulated by ERRα.

Because ERRs modulate the transcription of a subset of estrogen responsive genes by divergent estrogen response elements (EREs) a study was conducted to determine whether human ERRα, β and γ might be involved in ovarian cancer (Sun, 2005). Analysis of hERRα, hERR, hERRβ-2, and hERRγ message from five ovarian cancer cell lines and 33 samples of ovarian cancer and 12 samples of normal ovary. Serum CA-125 levels were also analyzed in all samples by ELISA. Progression-free survival and overall survival of patients with different expression of ERRs were analyzed by the Kaplan-Meier method. ERRα-GFP transfection in OVCAR-3 cells showed nuclear expression. ERRα (P=0.020) and hERRγ (P=0.045) were upregulated in ovarian cancers compared to normal ovaries, while hERRβ was only observed in 9.1% of ovarian cancers. Serum CA-125 levels were positively correlated hERRα expression (P=0.012), but not hERRβ and hERRγ expression. The hERRα-positive group had a reduced survival (P=0.015), and the ERRγ-positive group has a longer progression-free survival (P=0.020). Expression of hERRα was an independent prognostic factor for poor survival (relative risk, 3.032; 95% CI, 1.27-6.06).

ERRs may play an important role in ovarian cancer: hERRα representing a biomarker of poor prognosis, and hERRγ representing a new therapeutic target.

The promoter of the human ERRα gene was cloned and characterized to examine the interaction of ERR expression with estrogen and PGC-1 signaling (Liu, 2005). Mutation and deletion studies showed a 53 bp region containing repeated core element AGGTCA motifs of the ERRα gene serves as a multi-hormone response element (MHRE) for several nuclear receptors in transient co-transfection studies of human endometrial carcinoma (HEC-1B) cells. ERRγ bound and robustly stimulated reporters containing at least two AGGTCA motifs. Ectopic expression of PGC-1α in HEC-1B cells enhanced the responsiveness. Overexpression or siRNA reduction of ERRγ increased and decreased, respectively, the PGC1-1α effect in a manner dependent on AF2 of ERRγ and L2 and L3 of PGC-1α. Further, PGC-1α increases ChIP of ERRγ. ERRα contains a MHRE that is responsive to ERRγ and PGC-1α, findings supported in the studies presented here.

The complex nature of the polymorphic ERRα promoter has been further explored in the context of human epidemiology (Kamei, 2005). A 23-base pair sequence in the 5'-flanking region referred to as ESRRA23 was examined in703 Japanese individuals. The 2.3-genotype was associated with a higher BMI. This locus is found in a simlar proportion in whites. However newer work fails to see this correlation (Larsen, 2006).

Because transcriptional activation of oxytocin by estrogen does not follow the classical model of estrogen receptor action (Koohi, 2005), regulation by ERRα and GCNF was explored in MDA-MB 231 cells. The oxytocin promoter does not contain an ERE, but does contain a high affinity binding site for NRs. Estrogen responsiveness is dependent on the nuclear orphan receptor binding site and ligand-activated ERα, but independent of ERα binding to DNA. Partial agonists tamoxifen and raloxifen and the pure antagonist ICI 182 780 all show agonistic activities on transcription, while exhibiting normal binding affinities to ERα. Binding of ERRα to the oxytocin promoter binding site implicates this receptor in regulation. Regulation by estrogen is dependent on ERK-1/ERK-2 MAP kinases. This mechanism of estrogen action is likely to underlie the diverse responsiveness of estrogen signaling.

Gastrulation is an embryonic process in vertebrates involving cellular commitment and movements to establish three fundamental germ layers. Due to the previous studies demonstrating ERRs in developmental processes, loss of function (morpholinos or a dominant-negative version of the protein) and gain of function (mRNA injection) strategies, were used to show that ERRα is involved in epiboly and convergent-extension (CE) processes in the zebrafish (Bardet, 2005a). From the beginning of gastrulation, ERRα is expressed at the margin of the blastoderm that represents the presumptive mesendoderm. ERRα may regulate fundamental developmental processes.

Amphioxus represents an evolutionary enigma due to the apparent lack of hindbrain segmentation, as seen in other vertebrates such as zebrafish which expresses the ERRs segmentally (Bardet, 2005b). However, the single amphioxus homolog, AmphiERR, is expressed in a segmented manner in a region considered homologous to the vertebrate hindbrain. In contrast to islet (a LIM-homeobox gene that also labels motorneurons), AmphiERR expression persists longer in the hindbrain homolog and does not later extend to additional posterior cells. Both AmphiERR and ERRα are expressed in the developing somatic musculature of amphioxus and zebrafish, respectively. These results suggest that the amphioxus hindbrain is in fact segmented and this and musculature segmentation can be demarcated by ERR expression. This suggests that anterior segmentation in protochordates was dictated by axial mesoderm prior to the evolution of a segmentation program that was transferred to and controlled by the neural tube.

The hypothesis that ERRα regulates genes encoding the enzymes involved in adrenal steroid production was examined (Seely, 2005). QPCR was used to determine the levels of ERRα mRNA in various human tissues where adrenal levels of ERRα were similar to the highly-expressing heart and confirmed by immunohistochemistry and Western blot. Reporter constructs with the 5'-flanking regions of steroidogenic acute regulatory protein (StAR), cholesterol side-chain cleavage (CYP11A), 3beta-hydroxysteroid dehydrogenase type II (HSD3B2), 17alpha-hydroxylase/17,20-lyase (CYP17), and dehydroepiandrosterone sulfotransferase (SULT2A1) were used to examine the effects of ERRα on steroidogenic capacity. These reporter constructs demonstrated ERRα enhanced reporter activity from CYP17 and SULT2A1. SULT2A1 promoter activity was most responsive to the ERRα and VP16-ERRα, increasing 2.6- and 79.5-fold, respectively: greater than the stimulation seen in response to steroidogenic

factor 1 (SF1). Deletion and EMSA experiments showed that this activity is dependent on an SFRE; however the physiological responsiveness of these promoters may be regulated by ERRs more than SF1.

Given the interaction of ERRs with estrogen signaling and demonstration of lactoferrin and MCAD as target genes, the role of ERRα in mammary gland biology was examined (Conner, 2005). Expression of ERα, ERβ, PR and ERRα was characterized in multiple stages of bovine mammary gland development using QPCR. Expression was evaluated in prepubertal heifers, primigravid cows, lactating non-pregnant cows, lactating pregnant cows and non-lactating pregnant cows. ERα, ERβ, PR and ERRα were mapped to chromosomes 9, 10, 15 and 29. Expression of ERα, PR and ERRα was high and coordinately regulated. Expression of ERβ is very low by QPCR or immunohistochemistry. The presence of ERRα during all stages of mammary development and lactation suggests involvement of ERRα.

The presence of ERRs in human colorectal tumor and normal mucosa by RT-PCR was investigated (Cavallini, 2005). ERRα was found in 100% of the patients and ERRγ in approximately 30% while ERRβ was not detected. Multiplex PCR showed elevated ERRα mRNA in tumor, whereas lower ERRγ message was detected in both tumor and normal tissue. ERα and ERβ mRNA levels were shown to be decreased in tumor tissues. A positive correlation was observed between ERα and ERβ and between ERα and ERRα, respectively, in normal mucosa but not in tumor tissue. ERRα expression in tumor increased from TNM stages II to IV, whereas both ERs progressively declined. ERRα and the two ERs may play a role in colorectal cancer.

Prior literature suggests that exons I.3 and PII are the two major exons present in aromatase mRNAs isolated from breast tumors and that promoters I.3 and II are the major promoters (Chen, 2005). The two elements near promoters I.3 and II, i.e., S1 and CREaro, were mapped by DNase footprinting and yeast one-hybrid analyses. The function of promoters I.3 and II is suppressed by binding of EAR-2, COUP-TFI, and RARγ to S1, and by the binding of Snail/Slug proteins to their binding site that quenches the CREaro activity. In cancer tissue, the expression levels of EAR-2, COUP-TF1, EARγ, Snail, and Slug decrease, and aromatase expression is up-regulated by binding ERRα to S1 and the binding of CREB1 or related factors to CREaro.

The hypothesis that mitochondrial impairment contributes to the pathogenesis of insulin resistance prompted the study of exercise induced mitofusin (Mfn) proteins which regulate the biogenesis and maintenance of the mitochondrial network, and when inactivated, cause a failure in the mitochondrial architecture and decreases in oxidative capacity and glucose oxidation (Cartoni, 2005). Mfn1, Mfn2 and levels of transcriptional regulators that control mitochondrial biogenesis and functions, including PGC-1α, NRF-1, NRF-2 and ERRα, were measured pre-, post-, 2 and 24 h post-exercise. Mfn1, Mfn2, NRF-2 and COX IV increased at 24 h post-exercise, while PGC-1α and ERRα mRNA increased at 2 h post-exercise. Mfn2 gene expression is driven by a PGC-1α program dependent on ERRα. The PGC-1α/ERRα-mediated induction of Mfn2 suggests a role of these two factors in mitochondrial fusion, expression of oxidative phosphorylation, and mitochondrial architecture.

The regulation of a key step in the reciprocal control of glucose oxidation and fatty acid oxidation is the Pyruvate Dehydrogenase Complex (PDC) which is negatively regulated by phosphorylation by Pyruvate Dehydrogenases 1 through 4 (PDKs 1-4). Negative regulation of PDC by PDKs results in decreased glucose oxidation and increased fatty acid oxidation. This occurs following exercise when glucose is converted into glycogen to replace stores and fatty acids are used instead of glucose. PGC1α is a key regulator of PDK4 in skeletal muscle and the PGC1α upregulation of the PDK promoter is ERRα dependent (Wende, 2005). While FOXO1, PPARα, and GR have been shown to regulate PDK4, ERRα is the key transcription factor for PGC1α regulation. PPARα has not been show to directly act on the PDK4 promoter and ERRα is the likely effector of PGC-1α upregulation of PDK4.

Given the ovariectomy-induced loss of estrogen and subsequent obesity observed in mice with a concomitant decrease in oxygen consumption, the expression of genes related to energy expenditure and lipid metabolism in mouse adipose tissue and skeletal muscle was examined (Kamei, 2005). In adipose tissue and skeletal muscle, at 2-4 wk after ovariectomy, ERRα, PPARα and PPARδ, and PGC-1α and PGC-1β as well as Mcad, PPARγ, Srebp1, Fas and Aco1, Acc, Dgat1 and 2 were lower than in control mice. The reduction in these enzymes is correlative with the observed phenotype.

ERRα is a phosphoprotein whose expression in human breast tumors correlates with the RTK ErbB2, suggesting that its transcriptional activity could be regulated by signaling cascades (Barry and

Giguere, 2005). ERRα is phosphorylated in MCF-7 breast cancer cells in response EGF which also enhances its DNA binding. PGC1α binding is dependent on dimerization and dimerization is dependent on phosphorylation. In vitro, the DBD of ERRα is selectively phosphorylated by PKCδ, and constitutively active PKCδ enhances TFF1 promoter activity via the ERRE, but not he action of ERRα on its own promoter. ChIP analysis shows that ERRα and RNA Pol II are preferentially recruited to the TFF1, but not ERRα, promoter after EGF treatment. Phosphorylation reveals a mechanism for growth factor signaling to selectively activate subsets of ERRα target genes in breast cancer cells.

The role of ERRα in endometrial cancer was examined in human tissue samples (Gao, 2005). Forty-six cancer samples were compared to twenty-four normal samples by RT-PCR and immunohistochemistry for ERα and ERRα, β and γ. All samples were classified ERα-positive or negative. All ERRs had positive correlations between mRNA and protein expression. ERRα expression was reduced in ERα-positive carcinoma, whereas ERRγ has higher expression. The numbers of patients of Federal International Gynecological Oncology (FIGO) stage II-IV and of deep myometrial invasion in ERRα mRNA positive endometrial carcinoma group were more than those in ERRα mRNA negative group ($P = 0.017$ and $P = 0.033$). ERRγ mRNA positive patients had a lower occurrence of lymph metastases than negative patients ($P = 0.021$).

Another example of comparative analyses in cancer and normal tissue with respect to nuclear receptors and their cofactors was undertaken in human colorectal cancer (Giannini, 2005). Four coactivators, p300, pCAF, TIF-2 and TRAP 220, and seven corepressors, N-CoR, REA, MTA1, MTA1L1, HDAC1, HDAC2 and HDAC3, that interact with ERs, measured by quantitative-PCR from forty tissue samples with matched normal mucosa. Tumor tissue showed an increase in NCoR, HDAC1, HDAC2 and MTA1 and decrease in all coactivators with REA, HDAC3 and MTA1L1 unchanged. Expression of ERβ correlated with p300, TIF-2 and REA in normal mucosa, and with REA in tumor tissue only. No association was found between ERα and coregulators and between each coregulator and different clinical parameters. The authors suggest that the co-induction of ERβ and some cofactors may play an important role during the development of human colorectal carcinoma.

During the acute phase response (APR) induced by infection and inflammation, FAO is decreased (associated with hypertriglyceridemia) however, little is known about how APR decreases FAO (Kim, 2005). The APR affects on the expression of MCAD, ERRα and PGC1α were studied. PGC-1α, ERRα and MCAD are markedly reduced in the liver, heart and kidney of mice during LPS-induced APR. Similar decreases in mRNA levels of these genes occur during zymosan and turpentine induced inflammation, indicating that suppression of PGC-1α, ERRα, and MCAD pathway is a general response during infection and inflammation.

A key node in the regulation of substrate utilization is pyruvate dehydrogenase. Because pyruvate dehydrogenase kinase 4 (PDK4) is altered during fasting or by the administration of a PPARα ligand, a study was undertaken to see if ERRα plays a role (Araki, 2006). ERRα binds (with PGC-1α) and activates the PDK4 promoter independent of PPARα. These findings were supported by mutation analysis of the PDK4 promoter that showed that elimination of an ERRα site abrogated both ERRα binding and PGC-1α binding. Additionally, overexpression enhanced and siRNA knockdown of ERRα enhanced and reduced the activity of PGC-1α. The authors point out that the tissue specific expression levels of the two factors serve to direct the expression of PDK4, although the actions of PGC-1α are not entirely dependent on ERRα.

Central to energy production is the mitochondrion—regulation of which requires hundreds of nuclear genes to be transcribed appropriately. One marker of mitochondrial activity is Mitofusin 2 (Mfn2) (Soriano, 2006). Mfn2 gene expression is induced in skeletal muscle and brown adipose tissue by physiologic stimuli such as cold exposure or β_3-adrenergic agonist. This upregulation appears to be by PGC-1α acting via the direct binding of ERRα at -413/-398 in the mitofusin promoter. ERRα alone is a positive regulator of the mitofusin promoter which is enhanced by PGC-1α. The stimulatory effect of PGC-1alpha on mitochondrial membrane potential is dependent on Mfn2. Heterozygous Mfn2 knock-out appear to be sensitized to cold exposure with increased Mfn2 and PGC-1α. The authors of this study suggest that ERRα, PGC-1α and Mfn2 may play a role in mitochondrial physiology and diabetes.

A study of human genetics demonstrating a linkage of ERRα to a human disease was undertaken (Larsen, 2006). ERRα is located on chromosome 11q13, a region with genetic linkage to BMI and fat

percentage. This study analyzed exons, exon-intron boundaries and 1000 base pairs of the ERRα promoter region from 48 overweight or obese humans. Seven variants were detected. Four variants had minor allele frequencies (MAF) below 1%: Pro369Pro, Gly406Asp, 3'UTR+418G>A, and 3'UTR+505C>A. Two variants were single-nucleotide polymorphisms, Pro116Pro and IVS6+65C>T (MAF 15%), in complete linkage disequilibrium (LD) (r (2)=1). This study confirmed the reported 23 bp microsatellite repeat (ESRRA23) (Kamei, 2005). However, the Pro116Pro and ESRRA23 variants were not associated with obesity, type 2 diabetes or related phenotypes in 6365 Danish whites. Nor did the variants interact with PGC-1α or β. This study is in disagreement with the Kamei, work and leaves the interaction of ERRs with diabetes and obesity uncertain.

Because estrogen has been reported to 1) have neuroprotective effects and 2) interacts with the ERRs, a study was undertaken to examine the interplay of these two transcription factors on neural markers, such as MAO-B, previously reported to be an ERRα target gene (Zhang, 2006, Willy, 2004). Both ERRα and ERRγ were demonstrated to upregulate MAO-B while liganded ERα and ERβ downregulate its transcription. This transcriptional regulation by ERRα correlated with protein and activities in ER-deficient HeLa cells, but was blunted in ER-containing MCF-7 and T47D cells. There are several AGGTCA motifs of the MAO-B promoter that can be ChIPed with ER or ERR which compete for binding. These competitive interactions are thought to alter the cofactor status of the promoter and therefore the expression characteristics.

ERRα Prospectus

The role of ERRα in modifying classical estrogen signaling in the processes of breast cancer development and progression, disturbances of bone mineralization, and endometrial biology are assured to gain understanding and clinical application. The role of ERRs in defining the tissue- and disease-specific transcriptional responsiveness to SERMs will prove to both: 1) improve the prognostic assessment of responsiveness to chemotherapeutic agents; and 2) appreciate the transcription modulating qualities of SERMs that produce positive clinical outcomes while reducing unwanted side-effects. In addition to modifying the established endocrine functions of estrogen, ERRs are proving to be potent and pervasive modifiers of the more recently appreciated actions of the PPARs and the related PGCs. It may be the case

that ERRs can modify metabolic function within individual rogue cells, as in cancer, as well as in whole organs, such as adipose or skeletal muscle in metabolic disease states, such as non-insulin dependent diabetes mellitus.

Estrogen-related Receptor β

ERRβ Gene Structure, Expression and Regulation

As mentioned above, Vincent Giguere in the Evans lab identified two cDNAs that bore similarity to the estrogen receptor by low-stringency hybridization (Giguere, 1988). One of the clones detected in a screen from mouse heart cDNAs was estrogen-related receptor beta (ERRβ, ERR2, NR3B2).

Early characterization of the ERRs reported that ERRα, and hERRβ can be activated by different ligand-independent pathways (Lydon, 1992). hERRα and hERRβ exhibited constitutive activity in the absence of exogenously added ligands. Furthermore, this constitutive activity is localized in the carboxy terminal domain of both receptors and can be transferred to other members of this superfamily using domain switch strategies.

A survey of the supraoptic nucleus (SON) to identify the role of nuclear receptors in the hypothalamic pituitary system identified the presence of ERRβ by an RT-PCR strategy directed at LBD conservation among AGGTCA binding receptors (Lopes DE Silva, 1995). Dot-blot detection of ERRβ showed expression in the testis, ovary, PVN, SON and pituitary, with very low expression in the liver.

The expression of NRs in mouse development was studied first in embryonal carcinoma stem cells by RT-PCR (which could be down-regulated by RA), then by expression in implanting embryos (Pettersson, 1996). This study detected the presence of ERRβ in trophoblast at E6.5 and E7.5, but by E8.5 the transcript could no longer be detected by in situ hybridization. The expression was detected in an ectodermally derived region of the amniotic fold that is formed by the juxtaposition of mesodermally derived cells at around E5.5-6.5. There was little expression detected in the mesodermally derived cells lining the ectodermal cells of the chorion. Highest expression was at the boundary between the chorion and the extraembryonic ectoderm. This expression is very transient and is gone by day E8.5. Molecular analysis of the binding characteristics of mERRβ was performed as well. By EMSA, Vaccinia virus expressed ERRβ binding was demonstrated on an ERE independent of RXR. Further studies were performed to

determine if ERRβ binds as a monomer or dimer. Gel shift and immunoprecipitation of in vitro expressed proteins resulted in the conclusion that ERRβ binds DNA as a homodimer and that this dimer is formed in solution, without an ERE. Interestingly, an experiment was performed to determine of ERRβ interacts with Hsp90. Proteins expressed in reticulocyte lysate were found to interact in a manner similar to ER or AhR, suggesting the possible regulation of ERRβ by Hsp90 or a Hsp90 related protein and those pathways regulated by Hsp90. Another study relates to these findings (Hunter, 1999). The developmental findings here are borne out in the study by Lu and coworkers in the generation of a knockout mouse that is embryonic lethal due to placental defects (Luo, 1997)

Having demonstrated that there is an embryonic lethality in ERRβ mice, a chromosomal mapping for human and mouse was performed (Sladek, 1997). F1 C57BL/6J x *mus spretus* females are crossed with male C57BL/6J. The mouse Estrra locus maps to chromosome 19 and the Estrrb locus to mouse chromosome 12. Using fluorescence in situ hybridization (FISH), the human ESRRA mapped gene to chromosome 11q12-q13 and the human ESRRB gene to chromosome 14q24.3. In addition, a processed human ERRα pseudogene mapped to chromosome 13q12.1: the first reported of a nuclear receptor superfamily pseudogene

ERRβ Gene Products

Using inverse PCR and ESTs investigators at Merck identified the human forms of ERRB and ERRG (Chen, 1999). The deduced protein sequences of hERRβ2 and hERRγ2 contain 500 and 458 amino acid (aa) residues respectively. Sequence analysis revealed that hERRβ2 and hERRγ2 respectively share 95% and 77% overall aa sequence identity with hERRβ. An extra C-terminal domain in hERRβ2 and extra N-terminal domain in hERRγ2 are not in hERRβ or mouse ERRβ (mERRβ). This study also showed that the hERRβ originally reported as a human gene is a rat gene (Giguere, 1988). Tissue distribution studies show that hERRγ2 is more highly and broadly expressed than hERRβ2. The hERRβ2 locus was mapped to cytogenetic locus 14q24.3 approximately -14q31, and linked (LOD = 7.1) to disease loci for Alzheimer's and insulin dependent diabetes mellitus.

The role of splicing and tissue specific isoform expression of nuclear receptors was furthered by the identification of two splicing isoforms of human ERRβ: hERRβ2-Δ10 and short-form hERRβ, during

the cloning of previously reported hERRβ-hERRβ2 (Zhou, 2006). The short-form hERRβ lacks an F domain and is the homolog of mouse and rat ERRβ proteins in humans and is widely expressed in 24 of 27 tissues and cell lines tested. However, hERRβ2-Δ10 and the previously reported hERRβ2 isoforms are primate specific and only expressed in the testis and kidney. The F domain of hERRβ2 alters the function of the nuclear localization signal resulting in immunostaining in the nucleus and cytoplasm of transfected COS-1 cells—compared to the exclusively nuclear staining of the other two isoforms.

Subtle aspects of nuclear receptor binding were identified by a study of SF-1 binding to DNA by MRI (Little, 2006). A region of SF-1 termed the FTZ-F1 box, which bears some similarity to other monomerically binding receptors, serves as a secondary recognition element by crossing over the minor groove and engaging sequences immediately 5' to the HRE. The observation that variation in the DNA elements can confer protein bind partner specificity by transmitting conformational information to distal portions of the receptor must take into account these additional DNA interaction surfaces.

ERRβ Interactions with Co-regulatory Proteins

A β-Geo gene trap screen identified a novel gene in that encodes a protein related to the DnaJ co-chaperone in E. coli named Mrj (mammalian relative of DnaJ) (Hunter, 1999)). It is widely expressed throughout development in the embryo and placenta. Expression was particularly high in trophoblast giant cells of the placenta, and moderate expression was seen in trophoblast cells of the chorion at embryonic day 8.5, and later in the labyrinth which arises from the attachment of the chorion to the allantois (a process called chorioallantoic fusion). Homozygous Mrj mutants died at mid-gestation due to a failure of chorioallantoic fusion at embryonic day 8.5. At E8.5, the chorion in mutants was morphologically normal and expressed the cell adhesion molecule β4 integrin that is known to be required for chorioallantoic fusion, but had reduced ERRβ and Gcm1 expression. Given the relationship of DnaJ protein to HSPs in mammals it is compelling to consider a regulatory interaction between the 40 or so DnaJ homologs in mammals and nuclear receptors.

The Evans Laboratory in collaboration with Heng Hong and the Stallcup Laboratory, extended the characterization of ERRα and ERRβ in demonstrating that the p160 coactivators GRIP1, SRC1, and ACTR/AIB can functionally interact with EREs and TREpal, but not GREs (Xie, 1999). Chimeric

ERRαLBD/GRDBD receptors demonstrate that the ERRα AF-1 does not contribute significantly to the constitutive activity of the ERRs. Reciprocal chimeric proteins demonstrated that the ERR AF-2 is constitutively active. All p160s physically interact with ERRs, by GST pull-down assay, with GRIP1 inducing the greatest transcriptional activity. VP16 chimeric ERRs have further increased constitutive transcriptional activation.

Possible crosstalk/combinatorial control between RTR and ERRα and ERRβ in placental development is suggested (Mehta, 2002). RTR is essential for neural tube closure and cardiovascular development, with RTR nulls lost at E10.5. ERRs can compete with RTR for binding to the RTRE: AGGTCAAGGTCA. Functional assays were performed in murine placenta and several human placental choriocarcinoma cell lines. Immunohistochemistry localized RTR to nuclei of giant trophoblasts and spongiotrophoblasts. RTR mRNA was detected in rat choriocarcinoma Rcho-1 cells and human placental choriocarcinoma cell lines BeWo, JAR, and JEG-3. In trophoblasts, RTR co-expressed with ERRαand ERRβ. Giant trophoblast differentiation in Rcho-1 cells, decreased in the expression of RTR mRNA and down-regulation of ERRβ but not ERRα. RTR inhibits VP16-ERRα transactivation through the RTRE by potential competition.

The actions of DAX-1 (NR0B1) to inhibit the constitutive activity of SF-1 (NR5A1) which shares a binding motif with the ERRs, were investigated (Suzuki, 2003). Yeast-two-hybrid and transient-transfection experiments showed that the three N-terminal LXXLL-related motifs in Dax-1 interact with SF-1 to allow inhibition by the C-terminal LBD-like region. DAX-1 target specificity was indicated by the observations that ERRβ, SF-1, ERα, LRH-1, and fly FTZ-F1 had LBD interactions with all the LXXLL-related motifs in Dax-1, whereas HNF4 and RORα did not. Like the Huss and Schreiber papers, combinatorial control of coactivators is diversified by varying LXXLL interaction specificities (Huss, 2001, Schreiber, 2003).

ERRβ Target Genes and Functional Significance

As discussed above, the interaction of ERRα and ERRβ on GR was studied in cell culture (CV-1, monkey kidney, COS-1, monkey kidney, SK-N-MC, human neuroblastoma, HeLa, human cervix carcinoma) grown in DMEM plus 10% charcoal-stripped steroid-free fetal calf serum (FCS) (Trapp and

Holsboer, 1996). In CV-1 cells, five-times more DEX had to be added to see the effects of GR on an MTV-Luc construct when ERRβ was co-expressed. These effects were not seen in HeLa cells. This result was not seen on the PR reporter; nor was GR expression affected by ERRβ expression. GR continues to bind the GRE in the presence of ERRβ, and ERRβ does not bind the GRE, nor do ERRβ and GR form a complex that alters DNA binding, as seen with c-jun, calreticulin, and the p65 subunit of NF-κB. They conclude that this inhibition is the trans sequestration of a factor that is in limiting concentrations in some cell types.

Collaboration with the Giguere and Rossant labs, resulted in a report on the phenotype of ERRβ-null animals (Luo, 1997). ERRβ-null embryos die at day 10.5 due to a defect in placentation. Histologic analysis revealed the presence of ERRβ transcript at E5.5 in extraembryonic ectoderm. At E6.5 the transcript is more highly expressed in the ectodermally derived regions of the amniotic fold, which gives rise to the chorion, and which appears normal in ERRβ null embryos. At day 7.5 the transcript is detected in the chorion, but expression decreases as the chorion fuses with the ectoplacental cone where by day 8.5, it is only detected in the free margin of the chorion. ERRβ null embryos had hypomorphic or absent chorion at day 7.5; and by day 8.5 had excessive trophoblast giant cells with a loss of diploid trophoblast. Chorioallantoic fusion did not occur in null embryos and by day 9.5, although ERRβ expression is not detected after E8.5 in wild-type embryos, embryos had excessive trophoblast giant cells with a loss of labyrinthine trophoblast and spongiotrophoblast. This defect was rescued by tetraploid aggregation experiments where the extraembryonic tissues were composed of wild-type cells, demonstrating that the lethal developmental defect is limited to placentation.

As previously mentioned, the cross talk of ERα, ERβ, ERRα and ERRβ was investigated (Vanacker, 1999). On ERE reporter constructs, all four receptors could bind and activate; the ERs being ligand dependent. On the SFRE, ERβ did not bind, but the others did. The osteopontin promoter was shown to retain these binding and activation characteristics. This study demonstrated the novel action of ERα on the SFRE, and the strong potential for cross talk between the ERs and ERRs on both EREs and SFREs. ERRγ was not investigated.

Given the pharmacologic actions of diethylstilbestrol (DES) as an ERRβ antagonist, the placental phenotypic similarities of ERRβ-null and DES-treated mice were investigated (Trembley, (2001). Loss of

ERRβ results in abnormal trophoblast proliferation and precocious differentiation toward the giant cell lineage (Luo, 1997). DES promotes coactivator release from ERRβ and inhibits its transcriptional activity. DES also leads to polyploid giant cell lineage from trophoblast stem cells and precocious placental development with overabundant trophoblast giant cells and loss of diploid trophoblast. Prenatal exposure to DES has been shown to affect male and female reproductive tract and increase the incidence of vaginal clear-cell adenocarcinoma. ERα and ERβ null mice do not have placental abnormalities, suggesting that the DES effects are mediated by the ERRs. This study reports, but does not show, that DES does not cause an increase in NCoR or SMRT interaction.

As discussed above, the action of SERMs, such as 4-hydroxytamoxifen was investigated on the activities of ERRβ and ERRγ in a study very similar to Coward and coworkers (Coward, 2001; Trembley, 2001). These FRET studies used an LLXXLL motif from GRIP-1 instead of SRC-1. Half inhibition was 500nM for ERRβ and 90 nM for ERRγ, with no effect on ERRα. 4-OHT also disrupted the interaction of ERRγ, but not ERRα, with SRC-1 in a mammalian two-hybrid. 4-hydroxytamoxifen (OHT) is a first generation SERM that functions as an antagonist in breast cancer cells but displays estrogen-like activities in the uterus and bone. 4-OHT disrupts the interaction of ERRs β and γ with coactivators and that their constitutive activity is dependent on this coactivator interaction. 4-OHT has no effect on ERRα. 4-OHT has been shown to be an estrogen agonist to maintain bone density, reduce circulating cholesterol, and increase uterine growth and to be an estrogen antagonist in breast.

ERRβ binds to a 5'-AGGTCA-3' ERE) half-site in the major groove and an upstream 5'-TNA-3' site in the minor groove (Gearhart, 2005). This minor groove interaction is mediated by a C-terminal extension (CTE) of the DBD unique to the ERRs. Synthetic pyrrole-imidazole polyamides, which bind specific sequences in the minor groove, demonstrate that hERRβ binding by is sensitive to polyamides in both the upstream minor groove CTE site and the minor groove of the ERE half-site. Polyamides block hERRβ by two mechanisms: 1) by direct steric blockage of CTE to minor groove DNA; and 2) by changing the helical geometry of DNA with subsequent major groove interaction weakening. These polyamines also block the binding of dimeric ERα to EREs suggesting a general mechanism of ER and ERR modulation.

Given the vagaries of cloning, eight genes critical for early placental development (Acrogranin, Cdx2, Eomes, ErbB3, ERRβ, Hand1, MRJ, and Rex1) were studied in single, in vivo, in vitro, and cloned bovine blastocysts (produced by hand-made cloning (HMC) and serial hand-made cloning (SHMC)) by RT-PCR (Hall, 2005). Aberrant expression of Acrogranin, Cdx2, and ERRβ was detected in a number of blastocysts produced by SHMC. Eomes and Hand1 were not detectable in suggesting differential expression between bovine and murine embryos. Control marker genes (Oct4, IFN-tau, and PolyA) were expressed in all single blastocysts analyzed. Failure of implantation may be due to aberrant expression of genes in the preimplantation cloned embryo, some of which are crucial for the early regulation and differentiation of the placenta.

ERRβ Prospectus

The neonatal lethality of ERRβ null mice limits the utility of the mouse model. Despite the potential to rescue the null fetuses to term with a tetraploid aggregation experiment, no large scale study of ERRβ-null animals has been reported. Personal communication with Vincent Giguere reveals that the ERRβ null animals have a severe motor disturbance. As mentioned above in regards to ERRα, the role of ERRs in modulating and mediating the effects of SERMs will gain increasing understating and application.

Estrogen-related Receptor γ

ERRγ Gene Structure, Expression and Regulation

Discovery of a third member of the estrogen related receptors: estrogen related receptor γ was reported ten years after the initial report of the ERRs (Eudy, 1998; Giguere, 1988). Despite the hope that this gene would shed some light of the etiology of Usher's Syndrome, due to the gross proximity of this novel gene to a known Usher's region, no statistically significant linkage was demonstrated.

Shortly after the initial report of ERRγ, the identification and properties of ERRγ in mouse was reported (Hong, 1999). A yeast-two-hybrid approach using GRIP1 as bait identified ERRγ as an interacting protein. This report that ERRγ bound and activated EREs, but not GREs or TREs in mammalian cells cultured in charcoal stripped media, in the absence of any added ligand. Deletion or alanine-substitutions in the AF-2 eliminated transcriptional activity and interaction with GRIP1 by GST pull-down or Y2H, whereas loss of AF-1 had little effect. The ERRγ AF-2 domain bound GRIP1 in a ligand-independent

manner both in vitro and in vivo, through the LXXLL motifs of GRIP1, and GRIP1 functioned as a transcriptional coactivator for ERRγ in both yeast and mammalian cells. ERRγ also interacted with SRC1 and ACTR in vitro. Post-translational modifications may not be required as ERRγ synthesized in bacteria, yeast or reticulocyte lysate all bind GRIP-1. Furthermore, synthesis in the presence of radioactive ATP did not detect any phosphorylation. Expression studies of ERRγ in adult mouse showed highest expression was observed in heart, kidney, and brain. Whole embryo expression studies showed no expression ad E7, and peak expression at E11-15.

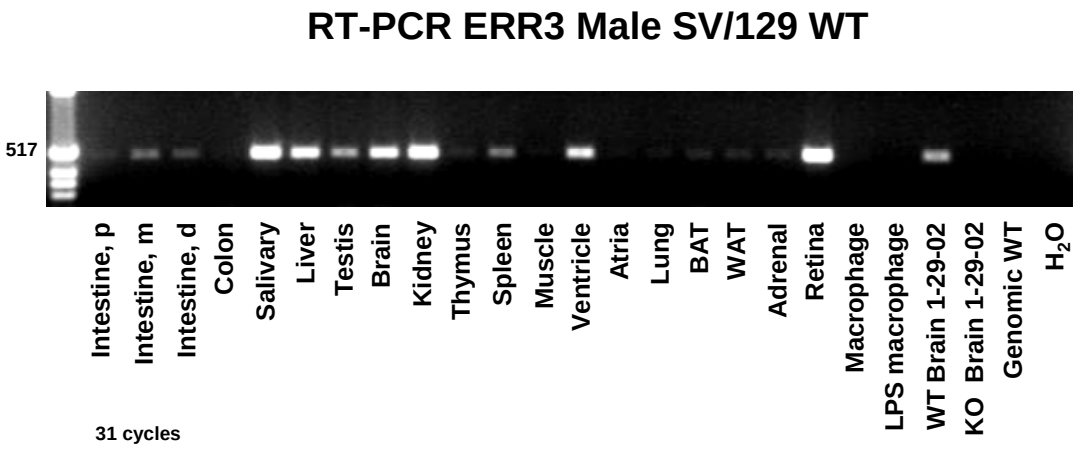

Figure 1.5: Reverse Transcriptase-PCR Analysis of ERRγ Expression in Mouse

A preliminary neural expression pattern study of ERRγ by in situ hybridization in developing mouse was performed (Hermans-Borgemeyer, 2000). Earliest expression was detected at E10.5. Cranial nerve motor and sensory nuclei were identified, as were catecholaminergic regions of the brainstem.

a highly conserved role of ERRγ in mammals was suggested by the identification of two transcripts in mouse that correspond to the transcripts found in human (Susens et al., 2000). Northern blot analysis revealed that ERRγ is expressed as early as E11. Whole mount in situ hybridization analysis shows major expression of ERRγ in the central nervous system at E12.5, but little expression was observed in other organs (heart, liver, and kidney) at this age. In the adult mouse a 5.7 kb transcript is detected in heart, brain, kidney, and skeletal muscle. One alternate splice form lacks the AF-1. These results confirm the work of

others, but prove to be much less sensitive than the genetic methods employed by the Evans Laboratory (Heard, 2000; Ibid).

The expression pattern of ERRγ in mouse brain by in situ hybridization was thoroughly reported (Lorke, (2000). No signal was observed in fiber tracts, suggesting expression in limited to neurons. Expression was detected in the mitral and granule cell layers of the olfactory bulb, and all four olfactory nuclei, with more intense labeling in the accessory bulb. The stria terminalis showed weaker hybridization signals. In the cerebral cortex, the ERRγ was differentially expressed: the frontal cortex was weakly and uniformly labeled over six layers , whereas the parietal cortex showed strong hybridization signals in layers V and VI, with labeling intensity decreasing towards layer II. The temporal and occipital cortex, labeling was most prominent in layer V; here, staining intensity increased rostro-caudally. In the piriform cortex, transcripts were confined to the lamina. In the hippocampus only a few cells in the CA3, increasing rostro-caudally, expressed ERRγ. Signal was not detected in striatum or amygdala, but was detected in the pallidum. The reticular nucleus of the thalamus, zona incerta and field of Forel had the highest forebrain expression. Other regions had moderate expression: lateral geniculate; parafasicular, dorsal nucleus and posterior complex of the thalamus; and a few cells in the habenula. The mid-hind brain had the highest expression: inferior colliculus, interpeduncular, pontine, dorsal raphe, parabrachial, red, and lateral mammillary nuclei. All three dopaminergic areas, retrorubral, substantia nigra and ventral tegmental area showed expression (not observed by in situ hybridization for tyrosine hydroxylase, T. Perlmann, personal communication). The reticular formation: pedunculopontine tegemental, pontine reticular, reticular gigantocellular, median parabrachial, nucleus Darkschewitch, locus coeruleus, and A5 noradrenergic nuclei. All acoustic nuclei: paraleminiscal, trapezoid, periolivary, and inferior colliculus. In the cerebellum many basket and a few stellate cells of the molecular layer, Golgi cells of the granular layer and the deep cerebellar nuclei. Among the cranial nerve nuclei: occulomotor, trochlear, principal, mesencephalic and motor nuclei of the trigeminal, facial, all vestibular and cochlear and in the trigeminal ganglion. , ERRγ distribution was clearly distinguished from that described for ERRα, for ERRβ, and for estrogen receptors (ER) pointing at functional differences between ERRγ and these receptors.

A potential role for ERRγ was suggested in systemic lupus erythematosus (SLE), a chronic autoimmune disease characterized by the production of autoantibodies to a wide range of self-antigens (Graham, 2001). Significant linkage for the genomic region of ERRγ was reported but lacked the resolution to implicate ERRγ in the etiology of this condition.

ERRγ Gene Products

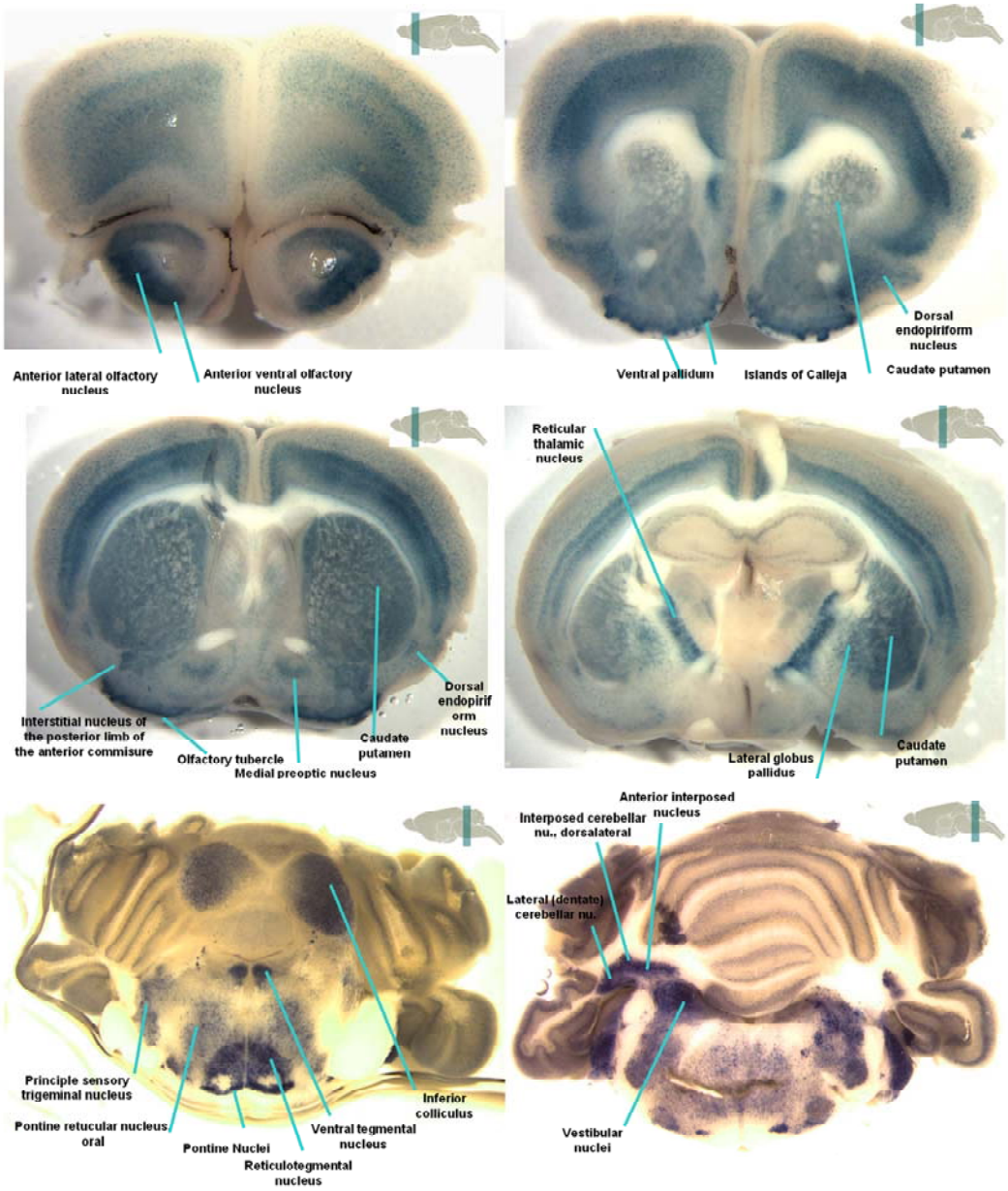

Figure 1.6: Detection of ERRγ in the CNS by X-gal Staining

Using inverse PCR and ESTs, the human forms of ERRB and ERRG were identified (Chen, 1999). The deduced protein sequences of hERRβ2 and hERRγ2 contain 500 and 458 amino acids, respectively. Sequence analysis revealed that hERRβ2 and hERRγ2 respectively share 95% and 77% overall amino acid sequence identity with hERRβ. An extra C-terminal domain in hERRβ2 and extra N-terminal domain in hERRγ2 are not in hERRβ or mouse ERRβ (mERRβ).

Various human ERRγ isoforms that appear in a tissue specific manner were identified by screening cDNA libraries from human placenta, pancreas, kidney, and skeletal muscle (Heard, 2000).

Message from these cDNA clones have a common start site, but variable splicing that predict the existence of six transcripts producing two proteins, one of which is varied in the N-terminus. Multiple cDNAs from kidney are named ERRγ1.1 to 1.4, and are similar to ERRγ2 (identical as previously identified Chen, 1999 and Eudy, 1998). ERRγ3, a skeletal muscle form has a non-AUG start site (AGA**GUG**G) thirty-four codons upstream of the ERRγ1 and 2. ERRγ1 is predicted to be 435aa (48.7kD), ERRγ2 458aa (51.3kD), ERRγ3 is predicted to be 469aa (52.6kD), unless the alternative start site is not used, when it would be the same as ERRγ1. Only two major protein forms are generated in reticulocyte lysates. Monomeric DNA binding is demonstrated by EMSA. Gal4-fusion studies indicate that ERRγ has the greatest constitutive transcriptional activity in HEK293 cells (ERRγ 65-fold, ERRα 10-fold, ERRβ no increase, relative to Gal 4 alone).

Investigators at the pharmaceutical firm, Tularik, published a report using a peptide sensor assay that identified the stilbenes diethylstilbestrol (DES), tamoxifen (TAM), and 4-hydroxytamoxifen (4-OHT) as high-affinity ligands for ERRγ (Coward, 2001). Indirect binding studies indicate 4-OHT had a K_d value of 35 nM, and both DES and TAM displaced radiolabeled 4-OHT with K_i values of 870 nM. In cell culture, 4-OHT binding caused dissociation of ERRγ and SRC-1, and reduction in ERRγ activity. Altering a single amino acid in the LBD of ERRα to a corresponding ERRγ residue conferred binding of 4-OHT to ERRα. ERRs can have high affinity ligands. This residue, located at the bottom of helix 3, is an alanine in ERα, ERRβ, and ERRγ, each of which bind 4-OHT, but is a phenylalanine in ERRα, which does not bind 4-OHT. In the clinic, TAM is indicated for the treatment of breast cancer, and patients taking the recommended dose of 20 mg per day achieve steady-state plasma levels that average 320 nM, within 3-fold

of the 870 nM Ki for ERRγ. Higher doses of tamoxifen, as used in salvage therapy, may reach serum levels capable of antagonizing ERRγ and producing side effects similar to those observed in ERRγ-null animals (Chang, 1998; Decaudin, 2004; Ibid).

The crystal structure of ERRγ LBD in association with an SRC-1 peptide was reported—the conformation of which resembles the holo-ERα active conformation (Greshik, 2002). The LBD ligand binding pocket contains residue side chains that sterically prohibit the binding of estradiol. ERR antagonists, diethylstilbestrol and 4-hydroxytamoxifen, enlarge the LBD pocket to an antagonist conformation that prevents coactivator binding. This filling of the LBD pocket by bulkier side chains allows interaction with SRC-1 in vitro and transcriptional activation, but prevents the binding of DES or 4-OHT. The apo form of ERRγ resembles the holo form of ER, therefore both are transcriptionally active in their respective forms. The cavity volume (220 $Å^3$) is the smallest observed so far, the next smallest pockets being those of the rat androgen receptor (340 $Å^3$) and hER (400 $Å^3$). ERRγ was observed to form a homodimer.

In subsequent crystal structure studies, the crystal structures of the ERRγ ligand-binding domain (LBD) complexed with diethylstilbestrol or 4-hydroxytamoxifen was reported (Greschik, 2004). Antagonist binding to ERRγ results in a rotation of the side chain of F435 that partially fills the cavity of the apo-LBD. The new rotamer of F435 displaces the 'activation helix' (helix 12) from the apo agonist conformation. Helix 12 is in the coactivator groove of ERα with 4-OHT or RAL, but is dissociated in the ERRγ. LBP differences result in a slight rotation of 4-OHT in the ERRγ compared to ERα. Cholic acid was found to fortuitously bind the surface of the ERRγ LBD near the opening of the LBP.

Splice variants are likely to play an important role in regulating the temporal and spatial regulation of nuclear receptors and are likely to be detected in finer detail in the future. An ERRγ splice variant cDNA termed ERRγ3 was found in human full-length cDNA libraries (Kojo, 2006). The ERRγ3 cDNA consists of 3362 base pairs and has an ORF of 1188bp. The ERRγ3 predicted peptide sequence differs from both ERRγ1 and ERRγ2 in missing 39 amino acid residues corresponding to the second zinc finger motif of the DNA binding domain (DBD). ERRγ3 gene consists of 8 exons including three unique 5'-terminal exons and lacks the exon encoding the second zinc finger motif. ERRγ3 expression is limited to adipocytes and

prostate while ERRγ2 is fairly widespread. ERRγ3 product does not activate ERE-controlled transcription but can modulate the activity of other NRs. ERRγ3 augmented the ligand-dependent transcriptional activities of ERα, ERβ, and TRα by 1.3-, 4-, and 2.1-fold whereas it inhibited fully the activity of GR. However, ERRγ3 had no effect on Vitamin D3 receptor, RARα or PPARα, δ, or γ. This *trans* modulatory activity of ERRγ3 may be critical in adipose and prostate tissue and may be induced in disease states in other tissues.

To better understand the ligand binding domains of ERRγ and ERα, a study of the amino acid residues of their LBDs was undertaken (Kim, 2005). Estrogen-dependent transcriptional activation by ERα depends on the conformation of helices 3 and 12 in the LBD. The role of charged residues in ERα helix 3 (which are conserved in most steroid receptors) was studied by the replacement of Asp-351 with lysine (D351K) or leucine (D351L). This abolished estrogen-dependent transactivation, and reduced AF2 activation and p160 interactions—but did not alter ERα's estrogen-binding, DNA-binding or homodimerization. The D351K mutant resulted in loss of the transcriptional activation activity of wild-type ERα. A critical Asp-351 was needed for 1) the estrogen-dependent conformational change of wild-type ERα; 2) constitutive activity and ligand-independent *holo*-conformation of ERα mutant Y537N. In ERRγ, the replacement of D273L (ERα Asp-351 corresponds to ERRγ Asp-273) had a reciprocal effect and reduced p160 interactions without altering DNA binding. It appears that Asp-351 acts to stabilize the *holo*-conformation of ERα, and Asp-351 of Helix 3 interacts with the amide hydrogen of L540 of Helix 12 to form a coactivator biding site on the LBD for p160 coactivators.

ERRγ Interactions with Co-regulatory Proteins

As discussed above for ERRα, the finding that PGC-1α can interact with ERRα and ERRγ through an alternate interaction region distinct from the LXXLL domain that interacts with ERα, PPARα, and HNF-4 was reported (Huss, 2002). ERRα was found to interact with PGC-1α by Y2H from a human adult cardiac cDNA library and is co-expressed in neonatal heart, along with MCAD and PGC-1α. Adenoviral-mediated ERRα overexpression in primary neonatal cardiac myocytes induced MCAD expression. PGC-1α enhanced both ERRα (22-fold) and ERRγ (6-fold) transcription from vitellogenin-derived ERE promoter and ERRα (8-fold) from the MCAD promoter. The ERRα AF-2 interacts with PGC-1α in an alternative

Leu-rich region at aa 209-213 termed, Leu-3, and utilizes additional LXXLL-containing domains as accessory binding sites. Gal4 fusion experiments indicate that PGC-1α activation involves, in part, displacement of co-repressor proteins. PGC-1α may regulate mitochondrial energy metabolism through interactions with ERRα and ERRγ that utilize alternate interaction domains. This paper provides a detailed discussion of LXXLL motifs and coactivator interactions. An unpublished observation is that ERRα and ERRγ expression follows FAO capacity in skeletal muscle Type II slow-twitch, and is nearly undetectable in fast-twitch Type I muscle. This and the observation that ERRα is highly expressed during the transition from glycolysis to FAO in the neonatal heart suggest that ERRs may play a role in FAO oxidation and fiber type. This study is supported by others (Bardet, 2004).

The expression of the coactivators PGC-1 (PGC-1α) and PERC (PGC-1β) in mammalian cells augments potently the transcriptional activation by ERRγ (Hentschke, 2002). The constitutive activation function 2 (AF-2) of the orphan receptor was important for the synergistic enhancement. Functional receptor truncation analysis revealed an additional amino-terminal activation function, specific for the ERRγ2 isoform and PGC-1. In vitro experiments showed a direct interaction of ERRγ with both coactivators. These findings suggest distinct regulatory functions for PGC-1 and PERC; expanding the combinatorial control by tissue-specific coactivators for ERRγ.

Subsequently, the same author tested whether calmodulin (CaM) interacts with ERRγ (Hentschke, 2003). In vitro pull-down experiments with calmodulin-Sepharose demonstrated a Ca^{2+}-dependent interaction with cellularly expressed ERRγ. The CaM binding site is unusual in being composed of two discontinuous elements. Surface plasmon resonance (SPR) biosensor assays detected direct interaction of immobilized bacterially expressed ERRγ fusion protein with Ca^{2+}-calmodulin. In vitro DNA binding is calmodulin-independent, but transient transfection revealed a Ca^{2+}-influx-dependent ERRγ transcription. An IQ-like domain in the LBD is probably not functional as ERRγ does not bind apo-calmodulin, but it may interact with related proteins such as S-100 and calretinin. Tamoxifen is an antagonist of ERα, ERRγ and calmodulin. βPDGF is proposed to be a potential ERRγ target gene.

In further extension of doctoral dissertation work, this author used the ERRγ AF-1 as bait to biopan for proteins that interact in a phage display of a human brain cDNA library (Hentschke, 2003). Two

proteins: PNRC2 (proline-rich nuclear receptor co-regulatory protein 2) and a Groucho homolog member of the bHLH TCF/Lef family, TLE1 were found to interact. These proteins share similar expression profiles, interact by GST pull-down, and are coactivating in CV-1 cells. TLE1, which is highly expressed in proliferating, and then in post-mitotic neurons, is normally a repressor, but acts as a coactivator with ERRγ. These two proteins expand the breadth of combinatorial control conferred by diverse coactivating proteins. PNRC2 was also found to interact with ERRα (Zhou and Chen, 2001).

The role of additional amino acids found between helices H6 and H7 in SHP and DAX-1, ERRγ-interacting proteins, was investigated (Park, 2004). Mutant SHP Delta28-139, deletion of 12 extra amino acids in H6-H7, failed to repress the transactivity of ERRγ, HNF4α or CAR, although these mutants still interact via Y2H and GST pull-down. DAX-1 and mutant DAX-1 Delta38-362, deletion of 25 extra amino acids in H6-H7, both interact and repress SF-1. Chimeric SHP that contains DAX-1 extra amino acids or a mutant with poly-alanine stretch in H6-H7 behaved like WT SHP. The chimeric SHP/DAX-1 extra amino acids interacted with EID-1, a SHP-interacting nuclear repressor that interacts with Myo D, p300, and Rb and which blocks muscle differentiation. The SHP Delta28-139 and EID-1 interaction was reduced. This study identifies the H6-H7 loop regions of SHP and DAX-1 as players in the subtle interplay of combinatorial controls.

The requirements for ERRγ-mediated gene regulation were addressed (Huppunen, 2004). ERRγ transactivates ERE_2tk-LUC 5-fold and $ERRE_3$tk-LUC 7.7-fold in HeLa (endometrial) and 2.5-fold in SaOs (osteosarcoma) cell cultures, independent of ligand, phenol red or serum (unlike ERRα, Vanacker, 1999). ERRα and ERRβ are weakly active in these cells. Activity is dependent on (at least) the first zinc finger and A-box, and AF-2, but not the N-terminal domain nor two mutations in the LBD that enlarge or reduce the putative pocket volume. The slightly bulkier 4-hydroxytoremifene (4-OHtor) inactivates like 4-OHT. On an AP-1 reporter, 4-OHT and 4-OHtor had activating effects independent of AF-1 or AF-2. ERα activates AP-1 with agonist and ERβ, like ERRγ, activates AP-1 with antagonists. PGC-1 increased the activation from $ERRE_3$tk-LUC in HeLa cells that was dependent on the DBD, but not LBD, AF-1, AF-2 or 4-OHT. PGC-1 does not interact with ERRγ like the p160 coactivators.

ERRγ Target Genes and Functional Significance

As discussed above, the action of SERMs, such as 4-hydroxytamoxifen weas investigated on the activities of ERRβ and ERRγ in a study very similar to Coward and coworkers (Trembley, 2001; Coward, 2001). FRET studies used an LLXXLL motif from GRIP-1 instead of SRC-1. Half inhibition was 500nM for ERRβ and 90 nM for ERRγ, with no effect on ERRα. 4-OHT also disrupted the interaction of ERRγ, but not ERRα, with SRC-1 in a mammalian two-hybrid. 4-hydroxytamoxifen (OHT) is a first generation SERM that functions as an antagonist in breast cancer cells but displays estrogen-like activities in the uterus and bone. 4-OHT disrupts the interaction of ERRs β and γ with coactivators and that their constitutive activity is dependent on this coactivator interaction. 4-OHT has no effect on ERRα. 4-OHT has been shown to be an estrogen agonist to maintain bone density, reduce circulating cholesterol, and increase uterine growth and to be an estrogen antagonist in breast.

In addition to regulation by SF-1, LRH-1 and FXR, SHP (NR0B2) is regulated by ERRγ, but not ERRα or ERRβ (Sanyal, 2002). Coexpression of ERRγ and SHP in pancreas, kidney and heart may indicate an in vivo interaction. Regulation is dependent on only one of five SF-1 sites and this site is divergent from previously reported ERREs: TCAAGGTTG. The HDAC inhibitor trichostatin A increased ERRα and ERRβ activity indicating that ERRα and -β may associate with co-repressor in vivo. DNA sequence of different response elements may cause allosteric modulation of ERR proteins, (as indicated by protease sensitivity), that may alter transcriptional activities as has been reported for GR, ER and TR. SHP inhibits ERRγ and interacts with all ERRs, in an AF-2 dependent manner, by Y2H and GST-pulldown. SHP mutations associated with moderate obesity in humans eliminate the inhibition of ERRγ. These results suggest an autoregulatory loop controlling SHP gene expression and significantly extend the potential functional roles of the three ERRs.

The DNA binding characteristics were explored by EMSAs (Hentschke, (2002). ERRγ binds as a homodimer to direct repeats (DR) without spacing of the NR half-site 5'-AGGTCA-3' (DR-0), to extended half-sites, and to the inverted ERE. Binding was found to be dependent on the presence of sequences in the ligand binding domain (LBD). A far-Western analysis revealed that ERRγ forms dimers even in the absence of DNA. Two elements, located in the hinge region and in the LBD, respectively, are necessary for DNA-independent dimerization. DNA binding of bacterial expressed ERRγ requires additional factors

present in the serum and in cellular extracts. Fusion proteins of the germ cell nuclear factor (GCNF/NR6A1) with ERRγ showed that the characteristic feature to be stimulated by additional factors can be transferred to a heterologous protein. The stimulating activity was further characterized and its target sequence narrowed down to a small element in the hinge region. Importantly, addition of albumin also increased binding activity, as well. Two fractions from P19 cell extracts have been identified that increase ERRγ activity.

As discussed above for ERRα, the expression of known clinicopathological prognostic indicators form a pool of 38 tumors and 9 normal enriched mammary epithelial cells was analyzed (Ariazi, 2002). Using QPCR assays, levels of ERα, ERβ, epidermal growth factor receptor, ErbB2, ErbB3, ErbB4, ERRα, ERRβ, and ERRγ were determined. ERRα showed potential as a biomarker of unfavorable clinical outcome and, possibly, hormonal insensitivity. ERRα mRNA was expressed at levels greater than or similar to ERα mRNA in 24% of unselected breast tumors, and generally at higher levels than ERα in the progesterone receptor (PgR)-negative tumors. Increased ERRα levels associated with ER-negative and PgR-negative tumor status. ERRα levels also correlated with expression of ErbB2, an indicator of aggressive tumor behavior. Thus, ERRα was the most abundant nuclear receptor in a subset of tumors that tended to lack functional ERα and expressed ErbB2 at high levels. Consequently, ERRα may potentiate constitutive transcription of estrogen response element-containing genes independently of ERα and antiestrogens in ErbB2-positive tumors. ERRγ may be a biomarker of favorable clinical course and, possibly, hormonal sensitivity. ERRγ was overexpressed in 75% of the tumors, resulting in the median ERRγ level being elevated in breast tumors compared with normal mammary epithelial cells. ERRγ overexpression associated with hormonally responsive ER- and PR-positive status. Additionally, ERRγ expression correlated with levels of ErbB4, a likely indicator of preferred clinical course, and associated with diploid-typed tumors. Hence, ERRα and ERRγ status may be predictive of sensitivity to hormonal blockade therapy, and ERRα status may also be predictive of ErbB2-based therapy such as Herceptin.

Investigators at the pharmaceutical firm, Novartis, described the application of the molecular dynamics (MD) and molecular mechanics-generalized Born/surface area (MM-GB/SA) to simulate the different structure-function effects of diethylstilbestrol (DES) on ERα (agonist) and ERRγ (antagonist)

(Nam, 2002) at Extrapolating from x-ray crystal structures of ERα in the agonist- and antagonist-bound forms, ERRγ models were constructed in two different conformations. MM-GB/SA binding free-energy calculations of DES in the ERα and ERRγ structures suggest that DES has a greater free energy of binding in the agonist conformation of ERα, while the antagonist conformation is favored in ERRγ. The van der Waals interactions of DES in the small ligand pocket ERRγ are less favorable and confer antagonist properties of DES in ERRγ.

The potential of DNA elements to transmit conformational information to protein-protein interaction domains which contribute to coactivator/corepressor combinatorial control was investigated (Sanyal, 2003. ERRγ is a constitutively, but variably active on reporter elements driven by SFREs and EREs and divergent elements such as the SFRE-like sft4. On the SHP promoter the sft4 has high ERRγ activity. ERRγ binds, but does not activate the TREpal. EMSA and ChIP demonstrated that ERRγ was bound to sft4, SF-1RE, and TREpal with different degrees of affinity, but only caused hyperacetylation of sft4 and SF-1RE templates. ERRγ bound to different elements showed differential trypsin sensitivity. Coregulators of ERRγ include RIP140 and PGC-1. The conformations induced by different elements confer variable coactivator binding affinities. TREpal does not induce an active conformation, therefore neither RIP140 nor PCG-1 are bound, whereas the other elements do allow binding due to an active ERRγ conformation. Coexpression of RIP140 and PGC-1 with ERRγ suggest coregulatory roles of these proteins. This study extends the variability of ERRγ responsiveness to the DNA-binding motif.

The promoter activities of the SHP promoter were investigated with respect to SF-1, ERRγ, and the basic helix-loop-helix (bHLH) transcription factors, and the E2A proteins (E47, E12 and E2/5), which activated the human but not the mouse SHP promoter (Kim, 2003). The tissue-specific E47 heterodimer partner B2 repressed the E47- mediated transactivation of the human SHP (hSHP) promoter. The authors found that E47 and SF-1 synergistically activate the human but not the mouse SHP promoter, while ERRγ additively activates. This suggests that E2A proteins may interact combinatorially with ERRγ and SF-1 on the SHP promoter, and perhaps others.

A regulatory feedback loop between two orphan nuclear receptors, ERRγ and DAX-1, has been suggested as a regulatory mechanism (Park, 2005). ERRγ activates the DAX-1 promoter, and DAX-1 then

negatively regulates transactivation by ERRγ. ERRγ was shown to regulate the DAX-1 promoter by gel shift assay, ChIP, and reporter assay in ERRE-containing regions between -129 to -121 bp and -334 to -326 bp. Overexpression of ERRγ can upregulate DAX-1 in MCF-7 breast cancer cells that co-express ERRγ and DAX-1. Y2H and GST-pull down experiments showed that ERRγ and DAX-1 interact and that DAX-1 inhibits ERRγ transactivation in an AF-2 dependent manner. It appears that DAX-1 may inhibit the activity of ERRγ by competing with PGC-1α for ERRγ AF-2 occupancy.

Further interaction between nuclear receptors was presented in work on the small heterodimer partner (SHP) which lacks the N-terminal ligand-independent activation domain and the DNA binding domain. (Macchiarulo, 2005) SHP inhibits transcriptional activity of a large set of nuclear receptors: ER, AR, CAR, RXR, GR, LXR and ERRγ. This transcriptional inhibition involves 1) competition with coactivator binding on the AF-2; and 2) recruitment of transcriptional inhibitors such as EID-1. Clinically, LOF SHP mutants may be involved in mild obesity, increased birth weight and insulin levels. Studies were done to determine the physical interactions between SHP and EID-1. In doing these experiments a possible ligand binding site was suggested. While these computational experiments are intriguing, they lack any experimental evidence.

In a physiologic study consistent with SHP studies in the past, SHP KO mice were examined for brown adipose (BAT) phenotypes (Wang, 2005). The high energy production of BAT is largely under the control of PGC-1α which exerts its effects through several nuclear receptors found to act in BAT, such as the PPARs and ERRs. Loss of SHP results in increased basal energy expenditure, increased PGC-1α expression and diet-induced obesity resistance. Both cultured and *in vivo* $SHP^{-/-}$ BAT has alterations suggesting β-adrenergic stimulation independence. Additionally, acute inhibition or overexpression *in vitro* of SHP increased and decreased, respectively, basal PGC-1α expression. In particular, ERRγ is expressed in BAT and PGC-1α promoter transactivation by ERRγ is inhibited by SHP. SHP appears to function as a negative regulator of energy production in BAT by competing with PGC-1α for binding with some nuclear receptors.

In addition to constitutively activating genes as a monomer, ERRγ can also form dimers via the LBD that increases its transcriptional activity (Huppunen and Aarnisalo. 2004). This report also shows that

ERRγ can form heterodimers with ERRα—which are mutually reduced in transcriptional activity. 4-OHT further reduces this activity and suggests that tamoxifen may indirectly act upon ERRα through heterodimerization with ERRγ. This study is corroborated by others (Hentchke, 2002)

Rat ERRγ was shown to exhibit binding affinities with a wide spectrum of sequences: inverted and direct repeat motifs composed of AGGTCA half-sites with various spacing, as well as a monovalent motif of the same sequence carrying extra T(C/G)A trinucleotides on the 5' side (Razzaque, 2004). An inverted repeat spaced by three nucleotides was dominantly efficient for the binding of ERα. ERRγ bound as a homodimer to all binding sequences tested, including a monovalent binding site, and ERRγ did not heterodimerize with ERα. ERRγ recognizes a broad range of sequences as a homodimer. SHP efficiently represses the transcriptional activity of ERRγ, even at low concentrations.

In order to develop agonist ligands that are specific for the estrogen-related receptors ERRβ/γ, a hydrazone with a 4-hydroxy group at one phenyl ring and a 4-diethylamino moiety at the other phenyl ring was synthesized (Yu and Forman, 2005). The compound 3 (DY131; N'-{(1E)-[4-(diethylamino)phenyl]methylene}-4-hydroxybenzohydrazide) effectively and selectively activates ERRβ/γ. DY131 had no effect on the structurally related receptors ERRα or ERα/β.

The first small molecule agonists of the estrogen-related receptors have been identified. GSK4716 (3) and GSK9089 (4) show binding to ERRγ with remarkable selectivity over the classical estrogen receptors (Zuercher, 2005). Notably, in cell-based reporter assays, GSK4716 mimics the protein ligand PGC-1α in activation of human ERRβ and ERRγ.

X-ray crystallography studies are key to the rational design of nuclear receptor ligands, such as derivatives of the ERRγ antagonist, tamoxifen (Chao, 2005). These studies suggest that analogs bearing hydroxyalkyl groups have higher selectivity for ERRγ than ERα. X-ray crystallography structure of one of the designed compounds in the ERRγ LBD explains this selectivity by key interactions with ligand binding pocket side chains that differ between ERRγ and ERα.

Due to the importance of hormonal signaling prostate physiology and disease, and the interactions of ERRs with ERs, crosstalk studies were performed in prostate cell lines to study ERRγ (Lui, 2006). ERRγ expression was examined in rat prostate and Nb rat prostate cancer model, as well as growth regulation in

prostatic cells. ERRγ expression, by QPCR, in castrated prostates was androgen-dependent. ERRγ was also expressed in prostatic epithelial cells, and appeared reduced in neoplastic prostates. Overexpression of ERRγ in stable transfectants of NbE-1 and MAT-Lu cells reduced proliferation in vitro, reduced anchorage-independent growth in soft-agar and reduced tumorigenicity in nude mice. This study suggests that ERRγ may be a favorable biomarker for prostatic cancers.

In order to better study and rapidly screen protein interactions with ERRγ, a fluorescence based assay was developed (Gowan, 2006). Because there appear to be no endogenous ligands for ERRγ, this assay serves to identify 'protein ligands' that interact during basal and antagonist-bound conditions (Kamei 2003). Two components were used in this study. Firstly, a GST-ERRγLBD fusion protein with terbium-labeled anti GST antibody was generated. Secondly, flouroscein-labeled peptides were used to screen for interactions with the ERRγ-LBD. When interactions occurred, a shift in the time-resolved fluorescence resonance energy transfer (TR-FRET) would occur. Initially, coregulator peptides bearing the coactivator LXXLL motif, the corepressor LXXI/HIXXXI/L motif were screened. Then other protein-protein interaction motifs from natural coactivator sequences or random phage display peptides were screened. These screens detected class III coregulator peptides such as, PGC-1α, D22, and SRC1-4. Both 4-OHT and DES displaced PGC-1α, although DES was less effective.

ERRγ Prospectus

The literature reflects an emerging role for ERRγ in energetics, through interactions with PGC-1α and β, that intersects with the PPARs. These roles may contribute to favorable biomarkers in cancer. The metabolic differentiation of the tissue undergoing neoplasia may be becoming more poorly differentiated. The retention of ERRγ as a favorable biomarker might represent the retention of more differentiated metabolic function. Loss of ERRγ as cells de-differentiate and become more primitive and malignant, may represent the emergence of a more primitive glycolytic metabolism that recapitulates the embryonic state.

Additional markers of terminal differentiation that are driven by ERRγ await identification.

REFERENCES

Adams M, Meijer OC, Wang J, Bhargava A, Pearce D. Homodimerization of the glucocorticoid receptor is not essential for response element binding: activation of the phenylethanolamine N-methyltransferase gene by dimerization-defective mutants. Mol Endocrinol.

Araki M, Motojima K. Identification of ERRα as a specific partner of PGC-1α for the activation of PDK4 gene expression in muscle. FEBS J. 2006 Apr;273(8):1669-80.

Ariazi EA, Clark GM, Mertz JE. Estrogen-related receptor alpha and estrogen-related receptor gamma associate with unfavorable and favorable biomarkers, respectively, in human breast cancer. Cancer Res. 2002 Nov 15;62(22):6510-8.

Ariazi EA, Jordan VC. Estrogen-related receptors as emerging targets in cancer and metabolic disorders. Curr Top Med Chem. 2006;6(3):203-15.

Bardet PL, Horard B, Laudet V, Vanacker JM. The ERRalpha orphan nuclear receptor controls morphogenetic movements during zebrafish gastrulation. Dev Biol. 2005 May 1;281(1):102-11.

Bardet PL, Obrecht-Pflumio S, Thisse C, Laudet V, Thisse B, Vanacker JM. Cloning and developmental expression of five estrogen-receptor related genes in the zebrafish. Dev Genes Evol. 2004

Bardet PL, Schubert M, Horard B, Holland LZ, Laudet V, Holland ND, Vanacker JM. Expression of estrogen-receptor related receptors in amphioxus and zebrafish: implications for the evolution of posterior brain segmentation at the invertebrate-to-vertebrate transition. Evol Dev. 2005 May-Jun;7(3):223-33.

Bardet PL, Laudet V, Vanacker JM. Studying non-mammalian models? Not a fool's ERRand! Trends Endocrinol Metab. 2006 May-Jun;17(4):166-71. Epub 2006 Mar 31.

Barrero MJ, Camarero N, Marrero PF, Haro D. Control of human carnitine palmitoyltransferase II gene transcription by peroxisome proliferator-activated receptor through a partially conserved peroxisome proliferator-responsive element. Biochem J. 2003 Feb 1;369(Pt 3):721-9

Barry JB, Giguere V. Epidermal growth factor-induced signaling in breast cancer cells results in selective target gene activation by orphan nuclear receptor estrogen-related receptor alpha. Cancer Res. 2005 Jul 15;65(14):6120-9.

Barry JB, Laganiere J, Giguere V. A Single Nucleotide in an Estrogen Related Receptor α Site Can Dictate Mode of Binding and PGC-1α Activation of Target Promoters. Mol Endocrinol. 2005 Sep 8

Bonnelye E, Aubin JE. Estrogen receptor-related receptor alpha: a mediator of estrogen response in bone. J Clin Endocrinol Metab. 2005 May;90(5):3115-21.

Bonnelye E, Kung V, Laplace C, Galson DL, Aubin JE. Estrogen receptor-related receptor alpha impinges on the estrogen axis in bone: potential function in osteoporosis. Endocrinology. 2002 Sep;143(9):3658-70.

Bonnelye E, Merdad L, Kung V, Aubin JE. The orphan nuclear estrogen receptor-related receptor alpha (ERRalpha) is expressed throughout osteoblast differentiation and regulates bone formation in vitro. J Cell Biol. 2001 May 28;153(5):971-84.

Bonnelye E, Vanacker JM, Spruyt N, Alric S, Fournier B, Desbiens X, Laudet V. Expression of the estrogen-related receptor 1 (ERR-1) orphan receptor during mouse development. Mech Dev. 1997 Jul;65(1-2):71-85.

Bonnelye E, Vanacker JM, Spruyt N, Alric S, Fournier B, Desbiens X, Laudet V. The ERR-1 orphan receptor is a transcriptional activator expressed during bone development. Mol Endocrinol. 1997 Jun;11(7):905-16.

Busch BB, Stevens WC Jr, Martin R, Ordentlich P, Zhou S, Sapp DW, Horlick RA, Mohan R. Identification of a selective inverse agonist for the orphan nuclear receptor estrogen-related receptor alpha. J Med Chem. 2004 Nov 4;47(23):5593-6.

Cao L, Bu R, Oakley JI, Kalla SE, Blair HC. Estrogen receptor-beta modulates synthesis of bone matrix proteins in human osteoblast-like MG63 cells. J Cell Biochem. 2003 May 1;89(1):152-64.
Castet A, Herledan A, Bonnet S, Jalaguier S, Vanacker JM, Cavailles V.

RIP140 Differentially regulates estrogen receptor related receptor transactivation depending on target genes. Mol Endocrinol. 2006 Jan 26

Carrier JC, Deblois G, Champigny C, Levy E, Giguere V. Estrogen-related receptor alpha (ERRalpha) is a transcriptional regulator of apolipoprotein A-IV and controls lipid handling in the intestine. J Biol Chem. 2004 Dec 10;279(50):52052-8

Cartoni R, Leger B, Hock MB, Praz M, Crettenand A, Pich S, Ziltener JL, Luthi F, Deriaz O, Zorzano A, Gobelet C, Kralli A, Russell AP. Mitofusins 1/2 and ERRalpha expression are increased in human skeletal muscle after physical exercise. J Physiol. 2005 Aug 15;567(Pt 1):349-58.

Cavallini A, Notarnicola M, Giannini R, Montemurro S, Lorusso D, Visconti A, Minervini F, Caruso MG. Oestrogen receptor-related receptor alpha (ERRalpha) and oestrogen receptors(ERalpha and ERbeta) exhibit different gene expression in human colorectal tumour progression.Eur J Cancer. 2005 Jul;41(10):1487-94.

Chang SM, Barker FG 2nd, Huhn SL, Nicholas MK, Page M, Rabbitt J, Prados MD. High dose oral tamoxifen and subcutaneous interferon alpha-2a for recurrent glioma. Neurooncol. 1998 Apr;37(2):169-76.

Chao EY, Collins JL, Gaillard S, Miller AB, Wang L, Orband-Miller LA, Nolte RT, McDonnell DP, Willson TM, Zuercher WJ. Structure-guided synthesis of tamoxifen analogs with improved selectivity for the orphan ERRgamma. Bioorg Med Chem Lett. 2006 Feb 15;16(4):821-4.

Chen F, Zhang Q, McDonald T, Davidoff MJ, Bailey W, Bai C, Liu Q, Caskey CT. Identification of two hERR2-related novel nuclear receptors utilizing bioinformatics and inverse PCR. Gene. 1999 Mar 4;228(1-2):101-9.

Chen H, Tini M, Evans RM. HATs on and beyond chromatin. Curr Opin Cell Biol. Apr;13(2):218-24. 2001
Chen S, Ye J, Kijima I, Kinoshita Y, Zhou D. Positive and negative transcriptional regulation of aromatase expression in human breast cancer tissue. J Steroid Biochem Mol Biol. 2005 May;95(1-5):17-23.

Chen S, Zhou D, Okubo T, Kao YC, Yang C. Breast tumor aromatase: functional role and transcriptional regulation. Endocr Relat Cancer. 1999 Jun;6(2):149-56. Review.

Chen S, Zhou D, Yang C, Okubo T, Kinoshita Y, Yu B, Kao YC, Itoh T. Modulation of aromatase expression in human breast tissue. J Steroid Biochem Mol Biol. 2001 Dec;79(1-5):35-40.

Chen S, Zhou D, Yang C, Sherman M. Molecular basis for the constitutive activity of estrogen-related receptor alpha-1. J Biol Chem. 2001 Jul 27;276(30):28465-70.

Cheung CP, Yu S, Wong KB, Chan LW, Lai FM, Wang X, Suetsugi M, Chen S, Chan FL. Expression and functional study of estrogen receptor-related receptors in human prostatic cells and tissues. J Clin Endocrinol Metab. 2005 Mar;90(3):1830-44.

Connor EE, Wood DL, Sonstegard TS, da Mota AF, Bennett GL, Williams JL, Capuco AV. Chromosomal mapping and quantitative analysis of estrogen-related receptor alpha-1, estrogen receptors alpha and beta and progesterone receptor in the bovine mammary gland. J Endocrinol. 2005 Jun;185(3):593-603.

Coward P, Lee D, Hull MV, Lehmann JM. 4-Hydroxytamoxifen binds to and deactivates the estrogen-related receptor gamma. Proc Natl Acad Sci U S A. 2001 Jul 17;98(15):8880-4.

Cross JC, Baczyk D, Dobric N, Hemberger M, Hughes M, Simmons DG, Yamamoto H, Kingdom JC. Genes, development and evolution of the placenta. Placenta. 2003 Feb-Mar;24(2-3):123-30.

Decaudin D, Etienne MC, De Cremoux P, Maciorowski Z, Vantelon JM, Voog E, Urien S, Tran-Perennou C, Renee N, Vielh P, Nemati F, Pouillart P. Multicenter phase II feasibility trial of high-dose tamoxifen in patients with refractory or relapsed multiple myeloma. J Natl Cancer Inst. 2004 Apr 21;96(8):636-7.

Devine C, Hinman VF, Degnan BM. Evolution and developmental expression of nuclear receptor genes in the ascidian Herdmania. Int J Dev Biol. 2002;46(4):687-92.

Eudy JD, Yao S, Weston MD, Ma-Edmonds M, Talmadge CB, Cheng JJ, Kimberling WJ, Sumegi J. Isolation of a gene encoding a novel member of the nuclear receptor superfamily from the critical region of Usher syndrome type IIa at 1q41. Genomics. 1998 Jun 15;50(3):382-4.

Evans, RM. Molecular characterization of the glucocorticoid receptor. Recent Prog Horm Res.;45:1-22; 1989

Forman, BM Evans RM. Nuclear hormone receptors activate direct, inverted, and everted repeats. Ann N Y Acad Sci. Jun 12;761:29-37. 1995

Gao M, Wei LH, Sun PM, Wang JL, Zhao D, Zhao C, Wang ZQ.[Regulation of orphan receptor ERR alpha by estrogen and progesterone in endometrial carcinoma cell line] Beijing Da Xue Xue Bao. 2005 Jun 18;37(3):281-3. Chinese.

Gao M, Wei LH, Sun PM, Zhao D, Wang JL, Wang ZQ, Zhao C. [Expression of estrogen receptor-related receptor isoforms in endometrial carcinoma tissues and its clinical significance] Zhonghua Fu Chan Ke Za Zhi. 2005 Nov;40(11):756-60. Chinese.

Gao M, Sun P, Wang J, Zhao D, Wei L. Expression of estrogen receptor-related receptor isoforms and clinical significance in endometrial adenocarcinoma. Int J Gynecol Cancer. 2006 Mar-Apr;16(2):827-33.

Gearhart MD, Dickinson L, Ehley J, Melander C, Dervan PB, Wright PE, Gottesfeld JM. Inhibition of DNA binding by human estrogen-related receptor 2 and estrogen receptor alpha with minor groove binding polyamides. Biochemistry. 2005 Mar 22;44(11):4196-203.

Geng Y, Tsai-Morris CH, Zhang Y, Dufau ML. The human luteinizing hormone receptor gene promoter: activation by Sp1 and Sp3 and inhibitory regulation. Biochem Biophys Res Commun. 1999 Sep 24;263(2):366-71.

Giannini R, Cavallini A. Expression analysis of a subset of coregulators and three nuclear receptors in human colorectal carcinoma. Anticancer Res. 2005 Nov-Dec;25(6B):4287-92.

Giguere V, Yang N, Segui P, Evans RM. Identification of a new class of steroid hormone receptors. Nature. 1988 Jan 7;331(6151):91-4.

Giguere V. Orphan nuclear receptors: from gene to function. Endocr Rev. 1999 Oct;20(5):689-725.

Giguere V. To ERR in the estrogen pathway. Trends Endocrinol Metab. 2002 Jul;13(5):220-5.

Glass CK, Rosenfeld MG. The coregulator exchange in transcriptional functions of nuclear receptors. Genes Dev. Jan 15;14(2):121-41 2000

Gowda K, Marks BD, Zielinski TK, Ozers MS. Development of a coactivator displacement assay for the orphan receptor estrogen-related receptor-gamma using time-resolved fluorescence resonance energy transfer. Anal Biochem. 2006 Jul 10

Gray PA, Fu H, Luo P, Zhao Q, Yu J, Ferrari A, Tenzen T, Yuk DI, Tsung EF,Cai Z, Alberta JA, Cheng LP, Liu Y, Stenman JM, Valerius MT, Billings N, Kim HA,Greenberg ME, McMahon AP, Rowitch DH, Stiles CD, Ma Q. Mouse brain organization revealed through direct genome-scale TF expression analysis. Science. 2004 Dec 24;306(5705):2255-7.

Greschik H, Flaig R, Renaud JP, Moras D. Structural basis for the deactivation of the estrogen-related receptor gamma by diethylstilbestrol or 4-hydroxytamoxifen and determinants of selectivity. J Biol Chem. 2004 May 24

Greschik H, Wurtz JM, Sanglier S, Bourguet W, van Dorsselaer A, Moras D, Renaud JP. Structural and functional evidence for ligand-independent transcriptional activation by the estrogen-related receptor 3. Mol Cell. 2002 Feb;9(2):303-13.

Hall VJ, Ruddock NT, French AJ. Expression profiling of genes crucial for placental and preimplantation development in bovine in vivo, in vitro, and nuclear transfer blastocysts. Mol Reprod Dev. 2005 Sep;72(1):16-24.

Hamm JK, Park BH, Farmer SR. A role for C/EBPbeta in regulating peroxisome proliferator-activated receptor gamma activity during adipogenesis in 3T3-L1 preadipocytes. J Biol Chem. 2001 May 25;276(21):18464-71.

Heard DJ, Norby PL, Holloway J, Vissing H. Human ERRgamma, a third member of the estrogen receptor-related receptor (ERR) subfamily of orphan nuclear receptors: tissue-specific isoforms are expressed during development and in the adult. Mol Endocrinol. 2000 Mar;14(3):382-92.

Hentschke M, Borgmeyer U. Identification of PNRC2 and TLE1 as activation function-1 cofactors of the orphan nuclear receptor ERRgamma. Biochem Biophys Res Commun. 2003 Dec 26;312(4):975-82.

Hentschke M, Schulze C, Susens U, Borgmeyer U. Characterization of calmodulin binding to the orphan nuclear receptor Errgamma. Biol Chem. 2003 Mar;384(3):473-82.

Hentschke M, Susens U, Borgmeyer U. Domains of ERRgamma that mediate homodimerization and interaction with factors stimulating DNA binding. Eur J Biochem. 2002 Aug;269(16):4086-97.

Hentschke M, Susens U, Borgmeyer U. PGC-1 and PERC, coactivators of the estrogen receptor-related receptor gamma. Biochem Biophys Res Commun. 2002 Dec 20;299(5):872-9.

Hermans-Borgmeyer I, Susens U, Borgmeyer U. Developmental expression of the estrogen receptor-related receptor gamma in the nervous system during mouse embryogenesis. Mech Dev. 2000 Oct;97(1-2):197-9.

Herzog B, Cardenas J, Hall RK, Villena JA, Budge PJ, Giguere V, Granner DK, Kralli A. Estrogen-related receptor alpha is a repressor of phosphoenolpyruvate carboxykinase gene transcription. J Biol Chem. 2006 Jan 6;281(1):99-106.

Hong H, Yang L, Stallcup MR. Hormone-independent transcriptional activation and coactivator binding by novel orphan nuclear receptor ERR3. J Biol Chem. 1999 Aug 6;274(32):22618-26.

Horard B, Castet A, Bardet PL, Laudet V, Cavailles V, Vanacker JM. Dimerization is required for transactivation by estrogen-receptor-related (ERR) orphan receptors: evidence from amphioxus ERR. J Mol Endocrinol. 2004 Oct;33(2):493-509.

Horard B, Rayet B, Triqueneaux G, Laudet V, Delaunay F, Vanacker JM. Expression of the orphan nuclear receptor ERRalpha is under circadian regulation in estrogen-responsive tissues. J Mol Endocrinol. 2004 Aug;33(1):87-97.

Horard B, Vanacker JM. Estrogen receptor-related receptors: orphan receptors desperately seeking a ligand. J Mol Endocrinol. 2003 Dec;31(3):349-57.

Hunter PJ, Swanson BJ, Haendel MA, Lyons GE, Cross JC. Mrj encodes a DnaJ-related co-chaperone that is essential for murine placental development. Development. 1999 Mar;126(6):1247-58.

Huppunen J, Aarnisalo P. Dimerization modulates the activity of the orphan nuclear receptor ERRgamma. Biochem Biophys Res Commun. 2004 Feb 20;314(4):964-70.

Huppunen J, Wohlfahrt G, Aarnisalo P. Requirements for transcriptional regulation by the orphan nuclear receptor ERRgamma. Mol Cell Endocrinol. 2004 Apr 30;219(1-2):151-60.

Huss JM, Kelly DP. Nuclear receptor signaling and cardiac energetics. Circ Res. 2004 Sep 17;95(6):568-78.

Huss JM, Kopp RP, Kelly DP. Peroxisome proliferator-activated receptor coactivator-1alpha (PGC-1alpha) coactivates the cardiac-enriched nuclear receptors estrogen-related receptor-alpha and -gamma. Identification of novel leucine-rich interaction motif within PGC-1alpha. J Biol Chem. 2002 Oct 25;277(43):40265-74.

Huss JM, Torra IP, Staels B, Giguere V, Kelly DP. Estrogen-related receptor alpha directs peroxisome proliferator-activated receptor alpha signaling in the transcriptional control of energy metabolism in cardiac and skeletal muscle. Mol Cell Biol. 2004 Oct;24(20):9079-91

Ichida M, Nemoto S, Finkel T. Identification of a specific molecular repressor of the peroxisome proliferator-activated receptor gamma Coactivator-1 alpha (PGC-1alpha). J Biol Chem. 2002 Dec 27;277(52):50991-5.

Igarashi M, Kawaguchi Y, Hirai K, Mizuno F. Physical interaction of Epstein-Barr virus (EBV) nuclear antigen leader protein (EBNA-LP) with human oestrogen-related receptor 1 (hERR1): hERR1 interacts with a conserved domain of EBNA-LP that is critical for EBV-induced B-cell immortalization. J Gen Virol. 2003 Feb;84(Pt 2):319-27.

Johnston SD, Liu X, Zuo F, Eisenbraun TL, Wiley SR, Kraus RJ, Mertz JE. Estrogen-related receptor alpha 1 functionally binds as a monomer to extended half-site sequences including ones contained within estrogen-response elements. Mol Endocrinol. 1997 Mar;11(3):342-52.

Kallen J, Schlaeppi JM, Bitsch F, Filipuzzi I, Schilb A, Riou V, Graham A, Strauss A, Geiser M, Fournier B. Evidence for ligand-independent transcriptional activation of the human estrogen-related receptor alpha

(ERRα): crystal structure of ERRα ligand binding domain in complex with peroxisome proliferator-activated receptor coactivator-1α. J Biol Chem. 2004 Nov 19;279(47):49330-7.

Kamei Y, Ohizumi H, Fujitani Y, Nemoto T, Tanaka T, Takahashi N, Kawada T, Miyoshi M, Ezaki O, Kakizuka A. PPARgamma coactivator 1beta/ERR ligand 1 is an ERR protein ligand, whose expression induces a high-energy expenditure and antagonizes obesity. Proc Natl Acad Sci U S A. 2003 Oct 14;100(21):12378-83. Epub 2003 Oct 06.

Kamei Y, Suzuki M, Miyazaki H, Tsuboyama-Kasaoka N, Wu J, Ishimi Y, Ezaki O. Ovariectomy in mice decreases lipid metabolism-related gene expression in adipose tissue and skeletal muscle with increased body fat. J Nutr Sci Vitaminol (Tokyo). 2005 Apr;51(2):110-7.

Kamei Y, Lwin H, Saito K, Yokoyama T, Yoshiike N, Ezaki O, Tanaka H. The 2.3 genotype of ESRRA23 of the ERR alpha gene is associated with a higher BMI than the 2.2 genotype. Obes Res. 2005 Oct;13(10):1843-4.

Kim HJ, Kim JY, Park YY, Choi HS. Synergistic activation of the human orphan nuclear receptor SHP gene promoter by basic helix-loop-helix protein E2A and orphan nuclear receptor SF-1. Nucleic Acids Res. 2003 Dec 1;31(23):6860-72.

Kim JH, Lee MH, Kim BJ, Kim JH, Han SJ, Kim HY, Stallcup MR. Role of aspartate 351 in transactivation and active conformation of estrogen receptor alpha.J Mol Endocrinol. 2005 Dec;35(3):449-64.

Kim JK, Levin ER. Estrogen signaling in the cardiovascular system. Nucl Recept Signal. 2006;4:e013.
Kim MS, Shigenaga JK, Moser AH, Feingold KR, Grunfeld C. Suppression of estrogen-related receptor-alpha and medium-chain acyl coenzyme A dehydrogenase in the acute phase response. J Lipid Res. 2005 Aug 1.

Klinge CM, Kaur K, Swanson HI. The aryl hydrocarbon receptor interacts with estrogen receptor alpha and orphan receptors COUP-TFI and ERRalpha1. Arch Biochem Biophys. 2000 Jan 1;373(1):163-74.

Klinge CM, Silver BF, Driscoll MD, Sathya G, Bambara RA, Hilf R. Chicken ovalbumin upstream promoter-transcription factor interacts with estrogen receptor, binds to estrogen response elements and half-sites, and inhibits estrogen-induced gene expression. J Biol Chem. 1997 Dec 12;272(50):31465-74.

Kojo H, Tajima K, Fukagawa M, Isogai T, Nishimura S. A novel estrogen receptor-related protein gamma splice variant lacking a DNA binding domain exon modulates transcriptional activity of a moderate range of nuclear receptors. J Steroid Biochem Mol Biol. 2006 Feb 3

Koohi MK, Ivell R, Walther N. Transcriptional activation of the oxytocin promoter by oestrogens uses a novel non-classical mechanism of oestrogen receptor action. J Neuroendocrinol. 2005 Apr;17(4):197-207.

Kraus RJ, Ariazi EA, Farrell ML, Mertz JE. Estrogen-related receptor alpha 1 actively antagonizes estrogen receptor-regulated transcription in MCF-7 mammary cells. J Biol Chem. 2002 Jul 5;277(27):24826-34.

Kressler D, Schreiber SN, Knutti D, Kralli A. The PGC-1-related protein PERC is a selective coactivator of estrogen receptor alpha. J Biol Chem. 2002 Apr 19;277(16):13918-25.

Laganiere J, Tremblay GB, Dufour CR, Giroux S, Rousseau F, Giguere V. A polymorphic autoregulatory hormone response element in the human estrogen related receptor a (ERRa) promoter dictates PGC-1a control of ERRa expression. J Biol Chem. 2004 Feb 20

Larsen LH, Rose CS, Sparso T, Overgaard J, Torekov SS, Grarup N, Jensen DP, Albrechtsen A, Andersen G, Ek J, Glumer C, Borch-Johnsen K, Jorgensen T, Hansen T, Pedersen O. Genetic analysis of the estrogen-related receptor alpha and studies of association with obesity and type 2 diabetes. Int J Obes (Lond). 2006 Jun 6;

Lee CH, Chawla A, Urbiztondo N, Liao D, Boisvert WA, Evans RM. Transcriptional Repression of Atherogenic Inflammation: Modulation by PPARγ. Science. 2003
Lichtenegger W. Expression of estrogen receptor-related receptors, a subfamily of orphan nuclear receptors, as new tumor biomarkers in ovarian cancer cells. J Mol Med. 2005 Jun;83(6):457-467.

Little TH, Zhang Y, Matulis CK, Weck J, Zhang Z, Ramachandran A, Mayo KE, Radhakrishnan I. Sequence-Specific DNA Recognition by Steroidogenic Factor 1: A Helix at the Carboxy-Terminus of the DNA Binding Domain is Necessary for Complex Stability. Mol Endocrinol. 2005 Dec 8

Liu D, Zhang Z, Gladwell W, Teng CT. Estrogen stimulates estrogen-related receptor alpha gene expression through conserved hormone response elements. Endocrinology. 2003 Nov;144(11):4894-904.

Liu D, Zhang Z, Teng CT. Estrogen-related receptor-gamma and peroxisome proliferator-activated receptor-gamma coactivator-1alpha regulate estrogen-related receptor-alpha gene expression via a conserved multi-hormone response element.J Mol Endocrinol. 2005 Apr;34(2):473-87.

Lopes da Silva S, Van Horssen AM, Chang C, Burbach JP. Expression of nuclear hormone receptors in the rat supraoptic nucleus. Endocrinology. 1995 May;136(5):2276-83.

Lorke DE, Susens U, Borgmeyer U, Hermans-Borgmeyer I. Differential expression of the estrogen receptor-related receptor gamma in the mouse brain. Brain Res Mol Brain Res. 2000 May 5;77(2):277-80.

Lu D, Kiriyama Y, Lee KY, Giguere V. Transcriptional regulation of the estrogen-inducible pS2 breast cancer marker gene by the ERR family of orphan nuclear receptors. Cancer Res. 2001 Sep 15;61(18):6755-61.

Lui K, Huang Y, Choi HL, Yu S, Wong KB, Chen S, Chan FL.Molecular cloning and functional study of rat estrogen receptor-related receptor gamma in rat prostatic cells. Prostate. 2006 Aug 22

Luo J, Sladek R, Bader JA, Matthyssen A, Rossant J, Giguere V. Placental abnormalities in mouse embryos lacking the orphan nuclear receptor ERR-beta. Nature. 1997 Aug 21;388(6644):778-82.

Luo J, Sladek R, Carrier J, Bader JA, Richard D, Giguere V. Reduced fat mass in mice lacking orphan nuclear receptor estrogen-related receptor alpha. Mol Cell Biol. 2003 Nov;23(22):7947-56

Lydon JP, Power RF, Conneely OM. Differential modes of activation define orphan subclasses within the steroid/thyroid receptor superfamily. Gene Expr. 1992;2(3):273-83.

Macchiarulo A, Rizzo G, Costantino G, Fiorucci S, Pellicciari R. Unveiling hidden features of orphan nuclear receptors: The case of the small heterodimer partner (SHP). J Mol Graph Model. 2005 Nov 7.

Maehara K, Hida T, Abe Y, Koga A, Ota K, Kutoh E. Functional interference between estrogen-related receptor alpha and peroxisome proliferator-activated receptor alpha/9-cis-retinoic acid receptor alpha heterodimer complex in the nuclear receptor response element-1 of the medium chain acyl-coenzyme A dehydrogenase gene. J Mol Endocrinol. 2003 Aug;31(1):47-60.

Mehta DV, Kim YS, Dixon D, Jetten AM. Characterization of the expression of the retinoid-related, testis-associated receptor (RTR) in trophoblasts. Placenta. 2002 Apr;23(4):281-7

Mertz JE. Simian virus 40 late gene expression is regulated by members of the steroid/thyroid hormone receptor superfamily. Proc Natl Acad Sci U S A. 1995 Sep 12;92(19):8586-90.

Mootha VK, Handschin C, Arlow D, Xie X, St Pierre J, Sihag S, Yang W, Altshuler D, Puigserver P, Patterson N, Willy PJ, Schulman IG, Heyman RA, Lander ES, Spiegelman BM. Errα and Gabpa/b specify PGC-1α-dependent oxidative phosphorylation gene expression that is altered in diabetic muscle. Proc Natl Acad Sci U S A. 2004 Apr 20

Nam K, Marshall P, Wolf RM, Cornell W. Simulation of the different biological activities of diethylstilbestrol (DES) on estrogen receptor alpha and estrogen-related receptor gamma. Biopolymers. 2003 Jan;68(1):130-8.

Nichol D, Christian M, Steel JH, White R, Parker MG. RIP140 expression is stimulated by ERRalpha during adipogenesis.J Biol Chem. 2006 Aug 21

Ostberg T, Jacobsson M, Attersand A, Mata de Urquiza A, Jendeberg L. A triple mutant of the Drosophila ERR confers ligand-induced suppression of activity. Biochemistry. 2003 Jun 3;42(21):6427-35.

Park YY, Kim HJ, Kim JY, Kim MY, Song KH, Park KC, Yu KY, Shong M, Kim KH, Choi HS. Differential role of the loop region between helices H6 and H7 within the orphan nuclear receptors SHP and DAX-1. Mol Endocrinol. 2004 Feb 12

Park YY, Ahn SW, Kim HJ, Kim JM, Lee IK, Kang H, Choi HS. An autoregulatory loop controlling orphan nuclear receptor DAX-1 gene expression by orphan nuclear receptor ERRgamma.Nucleic Acids Res. 2005 Nov 28;33(21):6756-68.

Pettersson K, Svensson K, Mattsson R, Carlsson B, Ohlsson R, Berkenstam A. Expression of a novel member of estrogen response element-binding nuclear receptors is restricted to the early stages of chorion formation during mouse embryogenesis. Mech Dev. 1996 Feb;54(2):211-23.

Powelka AM, Seth A, Virbasius JV, Kiskinis E, Nicoloro SM, Guilherme A, TangX, Straubhaar J, Cherniack AD, Parker MG, Czech MP. Suppression of oxidative metabolism and mitochondrial biogenesis by the transcriptional corepressor RIP140 in mouse adipocytes. J Clin Invest. 2006 Jan;116(1):125-36.

Razzaque MA, Masuda N, Maeda Y, Endo Y, Tsukamoto T, Osumi T. Estrogen receptor-related receptor gamma has an exceptionally broad specificity of DNA sequence recognition. Gene. 2004 Oct 13;340(2):275-82.

Reichardt HM, Kaestner KH, Tuckermann J, Kretz O, Wessely O, Bock R, Gass P, Schmid W, Herrlich P, Angel P, Schutz G. DNA binding of the glucocorticoid receptor is not essential for survival. Cell. May 15;93(4):531-41 1998.

Rollerova E, Urbancikova M. Intracellular estrogen receptors, their characterization and function (Review). Endocr Regul. 2000 Dec;34(4):203-18.

Scarpulla RC. Nuclear control of respiratory gene expression in mammalian cells. J Cell Biochem. 2006 Mar 1;97(4):673-83.

Sanyal S, Kim JY, Kim HJ, Takeda J, Lee YK, Moore DD, Choi HS. Differential regulation of the orphan nuclear receptor small heterodimer partner (SHP) gene promoter by orphan nuclear receptor ERR isoforms. J Biol Chem. 2002 Jan 18;277(3):1739-48.

Sanyal S, Matthews J, Bouton D, Kim HJ, Choi HS, Treuter E, Gustafsson JA.Deoxyribonucleic acid response element-dependent regulation of transcription by orphan nuclear receptor estrogen receptor-related receptor gamma. Mol Endocrinol. 2004 Feb;18(2):312-25. Epub 2003 Nov 26.

Schlecht C, Klammer H, Jarry H, Wuttke W. Effects of estradiol, benzophenone-2 and benzophenone-3 on the expression pattern of the estrogen receptors (ER) alpha and beta, the estrogen receptor-related receptor 1 (ERR1) and the aryl hydrocarbon receptor (AhR) in adult ovariectomized rats. Toxicology. 2004 Dec 1;205(1-2):123-30.

Schreiber SN, Emter R, Hock MB, Knutti D, Cardenas J, Podvinec M, Oakeley EJ, Kralli A. The estrogen-related receptor (ERR) functions in PPARγ coactivator 1γ (PGC-1γ)-induced mitochondrial biogenesis. Proc Natl Acad Sci U S A. 2004 Apr 15
Schreiber SN, Knutti D, Brogli K, Uhlmann T, Kralli A. The transcriptional coactivator PGC-1 regulates the expression and activity of the orphan nuclear receptor estrogen-related receptor alpha (ERRalpha). J Biol Chem. 2003 Mar 14;278(11):9013-8. Epub 2003 Jan 08.

Seely J, Amigh KS, Suzuki T, Mayhew B, Sasano H, Giguere V, Laganiere J, Carr BR, Rainey WE. Transcriptional regulation of dehydroepiandrosterone sulfotransferase (SULT2A1)by estrogen-related receptor alpha. Endocrinology. 2005 Aug;146(8):3605-13.

Shi H, Shigeta H, Yang N, Fu K, O'Brian G, Teng CT. Human estrogen receptor-like 1 (ESRL1) gene: genomic organization, chromosomal localization, and promoter characterization.Genomics. 1997 Aug 15;44(1):52-60.

Shigeta H, Zuo W, Yang N, DiAugustine R, Teng CT. The mouse estrogen receptor-related orphan receptor alpha 1: molecular cloning and estrogen responsiveness.J Mol Endocrinol. 1997 Dec;19(3):299-309.

Sladek R, Bader JA, Giguere V. The orphan nuclear receptor estrogen-related receptor alpha is a transcriptional regulator of the human medium-chain acyl coenzyme A dehydrogenase gene. Mol Cell Biol. 1997 Sep;17(9):5400-9.

Sladek R, Beatty B, Squire J, Copeland NG, Gilbert DJ, Jenkins NA, Giguere V. Chromosomal mapping of the human and murine orphan receptors ERRalpha (ESRRA) and ERRbeta (ESRRB) and identification of a novel human ERRalpha-related pseudogene. Genomics. 1997 Oct 15;45(2):320-6.

Sladek R, Giguere V. Orphan nuclear receptors: an emerging family of metabolic regulators. Adv Pharmacol. 2000;47:23-87.

Smith EP, Boyd J, Frank GR, Takahashi H, Cohen RM, Specker B, Williams TC, Lubahn DB, Korach KS. Estrogen resistance caused by a mutation in the estrogen-receptor gene in a man. N Engl J Med. 1994 Oct 20;331(16):1056-61.

Soriano FX, Liesa M, Bach D, Chan DC, Palacin M, Zorzano A. Evidence for a Mitochondrial Regulatory Pathway Defined by Peroxisome Proliferator-Activated Receptor-γ Coactivator-1α, Estrogen-Related Receptor-α, and Mitofusin 2. Diabetes. 2006 Jun;55(6):1783-91

Suetsugi M, Su L, Karlsberg K, Yuan YC, Chen S. Flavone and isoflavone phytoestrogens are agonists of estrogen-related receptors. Mol Cancer Res. 2003 Nov;1(13):981-91.

Sumi D, Ignarro LJ. Estrogen-related receptor alpha 1 up-regulates endothelial nitric oxide synthase expression. Proc Natl Acad Sci U S A. 2003 Nov 25;100(24):14451-6.

Sumi D, Ignarro LJ. Sp1 transcription factor expression is regulated by estrogen-related receptor alpha1. Biochem Biophys Res Commun. 2005 Mar 4;328(1):165-72.

Sun P, Sehouli J, Denkert C, Mustea A, Konsgen D, Koch I, Wei L, Lichtenegger W. Expression of estrogen receptor-related receptors, a subfamily of orphan nuclear receptors, as new tumor biomarkers in ovarian cancer cells. J Mol Med. 2005 Jun;83(6):457-467.

Susens U, Hermans-Borgmeyer I, Borgmeyer U. Alternative splicing and expression of the mouse estrogen receptor-related receptor gamma. Biochem Biophys Res Commun. 2000 Jan 19;267(2):532-5.

Suzuki T, Kasahara M, Yoshioka H, Morohashi K, Umesono K. LXXLL-related motifs in Dax-1 have target specificity for the orphan nuclear receptors Ad4BP/SF-1 and LRH-1. Mol Cell Biol. 2003 Jan;23(1):238-49.

Suzuki T, Miki Y, Moriya T, Shimada N, Ishida T, Hirakawa H, Ohuchi N, Sasano H. Estrogen-Related Receptor α in Human Breast Carcinoma as a Potent Prognostic Factor. Cancer Res. 2004 Jul 1;64(13):4670-4676.

Tarrant AM, Greytak SR, Callard GV, Hahn ME. Estrogen receptor-related receptors in the killifish Fundulus heteroclitus: diversity, expression, and estrogen responsiveness. J Mol Endocrinol. 2006 Aug;37(1):105-20.

Trapp T, Holsboer F. Nuclear orphan receptor as a repressor of glucocorticoid receptor transcriptional activity. J Biol Chem. 1996 Apr 26;271(17):9879-82.

Tremblay GB, Bergeron D, Giguere V. 4-Hydroxytamoxifen is an isoform-specific inhibitor of orphan estrogen-receptor-related (ERR) nuclear receptors beta and gamma. Endocrinology. 2001 Oct;142(10):4572-5.

Tremblay GB, Kunath T, Bergeron D, Lapointe L, Champigny C, Bader JA, Rossant J, Giguere V. Diethylstilbestrol regulates trophoblast stem cell differentiation as a ligand of orphan nuclear receptor ERR beta. Genes Dev. 2001 Apr 1;15(7):833-8.

Vanacker JM, Bonnelye E, Chopin-Delannoy S, Delmarre C, Cavailles V, Laudet V. Transcriptional activities of the orphan nuclear receptor ERR alpha (estrogen receptor-related receptor-alpha). Mol Endocrinol. 1999 May;13(5):764-73.

Vanacker JM, Bonnelye E, Delmarre C, Laudet V. Activation of the thyroid hormone receptor alpha gene promoter by the orphan nuclear receptor ERR alpha. Oncogene. 1998 Nov 12;17(19):2429-35.

Vanacker JM, Delmarre C, Guo X, Laudet V. Activation of the osteopontin promoter by the orphan nuclear receptor estrogen receptor related alpha. Cell Growth Differ. 1998 Dec;9(12):1007-14.

Vanacker JM, Pettersson K, Gustafsson JA, Laudet V. Transcriptional targets shared by estrogen receptor-related receptors (ERRs) and estrogen receptor (ER) alpha, but not by ERbeta. EMBO J. 1999 Aug 2;18(15):4270-9.

Vega RB, Kelly DP. A role for estrogen-related receptor alpha in the control of mitochondrial fatty acid beta-oxidation during brown adipocyte differentiation. J Biol Chem. 1997 Dec 12;272(50):31693-9.

Vlaeminck-Guillem V, Vanacker JM, Verger A, Tomavo N, Stehelin D, Laudet V, Duterque-Coquillaud M. Mutual repression of transcriptional activation between the ETS-related factor ERG and estrogen receptor. Oncogene. 2003 Nov 6;22(50):8072-84.

Wang L, Liu J, Saha P, Huang J, Chan L, Spiegelman B, Moore DD. The orphan nuclear receptor SHP regulates PGC-1alpha expression and energy production in brown adipocytes. Cell Metab. 2005 Oct;2(4):227-38.

Wang LH, Ing NH, Tsai SY, O'Malley BW, Tsai MJ. The COUP-TFs compose a family of functionally related transcription factors. Gene Expr. 1991;1(3):207-16.

Watanabe A, Kinoshita Y, Hosokawa K, Mori T, Yamaguchi T, Honjo H. Function of estrogen-related receptor alpha in human endometrial cancer. J Clin Endocrinol Metab. 2006 Feb 7.

Wende AR, Huss JM, Schaeffer PJ, Giguere V, Kelly DP. PGC-1alpha coactivates PDK4 gene expression via the orphan nuclear receptor ERRalpha: a mechanism for transcriptional control of muscle glucose metabolism. Mol Cell Biol. 2005 Dec;25(24):10684-94.

Wiley SR, Kraus RJ, Zuo F, Murray EE, Loritz K, Mertz JE. SV40 early-to-late switch involves titration of cellular transcriptional repressors. Genes Dev. 1993 Nov;7(11):2206-19.

Willy PJ, Murray IR, Qian J, Busch BB, Stevens WC Jr, Martin R, Mohan R, Zhou S, Ordentlich P, Wei P, Sapp DW, Horlick RA, Heyman RA, Schulman IG. Regulation of PPARγ coactivator 1α (PGC-1α) signaling by an estrogen-related receptor α (ERRα) ligand. Proc Natl Acad Sci U S A. 2004 Jun 7

Wilson TE, Fahrner TJ, Milbrandt J. The orphan receptors NGFI-B and steroidogenic factor 1 establish monomer binding as a third paradigm of nuclear receptor-DNA interaction.Mol Cell Biol. 1993 Sep;13(9):5794-804.

Xie W, Hong H, Yang NN, Lin RJ, Simon CM, Stallcup MR, Evans RM. Constitutive activation of transcription and binding of coactivator by estrogen-related receptors 1 and 2. Mol Endocrinol. 1999 Dec;13(12):2151-62.

Xie X, Lu J, Kulbokas EJ, Golub TR, Mootha V, Lindblad-Toh K, Lander ES, Kellis M.Systematic discovery of regulatory motifs in human promoters and 3' UTRs by comparison of several mammals. Nature. 2005 Mar 17;434(7031):338-45.

Yan Z, Jetten AM. Characterization of the repressor function of the nuclear orphan receptor retinoid receptor-related testis-associated receptor/germ cell nuclear factor. J Biol Chem. 2000 Nov 10;275(45):35077-85.

Yang C, Chen S. Two organochlorine pesticides, toxaphene and chlordane, are antagonists for estrogen-related receptor alpha-1 orphan receptor. Cancer Res. 1999 Sep 15;59(18):4519-24.

Yang C, Yu B, Zhou D, Chen S. Regulation of aromatase promoter activity in human breast tissue by nuclear receptors. Oncogene. 2002 Apr 25;21(18):2854-63.

Yang C, Zhou D, Chen S. Modulation of aromatase expression in the breast tissue by ERR alpha-1 orphan receptor. Cancer Res. 1998 Dec 15;58(24):5695-700.

Yang N, Shigeta H, Shi H, Teng CT. Estrogen-related receptor, hERR1, modulates estrogen receptor-mediated response of human lactoferrin gene promoter. J Biol Chem. 1996 Mar 8;271(10):5795-804.
Yu DD, Forman BM. Identification of an agonist ligand for estrogen-related receptors ERRbeta/gamma. Bioorg Med Chem Lett. 2005 Mar 1;15(5):1311-3.

Zhang Z, Teng CT. Estrogen receptor alpha and estrogen receptor-related receptor alpha1 compete for binding and coactivator. Mol Cell Endocrinol. 2001 Feb 14;172(1-2):223-33.

Zhang Z, Teng CT. Estrogen receptor-related receptor alpha 1 interacts with coactivator and constitutively activates the estrogen response elements of the human lactoferrin gene. J Biol Chem. 2000 Jul 7;275(27):20837-46.

Zhang Z, Chen K, Shih JC, Teng CT. Estrogen-related receptors-stimulated monoamine oxidase B promoter activity is down-regulated by estrogen receptors. Mol Endocrinol. 2006 Jul;20(7):1547-61.
Zhou D, Chen S. PNRC2 is a 16 kDa coactivator that interacts with nuclear receptors through an SH3-binding motif. Nucleic Acids Res. 2001 Oct 1;29(19):3939-48

Zhou W, Liu Z, Wu J, Liu JH, Hyder SM, Antoniou E, Lubahn DB. Identification and characterization of two novel splicing isoforms of human estrogen-related receptor beta. J Clin Endocrinol Metab. 2006 Feb;91(2):569-79.

Zuo F, Zhou D, Quach KM, Yang C, Lee SY, Pohajdak B, Chen S. PNRC: a proline-rich nuclear receptor coregulatory protein that modulates transcriptional activation of multiple nuclear receptors including orphan receptors SF1 (steroidogenic factor 1) and ERRalpha1 (estrogen related receptor alpha-1). Mol Endocrinol. 2000 Jul;14(7):986-98.

Zuercher WJ, Gaillard S, Orband-Miller LA, Chao EY, Shearer BG, Jones DG, Miller AB, Collins JL, McDonnell DP, Willson TM. Identification and structure-activity relationship of phenolic acyl hydrazones as selective agonists for the estrogen-related orphan nuclear receptors ERRbeta and ERRgamma. J Med Chem. 2005 May 5;48(9):3107-9.

Chapter 2

Initial Characterization of ERRγ Mutant Mice

Generation and Initial Characterization of ERRγ Mutant Mice

Targeted disruption of ERRγ was achieved by the introduction of a LacZ-neomycin resistance (neomycin phosphotransferase II (EC 2.7.1.95)) fusion gene into the second exon. The site for insertion was created between 5' BamH I and 3' Asp718 restriction sites (Figure 1A). Chimeric mice were created

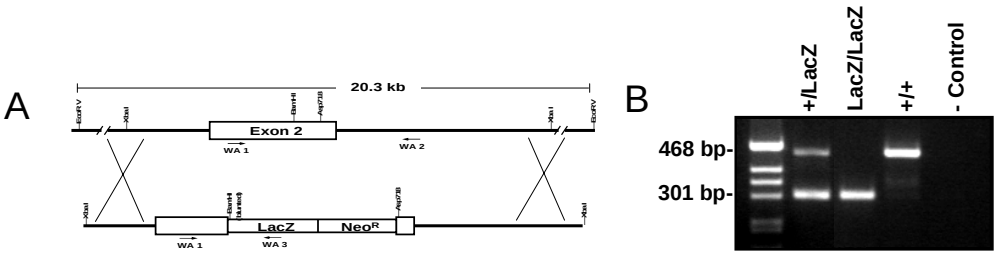

Figure 2.1: Targeting Strategy and Genotyping of ERRγ Knockout Mice

and multiplex polymerase chain reaction (PCR) was used to determine genotype of offspring using the following primers: 5' Common exonic, tgacggacacgctcaaccaccacagc; 3' WT exonic, gtcccacagtgaaacaggaaggggc; 3' LacZ exonic, tgcgggcctcttcgctattacgcc. The PCR reaction produced a 468

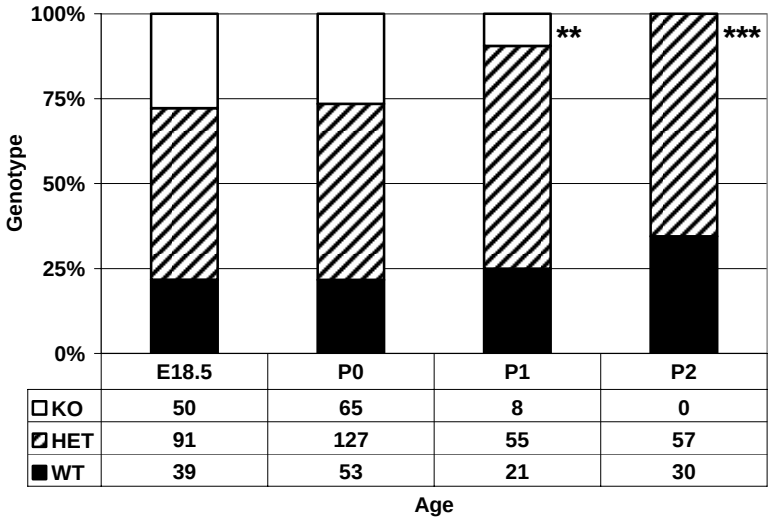

	E18.5	P0	P1	P2
KO	50	65	8	0
HET	91	127	55	57
WT	39	53	21	30

Figure 2.2: ERRγ is Essential During Early Postnatal Life

bp amplicon for the WT allele and a 301 bp amplicon for the mutant allele (Figure 1B).

Crosses between ERRγ$^{+/LacZ}$ mice produced offspring in a 1:2:1 Mendelian ratio until postnatal day zero (P0, 0 to 24 hours after birth) as predicted by this cross ($chi^2 = 0.3$; $p = 0.86$; $n = 895$). However by postnatal day one (P1, 24-48 hours after birth), there was a significant reduction in the number of ERRγ$^{LacZ/LacZ}$ (ERRγ-KO, ERRγ-null, KO) animals observed under standard breeding conditions ($chi^2 = 12.07$; $p = 0.0024$; $n = 84$). At postnatal day two (P2, 48 to 72 hours after birth), no ERRγ-null animals were observed ($chi^2 = 28.34$; $p < 0.0001$; $n = 87$).

Body weight weights of neonatal mice were recorded and while ERRγ$^{+/+}$ and ERRγ$^{+/LacZ}$ animals were statistically indistinguishable, the weight of the ERRγ null mice was significantly less that WT littermate controls (WT = 1.52g ± 0.02 SEM; KO = 1.39g ± 0.01 SEM; $p < 5x10^{-6}$; n=152). While ERRγ WT and HET littermates continued to steadily gain weight during P1 and P2, ERRγ-null mice did not gain

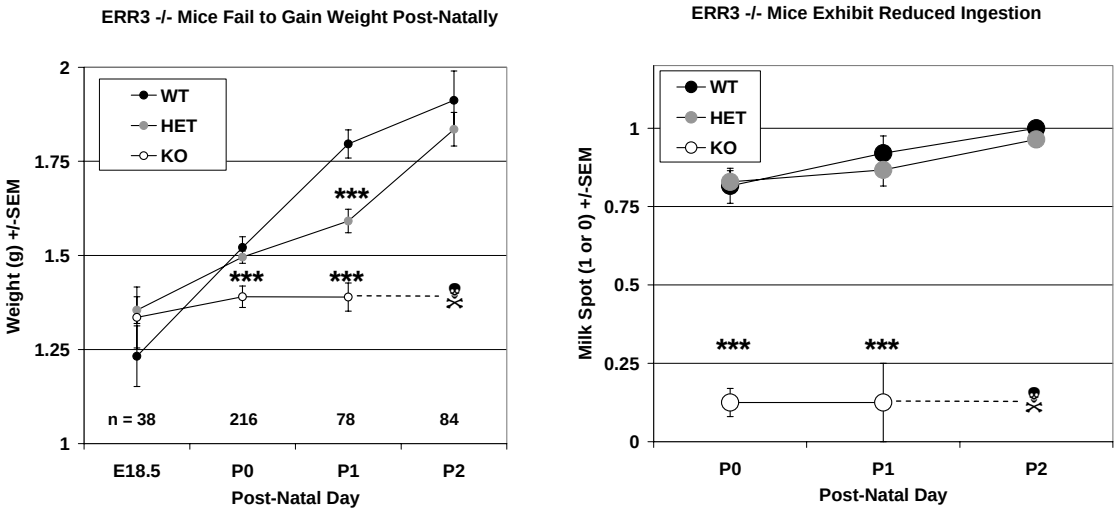

Figure 2.3: ERRγ-null Mice Die from Inanition.

weight and appeared to die from inanition. Feeding status of the mice scored by direct visualization of the milk-filled stomach (milk-spot) through the translucent body wall with milk observation assigned "1" and no milk-spot assigned a "0". At P0 and P1, ERRγ-null mice had a significant reduction in observed milk spots compared to WT and HET littermate controls ($p < 0.0001$ ANOVA; $n = 178$).

The introduction of the beta-galactosidase gene into the ERRγ locus allows the use of a chromogenic substrate, X-gal (5-bromo-4-chloro-3-indolyl-beta-D-galactopyranoside) to visualize regions of ERRγ expression in whole-mounted embryos or tissues.

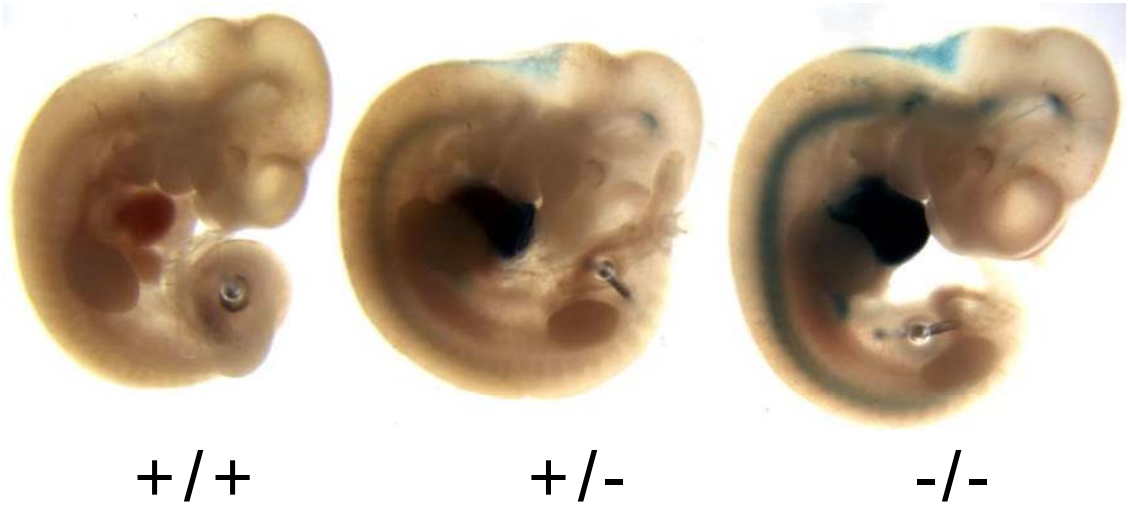

Figure 2.4: Whole Mount X-Gal Staining of E10.5 Embryos

At embryonic day 10.5 (E10.5) whole mount embryo staining revealed robust expression in the heart, CNS and kidney precursors. Of note is the staining present in the third cranial (occulomotor) nucleus and nerve. This indicated that ERR3 is present in cholinergic motor neuron. Because development proceeds in a rostrocaudal fashion, the cranial motor nuclei are more developmentally advanced than the motor

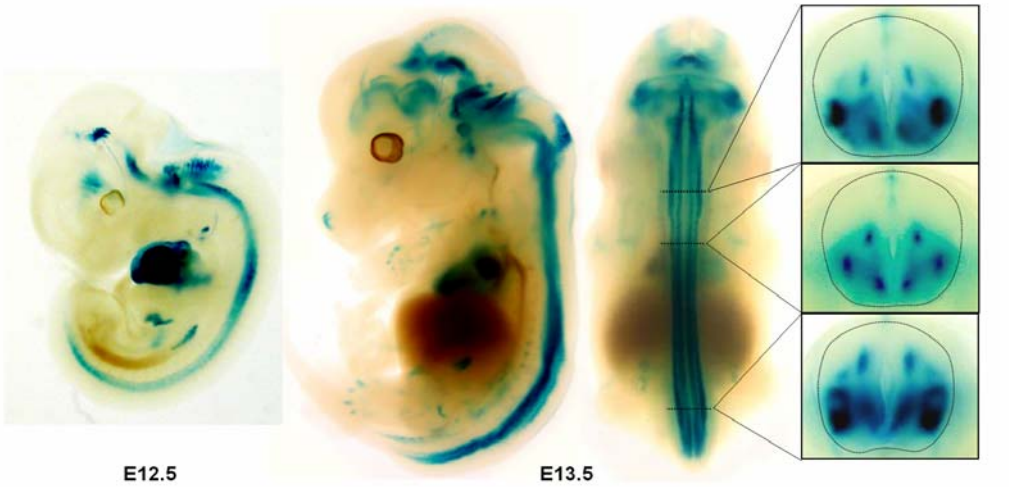

Figure 2.5: Whole Mount X-Gal Expression of E12.5 and E13.5 ERRγ$^{LacZ/LacZ}$ Embryo

nuclei found in the caudal regions of the spinal cord.

The peripheral nervous system expresses ERRγ as well. In addition to ERRγ expression in the occulomotor nucleus and occulomotor nerve, there is robust expression in the dorsal root ganglia (DRG) which contain the cell bodies of the sensory nervous system. Utilizing the enzymatic activity of the beta galactosidase gene targeted to the ERRγ locus, expression of ERRs was detected by X-gal staining. At E18.5, robust expression is detected in the DRG. In collaboration with the laboratory of Thomas Jessell and his post-doctoral fellow, Jorienne De Nooij, studies were undertaken to follow their observations that in the

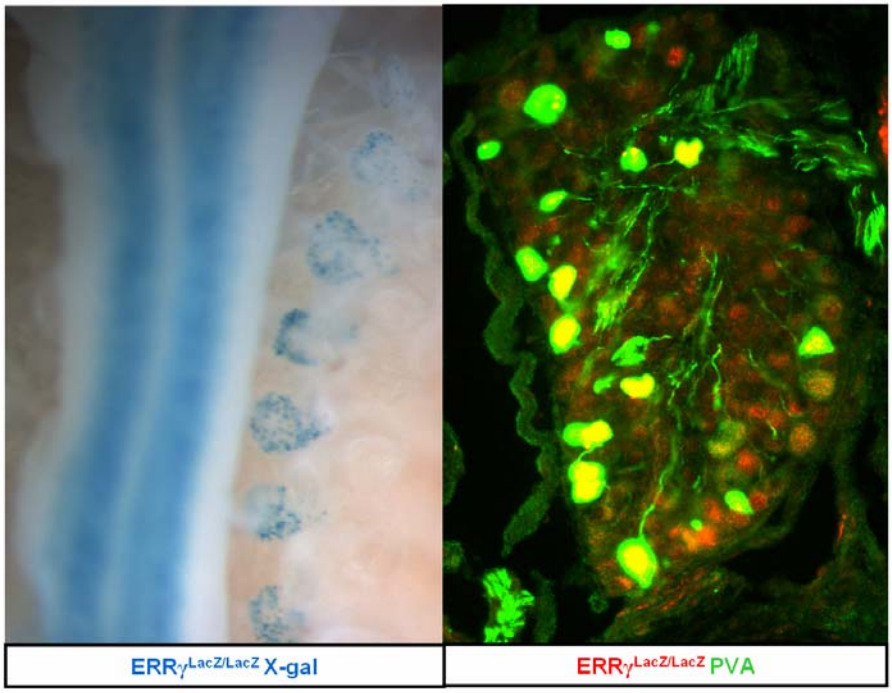

Figure 2.6: ERRγ is Expressed in Parvalbumin-positive Cells of the DRG

absence of trkC, ER81 or Runx3, ERRγ expression in the DRG is not detected by in situ hybridization. Loss of ngn1 has increases the percentage of ERRγ expressing neurons in the DRG. ER81 mice have excess GTOs at the expense of spindles.

Studies were undertaken to assess how loss of ERRγ would effect these markers. ERRγ is expressed in a subset of dorsal root ganglion neurons. These neurons express parvalbumin (PVA) and are Ia and Ib afferents that innervate the intrafusile fibers and Golgi tendon organs (GTO) respectively. Ia afferents have axonal projections that terminate directly on motor neurons in the ventral cord. These fibers sense the

stretch of the muscle. Ib afferents terminate in the dorsal cord and form disynaptic connection to the motor neurons in the ventral cord. These fibers sense the force generation of the muscle as detected by the GTOs.

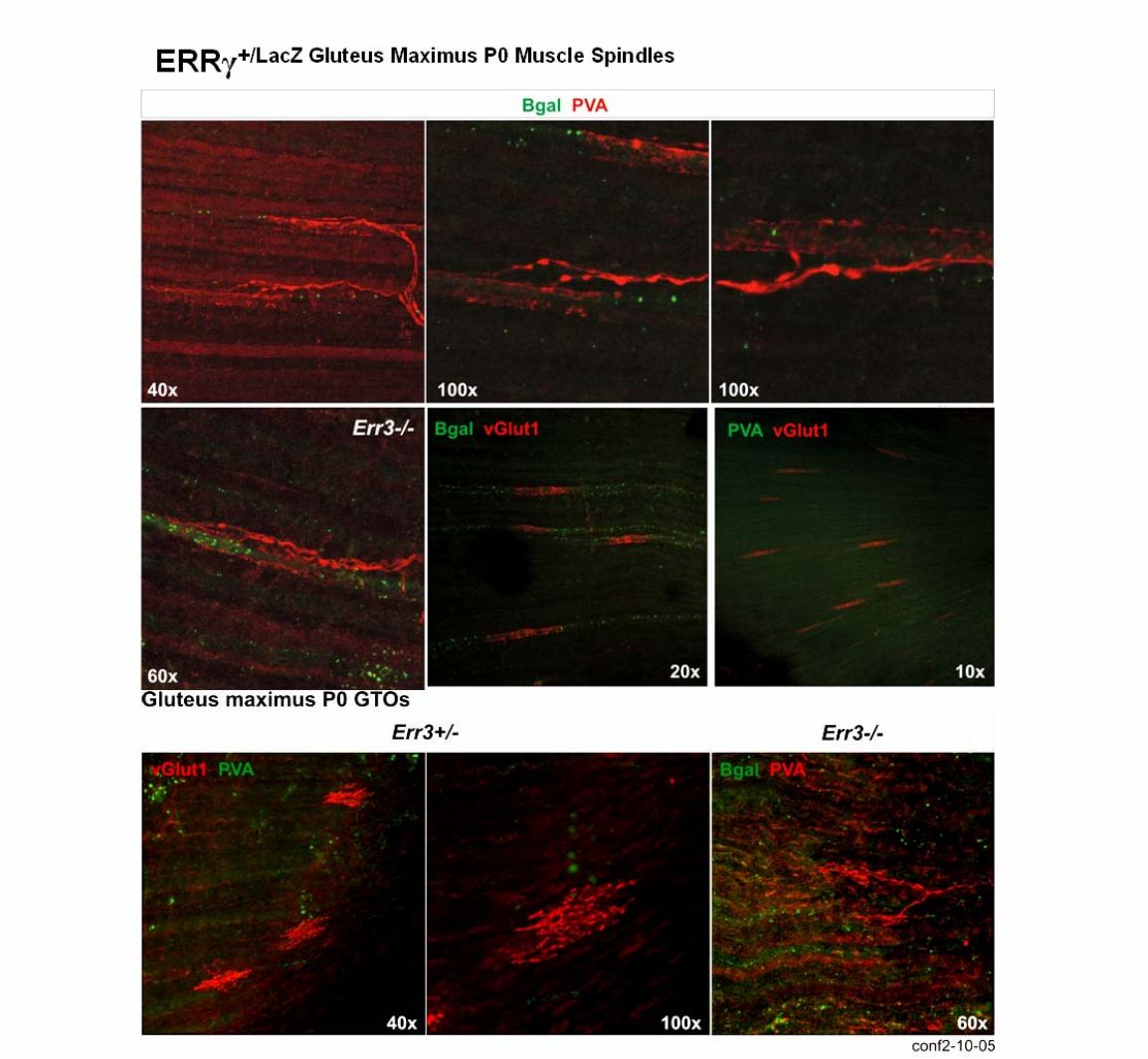

Figure 2.7: ERRγ is Expressed in Muscle Spindles and Golgi Tendon Organs

Expression in Muscle

In collaboration with Vihang Narkar, robust expression of ERRγ is detected in the slow twitch muscles. Skeletal muscles from male 9-week-old 99.9% C57Bl6 mice were subjected to X-gal staining to detect betagalactosidase expression as a surrogate marker of ERRγ expression. Despite visualization of ERRγ expression in intrafusile fibers of the muscle spindles and within the Golgi tendon organs of the

gluteus maximus muscle composed of mixed fiber types, ERRγ was not demonstrably expressed in fast twitch or mixed fiber type muscle.

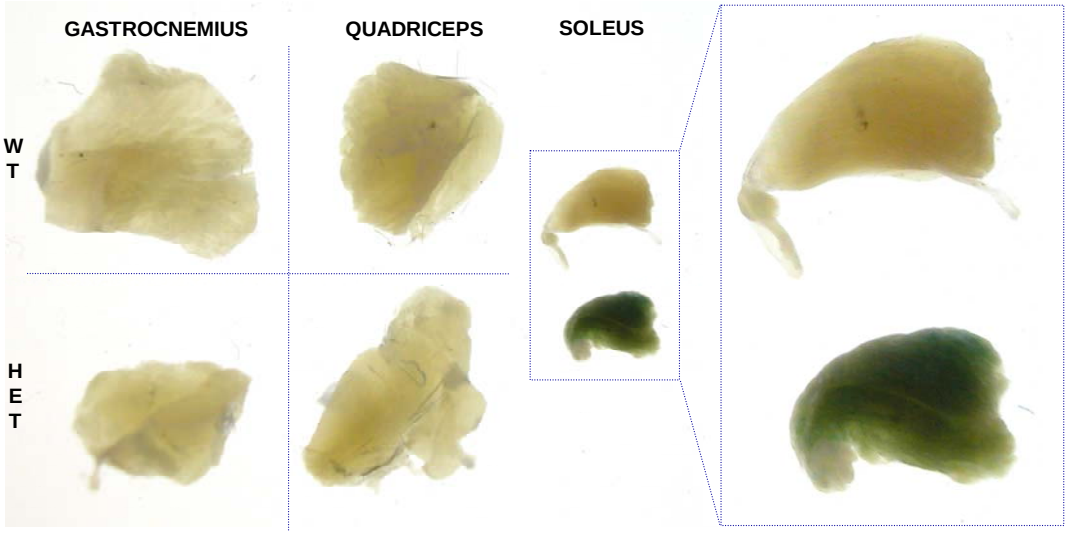

Figure 2.8: ERRγ is Expressed in Slow Twitch Muscles

Antibody Generation

A critical reagent in the characterization of the role of ERRγ was the development of a polyclonal rabbit antibody. A modified pGEX vector was used to express a GST-LBD fusion protein. The LBD of ERRγ is amino acids 230-458. The fusion protein was expressed in E. coli and isolated by sonication in the presence of a non-ionic detergent, NDSB (Eiler, 2001). The supernatant was affinity purified by the GST tag. The GST-LBD fusion protein was injected into three rabbits, one of which produced serum that worked for immunohistochemistry at a 1:10,000 dilution. In order to improve the specificity of the serum, the serum was subjected to two rounds of negative and one round of positive enrichment. First, the serum was passed across an immobilized GST column to remove antibodies against GST. Second, the serum was passed over a column with an immobilized E. coli lysate to remove antibodies generated against the impurities of the GST-LBD fusion protein. Third, an affinity column was prepared with Affy-gel that had bound GST-LBD protein to positively select anti-LBD reactive antibodies. This antibody has proved to work in Western blots, chromatin immunoprecipitation and immunohistochemistry.

Established MEF Line

Primary mouse embryonic fibroblasts were collected from embryonic null mice and subjected to a serial passaging protocol called the 3T3-rule (Todaro and Green, 1963). By passaging $3x10^3$ cells per 10cm plate every three days, the cells go through a crisis and will undergo chromosomal rearrangements that will produce a stable, immortalized cell line after 18-25 passages. ERRγ-null MEFs were serially passaged twenty-five times to establish a stable line.

Bone stain

Given the implications for bone development and mineralization, a bone stain was performed using alizarin red and alcian blue (Bonnelye, 1997; Menegola, 2001). No gross abnormalities in bone were noted. Alizarin red stains bone while alcian blue stains cartilage.

Figure 2.9: Bone Development is Grossly Normal in ERRγ-null Mice.

REFERENCES

Bonnelye E, Vanacker JM, Spruyt N, Alric S, Fournier B, Desbiens X, Laudet V. The ERR-1 orphan receptor is a transcriptional activator expressed during bone development. Mol Endocrinol. 1997 Jun;11(7):905-16.

Eiler S, Gangloff M, Duclaud S, Moras D, Ruff M. Overexpression, purification, and crystal structure of native ER alpha LBD. Protein Expr Purif. 2001 Jul;22(2):165-73.

Menegola E, Broccia ML, Giavini E. Atlas of rat fetal skeleton double stained for bone and cartilage. Teratology. 2001 Sep;64(3):125-33.

Todaro GJ, Green H. Quantitative studies of the growth of mouse embryo cells in culture and their development into established lines. J Cell Biol. 1963 May;17:299-313.

Acknowlegements

Collaborators subject to authorship deriving from this work include:

Matthew Bloch	Michael Downes, Ph.D.
Catherine Dufour , M.S.	Ronald M. Evans, Ph.D.
Benjamin W. Gallarda	Vincent Giguere, Ph.D.
Wayne R. Giles, Ph.D.	Johann W. Jonker, Ph.D.
Richard Kondo, Ph.D.	Alexander Lehrman, M.S.
Christopher P Myers, M.D. Ph.D.	Robert K. Naviaux, M.D. Ph.D.
Jordan Nevo	Samuel L. Pfaff, Ph.D.
Wen Xie, M.D. Ph.D.	Ruth T. Yu, M.D. Ph.D.

Alaynick WA; Myers CP; Gallarda BW; Pfaff SL, Evans RM. “Locomotor Defects in Estrogen-related Receptor Gamma Mutant Mice” In Preparation.

Alaynick WA; Kondo R; Xie W; Downes M; Dufour C; Jonker JW; Yu RT; Lehrman A; Nevo J; Bloch M; Naviaux RK; Giles WR; Giguere V; Evans RM. “Cardiac conduction Defects in Estrogen-related Receptor Gamma Mutant Mice”. In Preparation

Chapter 3

Motor and Central Pattern Generator Defects

Locomotor Circuits of the Spinal Cord

In the developing embryonic spinal cord, the generation of neuronal classes with specific phenotypic properties is dependent on the temporal and spatial establishment of morphogen and transcriptional gradients. Within the ventral spinal cord, neurons controlling locomotion are generated through the coordinate actions of sonic hedgehog (Shh) and delta, which identify the subclass, timing of differentiation, number, and spatial arrangement of cells (Bertrand et al., 2002; Briscoe and Ericson, 2001; Jessell, 2000; Tanabe and Jessell, 1996). The actions of multiple well-defined classes of transcription factors are influenced by these signaling pathways to modulate gene expression (Edlund and Jessell, 1999). Within the ventricular zone of the developing spinal cord, these transcription factors have been shown to act in defining five progenitor (P) pools of neurons. P0-P3 domains give rise to ipsilateral and commissural ventral (V) interneuron classes V0-V3 defined by the expression of Evx1, En1, Chx10 and Sim1, respectively, while the PMN domain gives rise to both motor neurons (defined by Hb9 or Isl1) and oligodendrocytes which express Olig2 (Lee and Pfaff, 2001). The coordinated actions of bHLH and HD factors—and undefined factors—contribute to the development and interaction of neurons to form functional networks of neurons, such as Central Pattern Generators (CPGs).

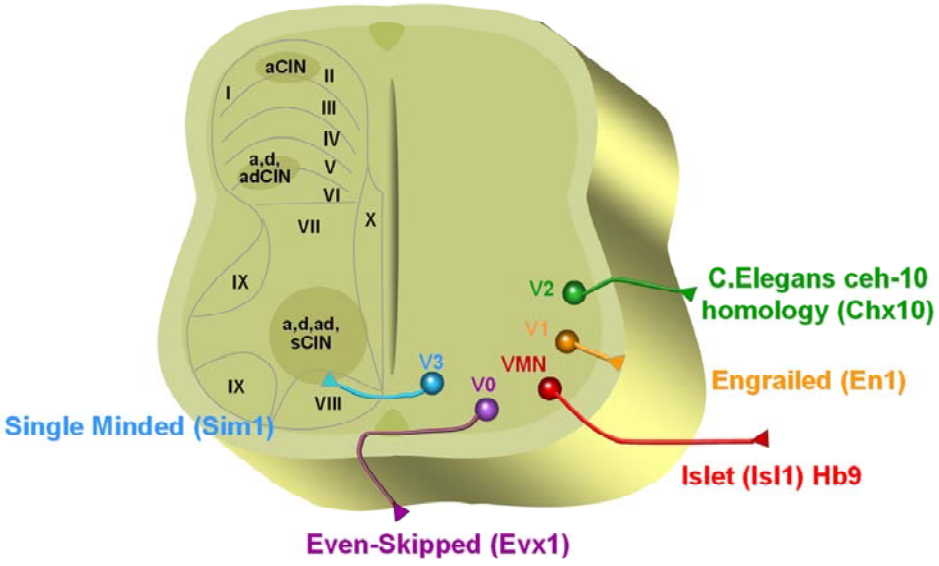

Figure 3.1: Developmental Markers of Ventral Spinal Cord Neurons

CPGs are regionally defined neuronal networks that can semiautonomously produce rhythmic movements in isolated systems deprived of movement-related sensory feedback. CPGs provide more delimited and tractable systems to study the principles upon which more complex neural networks are built. CPG have been described across phyla, including humans, and in diverse processes such as respiration, feeding and locomotion. (Keihn and Kullander, 2004). Locomotor networks have been well described in two aquatic vertebrates (Roberts, 2000; Grillner et al., 1998), however the mouse offers the advantages of genetic malleability, an emerging understanding of the molecular basis of spinal cord development (Jessell, 2000; Lee and Pfaff, 2001; Goulding et al., 2002), and more similar behavioral and locomotor repertoire in which to discover many unresolved issues in locomotor CPG cellular components, wiring and function (Hultborn et al., 1998). A network of neurons comprising a CPG within the lumbar spinal cord is capable of semi-autonomously mediating limb locomotor patterns (Kiehn, 2003). This network of neurons provides for alternating movements of the hind limbs by stimulating an extensor set of muscles ipsilaterally while inhibiting both ipsilateral flexors (synergist muscles) and contralateral extensors (homonymous muscles) (Butt, 2002). The use of an in vitro perinatal mouse spinal cord preparation allows the integrative analysis of genetic, molecular and pharmacologic perturbations of the locomotor CPG (Kiehn and Kullander, 2004).

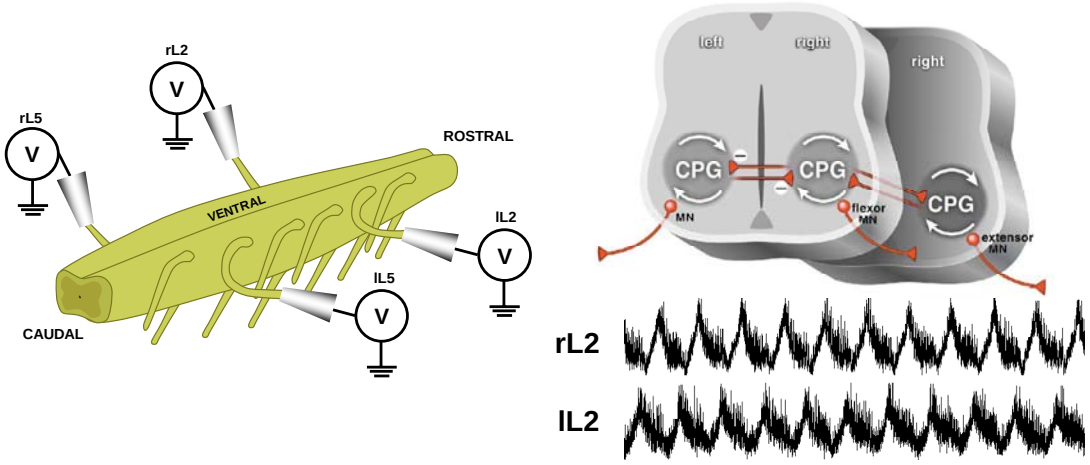

Figure 3.2: Electrophysiologic Recording of CPG Activity

In the presence of oxygenated artificial cerebrospinal fluid (aCSF) and neurotransmitters (*N*-methyl-aspartate (NMA), dopamine (DA), and serotonin (5-HT)) the isolated lumbar spinal cord produces rhythmic electrical activity resembling the components of locomotor limb movements that can be recorded by electrodes at the ventral roots (Kudo and Yamada, 1987a; Cazalets et al., 1992; Kiehn and Kjaerulff, 1996). The circuits responsible for generating such activity are located in the ventromedial area of the lumbar spinal cord and include commissural interneurons (CINs) necessary for correct left-right coordination, ipsilateral inhibitory neurons, and motor neurons to effect electrical and behavioral output (Kjaerulff and Kiehn, 1996; Kiehn and Kjaerulff, 1998).

Careful analysis of P0 animals in a simple test of motor functions suited to the limited behavioral repertoire of neonatal mice demonstrated a reduced capacity of ERRγ-null mice to execute forward movement (Figure 3C; Le Roy, 1999; Crawley, 2000). This analysis reveals that ERRγ-null mice can move all limbs, maintain an upright posture and react appropriately to vestibular cues. However, unlike WT and HET mice—which adopt a prone posture and paddling limb movements which are occasionally alternating—null mice instead will extend hindlimbs and arch (kyphosis/ dorsiflex) their backs. The limb movements of nulls were generally inappropriate, disorganized and ineffective. This assay, while effective in identifying a defect in ERRγ-null animals, is not an established behavioral assay, nor does it have the sensitivity to detect defects in the heterozygous animals.

Adaptation of a righting reflex assay to P0 animals allows examination of whole animal motor function in executing a robust and reflexive motor task (Crawley, 2000). Neonatal mice do not perform the righting reflex consistently because they do not have a consistent state of behavioral arousal and latency to right may be erroneously extended due to sleep or quiet resting. To assure a consistently aroused behavioral state, the mice were stimulated by a gentle, although noxious, pinch with fine forceps at 1, 15, 30 and 45 seconds. Mice were placed supine and righting was defined as having both forepaws in the surface as a brief prone position while rolling from one side to the other. With this adaptation, the righting reflex assay is sensitive enough to discern statistically significant differences in righting latency between WT, HET and KO animals collected from four litters (Figure 3c. WT = 8.3±1s, n = 9 ; HET = 14.7 ± 1.5s, n = 19; KO =

50.4 ± 1.4s, n = 7; WT v HET: $p < 0.025$; WT v KO: $p < 0.0001$; Student's T-test with Bonferonni post hoc correction).

Reducing the requirement for normal motor function through removal of competing littermates allows ERRγ-null mice to live beyond the P1 lethality observed in birth litters (data not shown). Empirically, this appears to be due to two factors: firstly, the KO neonates are less capable of competing for access to milk than their littermates; secondly, the dam rejects and refuses to nurture ERRγ-null animals

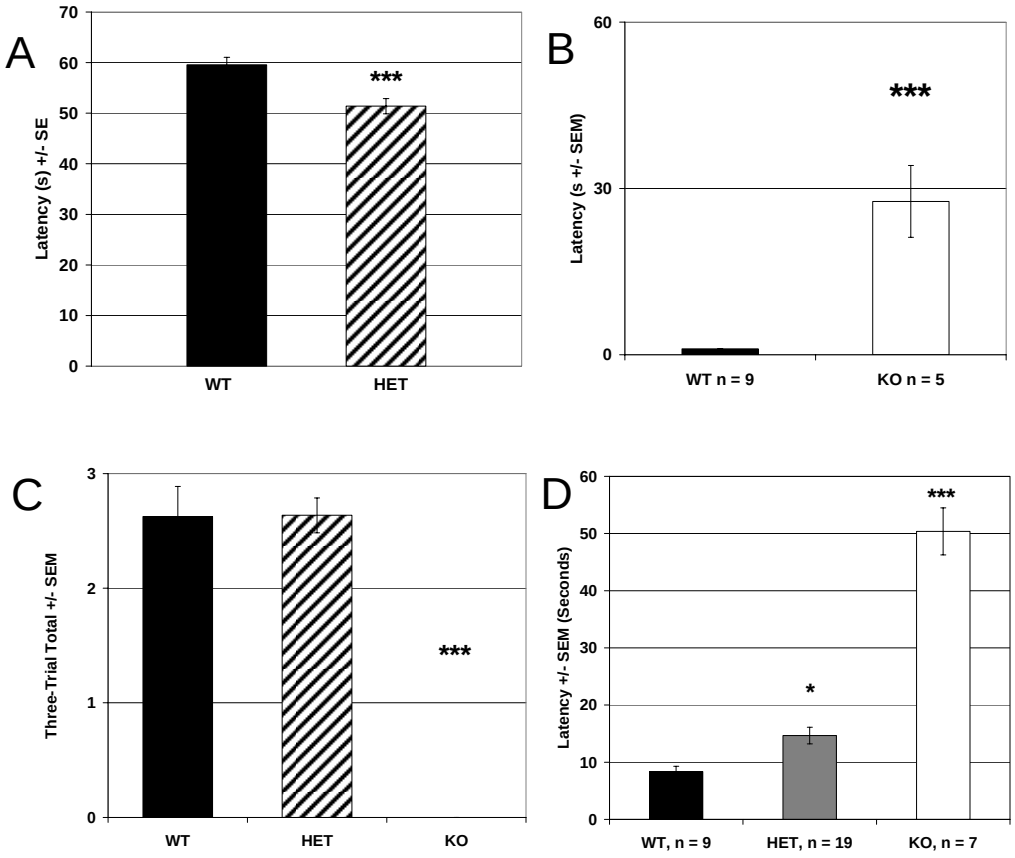

Figure 3.3: Loss of ERRγ Disturbs Motor Function

due to a yet unappreciated criteria, perhaps a motor/behavioral cue or metabolic/olfactory cue. However, under culled litter conditions, occasional pups have been observed at ten days of age (n = 5) which are not significantly different in weight from littermate controls raised separately (WT = 5.7g±0.2 SEM, n = 7; KO = 5.2g ± 0.2SEM, n = 5). ERRγ-null mice have a significant deficit in the righting reflex and maintenance of a prone tetrapod posture at post natal day 10, despite normal growth and weight gain when compared to littermate, foster-mother-reared controls (Figure 3B).

The effect of ERRγ heterozygosity on motor function was also examined in $ERR\gamma^{+/+}$ and $ERR\gamma^{+/LacZ}$ animals at 17±1 weeks of age. $ERR\gamma^{+/LacZ}$ mice have a modest, yet significant, reduction in motor function as assayed by Roto-Rod test ($ERR\gamma^{+/+}$, 60.5 ± 1.9 SEM; $ERR\gamma^{+/LacZ}$, 51.2 ± 2 SEM seconds. Student's T-test $P<0.001$, N = 55, in each group) that is not sex dependent (data not shown).

In addition to the whole animal righting reflex, the CPG activity can be studied in the intact conscious animal by administration of L-DOPA (100 mg/kg s.c.; the BBB-penetrating precursor to dopamine) and quipazine (4mg/kg s.c; a serotonin agonist) to elicit *airstepping* (Van Hartesveldt, 1991). Under these conditions, limb movement is generated for tens of minutes and can be video recorded and quantitated. Twenty-four neonatal mice were collected, numbered and arranged in an orderly manner, secured supine and recorded for one minute 15 minutes after the administration of a PBS vehicle. Under these conditions, mice displayed approximately 1 left-right alternation of the forelimbs over a one minute period independent of genotype (data not shown). The mice were administered the airstepping drug cocktail and video recorded 15 minutes after drug administration. WT and HET mice had robust and well-ordered left-right alternation of the forelimbs in contrast to the less orderly and grossly inappropriate movements of the null animals (Figure 4. WT = 42.0s±1.3 SEM, n = 9; HET = 43.4s±3.1SEM, n = 10; KO = 5.7s±5.7SEM, n = 5. WT v KO: $p < 0.0001$, Student's T-test). The airstepping preparation indicates that under pharmacologic treatments that mimic descending locomotor drive, the ERRγ-null animals have a defect in the organization and execution of alternating limb movements, suggestive of a limb central pattern generator defect. However the airstepping preparation cannot differentiate between forebrain and spinal cord, nor does it eliminate the influence of sensory systems.

Electrophysiologic Recordings

Under a more reduced *in vitro* "fictitious locomotion" preparation the ventral cord is exposed to an oxygenated artificial cerebral spinal fluid bath while the hindlimb innervating nerves and hind limbs are left intact. This preparation can be activated in the presence of drugs such that limb movements can be directly visualized. This eliminates neural structures above the spinal cord, but does not eliminate sensory or musculoskeletal systems. The protocol is a modification of preparations described previously (see Landmesser and O'Donovan, 1984; Whelan et al., 2000). P0 mouse embryos were decapitated and

eviscerated. The remaining tissue was then placed in a dissecting chamber containing artificial cerebrospinal fluid (aCSF) (concentrations in mM: 128 NaCl, 4 KCl, 1.5 $CaCl_2$, 1 $MgSO_4$, 0.5 NaH_2PO_4, 21 $NaHCO_3$, 30 D-glucose), and oxygenated with 95% O_2-5% CO_2. The embryos were pinned down onto a silicone elastomer (Sylgard) base and a ventral laminectomy was performed though spinal level T13 to expose the spinal cord and allow oxygenation. Following these dissection procedures, the preparation was continuously re-circulated oxygenated with aCSF. The aCSF solution was gradually warmed to 30°C for the duration of the experiment. Tissue was allowed to equilibrate to this temperature before were begun.

By further reduction, the electrophysiologic properties of the isolated lumbar locomotor network can be directly recorded from ventral nerve roots and characterized by the periodicity of the movements, the amplitude of the flexor and extensor signals and the phase of these movements relative to the contralateral side or across spinal segmental levels. Preparation is as for fictitious locomotion with the following exceptions. E18.5 mouse embryos were decapitated and eviscerated. After ventral laminectomy, the ventral and dorsal roots were cut and the spinal cord was then transected between T5 and T7 and carefully removed from the spinal column. Following these dissection procedures, the preparation was transferred to the recording chamber and continuously re-circulated with oxygenated aCSF.

Motor neuronal electrical activity was recorded with extra fine-tip suction electrodes pulled from polyethylene tubing (PE 190; Clay Adams, Parsippany, NJ), into which lumbar ventral roots were drawn. The resultant neurograms were amplified (1,000 to 5,000 times), filtered (0.01 Hz to 3 kHz), digitized (National Instruments), and recorded continuously directly to computer using Polyview (Grass Instruments, Rhode Island). Rhythmic alternating ventral root discharge was induced by bath application of a combination of the following drugs (serotonin (5-HT), 10 μM; N-methyl-D,L-aspartate (NMA), 5-10μM; dopamine, 50 μM). A single dose of the chemicals applied to the bath usually produced alternating activity within 5-10 minutes.

For some experiments, the ventral commissure was transected along the entire length of the isolated cord (mid-thoracic to sacral). For this procedure, a fine tungsten needle was utilized**.** In some studies, the glycine re-uptake inhibitor, sarcosine (100μM), was bath-applied. This drug was applied for a

minimum of 20 minutes before assessing its effect on drug-evoked activity by quantifying the change in episode frequency, burst duration, and/or cycle period.

Data Analysis

Data analyses were performed off-line using Polyview (Grass Instruments) acquisition software along with Axograph (Axon instruments) analysis software to determine episode frequency, burst duration, cycle period, and phase angles. If necessary, rectification and smoothing of drug-evoked rhythmic alternating discharges were performed digitally (moving average over 50-500 points). The cycle period of drug-evoked activity was determined by measuring the peak activity of the low-pass filtered record (0.1-10 Hz). Burst durations and cycle periods for drug-evoked alternating activity were determined through an analysis of ≥30 bursts per embryo. At least 7 embryos were used in the determination of average locomotor burst parameter values.

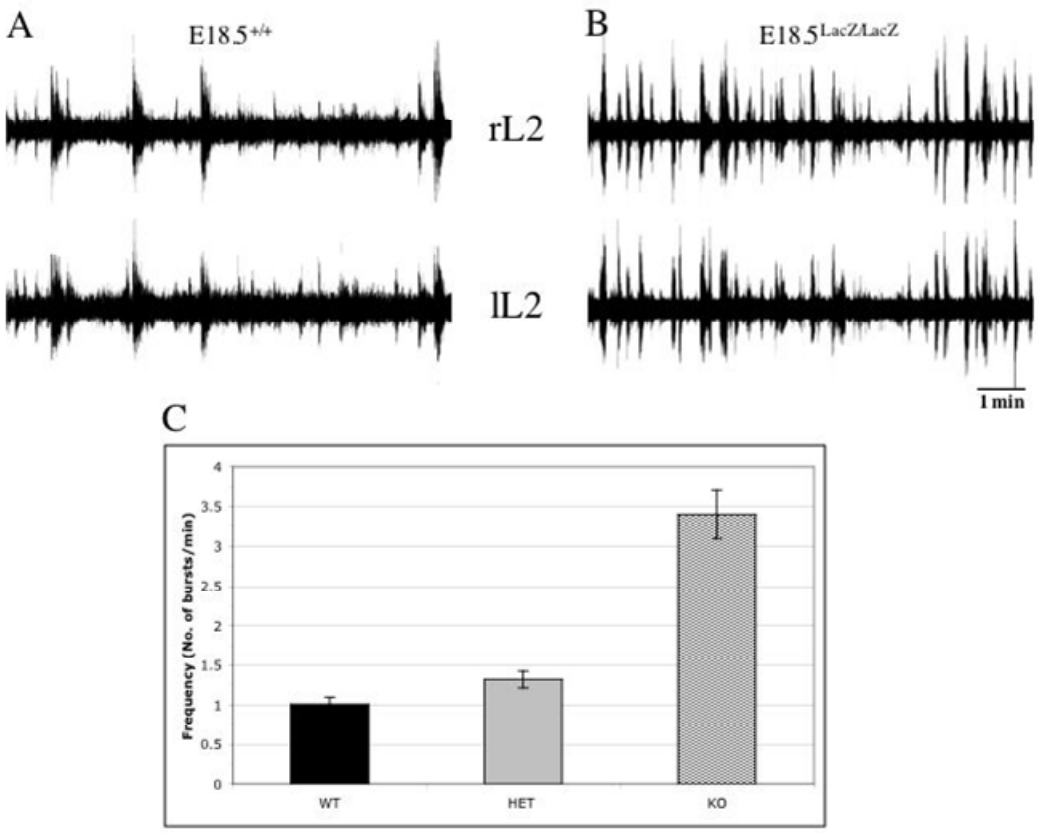

Figure 3.4: Increased Spontaneous Bursting in ERRγ-null Cord.

Coupling between the bursting of left and right L2 or ipsilateral L2 and L5 roots was determined using circular statistics to generate phase values (Kjaerulff and Kiehn, 1996). In short, lumbar root phase values were plotted on a circle representing the interval of possible phases from 0 to 1. The phase values 0 and 1 are equivalent and reflect synchrony, whereas the value 0.5 reflects alternation. The mean phase is indicated by the direction of the vector originating from the center of the circle. A measure, r, indicates the concentration of phase values around the mean. Its value ranges from 0 to 1 and is represented graphically by the length of the vector. All data for the burst parameters (burst durations and cycle periods) are given as mean ± SEM. The significance of differences was evaluated using a Student's *t* test, which determined the p value; $p < 0.05$ was considered significant. Spontaneous activity is a characteristic feature of the developing vertebrate spinal cord (Landmesser and O'Donovan, 1984; Nishimaru et al., 1996) that is important in the formation of spinal locomotor circuits. In order to evaluate the effect of ERRγ deficiency on the pattern and frequency of spontaneous activity, electrophysiological measurements of burst frequency and burst duration were performed on the second lumbar (L2) ventral roots of E18.5 isolated spinal cord preparations (Figure 4A; Experimental Procedures). The general pattern of rhythmic spontaneous bursting displayed similar frequent, synchronized bursts of variable duration, independent of genotype (Figure 4B). However, the frequency of bursting was observed to be approximately three-fold higher in the ERRγ null cord (3.40 ± 0.31 SEM bursts/min, N=11) than in the cords of littermate controls ($ERR\gamma^{+/+}$ 1.01 ± 0.09 SEM, n = 12; $ERR\gamma^{+/LacZ}$ 1.32 ± 0.11 SEM n=10 bursts/min, $P<0.001$).

ERRγ-null Mice Have an Electrophysiological CPG Defect

Application of neurotransmitter agonists, including N-methyl-D-aspartate (NMDA) and serotonin (5-HT), to the isolated spinal cord of late embryonic and neonatal rodents results in rhythmic alternating burst-firing of motor neuron pools in the lumbar cord, as recorded from either ventral roots or hindlimb muscles (Kudo and Yamada, 1987; Smith and Feldman, 1987; Experimental Procedures). This locomotor-like activity is defined by alternating bursts between left and right ventral roots within segments, and between ipsilateral L2 (flexor-related) and L5 (extensor-related) ventral roots across segments.

Exposure of isolated, equilibrated cord to a neurotransmitter agonist cocktail [5-HT, 10 μM; N-methyl-$_{D,L}$-aspartate (NMA), 5-10μM; dopamine, 50 μM)] generates a stereotypical rhythm of left-right

alternating firing in L2 ventral roots within 5-10 minutes, independent of genotype (Figure 4C). In the

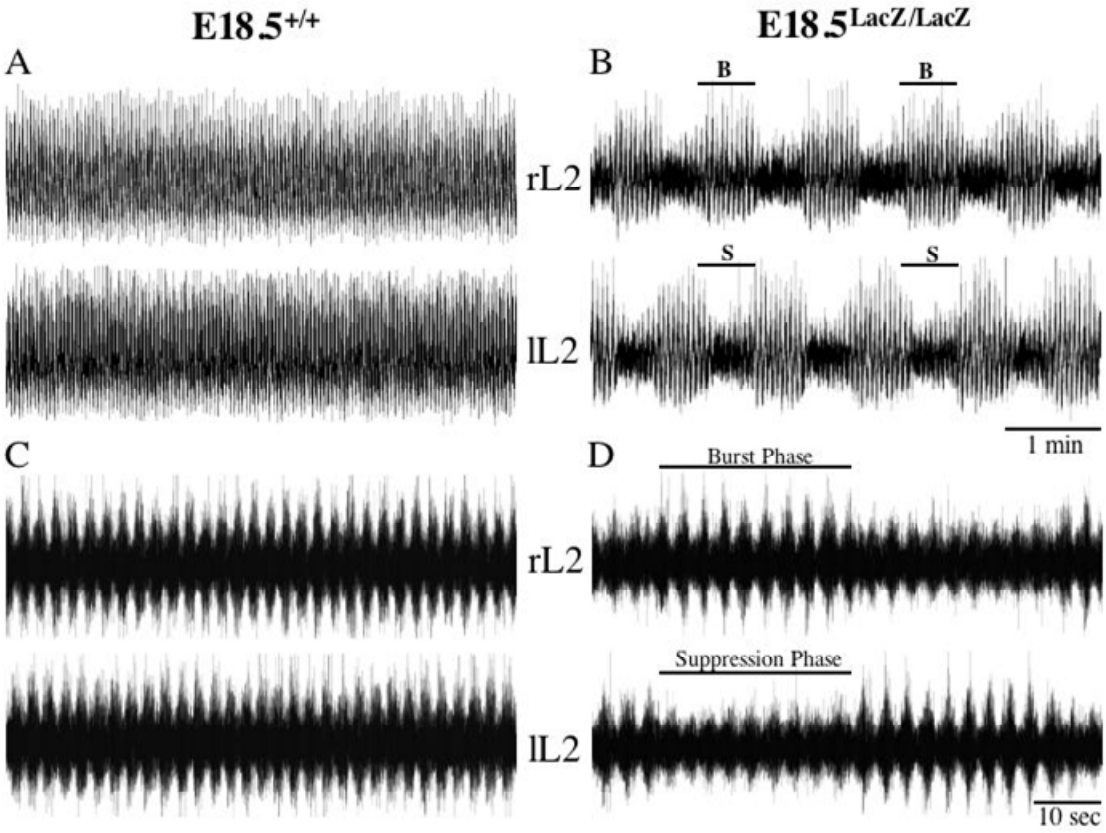

Figure 3.5: Superimposed Pattern of Alternating Suppression: SPAS

ERRγ-null however, a superimposed low frequency (~0.025 Hz) alternating rhythm was observed in the presence of higher frequency (0.5 Hz) stereotypic locomotor alternation (Figure 4C). This lower frequency left-right alternating rhythm can be characterized by having two phases of activity in either L2 root. In the first, or 'burst' phase, a series of bursts of normal amplitude is produced. In the second, or 'suppression' phase, a series of very low amplitude attenuated bursts is produced. Like the 0.5 Hz stereotypical alternating locomotor pattern, the superimposed 0.025 Hz pattern also displays strict left-right alternation that also has a phase angle of 180-degrees (Figure 4C). In the ERRγ-null there are effectively two patterns of alternation: a stereotypic type at 0.5 Hz and a novel superimposed form at 0.025 Hz that we term a *superimposed pattern of alternating suppression* (SPAS). The durations of the 'burst' and 'suppression' phases of the ERRγ null cord were determined to be 26.07 ± 1.94 and 25.95 ± 2.39 seconds.

Quantization of L2 burst duration reveals that loss of ERRγ results in a very significantly decreased burst-firing component of the CPG cycle in either root ($ERR\gamma^{+/+}$: 1.47s ± 0.09 SEM, N=8; $ERR\gamma^{+/LacZ}$: 1.73s ± 0.16 SEM, N=10; $ERR\gamma^{LacZ/LacZ}$: 1.08s ± 0.04 SEM, N=8) during the burst phase of the SPAS, relative to WT controls ($P<0.001$) or the ERRγ-null during the suppression phase of SPAS (1.80s ± 0.11 SEM, $P<0.001$). Furthermore, the burst duration was significantly longer during the suppression phase

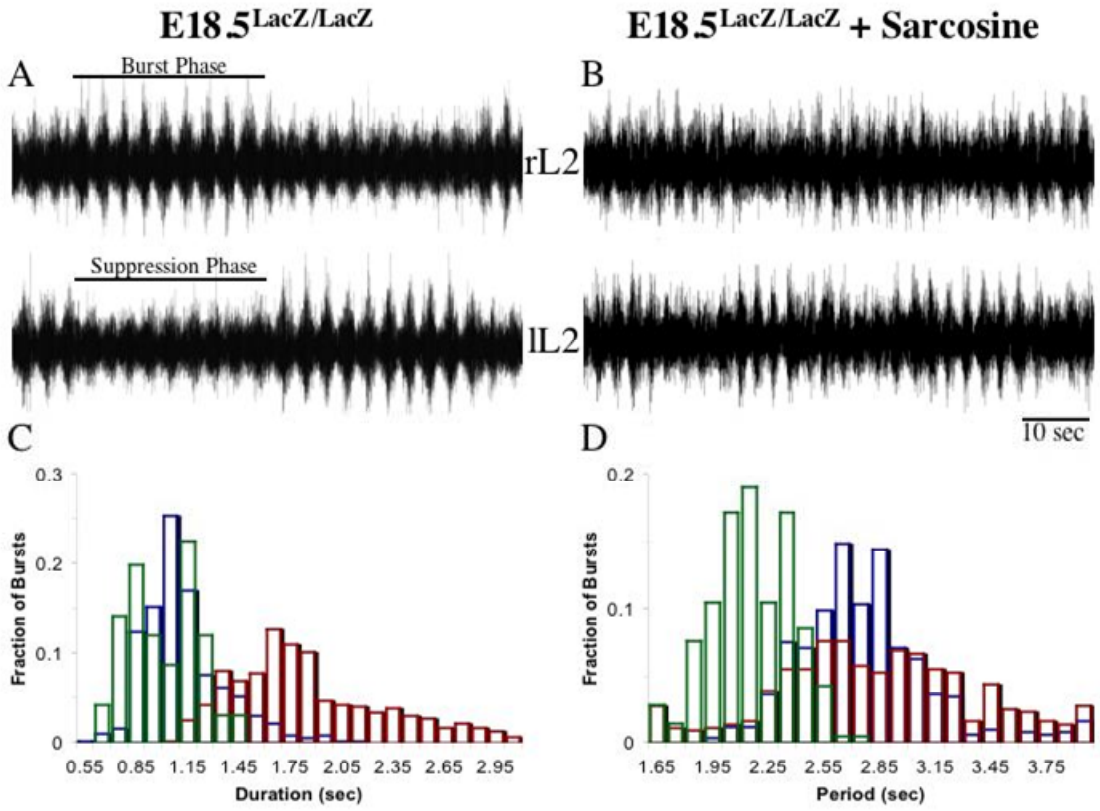

Figure 3.6: Sarcosine Attenuates SPAS

of SPAS, relative to WT controls. ($P<0.05$). Interestingly, there is a significant difference in the burst duration of $ERR\gamma^{+/+}$ and $ERR\gamma^{+/LacZ}$ cord ($p<0.05$), with $ERR\gamma^{+/LacZ}$ cord demonstrating longer burst durations. While the SPAS influenced the burst-firing component of the cycle, the SPAS did not alter the cycle period ($ERR\gamma^{+/+}$: 2.49 ± 0.25 SEM, N=8; $ERR\gamma^{+/LacZ}$: 2.82 ± 0.22 SEM, N=10; $ERR\gamma^{LacZ/LacZ}$: 2.72 ± 0.15 SEM [Burst], 2.92 ± 0.13 SEM [Suppression] , N=8). Consistent approximately 180-degree phase angle measurements, ($ERR\gamma^{+/+}$:179.2º ± 0.50°, r=0.998; $ERR\gamma^{+/}$LacZ:183.0º ± 0.51°, r=0.997;

ERRγ$^{LacZ/LacZ}$: 184.2º ± 0.52°, r=0.995) between right and left L2 burst firing, reflects the cycle period independence from genotype or SPAS phase.

Sarcosine Eliminates SPAS

In light of the three-fold increase in spontaneous activity observed in ERRγ-null isolated cords, an increase inhibitory neurotransmission was made with sarcosine, an inhibitor of the glycine reuptake transporters 1 and 2, in an attempt to eliminate the SPAS. The amino acid neurotransmitter, glycine, has an inhibitory role in spinal cord, and perturbations in glycinergic reuptake have severe effects on motor function and viability that superficially resembles the phenotype of ERRγ-null animals (Gomeza, 2003a, 2003b). Addition of 100 μM sarcosine effectively eliminates the SPAS, but significant differences in burst durations (0.90 ± 0.04 SEM, N=?, P?) or cycle periods (2.05s ± 0.11 SEM P?) persist relative to WT values (WT VALUES) in the presence of sarcosine.

Histogram plots of electrophysiologic characteristics of ERRγ-null cords demonstrate a bi-modal, SPAS-dependent, distribution of burst durations that is restored to a uni-modal distribution (0.90s ± 0.04s) in the presence of sarcosine that more closely resembles the wild-type distribution (Figures 6A and 6F). Application of sarcosine largely, but incomplete eliminates the SPAS, however this experiment cannot discern between an enhanced excitatory tone and a decreased inhibitory tone in the ERRγ-null cord.

SPAS is Dependent on Commissural Projections

CPG functions resident in each hemicord communicate contralaterally via reciprocal projections resident in the ventral commissure; the interruption of which eliminates left-right phase alignment between hemicords, but not firing within either hemicord. The strictly alternating CPG nature of the SPAS suggests a contribution by direct, reciprocal projections resident in the ventral commissure that can be examined experimentally by recording from a 'split-cord' preparation in which the commissural connections have been interrupted. In ERRγ$^{+/+}$ split-cord, the loss of contralateral inhibitory projections within the ventral commissure results in an increase in the burst duration and cycle period (Figures 6C and D). Histogram plots of ERRγ-null split cords reflect a loss of SPAS as indicated by loss of the bi-modal distribution of burst duration and the appearance of a broad uni-modal distribution (2.47s ± 0.30 SEM) resembling firstly, the WT split-cord condition (2.89s ± 0.28 SEM) and secondly, the suppression phase of the SPAS (1.80s ±

0.11 SEM). This finding suggests that, during the suppression phase of SPAS, contralateral CPG projections are ineffective and the independent hemicord, split-cord-like, distribution of burst durations is revealed. Split cord preparations also produce a significant slowing of cycle period in both WT (7.60s ± 0.18 SEM) and ERRγ-null (4.40s ± 0.43 SEM) cords, with a significantly attenuated expansion of cycle

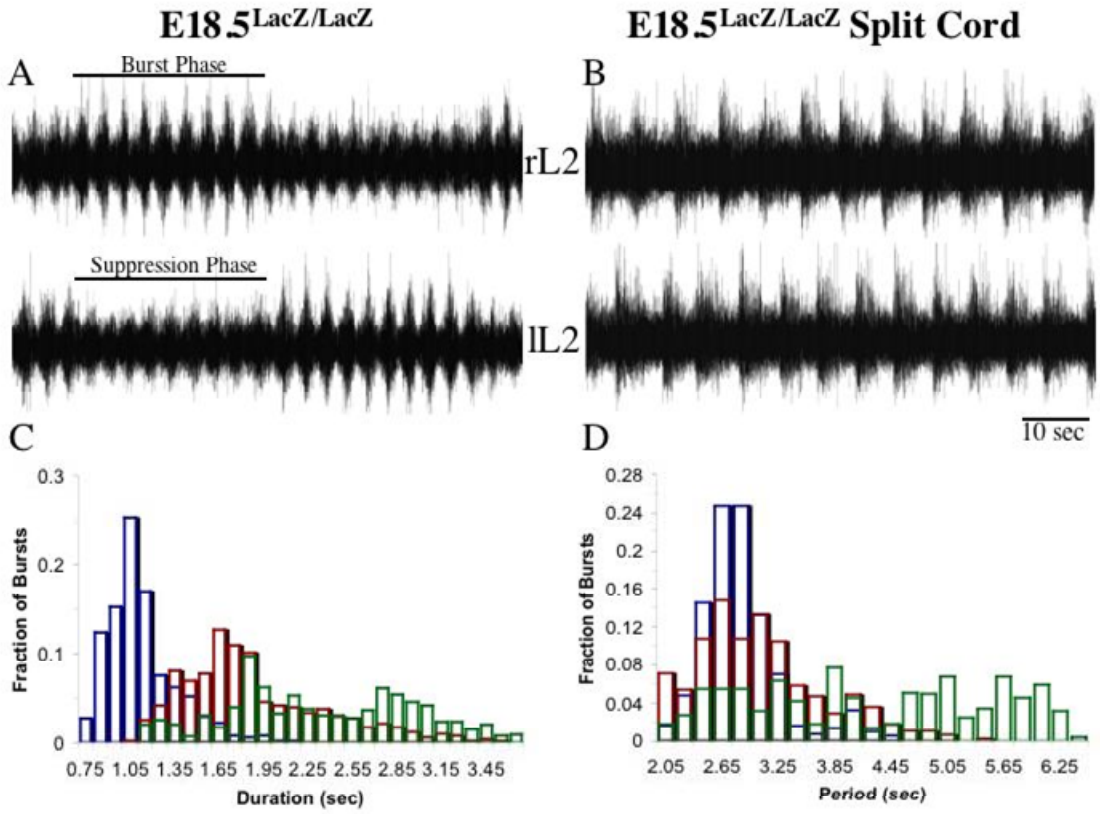

Figure 3.7: Split Cord Attenuates SPAS.

period observed in the ERRγ-null (P<0.001). This finding demonstrates that there is an inherent ipsilateral hemicord alteration in the ERRγ-null CPG that maintains an approximately two-fold higher bursting rate, relative to split-cord controls, in the absence of contributions from commissural projections that is consistent with higher observed spontaneous firing (Figure 4A).

An imbalance in excitation and inhibition is reflected firstly, in higher spontaneous activity in a drug-free preparation, and secondly, by the correction of SPAS in the presence of sarcosine, an inhibitor of glycine transporters. Lesion of the commissural neurons also eliminates the SPAS suggesting that this defect is the result of dysfunction in commissural neurons.

Motor Circuits in the ERRγ Null Cord: An Imbalance of Excitation and Inhibition

Spontaneous activity is a characteristic feature of developing circuits in virtually every part of the nervous system that has been examined (Ben-Ari et al, 1989; Christie et al, 1989; Fortin et al., 1995). This type of network-driven embryonic activity is remarkably similar in tissues as diverse as the hippocampus, retina, and spinal cord (O'Donovan, 1999) and is manifest as recurrent depolarizing events, during which cells within the network are synchronously activated. During these events, intracellular calcium is elevated (Garaschuk, 1998; Kulik, 2000; Leinekugel, 1995; O'Donovan, 1994), suggesting a role in developmental or trophic processes.

Recordings from the L2 roots of the ERRγ-null cord reveal an approximately three-fold increase in the frequency of spontaneous bursting, relative to ERR$\gamma^{+/+}$ and ERR$\gamma^{+/LacZ}$ control cords, suggesting an imbalance in excitatory and inhibitory neurotransmission in the null cord.. This imbalance could result from: firstly, an increase in excitatory input; secondly, a decrease in inhibitory input; or thirdly, some combination of these events. The expression of ERRγ in a subset of glycinergic neurons suggests that loss of ERRγ may alter the functional contribution of these cells to the CPG. In the ERRγ-null, loss of the glycinergic inhibitory potential of these cells could increase the overall level of network excitability.

Histologic Analysis of ERRγ in Spinal Cord

Histochemistry and Immunofluorescence

For X-gal staining, whole embryos (E9.5-E13.5) or dissected tissues from older animals (E18.5-P2) were utilized. Whole mount embryos were then post-fixed in 10% buffered formalin for 1 week, followed by clearing in glycerol at room temperature. Cryosectioned X-gal stains were not cleared by glycerol, but were instead cryoprotected by sinking in 30% sucrose/PBS and embedding in OCT. Frozen sections (12-25 microns) were cut on a Leica cryostat and mounted on Superfrost Plus (Fisher) glass microscope slides. Rabbit anti-ERRγ antiserum was generated by insertion of the ERRγ ligand binding domain RT-PCR product encoding amino acids 228-458 (5'GGATCGATCCAGCCAAAAAGCCATATAAC; 3' CCGGATCCGACCTTGGCCTCCAGCATTTC with 5' ClaI and 3' BamHI restriction sites) into a modified pGEX vector and expression of a GST-ERRγLBD fusion protein in *E. coli*. Immunohistochemistry was performed as described previously (Thaler

et al., 1999). Additional antibodies were as follows: guinea pig anti-Lhx3, guinea pig anti-Isl1/2, guinea pig anti-Hb9, Rabbit anti-Evx1, Goat anti-beta galactosidase, guinea pig anti-VAChT, and guinea pig-anti-GlyT2, Rabbit anti-Sim1 (kind gift of Chen-Ming Fan), mouse anti-GAD67 (kind gift of Paul Sawchenko).

Abnormalities in motor function may be the result of dysfunction in various regions of the central nervous system (CNS) including the cortex, pyramidal and extra-pyramidal motor systems, cerebellum, or spinal cord, as well as various regions of the peripheral nervous system (PNS), including motor nerves and

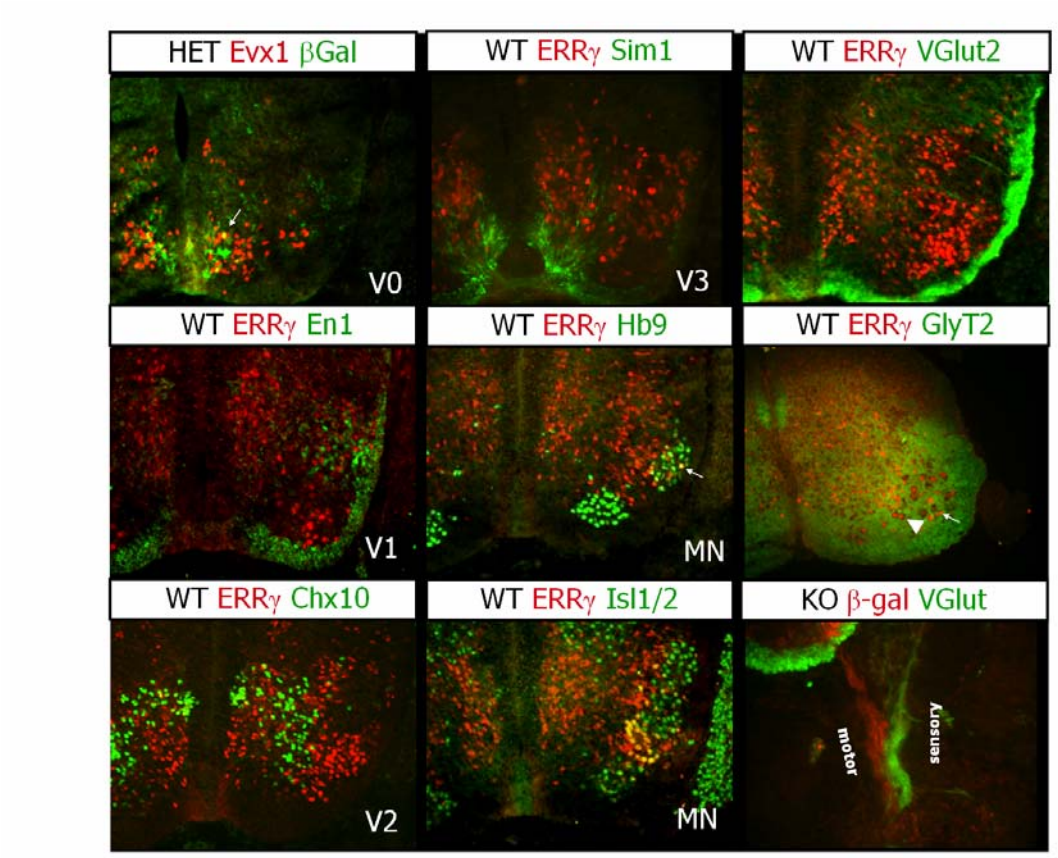

Figure 3.8: Co-localization of Developmental Markers with ERRγ

their muscle targets. To determine which of these structures contribute to the observed motor deficit, whole mount X-gal stains were preformed on developing mice carrying a LacZ knock-in gene under the transcriptional control of the ERRγ locus. Striking ERRγ-dependent LacZ expression is detected in the ventral spinal cord at E10.5 and high expression is retained throughout development and adulthood (Figure 2A). At E13.5, robust expression in detected in ventromedial, ventrolateral, and medial regions of the cord, with enrichment at limb levels (Figure 2A). At the lumbar level, particularly robust expression can be

detected in the lateral motor column. To refine the localization of ERRγ, we generated a polyclonal antibody directed against a divergent portion of the protein, the ligand binding domain (LBD; Experimental Procedures). Immunofluorescent detection of ERRγ protein confirms the regional expression pattern detected by X-gal staining and refines the expression pattern to a cellular resolution allowing localization with known cellular markers (Figure 2A). The enhanced X-gal staining at the lumbar level is due to presence of large, limb-innervating, Isl1/2-positive and Lim3-positive motor neurons in the medial portion of the lateral motor column (LMCm) that express very low levels of Hb9 (Figure 3A). At E13.5, axonal projections of ERRγ positive motor neurons can be detected by immunofluorescent localization of ERRγ directed expression of beta-galactosidase that fills the cytoplasm and axoplasm of ventral, but not dorsal roots (Figure 3.8). The relative contribution of ERRγ cells to regions of motor function was determined by

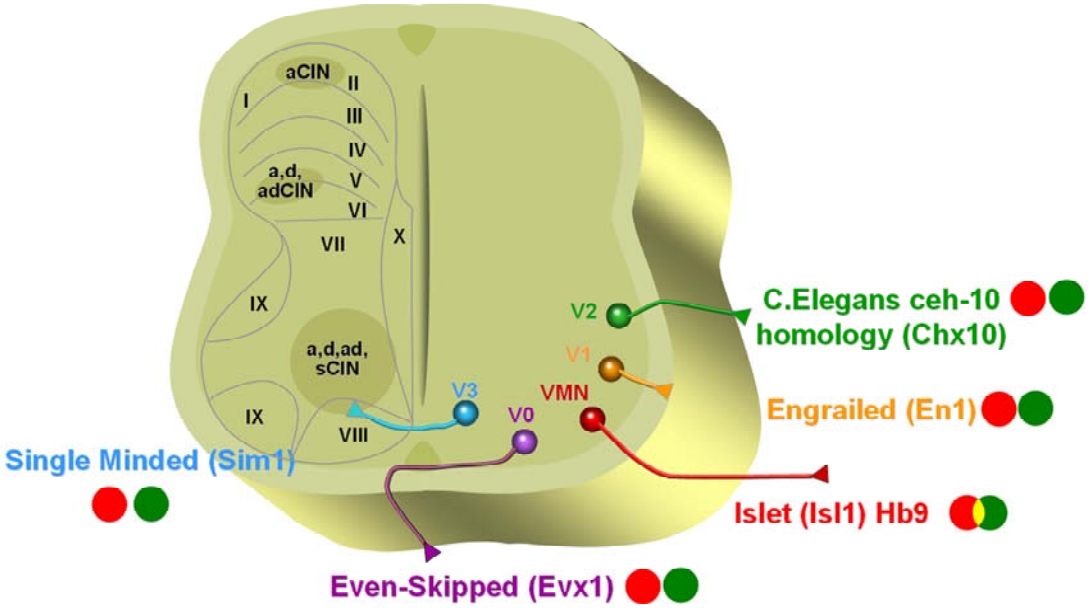

Figure 3.9: ERRγ Defines a Novel Class of Ventral Interneurons

counting ERRγ-positive cells at lumbar, thoracic and brachial levels and comparing them to a known marker for motor neuron specification, Isl1/2. Along the rostro-caudal axis of the spinal cord, ERRγ- and Isl1/2-positive cells were observed in greater numbers at limb levels (Figure 2C) than at thoracic levels.

ERRγ Defines a Heterogeneous Pool of Interneurons and Motor Neurons

Because ERRγ null and heterozygous animals display a motor deficit and have strong expression of ERRγ in motor regions of the spinal cord, immunofluorescent co-localization experiments were performed to define ERRγ-positive cells in reference to known markers of ventral neuron development (Lee and Pfaff, 2001; Goulding and Lamar, 2000). Despite robust and discreet expression of both ERRγ and a panel of known markers in both embryonic mouse and chick, only small subsets of neurons were positive for both ERRγ and particular developmental markers (Figure 3A) Minimal co-expression was detected for the VO Evx1-positive locally projecting intersegmental commissural interneurons, V1 En1-positive ipsilateral intrasegmentally locally projecting interneurons, V2 Chx10-positive intrasegmentally

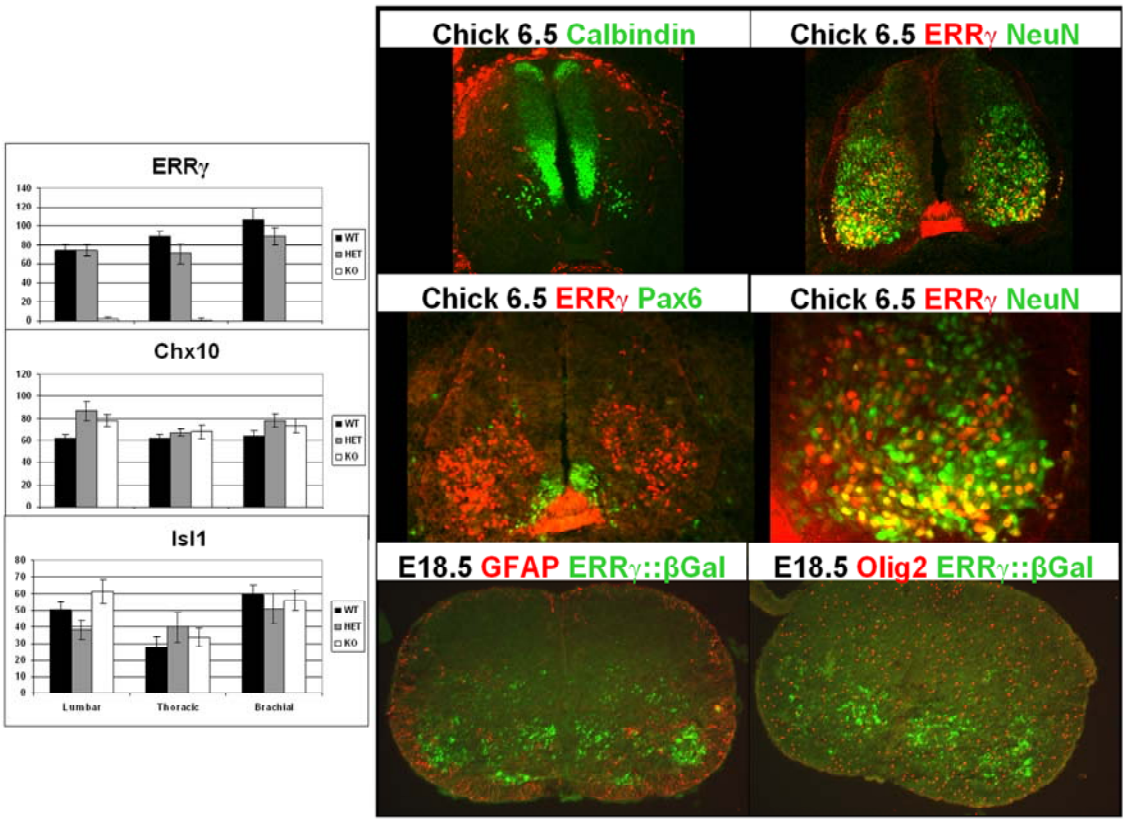

Figure 3.10: Characterization of ERRγ in Spinal Cord

projecting interneurons, or V3 Sim1::LacZ-positive local commissural interneurons with ERRγ-positive nuclei. Only small numbers of Lim3-positive MNs, Isl1/2-positive MNs or Hb9-positive MNs also expressed ERRγ. Less than five-percent of any cell population identified by these developmental markers was also ERRγ positive.

ERRγ-Positive Neurons Express Varied Biosynthetic Markers

To better characterize the phenotype of ERRγ-positive neurons, we employed a panel of biosynthetic and molecular markers of neurotransmitter function. GABAergic neurons express glutamic acid decarboxylase (GAD), glycinergic neurons are characterized by the expression of glycine transporter 2 (GlyT2) primarily localized at synaptic boutons of glycinergic interneurons. ERRγ-positive neurons with cytoplasmic compartments staining for GlyT2 or GAD67 were identified (Figure 3B). Larger ERRγ-positive neurons within Rexed laminae IX were positive for choline acetyltransferase (ChAT) consistent with their localization in a zone containing motor neurons and their expression of motor neuron developmental markers. A subset of motorneurons of the lateral portion of the lateral motor column (LMCl) display co-expression of ERRγ and Islet-1 (Isl1). These cholinergic motor neurons are further

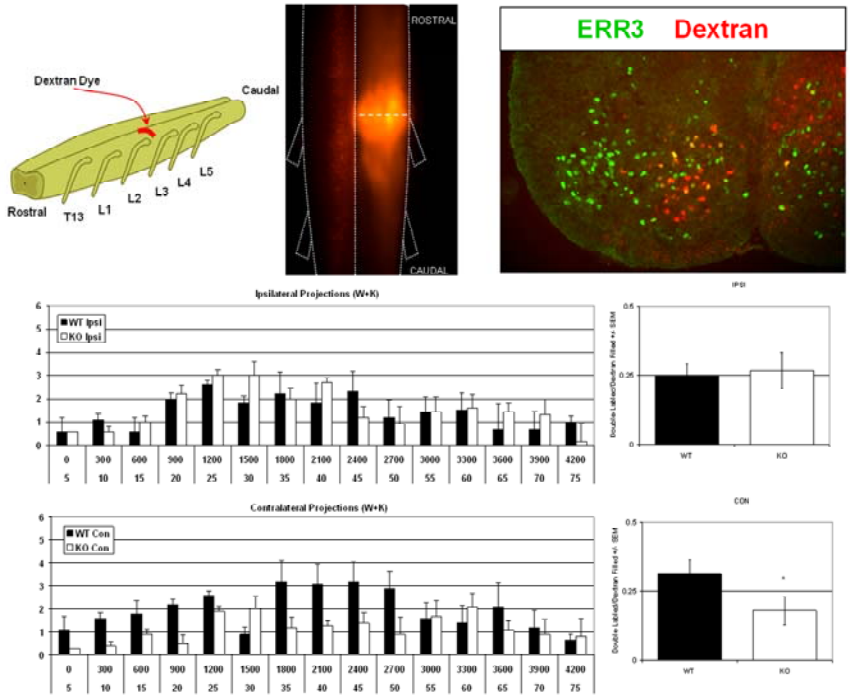

Figure 3.11: ERRγ-null mice have reduced contralateral projections

characterized by low expression of Hb9. Given that the ERRγ cord preparations are grossly normal by several electrophysiologic parameters (phase, burst duration, interburst interval) the defect may not reflect a defect in cell specification, but may be a more subtle defect in wiring or in neurotransmission at the level of neurotransmitter, receptor, second messenger, or ionic flux.

Analysis of the neuronal projections within the lumbar spinal cord was performed by the use of an actively transported dextran-conjugated rhodamine dye. By disrupting the ventral funiculus and placing dextran crystals in the disrupted area during an overnight incubation in oxygenated aCSF, the neurons that have projections through the ventral funiculus can be observed following the uptake of the dextran dye into the cell body. ERRγ-positive cells are identified by immunostaining of the dextran filled section and co-labeled cells quantified. This analysis demonstrated that there are a significantly reduced number of commissural motor neurons in the ERRγ-null animals. This result is compelling given the clear left-right synchrony of the SPAS and that the disruption of the ventral commissure (split-cord preparation) attenuates the SPAS.

Developmental studies in chicken provide several advantages that compliment mouse developmental studies. The developing chick embryo can be directly accessed and manipulated by preparing a fenestrated egg. Introduction of expression and reporter constructs into a hemicord by electroporation allows the detection and alteration of neural lineages. Fluorescent protein under the control of the ERRγ promoter will allow the detection of ERRγ expressing cells in chick in relation to known markers of neuronal development (Lee and Pfaff, 2003). Additionally, antiserum directed against mouse ERRγ recognizes chicken ERRγ. Perturbations in the pattern of known markers can be achieved by ectopic or overexpression of WT ERRγ or its dominant-negative form to address the transcriptional hierarchy that defines the specificity of neurons that contribute to motor function.

REFERENCES

Bai J, Ramos RL, Ackman JB, Thomas AM, Lee RV, LoTurco JJ. RNAi reveals doublecortin is required for radial migration in rat neocortex. Nat Neurosci. 2003 Dec;6(12):1277-83.

Bertrand, S. and Cazalets, J.R. (2002). The respective contribution of lumbar segments to the generation of locomotion in the isolated spinal cord of newborn rat. Eur. J. Neurosci. *16*, 1741-1750.

Blumberg, B. and Evans, R.M. (1998). Orphan nuclear receptors—new ligands and new possibilities. Genes Dev. *12*, 3149-3155.

Bonnelye, E., Vanacker, J.M., Dittmar, T., Begue, A., Desbiens, X., Denhardt, D.T., Aubin, J.E., Laudet, V., and Fournier, B. (1997). The ERR-1 orphan receptor is a transcriptional activator expressed during bone development. Mol. Endocrinol. *11*, 905-916.

Butt SJ, Kiehn O. (2003). Functional identification of interneurons responsible for left-right coordination of hindlimbs in mammals. Neuron *38* 953-63.

Butt SJ, Lebret JM, Kiehn O. Organization of left-right coordination in the mammalian locomotor network. Brain Res Brain Res Rev. Oct;40(1-3):107-17. 2002

Cazalets, J.R., Sqalli-Houssaini, Y., and Clarac, F. (1992). Activation of the central pattern generators for locomotion by serotonin and excitatory amino acids in neonatal rat. J. Physiol. *455*, 187-204.

Chawla, A., Repa, J.J., Evans, R.M., and Mangel SEMorf, D.J. (2001). Nuclear receptors and lipid physiology: opening the X-files. Science *294*, 1866-1870.

Chen H, Tini M, Evans RM. HATs on and beyond chromatin. Curr Opin Cell Biol. Apr;13(2):218-24. Review. 2001

Coward, P., Lee, D., Hull, M.V., and Lehmann, J. (2001). 4-Hydroxytamoxifen binds to and deactivates the estrogen-related receptor γ. Proc. Natl. Acad. Sci. USA *98*, 8880-8884.

Crawley, J.N. (2000) What's Wrong with my Mouse? Behavioral Phenotyping of Transgeneic and Knockout mice. (New York, Wiley-Liss)

Edlund, T. and Jessell, T.M. (1999). Progression from extrinsic to intrinsic signaling in cell fate specification: a view from the nervous system. Cell *96*, 211-224.

Evans, R.M. (1988). The steroid and thyroid hormone receptor superfamily. Science *240*, 889-895.

Evans, RM. Molecular characterization of the glucocorticoid receptor. Recent Prog Horm Res.;45:1-22; 1989

Forman, BM Evans RM. Nuclear hormone receptors activate direct, inverted, and everted repeats. Ann N Y Acad Sci. Jun 12;761:29-37. Review 1995

Giguère, V. (1999). Orphan nuclear receptors: from gene to function. Endocr. Rev. *20*, 689-725.

Giguère, V., Yang, N., Segui, P., and Evans, R.M. (1988). Identification of a new class of steroid hormone receptors. Nature *331*, 91-94.

Glass CK, Rosenfeld MG. The coregulator exchange in transcriptional functions of nuclear receptors. Genes Dev. Jan 15;14(2):121-41 2000

Gomeza J., Hulsmann S., Ohno K., Eulenburg V., Szoke K., Richter D., Betz H. (2003a) Inactivation of the glycine transporter 1 gene discloses vital role of glial glycine uptake in glycinergic inhibition. Neuron *40* 785-96.

Gomeza J., Ohno K., Hulsmann S., Armsen W., Eulenburg V., Richter D.W., Laube B., Betz H. (2003b) Deletion of the mouse glycine transporter 2 results in a hyperekplexia phenotype and postnatal lethality. Neuron *40* 797-806.

Grillner, S., Parker, D., and El Manira, A. (1998). Vertebrate locomotion—a lamprey perspective. Ann. N Y Acad. Sci. *860*, 1-18.

Hamburger, V. and Hamilton, H. (1951). A series of normal stages in the development of chick embryo. J. Morphol. *88*, 49-92.

Hamm JK, Park BH, Farmer SR. A role for C/EBPbeta in regulating peroxisome proliferator-activated receptor gamma activity during adipogenesis in 3T3-L1 preadipocytes. J Biol Chem. 2001 May 25;276(21):18464-71.

Heard, D.J., Norby, P.L., Holloway, J., and Vissing, H. (2000). Human ERRgamma, a third member of the estrogen-related receptor receptor (ERR) subfamily of orphan nuclear receptors: tissue-specific isoforms are expressed during development and in the adult. Mol. Endocrinol. *14*, 382-392.

Hong, H., Yang, L., and Stallcup, M.R. (1999). Hormone-independent transcriptional activation and coactivator binding by novel orphan receptor ERR3. J. Biol. Chem. *274*, 22618-22626.

Hultborn, H., Conway, B.A., Gossard, J.P., Brownstone, R., Fedirchuk, B., Schomburg, E.D., Enriquez-Denton, M., and Perreault, M.C. (1998). How do we approach the locomotor network in the mammalian spinal cord?. Ann. N Y Acad. Sci. *860*, 70-82.

Ibdah JA, Paul H, Zhao Y, Binford S, Salleng K, Cline M, Matern D, Bennett MJ, Rinaldo P, Strauss AW.Lack of mitochondrial trifunctional protein in mice causes neonatal hypoglycemia and sudden death. J Clin Invest. Jun;107(11):1403-9 2001.

Jessell, T.M. (2000). Neuronal specification in the spinal cord: inductive signals and transcriptional codes. Nat. Rev. Genet. *1*, 20-29.

Kiehn O, Butt SJ. Physiological, anatomical and genetic identification of CPG neurons in the developing mammalian spinal cord. Prog Neurobiol. Jul;70(4):347-61. 2003

Kiehn O., Kullander K (2004). Central pattern generators deciphered by molecular genetics. Neuron *41* 317-21.

Kiehn, O. and Kjaerulff, O. (1996). Spatiotemporal characteristics of 5-HT and dopamine-induced rhythmic hindlimb activity in the in vitro neonatal rat. J. Neurophysiol. *75*, 1472-1482.

Kiehn, O. and Kjaerulff, O. (1998). Distribution of central pattern generators for rhythmic motor outputs in the spinal cord of limbed vertebrates. Ann. N Y Acad. Sci. *860*, 110-129.

Kjaerulff, O. and Kiehn, O. (1996). Distribution of networks generating and coordinating locomotor activity in the neonatal rat spinal cord in vitro. A lesion study. J. Neurosci. *16*, 5777-5794.

Kudo, N. and Yamada, T. (1987). Morphological and physiological studies of development of the monosynaptic reflex pathway in the rat lumbar spinal cord. J. Physiol.

Kudo, N. and Yamada, T. (1987). N-methyl-D,L-aspartate-induced locomotor activity in a spinal cord-hindlimb muscles preparation of the newborn rat studied in vitro. Neurosci. Lett. *75*, 43-48.

Kullander K, Butt SJ, Lebret JM, Lundfald L, Restrepo CE, Rydstrom A, Klein R, Kiehn O. Role of EphA4 and EphrinB3 in local neuronal circuits that control walking. Science. Mar 21;299(5614): 1889-92. 2003

Landmesser L.T., O'Donovan, M.J. (1984) Activation patterns of embryonic chick hindlimb muscles recorded in ovo and in an isolated spinal cord preparation. J Physiol. *347* 189-204.

Lanuza GM, Gosgnach S, Pierani A, Jessell TM, Goulding M. Genetic identification of spinal interneurons that coordinate left-right locomotor activity necessary for walking movements. Neuron. 2004 May 13;42(3):375-86

Le Roy I., Perez-Diaz F., Cherfouh A., Roubertoux P.L. (1999) Preweanling sensorial and motor development in laboratory mice: quantitative trait loci mapping. Dev Psychobiol. *34* 139-58.

Lee CH, Chawla A, Urbiztondo N, Liao D, Boisvert WA, Evans RM. Transcriptional Repression of Atherogenic Inflammation: Modulation by PPARδ. Science. 2003

Lee SK, Pfaff SL. Synchronization of neurogenesis and motor neuron specification by direct coupling of bHLH and homeodomain transcription factors. Neuron. 2003 Jun 5;38(5):731-45.

Lee SK, Pfaff SL.Transcriptional networks regulating neuronal identity in the developing spinal cord. Nat Neurosci. Nov;4 Suppl:1183-91. 2001

Lee, S.K. and Pfaff, S.L. (2001). Transcriptional networks regulating neuronal identity in the developing spinal cord. Nat. Neurosci. *4*, 1183-1191.

Lehman JJ, Kelly DP. Transcriptional activation of energy metabolic switches in the developing and hypertrophied heart. Clin Exp Pharmacol Physiol. Apr;29(4):339-45. Review 2002

Lipshutz RJ, Fodor SP, Gingeras TR, Lockhart DJ. High density synthetic oligonucleotide arrays.Nat Genet. Jan;21(1 Suppl):20-4. 1999

Lockhart DJ, Barlow C. Expressing what's on your mind: DNA arrays and the brain. Nat Rev Neurosci. Jan;2(1):63-8. 2001

Mangelsdorf, D. and Evans, R.M. (1995). The RXR heterodimers and orphan receptors. Cell. 1995 83(6), 841-50.

Miles PD, Barak Y, Evans RM, Olefsky JM. Effect of heterozygous PPARgamma deficiency and TZD treatment on insulin resistance associated with age and high-fat feeding. Am J Physiol Endocrinol Metab. Mar;284(3):E618-26. 2003

Misner DL, Jacobs S, Shimizu Y, de Urquiza AM, Solomin L, Perlmann T, De Luca LM, Stevens CF, Evans RM. (2001) Vitamin A deprivation results in reversible loss of hippocampal long-term synaptic plasticity. Proc Natl Acad Sci U S A.*98* 11714-9.

Nakamura, H., Watanabe, Y., and Funahashi, J. (2000). Misexpression of genes in brain vesicles by in ovo electroporation. Dev. Growth Differ. *42*, 199-201.

Nishimaru H, Iizuka M, Ozaki S, Kudo N. (1996) Spontaneous motoneuronal activity mediated by glycine and GABA in the spinal cord of rat fetuses in vitro. J Physiol. *49*7 131-43.

Palmiter RD, Brinster RL, Hammer RE, Trumbauer ME, Rosenfeld MG, Birnberg NC, Evans RM.Dramatic growth of mice that develop from eggs microinjected with metallothionein-growth hormone fusion genes.Nature. 1982 Dec 16;300(5893):611-5.

Razzaque MA, Masuda N, Maeda Y, Endo Y, Tsukamoto T, Osumi T. Estrogen receptor-related receptor gamma has an exceptionally broad specificity of DNA sequence recognition. Gene. 2004 Oct 13;340(2):275-82

Reichardt HM, Kaestner KH, Tuckermann J, Kretz O, Wessely O, Bock R, Gass P, Schmid W, Herrlich P, Angel P, Schutz G. DNA binding of the glucocorticoid receptor is not essential for survival. Cell. May 15;93(4):531-41 1998.

Smith J.C., Feldman J.L. (1987) In vitro brainstem-spinal cord preparations for study of motor systems for mammalian respiration and locomotion.J Neurosci Methods. *21* 321-33.

Susens U, Hermans-Borgmeyer I, Borgmeyer U.Alternative splicing and expression of the mouse estrogen receptor-related receptor gamma. Biochem Biophys Res Commun. Jan 19;267(2):532-5. 2000

Todaro GJ, Green H. Quantitative studies of the growth of mouse embryo cells in culture and their development into established lines. J Cell Biol. May;17:299-313. 1963

Tronche F, Kellendonk C, Kretz O, Gass P, Anlag K, Orban PC, Bock R, Klein R, Schutz G. Disruption of the glucocorticoid receptor gene in the nervous system results in reduced anxiety. Nat Genet. Sep;23(1):99-103. 1999

Umesono K., Evans R.M. (1989) Determinants of target gene specificity for steroid/thyroid hormone receptors. Cell *57* 1139-46.

Van Hartesveldt C, Sickles AE, Porter JD, Stehouwer DJ. L-dopa-induced air-stepping in developing rats. Brain Res Dev Brain Res. 1991 Feb 22;58(2):251-5.

Wang YX, Lee CH, Tiep S, Yu RT, Ham J, Kang H, Evans RM. Peroxisome-proliferator-activated receptor delta activates fat metabolism to prevent obesity. Cell. Apr 18;113(2):159-70. 2003

Whelan P.J.. (2003) Developmental aspects of spinal locomotor function: insights from using the in vitro mouse spinal cord preparation. J Physiol. *553* 95-706.

Xie, W., Hong, H., Yang, N.N., Lin, R.J., Simon, C.M., Stallcup, M.R., and Evans, R.M. (1999). Constitutive activation of transcription and binding of coactivator by estrogen-related receptors 1 and 2. Mol. Endocrinol. *13*, 1594-1604.

Yu RT, McKeown M, Evans RM, Umesono K. (1994). Relationship between Drosophila gap gene tailless and a vertebrate nuclear receptor Tlx. Nature *370* 375-9.

Zetterstrom R.H., Solomin L., Jansson L., Hoffer B.J., Olson L., Perlmann T. (1997). Dopamine neuron agenesis in Nurr1-deficient mice. Science 276248-50.

Acknowlegements

Collaborators subject to authorship deriving from this work include:

Matthew Bloch Michael Downes, Ph.D.

Catherine Dufour , M.S.	Ronald M. Evans, Ph.D.
Benjamin W. Gallarda	Vincent Giguere, Ph.D.
Wayne R. Giles, Ph.D.	Johann W. Jonker, Ph.D.
Richard Kondo, Ph.D.	Alexander Lehrman, M.S.
Christopher P Myers, M.D. Ph.D.	Robert K. Naviaux, M.D. Ph.D.
Jordan Nevo	Samuel L. Pfaff, Ph.D.
Wen Xie, M.D. Ph.D.	Ruth T. Yu, M.D. Ph.D.

Alaynick WA; Myers CP; Gallarda BW; Pfaff SL, Evans RM. "Locomotor Defects in Estrogen-related Receptor Gamma Mutant Mice" In Preparation.

Alaynick WA; Kondo R; Xie W; Downes M; Dufour C; Jonker JW; Yu RT; Lehrman A; Nevo J; Bloch M; Naviaux RK; Giles WR; Giguere V; Evans RM. "Cardiac conduction Defects in Estrogen-related Receptor Gamma Mutant Mice". In Preparation

Chapter 4

Cardiac Dysfunction

The Role of ERRγ in Cardiac Function

ERRγ is highly expressed throughout cardiac development, from E8.5 through adulthood. Given the profound phenotype of the ERRγ-null spinal cord central pattern generator combined with the diffuse expression in this excitable tissue, studies were directed towards characterizing the role of ERRγ in the heart: a more homogeneously expressing excitable tissue amenable to electrophysiologic analysis and to molecular analyses frustrated by the diffuse ERRγ expression in the spinal cord.

The measurement of the electrical activity of the heart was established in the late 19th century by Ludwig and Waller followed by the precursor of the modern electrocardiograph (ECG or EKG) in 1901 by Einthoven (Dubin, 1994). The heart can be divided into two forms of electrically excitable muscle tissue: firstly, the working myocardium composed of force generating muscle tissue; and secondly, the conducting myocardium composed of specialized nerve-like muscle tissue that serves to transmit depolarizing electrical activity to the working myocardium in an organized manner so as to coordinate the pumping actions of the atria and ventricles. The action potentials and depolarizations of the conducting myocardium are too feeble to be measured by electrodes on the body surface. The electrical activity of the larger working myocardium can be measured by body surface electrodes in the form of an ECG and many properties of the working and conducting myocardium deduced from the properties of the ECG.

The heart beats at a rate appropriate to address the flow and pressure requirements needed to deliver oxygenated blood to the body. The rate is determined by the sino-atrial node, a collection of conducting myocardium cells that act as a pacemaker. Action potentials from the SA node travel through and depolarize the atria to create a positive deflection in a Lead II ECG called the P wave. The P wave is a measure of the electrical depolarization of the atria that is associated with the muscular contraction of the working atrial myocardium that forces blood from the left and right atria into the left and right ventricles. The P wave is followed by a period of electrical inactivity called the PR interval that represents a pause in the conduction system that allows the ventricles to remain relaxed while blood from the atria fills the ventricles. This pause is generated by the atrioventricular (AV) node and the PR interval is measure of AV function.

The most prominent feature of the ECG is the QRS complex which represents the electrical depolarization of the working ventricular myocardium which forces blood from the right ventricle towards the lungs and from the left ventricle through the aorta to the body. The duration of the QRS is determined

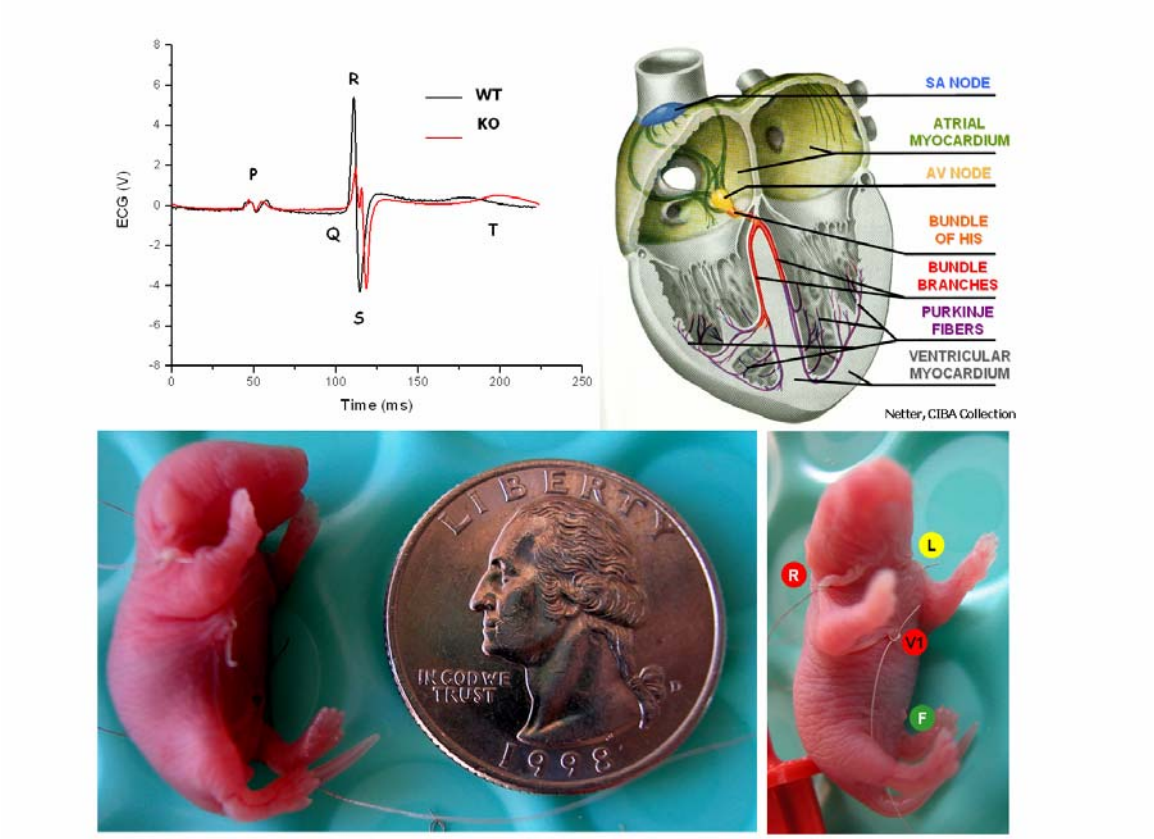

Figure 4.1: Electrocardiographic Analysis of ERRγ Mice

by two components. Firstly, the amount of time is takes the depolarizing electrical stimulus produced by the AV node to traverse the ventricular conducting system. The ventricular conduction system (composed of conducting myocardium) is made up of the bundle of His, the right and left bundle branches and their fine ramifications, the Purkinje fibers which are electrically coupled directly to the working myocardium via gap junctions composed of connexins. Secondly, the duration of the QRS is dependent on the rate at which the working myocardium depolarizes in response to the electrical stimulus delivered by the conduction system. Depolarization is mediated by sodium current crossing the cardiomyocyte membrane via voltage gated sodium channels, the major form of which, $Na_V1.5$, is encoded by the Scn5a gene.

Following depolarization of the ventricle, contraction of the working myocardium and ejection of blood, there is a second period of electrical inactivity, the ST interval. This period is followed by a positive ECG voltage reading produced by the repolarization of the working myocardium called the T-wave. Metabolic or ionic disturbances in the ventricular working myocardium can cause a prolongation in the occurrence of the T-wave, termed prolonged QT-interval that is pathomnemonic for potential arrhythmia and sudden death. Because of the long history and strong diagnostic power of the ECG, the ERRγ-mutant mice were subjected to ECG analysis.

Standard Lead II and V1 electrocardiographic recording were adapted to neonatal (E18.5 to P0, ~1.25g) mice in combination with computer analysis and quantification of the ECG waveform, analyses were undertaken to study the effects of loss of ERRγ on heart function. Chlorided 0.004-inch sterling silver wires (Fine ChemMetals) were sutured above the right forelimb and left hind limb (for Lead II) with the addition of leads above the left forelimb and at the second intercostal space (for V1). The electrode wires were attached to a head stage which was attached in series to a noise filter to remove sixty-cycle interference (HumBug) and oscilloscope (BK Precision) an analog to digital converter (National Instruments) and a personal computer. The signal was recorded with software (QRS) and stored for later analysis. Recording were performed for approximately 100 seconds at 6 kilohertz to obtain approximately 400 beats. The analysis program then grouped the individual beats by a component of the waveform termed the *zero crossing* where the QRS complex crosses the isoelectric line of the ECG recording. The software then selected the 100 most similar beats and compiled them to form an averaged *mean beat* from which quantitative measurements were derived by the software. Mice were recorded while placed left-recumbent on a 37°C water blanket. Neonatal mice do not regulate their body temperature and core body temperatures were recorded from a subset of animals by decapitation followed by insertion of thermistor probe in to the thoracic space. No significant difference was observed in core body temperature with regards to genotype.

Initial studies were preformed on litters obtained from $ERR\gamma^{+/LacZ}$ x $ERR\gamma^{+/LacZ}$ crosses under standard breeding conditions. Under these conditions, ERRγ-null mice have significantly reduced body weight (WT = 1.53g±0.03SEM; HET = 1.54±0.03SEM; KO = 1.40g±0.03SEM; WT v KO: $p < 0.001$, Student's T-test), milk intake (WT = 87%; HET = 84%; KO = 5%; WT v KO: $p < 0.0001$, Student's T-

test) and significantly and dramatically reduced serum glucose values (WT = 66±3SEM; HET = 62±2SEM; KO = 29±3SEM; WT v KO: $p < 0.0001$, Student's T-test). Measures of ECG parameters showed that all aspects of the ECG were significantly altered in the calorically-deprived ERRγ-null mice. Importantly, the

Table 4.1: E18.5 Caesarean Sectioned Mouse ECG Parameters (in milliseconds ± SEM)

	RR	P	PR	QRS	ST	QT	QTc
WT n=61	159.09 ± 2.58	12.45 ± 0.35	56.86 ± 1.07	9.05 ± 0.15	70.64 ± 1.19	79.70 ± 1.21	199.95 ± 2.19
HET n=104	162.50 ± 2.02	12.76 ± 0.26	58.22 ± 0.69	10.21 ± 0.18	72.67 ± 1.04	82.89 ± 1.07	205.53 ± 1.92
KO n=55	164.33 ± 2.49	12.61 ± 0.29	56.38 ± 0.89	11.77 ± 0.23	76.82 ± 1.34	87.89 ± 1.25	216.82 ± 2.11

heterozygous mice which have normal weights, milk scores, core body temperatures and blood glucose values, displayed a significant prolongation of the QRS complex. This suggested that the QRS complex may be perturbed in an ERRγ-dependent manner independent of caloric state.

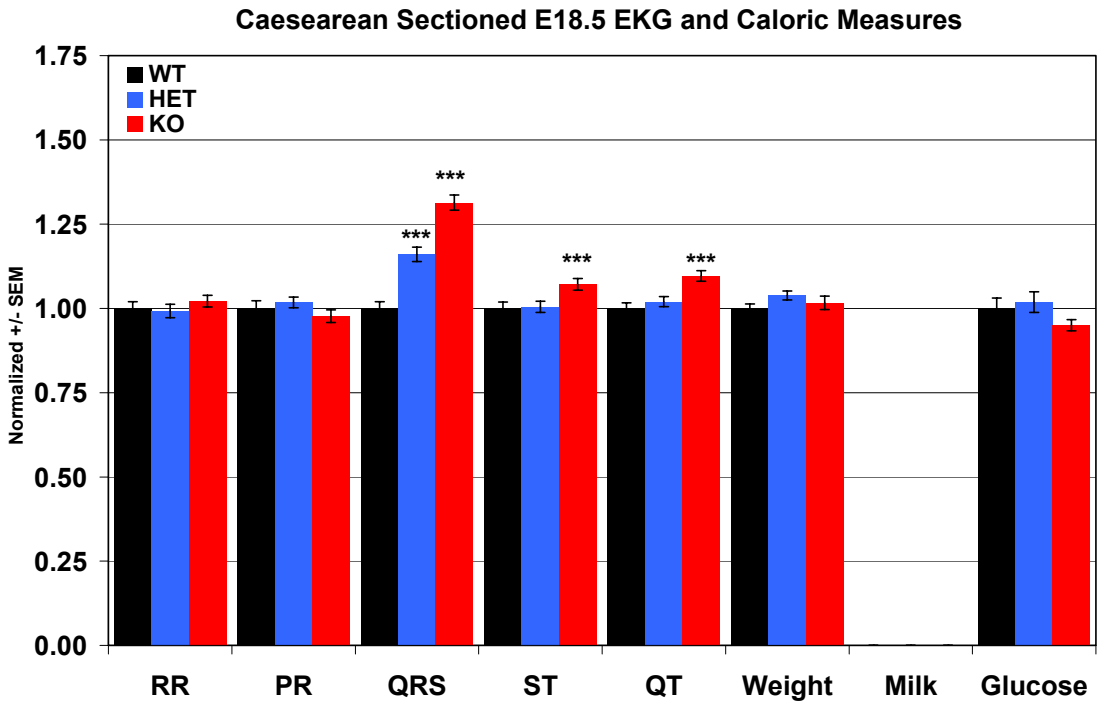

Figure 4.2: ECG Reveals Prolonged QRS and QT with Loss of ERRγ

In order to evaluate ERRγ-null mice during an energy-replete status, E18.5 mice were delivered by caesarean section and evaluated within one hour of birth. Under these conditions, ERRγ-null mice have normal body weights and blood glucose values. Analysis of neonatal mouse ECGs under caesarean-sectioned conditions revealed in the ERRγ-null animals a normal heart rate, PR-interval and ST interval.

Despite the normalization of these parameters, the QRS duration was prolonged by 35% in null animals and by 10% in heterozygous animals relative to WT littermate controls. The QT interval, prolongation of which is predisposing for arrhythmia and sudden death, was also prolonged in the null animals entirely due to the contribution of the QRS duration, with no statistically significant increase in the ST interval in ERRγ-null mice. The observation of a normal RR interval or heart rate indicates that the sinoatrial (SA) node is functioning properly. The contraction of the atria occurs normally in ERRγ-null animals as indicated by the normal P-wave duration. The normal PR interval indicates that the AV node is capable of generating an appropriate pause to allow blood from the atria to fill the ventricles prior to ventricular contraction. The prolongation of the QRS indicates that the depolarization of the ventricular myocardium is not occurring

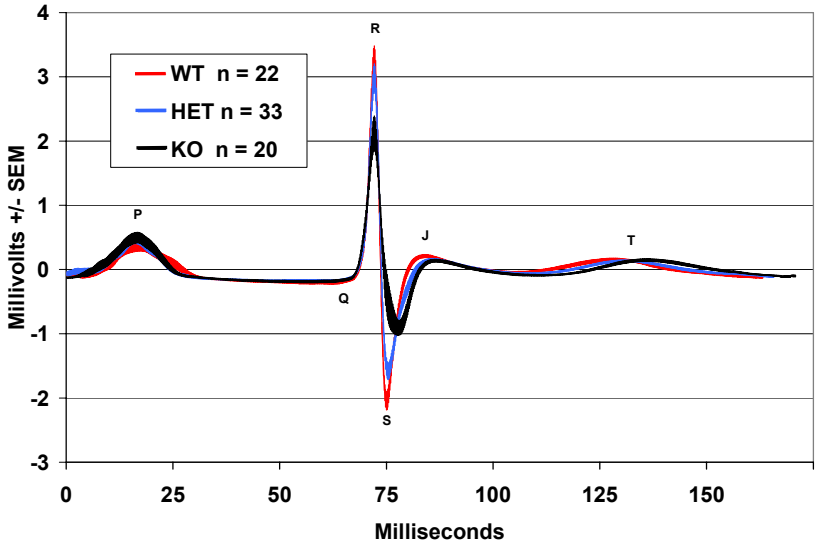

Figure 4.3: Altered ECG Morphologies in ERRγ-null Mice

properly. There are two explanations for this. First, a condition known as bundle block can occur where the repolarizing potential produced by the AV node is not propagated well through ventricular conducting system composed of the Bundle of His and the right and left bundle branches which are derived from specialized muscle tissue with nerve-like qualities. The right bundle branch is smaller and most susceptible to defects in conduction, termed *block*, which are variable in severity. ECG analysis produces characteristic waveforms under conditions of bundle branch block (BBB) that are diagnostic of left or right BBB.

Secondly, the ventricular conduction system (conducting myocardium) may be functioning properly and the defect may occur at the working myocardium. An inability of the working cardiomyocytes to generate a robust depolarizing action potential would appear on the ECG as a BBB. The ECG only records the depolarization of the working myocardium and therefore cannot distinguish between delayed or attenuated conduction and blunted depolarizing action potentials in the working myocardium. The depolarization of the action potential is mediated by sodium current through the sodium channel $Na_{v1.5}$ which is encoded by the Scn5a gene in mouse. The sodium channel forms functional channels in association with accessory subunits encoded by the Scn1b, Scn2b and Scn3b genes.

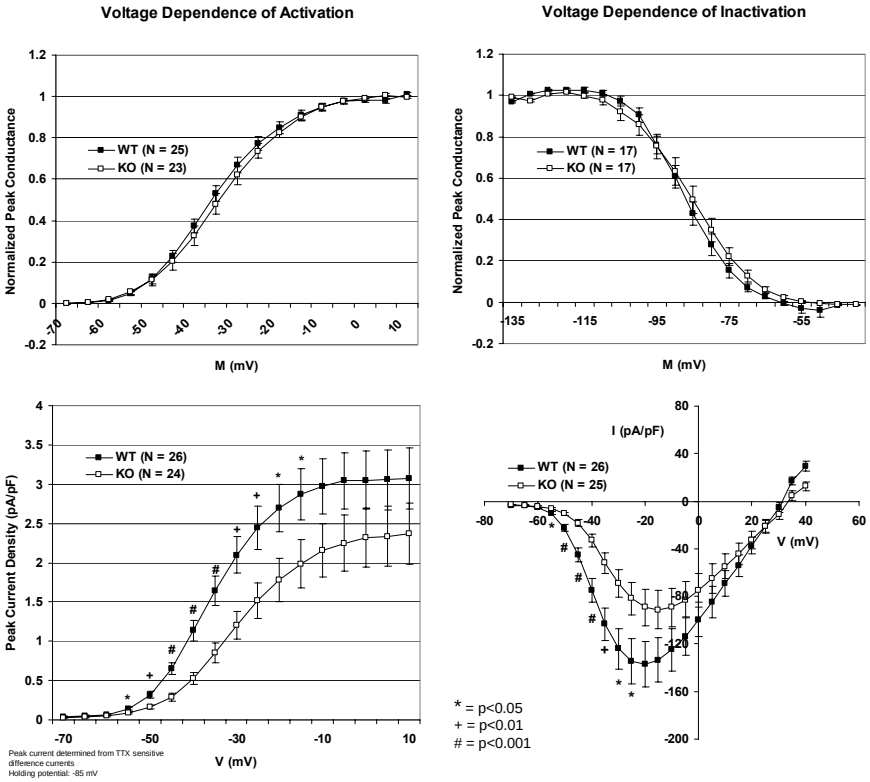

Figure 4.4: ERRγ-null Cardiomyocytes Have Reduced Sodium Current

The sodium conducting properties of the working cardiomyocytes were studied by enzymatic and mechanical dissociation and isolation of primary cardiomyocytes from E18.5 mice delivered by caesarean section and genotyped prior to collection of ventricular myocardium. Single ventricular neonatal myocytes

were isolated from perinatal pups delivered by caesarian section at embryonic day 18.5. Dissociated ventricular myocytes were cultured in MEM media for 36 hours before the commencement of electrophysiological studies which were performed at room temperature (18-22° C). The voltage dependent sodium current was recorded using the whole cell, voltage clamp technique with an Axopatch 200B patch clamp amplifier (Axon Instruments) and PC based data acquisition system. The culture plates containing the myocytes were positioned on the stage of an Axiovert 10 (Zeiss) invert microscope and the myocytes were superfused with a modified Tyrode's solution (100 TEA-Cl, 40 NaCl, 1 $MgCl_2$, 1 $CaCl_2$, 10 HEPES, 10 glucose, pH 7.4). Recording microelectrodes were pulled from 1.5mm OD capillary glass (WPI Instruments, PG52151) to a final pipette resistance of 1.5 to 2.5 megaohms after filled with the patch

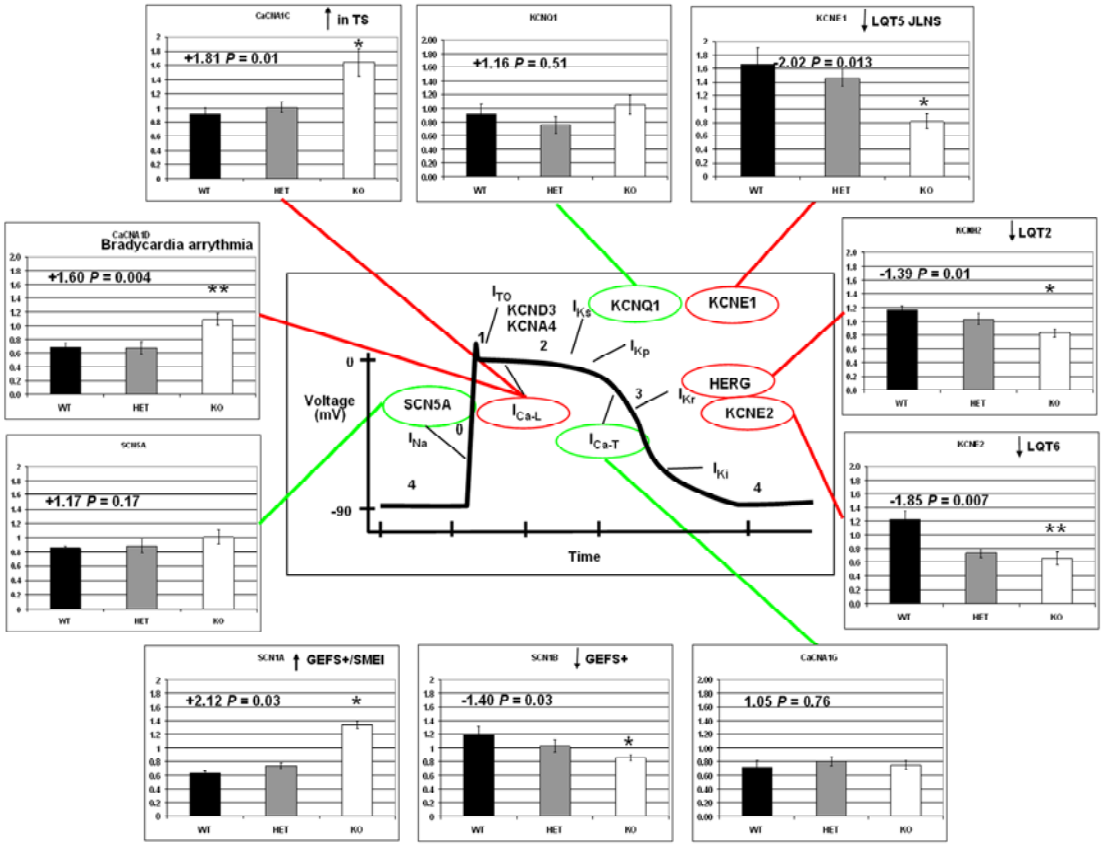

Figure 4.5: QPCR Analysis of Ion Channels in Heart

pipette solution (120 CsCl, 18 NaCl, 1 $MgCl_2$, 1 $CaCl_2$, 10 EGTA, 4 MgATP, 5 HEPES, 10 TEA-Cl, pH 7.2). Following formation and rupture of a gigaseal, access resistance was in the range of 5-8 megaohms and leak currents were typically less than 100pA at a holding potential of -90mV. Membrane potentials

were corrected for liquid junction potential offset by -5mV. Cell capacitance was assessed from capacitance transients recorded during a voltage step from -75mV to -70mV and quantified as the ratio of the integral of the transient to the size of the voltage step (5mV). The average cell capacitance was 13.9 ± 1 pF (N=30) for WT myocytes and 14.2 ± 1.2 pF (N=36) for ERRγ KO myocytes. Prior to recording of sodium currents, whole cell capacitance was compensated, and access resistance was corrected and subtracted by 80-85%, giving a voltage error of <5mV. I_{Na} was recorded using a depolarizing voltage clamp protocol which depolarized the membrane potential in incremental 5mV steps of 100 ms duration,

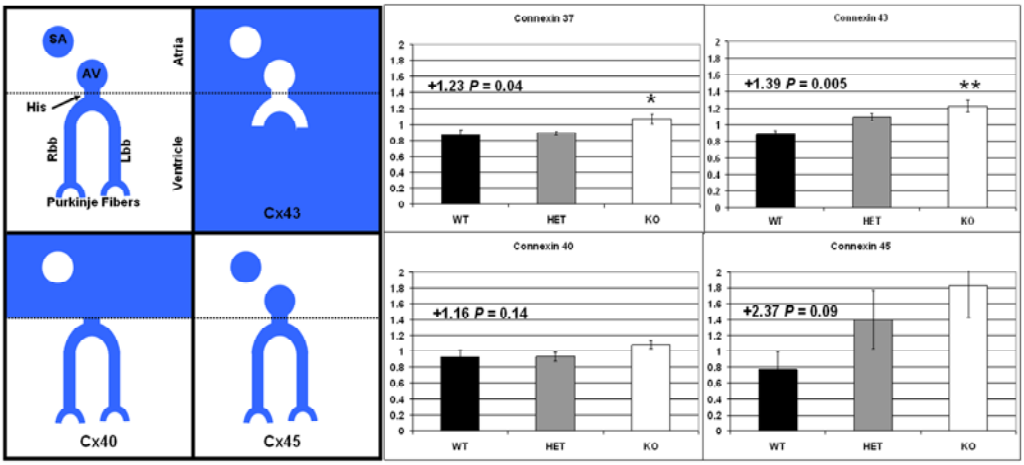

Figure 4.6: Altered Gap Junction Expression in ERRγ-null Heart

from a holding potential of -90mV to potentials of -75mV to +35mV. Subsequent recordings were made in the presence of 30μM tetrodotoxin (TTX) to block the sodium current and the sodium current was defined as the difference current recorded with and without TTX. All currents were normalized to whole cell capacitance and the extent of current activation was assessed from the peak current density.The isolated cells were plated for 48 hours prior to patch clamp recording. Tetrodotoxin sensitive currents were found to be significantly reduced in ERRγ-null cells, despite normal voltage activation and inactivation curves. Capacitance was not significantly reduced in the null cells, indicating similar size of the null cells.

Molecular analysis of the channel composition of ERRγ-null hearts was studied by QPCR. RNA from six animals from each genotype was collected from whole (atria and ventricle) E18.5 heart with RNeasy columns with on column DNase treatment (Qiagen). First-strand cDNA was synthesized with 1 μg of purified RNA using SuperScript II and Random Primers (Invitrogen). Samples were subsequently

treated with RNase H (Invitrogen). A 384-well microtiter dish format was utilized for qPCR reactions with SYBR green (Sigma) and final reaction volumes were 10 microliters. High throughput processing was achieved using a semiautomated Beckman liquid handler, an ABI Prism 7900HT and sequence detection system software. For each biological sample, QPCR reactions were performed in quadruplicate and expression was normalized to 36B4 expression. Bar graphs represent the averaged relative expression of the six biological samples and the standard error of the mean, assigning WT a relative expression of 100% for each indicated transcript.

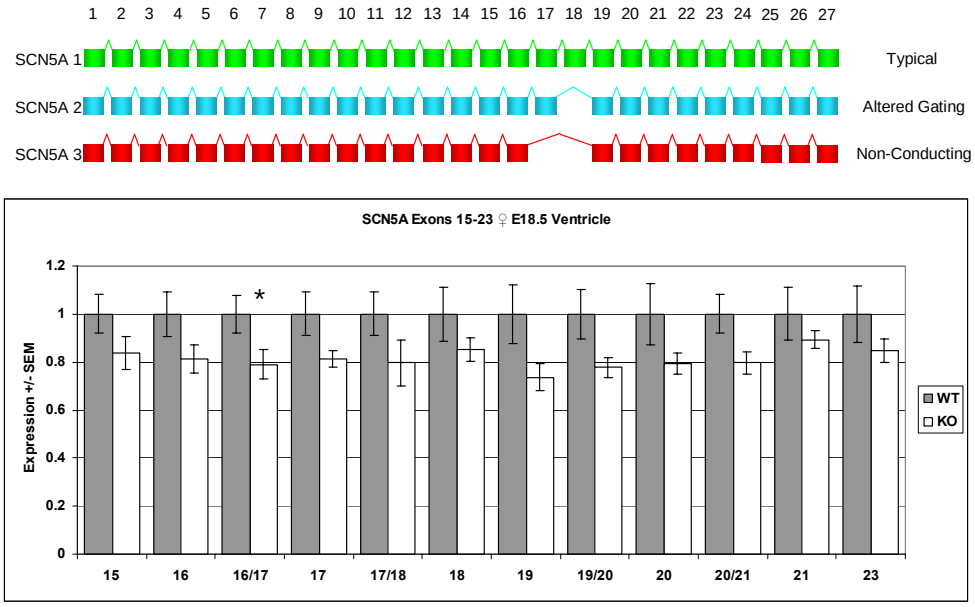

Figure 4.7: Sodium Channel SCN5A is not Alternatively Spliced in ERRγ-null Heart

Despite a prolonged QRS with Lead II morphology consistent with right bundle branch block and reduced sodium current measurements as measured from primary cardiomyocytes by patch clamping, no difference in RNA transcript for the major cardiac sodium channel, SCN5A, was detected. However, in a subsequent experiment designed to detect potential splicing variants in SCN5A which utilized only ventricle, while no evidence of alternative splicing was detected, a consistent overall reduction of approximately 20% was observed in the ERR3-null ventricular tissue.

In addition to SCN5A, thirty-two additional channels and channel subunits were evaluated by QPCR. Of these, seven were found to be significantly altered in their expression. However, despite

significant and robust reductions in potassium channel expression (KCNE2, KCNE1, Table 1) in ERR3-null mice, changes in potassium current are not consistent with the observed phenotype. Calcium channel expression was upregulated in ERR3-null heart; however increased calcium current is not consistent with the observed phenotype.

Fatty-Acid Oxidation in Primary Cardiomyocytes

Primary cardiomyocytes were isolated as described above for the electrophysiologic measures. The oxidation of fats converts the carbons into carbon dioxide and the hydrogens in to water, either of which can be detected by the use of radiolabeled fats. Cells (5×10^5) were cultured in the presence of H^3-

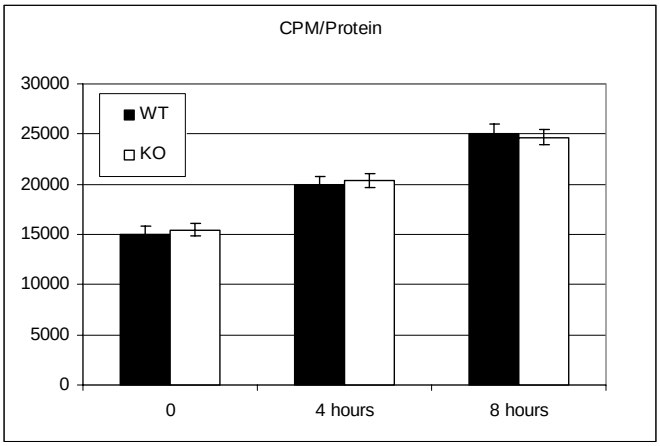

Figure 4.8: ERRγ-null Cardiomyocytes Have Normal Fatty-Acid Oxidation

labeled palmitoylate for four hours. Supernatant was collected at zero, two and four hours and waster was purified by trichloroacetic acid precipitation of proteins, and chloroform extraction of lipids. The tritiated water was mixed with Ecolume and radioactivity quantified by the use of a luminometer. Total counts were normalized to protein as a surrogate measure of cellularity. No difference in protein, or tritiated water was detected between KO and WT littermate-obtained ventricular cardiomyocytes.

Careful analysis of E18.5 mice showed a significant reduction in the ventricular myocardial mass of both $ERR\gamma^{+/LacZ}$, and $ERR\gamma^{LacZ/LacZ}$ mice—despite no alteration in the body mass of the animals at this time point. The weights were (in milligrams±SEM): WT: 5.31±0.07, n=86; HET: 4.97±0.1, n=68, $p<0.01$; KO: 4.86±0.07, n=78, $p<0.001$ (Figure 4.9).

Having limited the defect to below the AV-node at E18.5, complimentary genomic analyses of mRNA expression microarrays and chromatin-immunoprecipitation combined with a promoter array were performed (See Chapter 6). From these analyses mitochondrial processes were detected as being altered at the mRNA level with the loss of ERRγ and having promoter occupancy of ERRγ. These finding were consistent with the ECG finding of a bundle branch block and the clinical observation in humans that mitochondrial diseases may manifest as conduction system defects. Another sign of mitochondrial dysfunction is the development of lactic acidosis under conditions of stress such as trauma, infection or fasting (Smeitink, 2006). Blood from E18.5 mice delivered by caesarean section was analyzed for lactate

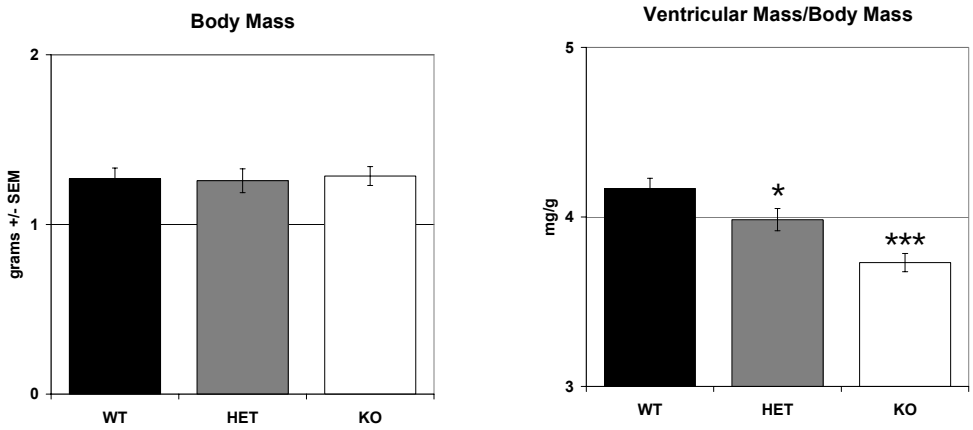

Figure 4.9: Reduced Ventricular Myocardial Mass in ERRγ-null Mice.

(Lactate Pro, SensLab, Leipzig) and glucose (OneTouch Ultra, Lifescan) collected in analytical cuvettes from the tail. At 4 hours, blood lactate and glucose values were normal in both ERRγ-null and heterozygous mice. However by eight hours, the ERRγ-null mice had developed a lactic acidosis that was significantly elevated to ~50% above control levels (Figure 6D; in mmol/L ± SEM, WT: 2.0±0.1; HET: 2.0±0.1; KO: 2.9±0.2). Despite this metabolic derangement, caesarean-sectioned E18.5 mice remained euglycemic, regardless of genotype, at both 4h and 8h post-partum (Figure 6E; in mg/dL ± SEM, 4h: WT: 31.5±2.5; HET: 30.1±1.4; KO: 32.3±2.0; 8h: WT: 46.4±2.7; HET: 39.8±3.6; KO: 42.3±5.0).

Further studies were undertaken to better characterize mitochondrial physiology in the $ERR\gamma^{LacZ/LacZ}$ mice, relative to wildtype littermate controls. Total DNA was prepared according to standard procedures and digested with 100 μg/ml RNase A for 30 min at 37°C. The relative copy numbers of mitochondrial and nuclear genomes from 1ng total DNA were determined by real-time PCR with primers

specific to mitochondrial Cytb (F-CCTTCATACCTCAAAGCAACGA, R-GATAAGTAGGTTGG CTACTAGGATTCAGT) and nuclear Rn18s (F-ACGGCCGGTACAGTGAAACT, R-GAGCGA GCGACCAAAGGA) genes. Serial dilutions of pooled DNA from 12 each E18.5 ERRγ$^{+/+}$, ERRγ$^{+/LacZ}$, and ERRγ$^{LacZ/LacZ}$ ventricular myocardia were analyzed in parallel to establish a standard curve. Examination of

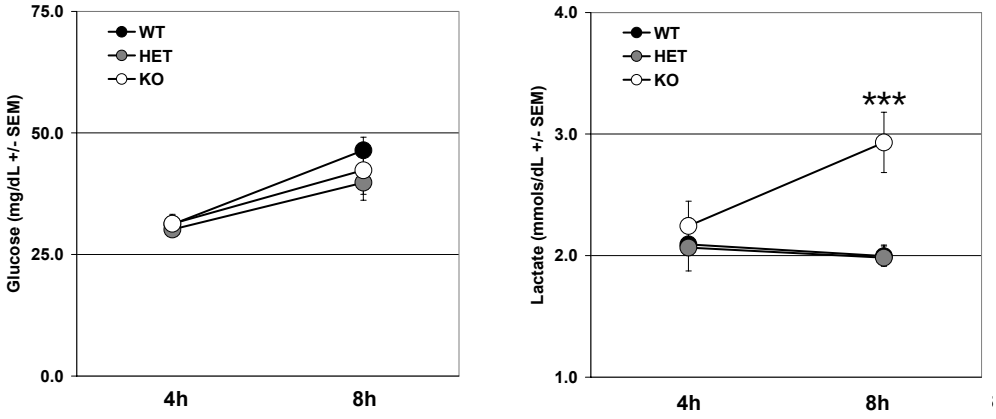

Figure 4.10: ERRγ$^{LacZ/LacZ}$ Mice Develop Fasting Lactic Acidosis

total genomic DNA from whole E18.5 cardiac ventricle and approximately 10mg of liver was performed by quantitative PCR for nuclear encoded 18S ribosomal gene (Rn18s) and the mitochondrial-encoded Cytochrome B (Cytb) gene reveals an increased number of mitochondrial genomes per nuclear genome in the ERRγ-null animals. The ratio of mtDNA to nDNA in WT heart was arbitrarily set to 1. In heart, the mtDNA:nDNA ratio was increased by 58% in ERRγ$^{+/LacZ}$ ($P<0.05$) and 90% in ERRγ$^{LacZ/LacZ}$ ($P<0.001$). While the mtDNA:nDNA ratio was reduced in liver relative to heart in all genotypes, because ERRγ is not highly expressed in liver, the mtDNA:nDNA ratio was not significantly altered by genotype and therefore serves as a negative control for ERRγ-expression.

To determine if alteration in substrate utilization could be detected in association with the observed alterations in mtDNA:nDNA and fasting blood lactate, direct measurements of isolated ventricular myocardium were preformed. Standard oximetry or polarography measurements have required larger tissue samples (~200mg) to perform experiments due to low resolution. The use of a high resolution oximeter allowed the use of much smaller tissue samples (~1.5mg) per experiment which permitted

analysis of individual E18.5 hearts. E18.5 mice were delivered by c-section, weighed, subjected to electrocardiographic, blood metabolite analysis (lactate and glucose) and genotyped by PCR. Four hours after delivery mice were sacrificed and tissue collected in ice-cold MiRO5 buffer (MiRO5 ref.). Heart tissue was weighed and prepared by blunt dissection of the myocardium with fine forceps in a teased-fiber method. 0.5 to 2.5 mg wet weight tissue samples were placed in to an oximeter containing 2ml MiRO5

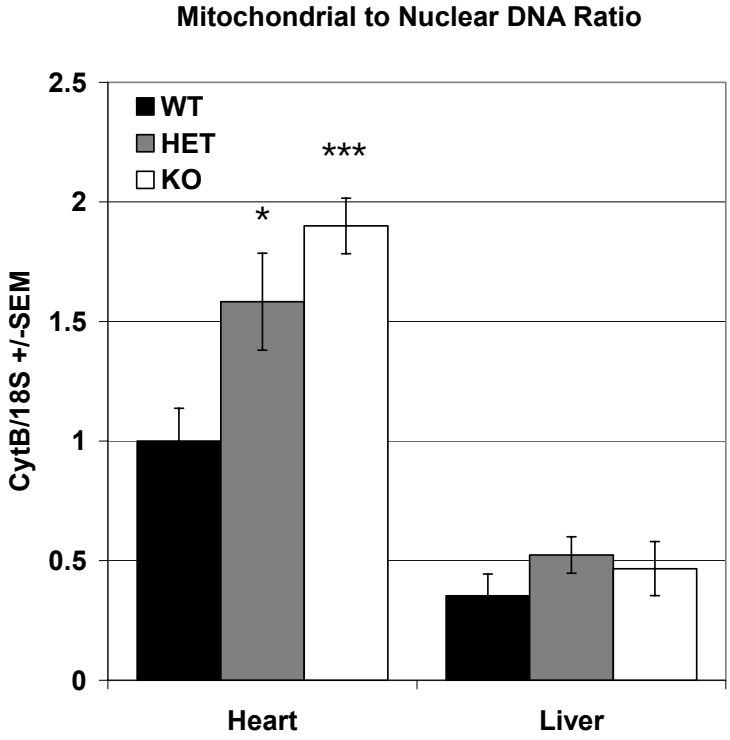

Figure 4.11: mtDNA:nDNA Alterations with Loss of ERRγ

buffer at 37°C while stirring at 750 rpm (Oroboros). After injection of oxygen to reach a partial pressure of 400mM/liter, the following substrates and inhibitors were injected via microsyringe (Hamilton): malate, 5ul 0.8M; dihydroorotate, 40ul 0.5M; octanoyl-carnitine, 20ul 0.1M; ADP 8ul 0.5M; cytochrome c, 5ul 4mM; glutamate, 10ul 2M; pyruvate 5ul 2M; succinate, 20ul 1M; FCCP 1ul 1mM; rotenone 1ul 1mM; antimycin A, 1ul 5mM; ascorbate, 5ul 0.8M; TMPD/ascorbate, 5ul 200/10mM; sodium azide, 100ul 4M. The negative derivative of the oxygen concentration was automatically calculated by the PC-based Oxygraph software. Trace segments were manually identified, exported and compiled for analysis. Teased ventricular

myocardium preparations from WT and KO animals displayed no overall differences in substrate utilization.

Alteration of several mitochondria-associated genes was detected by microarray mRNA expression analysis. To determine if protein levels of labile subunits electron transport chain complexes were altered, western blotting was performed (Figure 4.13). Male mice were collected by caesarean section

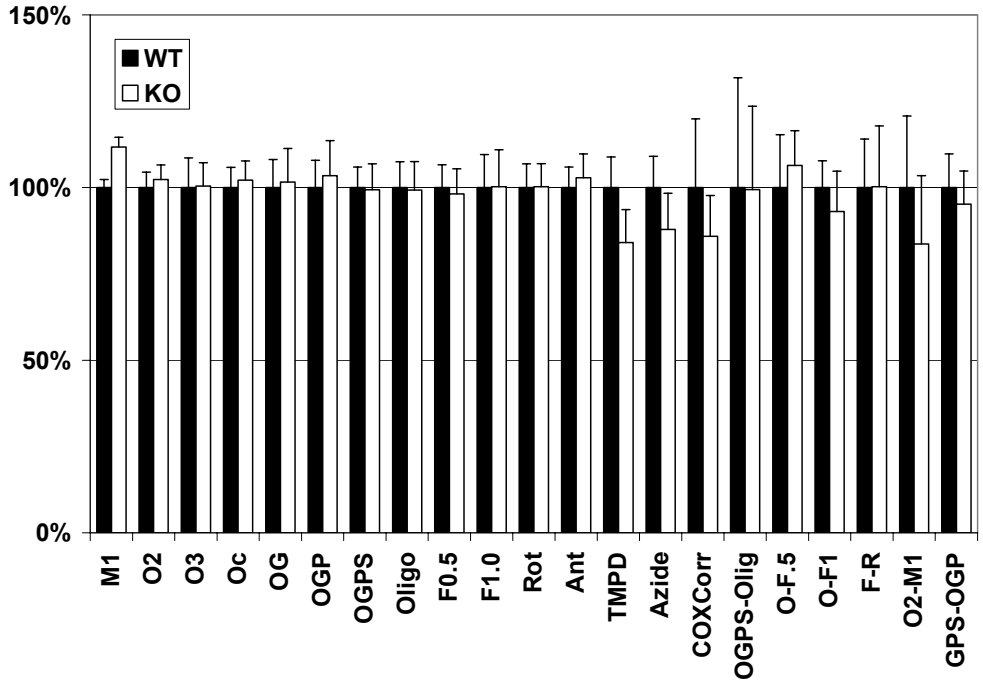

Figure 4.12: Mitochondrial Substrate Utilization is Not Altered by Loss of ERRγ

at E18.5 and ventricular myocardia were collected and stored at -80°C. Tissue was disrupted and resolved on a 10-20% BisTris gradient gel (Invitrogen). Five monoclonal antibodies against the 20 kDa subunit of complex I, probably ND6 (MS105), CII-30kDa (MS203), CIII-Core protein 2 (MS304) CIV subunit I (MS404) and CV α subunit (MS507) respectively as a premixed cocktail (MS601m, MitoSciences) were incubated with and exposed by chemoluminesence. Protein from two hearts was pooled and three lanes per genotype were run on a single gel allowing six hearts per genotype to be assayed. Under these conditions,

no genotype-dependent alteration in the mitochondrial proteins assayed was detected. It remains possible that other mitochondrial components are significantly altered.

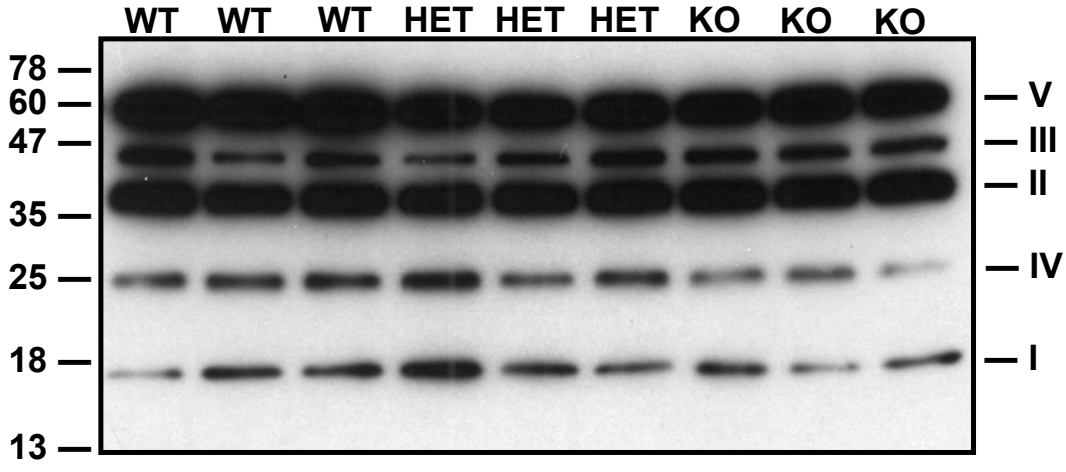

Figure 4.13: Key Electron Transport Proteins Are Not Altered in ERRγ$^{LacZ/LacZ}$ Mice

In contrast to the findings that key electron transport chain subunits are present at comparable levels in the ERRγ heterozygous and null animals by western blot, and that substrate utilization is grossly normal in intact mitochondria, biochemical assays of enzyme activity from ten E18.5 hearts per genotype revealed interesting findings. First, citrate synthase specific activity is significantly reduced by approximately 26% (P<0.001) in null animals, relative to wildtype. This indicates that mitochondrial mass is reduced in the null animals--despite normal electron micrographic, western blot, and substrate utilization findings (Figure 14.14). Secondly, Complex IV activity is significantly increased by 53% (P<0.001) in the ERRγ-null animals relative to wildtype when normalized to citrate synthase activity (Figure 14.14).

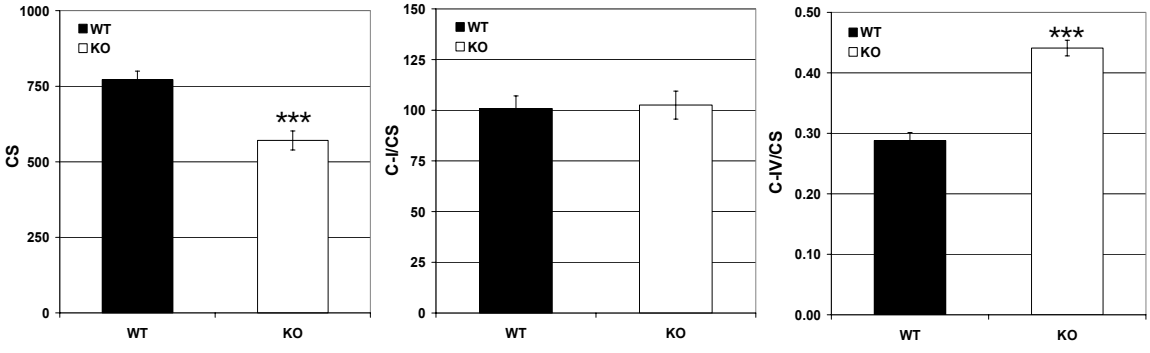

Figure 14.14: Biochemical Analysis of ERRγ$^{LacZ/LacZ}$ Mitochondria

REFERENCES

Barak Y, Nelson MC, Ong ES, Jones YZ, Ruiz-Lozano P, Chien KR, Koder A, Evans RM. PPAR gamma is required for placental, cardiac, and adipose tissue development. Mol Cell. 1999 Oct;4(4):585-95.

Chang SM, Barker FG 2nd, Huhn SL, Nicholas MK, Page M, Rabbitt J, Prados MD. High dose oral tamoxifen and subcutaneous interferon alpha-2a for recurrent glioma. J Neurooncol. 1998 Apr;37(2):169-76.

Costa LE, Boveris A, Koch OR, Taquini AC. Liver and heart mitochondria in rats submitted to chronic hypobaric hypoxia. Am J Physiol. 1988 Jul;255(1 Pt 1):C123-9.

Decaudin D, Etienne MC, De Cremoux P, Maciorowski Z, Vantelon JM, Voog E, Urien S, Tran-Perennou C, Renee N, Vielh P, Nemati F, Pouillart P. Multicenter phase II feasibility trial of high-dose tamoxifen in patients with refractory or relapsed multiple myeloma. J Natl Cancer Inst. 2004 Apr 21;96(8):636-7.

Giguere V, Yang N, Segui P, Evans RM. Identification of a new class of steroid hormone receptors. Nature. 1988 Jan 7;331(6151):91-4.

Hentschke M, Borgmeyer U. Identification of PNRC2 and TLE1 as activation function-1 cofactors of the orphan nuclear receptor ERRgamma. Biochem Biophys Res Commun. 2003 Dec 26;312(4):975-82.

Hentschke M, Susens U, Borgmeyer U. PGC-1 and PERC, coactivators of the estrogen receptor-related receptor gamma. Biochem Biophys Res Commun. 2002 Dec 20;299(5):872-9.

Hong H, Yang L, Stallcup MR. Hormone-independent transcriptional activation and coactivator binding by novel orphan nuclear receptor ERR3. J Biol Chem. 1999 Aug 6;274(32):22618-26.

Hsiao A, Ideker T, Olefsky JM, Subramaniam S. VAMPIRE microarray suite: a web-based platform for the interpretation of gene expression data.
Nucleic Acids Res. 2005 Jul 1;33

Huss JM, Kopp RP, Kelly DP. Peroxisome proliferator-activated receptor coactivator-1alpha (PGC-1alpha) coactivates the cardiac-enriched nuclear receptors estrogen-related receptor-alpha and -gamma. Identification of novel leucine-rich interaction motif within PGC-1alpha. J Biol Chem. 2002 Oct 25;277(43):40265-74.

Kulandavelu S, Qu D, Sunn N, Mu J, Rennie MY, Whiteley KJ, Walls JR, Bock NA, Sun JC, Covelli A, Sled JG, Adamson SL. Embryonic and neonatal phenotyping of genetically engineered mice. ILAR J. 2006;47(2):103-17.

Luo J, Sladek R, Bader JA, Matthyssen A, Rossant J, Giguere V. Placental abnormalities in mouse embryos lacking the orphan nuclear receptor ERR-beta. Nature. 1997 Aug 21;388(6644):778-82.

Luo J, Sladek R, Carrier J, Bader JA, Richard D, Giguere V. Reduced fat mass in mice lacking orphan nuclear receptor estrogen-related receptor alpha.Mol Cell Biol. 2003 Nov;23(22):7947-56.

Mangelsdorf DJ, Thummel C, Beato M, Herrlich P, Schutz G, Umesono K, Blumberg B, Kastner P, Mark M, Chambon P, Evans RM. The nuclear receptor superfamily: the second decade. Cell. 1995 Dec 15;83(6):835-9.

Papadopoulou, L. C.; Sue, C. M.; Davidson, M. M.; Tanji, K.; Nishino, I.; Sadlock, J. E.; Krishna, S.; Walker, W.; Selby, J.; Glerum, D. M.; Van Coster, R.; Lyon, G.; and 9 others Fatal infantile

cardioencephalomyopathy with COX deficiency and mutations in SCO2, a COX assembly gene. Nature Genet. 23: 333-337, 1999.

Razzaque MA, Masuda N, Maeda Y, Endo Y, Tsukamoto T, Osumi T. Estrogen receptor-related receptor gamma has an exceptionally broad specificity of DNA sequence recognition. Gene. 2004 Oct 13;340(2):275-82.

Ruiz-Lozano P, Smith SM, Perkins G, Kubalak SW, Boss GR, Sucov HM, Evans RM, Chien KR. Energy deprivation and a deficiency in downstream metabolic target genes during the onset of embryonic heart failure in RXRalpha-/- embryos. Development. 1998 Feb;125(3):533-44.

Sharieff GQ, Rao SO.The pediatric ECG. Emerg Med Clin North Am. 2006 Feb;24(1):195-208, vii-viii. Review.

Smeitink JA, Zeviani M, Turnbull DM, Jacobs HT. Mitochondrial medicine: a metabolic perspective on the pathology of oxidative phosphorylation disorders. Cell Metab. 2006 Jan;3(1):9-13.

Sucov HM, Dyson E, Gumeringer CL, Price J, Chien KR, Evans RM. RXR alpha mutant mice establish a genetic basis for vitamin A signaling in heart morphogenesis. Genes Dev. 1994 May 1;8(9):1007-18.

Trump DL, Smith DC, Ellis PG, Rogers MP, Schold SC, Winer EP, Panella TJ, Jordan VC, Fine RL. High-dose oral tamoxifen, a potential multidrug-resistance-reversal agent: phase I trial in combination with vinblastine. J Natl Cancer Inst. 1992 Dec 2;84(23):1811-6.

Xie W, Hong H, Yang NN, Lin RJ, Simon CM, Stallcup MR, Evans RM. Constitutive activation of transcription and binding of coactivator by estrogen-related receptors 1 and 2. Mol Endocrinol. 1999 Dec;13(12):2151-62.

Xie X, Lu J, Kulbokas EJ, Golub TR, Mootha V, Lindblad-Toh K, Lander ES, Kellis M. Systematic discovery of regulatory motifs in human promoters and 3' UTRs by comparison of several mammals. Nature. 2005 Mar 17;434(7031):338-45. Epub 2005 Feb 27.

Acknowlegements

Collaborators subject to authorship deriving from this work include:

Matthew Bloch	Michael Downes, Ph.D.
Catherine Dufour , M.S.	Ronald M. Evans, Ph.D.
Benjamin W. Gallarda	Vincent Giguere, Ph.D.
Wayne R. Giles, Ph.D.	Johann W. Jonker, Ph.D.
Richard Kondo, Ph.D.	Alexander Lehrman, M.S.
Christopher P Myers, M.D. Ph.D.	Robert K. Naviaux, M.D. Ph.D.
Jordan Nevo	Samuel L. Pfaff, Ph.D.
Wen Xie, M.D. Ph.D.	Ruth T. Yu, M.D. Ph.D.

Alaynick WA; Myers CP; Gallarda BW; Pfaff SL, Evans RM. “Locomotor Defects in Estrogen-related Receptor Gamma Mutant Mice” In Preparation.

Alaynick WA; Kondo R; Xie W; Downes M; Dufour C; Jonker JW; Yu RT; Lehrman A; Nevo J; Bloch M; Naviaux RK; Giles WR; Giguere V; Evans RM. “Cardiac conduction Defects in Estrogen-related Receptor Gamma Mutant Mice”. In Preparation

Chapter 5

Genomic Analysis

DNA Microarrays

The principle of hybridization between consensus sequences in nucleic acids allows for large scale parallel analysis of nucleic acids obtained from tissues or cells of interest (Lipshutz, 1999). DNA microarrays, or chips, are made by placing nucleic acids of known sequence on substrate in a known location, to produce an array of nucleic acid probes. These probes are then hybridized with labeled nucleic acids obtained by various methods, most commonly by generating cDNA from mRNA. This cDNA is then labeled and hybridized to an array of known expression products to produce an expression array. Alternatively, non-coding regions of the genome, such as the promoter regions of genes, can be arrayed. DNA from tissue or cells of interest is immunoprecipitated by targeting an antigen which interacts with DNA or chromatin. This DNA is then broken into small pieces, amplified, labeled and hybridized with the array in a process called ChIP on chip. Differentially regulated transcripts detected in an expression array can then be compared to promoter regions detected in the ChIP on chip array to determine direct and indirect transcriptional targets. We have developed antibodies against ERRγ that work very well for ChIP. Collaboration with Vincent Giguere at McGill has allowed access to an array containing approximately 19,000 one-kilobase promoter regions arrayed in triplicate.

Chromatin-immunoprecipitated material against ERRγ was obtained from adult heart and hybridized to the 20,000 promoter array in three separate experiments. Several hundred direct promoter targets of ERRγ have been identified and independently confirmed by additional ChIP-PCR experiments (Appendix III). Additionally, neonatal heart tissue was analyzed by ChIP-chip experiments in neonatal animals to allow comparison with expression arrays performed at E18.5 on ERRγ $^{+/+}$, ERRγ $^{+/LacZ}$ and ERRγ $^{LacZ/LacZ}$ mice.

Having limited the electrophysiologic defect to below the AV node in E18.5 mice, ventricular tissue from E18.5 mice was subjected to expression analysis with commercially available microarrays (Affymetrix 430 2.0, Santa Clara, CA). Hearts from nine animals per genotype were collected and atria removed prior to storage at -20C (RNALater, Ambion). Tissue was then pooled into groups of three and processed for total RNA (Qiagen). Total RNA (10 μg) was reverse transcribed with the SuperScript Choice system (Invitrogen). The cDNA (1 μg) was *in vitro* transcribed by using the EnzoBioArray High Yield

RNA system (Enzo Diagnostics). The cRNA (10 μg) was fragmented and hybridized to a HG-U133A GeneChip (Affymetrix, Santa Clara, CA) by using standard procedure (45°C, 16 h). Washing and staining were performed in a Fluidics Station 400 (Affymetrix) by using the protocol EukGE-WS2v4 and scanned in an Affymetrix GeneChip 2500 scanner.

Data from three experiments per genotype were analyzed with MICROARRAY SUITE 5 software (Affymetrix) and a server-based analysis suite (VAMPIRE) (Hsiao, 2005). The ‘‘change’’ *P*-value threshold was <0.003. Genes whose detection *P*-value was >0.05 in all experimental conditions were excluded from the analysis. Unbiased gene ontologies were assigned to within the VAMPIRE online microarray analysis suite (Goby). Classification into genes encoding mitochondrial proteins was based on annotations of the Affymetrix NetAffx Analysis Center, SOURCE and the National Center for Biotechnology Information PubMed, and the OXPHOS and human_mitoDB_6_2002 lists curated at the Whitehead Institute Center for Genome Research. Gene lists were further limited to transcripts with abundance values greater than 200. Lists were compared in and intersection determined with Access data base software (Microsoft, Redmond WA).

Human Promoter Microarray Design.

The strategy adopted to design the promoter microarray is similar to the one used by the Young group (Odum et al., 2004). Full-length complementary DNAs were extracted from Reference Sequence (Refseq) and Mammalian Gene Collection (MGC) databases and filtered to eliminate redundancy and incomplete cDNAs. Their transcription start sites were then located by using the University of California at Santa Cruz (UCSC) genome browser (Karolchik et al., 2003), and the sequence ranging from 800 bp upstream of the transcription start sites to 200 bp downstream of the transcription start sites was extracted by using the UCSC database assemblage July 2003. Primer pairs were designed by using the Primer3 algorithm, and the specificity was tested *in silico* by using a virtual PCR algorithm (Lexa et al., 2001; Rosen and Skaletsky, 2000). When the primer pair gave no satisfactory virtual PCR results, a new primer pair was designed by using Primer3 and tested again. The process was iterated three times to generate primer pairs predicted to be efficient to amplify promoter regions from human genomic DNA for almost all of our selected genes. This strategy was adopted after preliminary results showed that a simpler primer

design approach did not generate good results when we tried to amplify promoter regions from human genomic DNA. This primer design pipeline allowed the design of primer pairs to amplify promoter regions from human genomic DNA with a success rate of ≈80%, which is slightly better than that reported previously (Odum et al., 2004). At the date of the download (July 2004) 21,416 RefSeq and 16,521 MGC entries were retrieved. After the filtering process, 18,741 of them were selected and submitted to primer design. Primers were obtained for 18,660 promoters, and 188 controls were added (located in exons and far from any known genes).

ChIP Assays for Target Validation

ChIP assays were performed on adult male murine hearts. Specifically, hearts were isolated, weighed and homogenized for 1 sec in 14 ml culture tubes containing 5 ml of cold PBS using a Brinkmann Polytron homogenizer. The samples were centrifuged at 2000 rpm for 2 min at 4°C and the cell pellets were resuspended in cell lysis buffer (5 mM HEPES pH 8, 85 mM KCl, 0.5% NP-40) containing a protease inhibitor cocktail (Roche) and incubated at 4°C for 15 min with rotation. Following centrifugation at 2000 rpm for 2 min at 4°C, the nuclei pellets were resuspended in PBS containing formaldehyde (1% final) and DNA-protein crosslinking was allowed to occur at room temperature for 20 min with rotation. Samples were then centrifuged at 2000 rpm for 2 min at 4°C and the nuclei pellets were washed twice with 10 ml cold PBS and stored at –80°C. Nuclear pellets were thawed and resuspended in nuclei lysis buffer (50 mM Tris-HCl, pH 8.1, 10 mM EDTA, 1% SDS) supplemented with protease inhibitors (Roche). The samples were sonicated in 50 ml Falcon tubes at power 10 for 30 sec pulses using a VirSonic 100 (Virtis) sonicator. Sonicated material was centrifuged at maximum speed for 15 min at 4°C in 1.5 ml tubes. For standard ChIP experiments, 10% input samples were prepared by incubating sonicated material corresponding to 0. 015g of starting cardiac weight and eluted in 150ul elution buffer (1% SDS, 0.1 M $NaHCO_3$) at 65°C for at least 6 h. Thereafter, the 10% inputs were purified using the QIAquick Spin Kit (Qiagen) and eluted from the column with 30 µl of elution buffer provided in the kit. For antibody-enriched and no-antibody control samples, chromatin corresponding to 0.15 g of initial heart mass was diluted in 2.5X ChIP dilution buffer (0.5% Triton X-100, 2 mM EDTA, 100 mM NaCl, 20 mM Tris-HCl, pH 8.1) in 1.5 ml tubes and pre-cleared using 50 µl of a 50% slurry of salmon sperm DNA/protein A beads (Upstate) for 1 h at 4°C. Pre-

cleared chromatin was either immunoprecipitated (target enriched material) or not (no antibody control) overnight with an anti-hERRα polyclonal antibody (developed in the Giguere Laboratory; specific for both human and mouse ERRα) or with an affinity purified anti-mERRγ polyclonal antibody with subsequent addition of 50 µl of a 50% slurry of salmon sperm DNA/protein A beads for 2h at 4°C. The beads were washed sequentially in 1 ml for 10 min at 4°C with three different buffers requiring centrifugation at 4000 rpm at 4°C after each wash. Initially, buffer I (1% Triton X-100, 0.1% SDS, 150 mM NaCl, 2 mM EDTA, pH 8.0, 20 mM Tris-HCl, pH 8.1) was used, then buffer II (1% Triton X-100, 0.1% SDS, 500 mM NaCl, 2 mM EDTA, pH 8.0, 20 mM Tris-HCl, pH 8.1) and finally with buffer III (1% NP-40, 0.25 mM LiCl, 1% Na-deoxycholate, 1 mM EDTA, pH 8.0, 10 mM Tris-HCl, pH 8.1). The beads were next washed briefly with TE buffer (10 mM Tris-HCl, pH 7.5, 1 mM EDTA, pH 8.0) and eluted in 150 µl elution buffer (1% SDS, 0.1 M $NaHCO_3$) at 65°C for at least 6 h. The eluate was purified using the QIAquick Spin Kit (Qiagen) and eluted from the column with 30 µl of elution buffer provided in the kit.

ChIP Assays for Genome-Wide Location Analysis

The 10% inputs, immunoprecipitated and no-antibody control samples were prepared as described in the standard ChIP protocol above for target validation with the following modifications: for the 10% inputs, sonicated material corresponding to 0.15 g of starting cardiac weight was incubated at 65°C for at least 6 h in SDS (1% final) and $NaHCO_3$ (0.1M final) and purified from QIAquick Spin columns with 2 consecutive 30 µl elutions with elution buffer supplied in the kit; 15 mL Falcon tubes were used for enriched and no-antibody control samples and sonicated material corresponding to 1.5 g initial heart mass was used; a volume of 400 µl of a 50% slurry of salmon sperm DNA/protein A beads was used for both a 2 h pre-clear and 3 h incubation prior to sequential washing with 10 ml volumes of wash buffers; samples were eluted in 1 ml elution buffer at 65°C for at least 6 h and purified from QIAquick Spin columns with 2 consecutive 30 µl elutions with elution buffer supplied in the kit.

Genome-Wide Location Analysis

Triplicate ERRα and ERRγ genome-wide location analysis experiments were performed. Sample preparation of enriched and input control material for hybridizations to mouse promoter microarrays

involves ligation-mediated PCR (LM-PCR) and Cy-dye labeling. First, the 10% inputs were diluted with H_2O to a total of 55 µl to the percentage required for the input samples to read at the same Q-PCR cycle as that for the enriched samples using control primers. Then, 55 µl of non-diluted purified enriched material and diluted control input samples were separately added to a 55 µl mixture containing 11 µl NEB buffer 2 (10X), 0.5 µl BSA (10 mg/ml), 1 µl 10 mM dNTP mix, 0.2 µl T4 DNA polymerase (3U/µl) and 42.3 µl of H_2O. The mixtures were incubated at 12°C for 20 min followed by addition of 12 µl of a solution containing 11.5 µl 3 M NaOAc, pH 5.2 and 0.5 µl glycogen (20 mg/ml). The samples were vortexed briefly and 120 µl of phenol/chloroform/isoamyl was added. The samples were vortexed again and centrifuged for 5 min at 13000 rpm at RT. The upper phase was transferred to a new tube followed by addition of 2 volumes of cold ethanol. The samples were vortexed and precipitated at –80°C for 1 hour. The precipitated material was centrifuged at 13000 rpm, 4°C for 30 min and the pellets were air-dried. The pellets were then resuspended with a 20 µl mixture of 2 µl 10X T4 DNA ligase buffer, 6.5 µl annealed linkers (15 µM) (Ren et al., 2000), 0.5 µl 0.1 M ATP, 1 µl T4 DNA ligase (400U/µl) and 10 µl H_2O. The resuspended samples were incubated at 16°C overnight. The next day, a 20 µl solution containing 13.5 µl H_2O, 4 µl 10X Thermopol buffer, 1.25 µl 10 mM dNTP mix and 1.25 µl of 40 µM oligo oJW102 (Ren et al., 2000) was added. The samples were initiated to an LM-PCR program consisting of 4 min at 55°C, 3 min at 72°C, 2 min at 95°C, 28 cycles of 30 sec at 95°C, 30 sec at 60°C and 1 min at 72°C, followed by 5 min at 72°C and kept at 4°C until ready. The PCR program was paused once step 1 reached 2 min at 55°C, then a 10 µl solution comprised of 8 µl of H_2O, 1 µl of 10X Thermopol buffer and 1 µl TAQ (5U/µl, Invitrogen) was added and the PCR run was continued. The LM-PCR samples were purified by QIAquick Spin kit and eluted twice with 30 µl of elution buffer provided in the kit. Purified enriched and input control samples were labeled with Cy5 and Cy3 dyes (Invitrogen), respectively. For each ChIP-on-chip sample, 1 µg purified LM-PCR'd sample was placed into two 1.5 ml tubes (2µg each of enriched and control input samples needed). Next, 20 µl 2.5X Random Primers (BioPrime Kit) was added and the samples were incubated at 95°C for 5 min. The samples were cooled on ice and 5 µl dUTP was added. Then, 1 µl of Cy5 or Cy3 was added with subsequent addition of 1 µl Klenow to each tube. The samples

were incubated at 37°C for 2 h covered with aluminum foil. The samples were then purified using the Invitrogen BioPrime kit and 2 μg of each sample was eluted with at total of 100 μl. To the purified samples, 1/10 volume 3M NaOAc, pH 5.2 and 2.5X volume of cold ethanol was added and the samples were precipitated at -80°C for 2 h. Subsequently, the samples were centrifuged at 4°C for 30 min at maximum speed and the pellets were washed with 70% ethanol, air-dried and stored at -20°C ready for hybridization.

Hybridizations of Cy5-labeled ERRα or ERRγ enriched material against Cy3-labeled control input DNA to mouse 19K promoter microarrays were performed at the Institut de Recherches Cliniques de Montréal (IRCM). First, microarray slides containing 19000 promoter regions spanning from 800 bp upstream to 200 bp downstream of promoter transcriptional start sites were blocked for 20 min in a 250 ml solution containing 4 g succinic anhydride, 239 ml 1-methyl-2-pyrrolidinone and 11 ml boric acid, pH 8. The slides were then emerged first briefly then for 20 sec into a dish containing 0.2% SDS solution, followed by 20 sec in RT water, 2 min in 95°C water and finally for a few seconds in RT water prior to centrifugation at 1500 rpm for 3 min. Cy5 labeled enriched material was resuspended in 5 μl H_2O and combined with Cy3 labeled non-enriched material. Then, 20 μl human Cot-1 DNA (1 mg/ml) and 5 μl yeast tRNA (8 mg/ml) were added to the samples, mixed and then dried using a speed vac. The dried samples were resuspended in 50 μl hybridization buffer prepared by mixing 125 μl formamide (25% final), 125 μl 20X SSC (5X final), 5 μl 10% SDS (0.1% final), 100 μl BSA (20% final), and 145 μl H_2O. The samples were incubated at 95°C for 5 min and kept on a 50°C hot plate after a quick spin. About 47-48 μl from each sample was transferred onto a blocked mouse 19K promoter microarray slide, placed into a hybridization chamber and incubated at 50°C for at least 20 h. The microarrays were then washed consecutively with three different washing buffers with agitation. First, the arrays were washed for 15 min in Wash I solution (2X SSC, 0.1% SDS), twice for 2 min in Wash II solution (0.1X SSC, 0.1% SDS) and twice for 1 min in Wash III solution (0.1X SSC). The slides were then dried by centrifugation at 1500 rpm for 3 min, scanned and a macro was run to calculate p-values and binding ratios for the hybridized promoters on the mouse microarrays.

Genomic Results

Expression array experiments detected several genes associated with mitochondrial physiology as determined by unbiased online analysis in the NetAffx Analysis Suite (http://www.affymetrix.com/analysis/index.affx). This analysis allowed assignment of gene ontologies to determine if detected transcripts were associated with specific cellular components, biological processes, or molecular functions. Nine lists of transcripts were generated and subjected to gene ontology (GO) analysis. The comparison of genes detected as significantly altered by either mRNA expression or ChIP-Chip were made within the database program, Access (Microsoft, USA). Lists of genes were compared to establish intersections. Intersections of mRNA expression and ChIP-Chip would indicate genes that are altered by loss of ERRγ and that have ERRγ in their promoter regions—suggesting direct regulation and not compensatory regulation.

Sample	Genes	% Mito	Mito GO *P*
1. KO UP	703	7%	2.6×10^{-2}
2. HET& KO UP	304	9%	4.6×10^{-3}
3. KO DOWN	446	10%	2.4×10^{-8}
4. HET & KO DOWN	100	11%	4.6×10^{-3}
5. ChIP	233	15%	ND
6. KO ChIP UP	14	21%	1.6×10^{-3}
7. HET & KO ChIP UP*	8	25%	3.4×10^{-3}
8. KO ChIP DOWN	10	20%	5.6×10^{-2}
9. HET ChIP DOWN*	3	67%	3.3×10^{-5}
10. HET & KO ChIP DOWN*	2	100%	1.2×10^{-7}

Up Intersection	Down Intersection
2810485I05Rik	2310042D19Rik
Cd59a	A130022J15Rik
Ets1	Apoa1bp
Fgl2	Casq2*
Mdh1*	Cep57
Ndufb5*	Ckmt2*
Oxnad1	Clybl*
Prei4	Eno1*
Qrsl1	Ldb3
Sdhd*	Slc41a3
Slc25a4*	Txn2*
Txnl2*	
Unc50	
Wdr77	

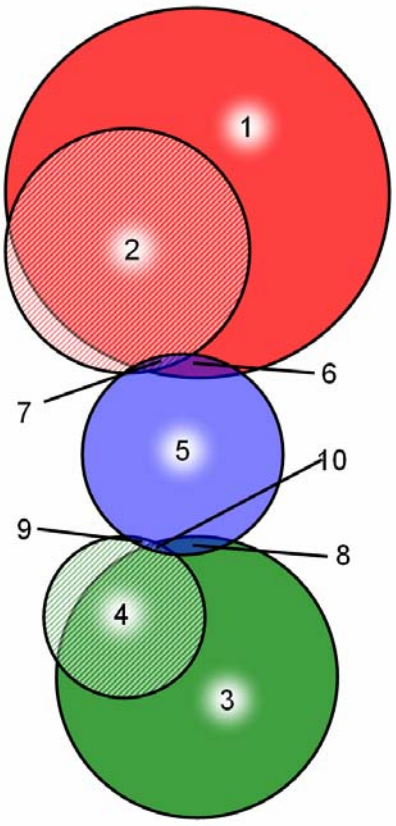

Figure 5.1: Complimentary Genomic Analysis.

A Venn diagram of the several groups of differentially detected transcripts was created to graphically depict the results of the complimentary genomic analyses of expression microarray and ChIP-chip. A table lists the domains of intersection or exclusivity. Region 1 represents the set of transcripts that are upregulated in the KO heart, relative to WT controls. This section has the lowest percentage of genes associated with mitochondrial biology (7%), and modest significance (P= 0.026) as determined by GO analysis. Region 2 represents the set of transcripts that are upregulated in the HET and KO hearts, relative to WT controls. Region 2 has a greater percentage of transcripts associated with mitochondrial biology (9%) and a greater statistical significance (P<0.005). This indicates that mitochondrial transcripts are most subject to upregulation by reductions or loss of ERRγ. Region 3 represents the set of transcripts that are down regulated in the KO heart, relative to WT controls. This section contains a substantial percentage of genes associated with mitochondrial biology (10%), with a very high statistical significance ($P=2.4 \times 10^{-8}$) as determined by GO analysis. This finding strongly supports that interpretation that ERRγ is an important regulator of mitochondrial function. Region 4 represents the set of transcripts that are down-regulated in the HET and KO hearts, relative to WT controls. This section has a high percentage of genes associated with mitochondrial biology (11%), and consistent with Region 3, this association has strong statistical significance (P< 0.005). The consideration of Regions 3 and 4 lends strong support to the hypothesis that ERRγ plays a role in mitochondrial biology.

The list of promoters detected by ChIP-chip is represented by Region 5. Region 5 is not amenable to the same analyses as the expression studies as these results do not utilize the proprietary Affymetrix nomenclature. However the intersections of Region 5 with gene expression studies are amenable to analysis in the NetAffyx analysis suite. Region 6 represents the 14 transcripts detect as upregulated in KO that were also detecteded by ChIP-chip as having ERRγ in their promoter region. 21% of these genes were associated with mitochondrial function, which represents a significant enrichment (P<0.002). Region 7 represents the 8 transcripts detected as upregulated in HET and KO that were also detected by ChIP-chip as having ERRγ in their promoter region. 25% of these genes were associated with mitochondrial function, which represents a significant enrichment (P<0.004). Region 8 represents the 10 transcripts detected as down-regulated in KO that were also detected by ChIP-chip as having ERRγ in their promoter region. 20% of these genes

were associated with mitochondrial function, however significant enrichment was not seen ($P<0.056$). Region 9 represents the 3 transcripts detected as downregulated in HET that were also detected by ChIP-chip as having ERRγ in their promoter region. 67%, or two, of these genes were associated with mitochondrial function, which represents a significant enrichment ($P<0.004$). Region 10 represents the 2 transcripts detected as upregulated in HET and KO that were also detected by ChIP-chip as having ERRγ in their promoter region. Both of these genes were associated with mitochondrial function, which represents a significant enrichment ($P< 1 \times 10^{-6}$).

The Up Intersection list (red text, Figure 1) denotes the several genes that are detected as most likely to be direct targets of ERRγ expression that are both: 1) up-regulated in the absence of ERRγ expression; and 2) contain ERRγ in their promoter regions. The Down Intersection list (green text, Figure 1) denotes the several genes that are detected as most likely to be direct targets of ERRγ expression that are both 1) down-regulated in the absence of ERRγ expression; and 2) contain ERRγ in their promoter regions. Of note is Ckmt2, the mitochondrial creatine kinase that serves to maintain the high-energy phosphate ATP pool by shuttling phosphoryl groups to AMP from phosphocreatine. Knockout studies of this gene suggest that reductions in this gene product may result in alteration in calcium handling (Steeghs, 1997).

Expression analysis can be analyzed in an unbiased manner, as was done in NetAffx, or by a candidate approach. While the unbiased analysis approach suggests changes in mitochondrial physiology, other phenotypic characteristics suggest other processes may be compromised in ERRγ-null mice, as well. Changes in ECG parameters, such as prolonged QRS, ST and QT intervals observed in association with loss of ERRγ, are very suggestive of changes in ion conductances. A candidate approach study of channel expression in E18.5 mouse heart by QPCR demonstrated significantly altered expression of several calcium and potassium channels associated with ECG alteration (Chapter 4, Figure 4). With these known alterations in hand, the array results were examined for expression changes or ERRγ promoter occupancy in genes encoding ion channels, ion binding proteins, or enzymes known to modify ion handling processes in cardiomyocytes. Some of the candidates examined were, Scn5a/Nav1.5/LQT3, Scn1a, Scn1b, Kcnh2/hERG/LQT2, Kcne1/MinK/LQT5, Kcne2/Mirp1/LQT6, Kcnq1/KvLQT1, Cacna1d, Cacna1c, gap

junctions, and calcium buffering genes. Only a few of the candidates detected by QPCR were also detected by the complimentary genomic techniques.

Despite the alterations of mitochondrial physiology that these studies indicate, there are several significant limitations of array technology. Firstly, the source material should be homogenous and display sufficient expression. A tissue or population of cells with low or diffuse expression will not produce a gene expression profile that adequately reflects the influence of the transcription factor of interest. Secondly, the technical aspect of hybridization must be done well, and due to the large number of parallel experiments, will undoubtedly produce spurious results. Thirdly, analysis of data is confounded by both the large number of observations and the yet developing analysis programs used to interpret these results. In order to reduce the spurious noise of the system, replicates must be used, which contribute considerable time, expense, and data to the experiments.

In addition to the use of replicates within one assay, complimentary assays can be undertaken to reduce inherent errors in either system. Results can be analyzed with quantitative PCR (QPCR) facilitated by a largely automated system that allows analysis of several dozen genes per day. A subset of the genes detected as altered was assayed by QPCR and appear in Table II of Chapter 5.

Overall, the results of the two complimentary genomic analyses of expression microarray and ChIP-chip provide compelling evidence that 1) the loss of ERRγ results in significantly altered expression of mitochondrial genes; and 2) that only a small proportion of these genes can be detected as having ERRγ occupancy of their proximal promoters (-800 to +200). These results served to direct studies of mitochondrial function discussed in Chapter 4.

REFERENCES

Adams M, Meijer OC, Wang J, Bhargava A, Pearce D. Homodimerization of the glucocorticoid receptor is not essential for response element binding: activation of the phenylethanolamine N-methyltransferase gene by dimerization-defective mutants. Mol Endocrinol. 2003

Bai J, Ramos RL, Ackman JB, Thomas AM, Lee RV, LoTurco JJ.RNAi reveals doublecortin is required for radial migration in rat neocortex. Nat Neurosci. 2003 Dec;6(12):1277-83

Butt SJ, Lebret JM, Kiehn O. Organization of left-right coordination in the mammalian locomotor network. Brain Res Brain Res Rev. Oct;40(1-3):107-17. 2002

Chen H, Tini M, Evans RM. HATs on and beyond chromatin. Curr Opin Cell Biol. Apr;13(2):218-24. Review. 2001

Evans, RM. Molecular characterization of the glucocorticoid receptor. Recent Prog Horm Res.;45:1-22; 1989

Forman, BM Evans RM. Nuclear hormone receptors activate direct, inverted, and everted repeats. Ann N Y Acad Sci. Jun 12;761:29-37. Review 1995

Glass CK, Rosenfeld MG. The coregulator exchange in transcriptional functions of nuclear receptors. Genes Dev. Jan 15;14(2):121-41 2000

Hamm JK, Park BH, Farmer SR. A role for C/EBPbeta in regulating peroxisome proliferator-activated receptor gamma activity during adipogenesis in 3T3-L1 preadipocytes. J Biol Chem. 2001 May 25;276(21):18464-71

Heard DJ, Norby PL, Holloway J, Vissing H.Human ERRgamma, a third member of the estrogen receptor-related receptor (ERR) subfamily of orphan nuclear receptors: tissue-specific isoforms are expressed during development and in the adult. Mol Endocrinol. Mar;14(3):382-92. 2000

Hentschke M, Schulze C, Susens U, Borgmeyer U.Characterization of calmodulin binding to the orphan nuclear receptor Errgamma. Biol Chem. Mar;384(3):473-82. 2003

Hong H, Yang L, Stallcup MR.Hormone-independent transcriptional activation and coactivator binding by novel orphan nuclear receptor ERR3. J Biol Chem. Aug 6;274(32):22618-26 1999

Ibdah JA, Paul H, Zhao Y, Binford S, Salleng K, Cline M, Matern D, Bennett MJ, Rinaldo P, Strauss AW.Lack of mitochondrial trifunctional protein in mice causes neonatal hypoglycemia and sudden death. J Clin Invest. Jun;107(11):1403-9 2001.

Lanuza GM, Gosgnach S, Pierani A, Jessell TM, Goulding M. Genetic identification of spinal interneurons that coordinate left-right locomotor activity necessary for walking movements. Neuron. 2004 May 13;42(3):375-86

Lehman JJ, Kelly DP. Transcriptional activation of energy metabolic switches in the developing and hypertrophied heart. Clin Exp Pharmacol Physiol. Apr;29(4):339-45. Review 2002

Lexa M, Horak J, Brzobohaty B. Virtual PCR. Bioinformatics. 2001 Feb;17(2):192-3.

Karolchik D, Baertsch R, Diekhans M, Furey TS, Hinrichs A, Lu YT, Roskin KM,Schwartz M, Sugnet CW, Thomas DJ, Weber RJ, Haussler D, Kent WJ; University of California Santa Cruz. The UCSC Genome Browser Database. Nucleic Acids Res. 2003 Jan 1;31(1):51-4.

Kiehn O, Butt SJ Physiological, anatomical and genetic identification of CPG neurons in the developing mammalian spinal cord. Prog Neurobiol. Jul;70(4):347-61. 2003

Kressler D, Schreiber SN, Knutti D, Kralli A. The PGC-1-related protein PERC is a selective coactivator of estrogen receptor alpha. J Biol Chem. 2002 Apr 19;277(16):13918-25.

Kullander K, Butt SJ, Lebret JM, Lundfald L, Restrepo CE, Rydstrom A, Klein R, Kiehn O. Role of EphA4 and EphrinB3 in local neuronal circuits that control walking. Science. Mar 21;299(5614): 1889-92. 2003

Lee CH, Chawla A, Urbiztondo N, Liao D, Boisvert WA, Evans RM. Transcriptional Repression of Atherogenic Inflammation: Modulation by PPARδ. Science. 2003

Lee SK, Pfaff SL. Synchronization of neurogenesis and motor neuron specification by direct coupling of bHLH and homeodomain transcription factors. Neuron. 2003 Jun 5;38(5):731-45.
Lee SK, Pfaff SL.Transcriptional networks regulating neuronal identity in the developing spinal cord. Nat Neurosci. Nov;4 Suppl:1183-91. 2001

Lipshutz RJ, Fodor SP, Gingeras TR, Lockhart DJ. High density synthetic oligonucleotide arrays.Nat Genet. Jan;21(1 Suppl):20-4. 1999

Lockhart DJ, Barlow C. Expressing what's on your mind: DNA arrays and the brain. Nat Rev Neurosci. Jan;2(1):63-8. 2001

Miles PD, Barak Y, Evans RM, Olefsky JM. Effect of heterozygous PPARgamma deficiency and TZD treatment on insulin resistance associated with age and high-fat feeding. Am J Physiol Endocrinol Metab. Mar;284(3):E618-26. 2003

Odom DT, Zizlsperger N, Gordon DB, Bell GW, Rinaldi NJ, Murray HL, Volkert TL, Schreiber J, Rolfe PA, Gifford DK, Fraenkel E, Bell GI, Young RA. Control of pancreas and liver gene expression by HNF transcription factors. Science. 2004 Feb 27;303(5662):1378-81.

Palmiter RD, Brinster RL, Hammer RE, Trumbauer ME, Rosenfeld MG, Birnberg NC, Evans RM.Dramatic growth of mice that develop from eggs microinjected with metallothionein-growth hormone fusion genes.Nature. 1982 Dec 16;300(5893):611-5.

Razzaque MA, Masuda N, Maeda Y, Endo Y, Tsukamoto T, Osumi T. Estrogen receptor-related receptor gamma has an exceptionally broad specificity of DNA sequence recognition. Gene. 2004 Oct 13;340(2):275-82

Reichardt HM, Kaestner KH, Tuckermann J, Kretz O, Wessely O, Bock R, Gass P, Schmid W, Herrlich P, Angel P, Schutz G. DNA binding of the glucocorticoid receptor is not essential for survival. Cell. May 15;93(4):531-41 1998.

Rozen S, Skaletsky H. Primer3 on the WWW for general users and for biologist programmers. Methods Mol Biol. 2000;132:365-86.

Steeghs K, Benders A, Oerlemans F, de Haan A, Heerschap A, Ruitenbeek W, Jost C, van Deursen J, Perryman B, Pette D, Bruckwilder M, Koudijs J, Jap P, Veerkamp J, Wieringa B. Altered Ca2+ responses in muscles with combined mitochondrial and cytosolic creatine kinase deficiencies. Cell. 1997 Apr 4;89(1):93-103.

Susens U, Hermans-Borgmeyer I, Borgmeyer U.Alternative splicing and expression of the mouse estrogen receptor-related receptor gamma. Biochem Biophys Res Commun. Jan 19;267(2):532-5. 2000

Todaro GJ, Green H. Quantitative studies of the growth of mouse embryo cells in culture and their development into established lines. J Cell Biol. May;17:299-313. 1963

Tronche F, Kellendonk C, Kretz O, Gass P, Anlag K, Orban PC, Bock R, Klein R, Schutz G.Disruption of the glucocorticoid receptor gene in the nervous system results in reduced anxiety. Nat Genet. Sep;23(1):99-103. 1999

Van Hartesveldt C, Sickles AE, Porter JD, Stehouwer DJ. L-dopa-induced air-stepping in developing rats. Brain Res Dev Brain Res. 1991 Feb 22;58(2):251-5.

Wang YX, Lee CH, Tiep S, Yu RT, Ham J, Kang H, Evans RM. Peroxisome-proliferator-activated receptor delta activates fat metabolism to prevent obesity. Cell. Apr 18;113(2):159-70. 2003

Xie W, Hong H, Yang NN, Lin RJ, Simon CM, Stallcup MR, Evans RM. Constitutive activation of transcription and binding of coactivator by estrogen-related receptors 1 and 2. Mol Endocrinol. Dec;13(12):2151-62. 1999

Acknowlegements

Collaborators subject to authorship deriving from this work include:

Matthew Bloch	Michael Downes, Ph.D.
Catherine Dufour , M.S.	Ronald M. Evans, Ph.D.
Benjamin W. Gallarda	Vincent Giguere, Ph.D.
Wayne R. Giles, Ph.D.	Johann W. Jonker, Ph.D.
Richard Kondo, Ph.D.	Alexander Lehrman, M.S.
Christopher P Myers, M.D. Ph.D.	Robert K. Naviaux, M.D. Ph.D.
Jordan Nevo	Samuel L. Pfaff, Ph.D.
Wen Xie, M.D. Ph.D.	Ruth T. Yu, M.D. Ph.D.

Alaynick WA; Myers CP; Gallarda BW; Pfaff SL, Evans RM. “Locomotor Defects in Estrogen-related Receptor Gamma Mutant Mice” In Preparation.

Alaynick WA; Kondo R; Xie W; Downes M; Dufour C; Jonker JW; Yu RT; Lehrman A; Nevo J; Bloch M; Naviaux RK; Giles WR; Giguere V; Evans RM. “Cardiac conduction Defects in Estrogen-related Receptor Gamma Mutant Mice”. In Preparation

Chapter 6

Conclusions

Conclusions

Loss of the orphan nuclear hormone receptor, estrogen-related receptor γ, results in motor disturbances in the lumbar spinal cord due to disruption of proper central pattern generator function. This disruption precludes normal feeding and the elicitment of maternal care. In another excitable tissue, the heart, the disruption of normal function is not acutely deleterious. By electrocardiographic analysis of the heart, a prolongation in the depolarization and repolarization of the working myocardium can be detected in the form of prolonged QRS and QT complexes, respectively. Interestingly, this prolongation is seen in the heterozygous animal as well.

Initial Findings and Characterization of Motor Defects

These experiments demonstrate that targeted disruption of the orphan nuclear hormone receptor ERRγ in mouse results in perinatal lethality due to motor abnormalities that occur both at the level of the whole mouse and within in vitro spinal cord preparations. Immunohistochemical studies have localized ERRγ-expressing neurons to ventromedial and ventrolateral areas of the lumbar cord, regions of the cord known to contain neurons of the locomotor CPG (Kiehn, 1996). These expression studies also indicate that ERRγ-positive neurons represent a complex family of neurons, including interneurons and a sub-population of motor neurons. Intriguingly, ERRγ-expressing interneurons do not fall into any of the well-described ventral interneuron classes (V0-V3), which have been defined by the expression of various cell-type specific transcription factors. This is the first report of a nuclear hormone receptor influencing the activity of a central pattern generating neural network in spinal cord. We conclude that ERRγ is responsible for conferring an electrophysiologic property to spinal interneurons by regulating the expression of a class of genes associated with inhibitory neural signaling.

Electrophysiological recordings from lumbar roots have demonstrated that the targeted disruption of the ERRγ locus results in significantly more spontaneous activity than is observed in control $ERR\gamma^{+/+}$ and $ERR\gamma^{+/LacZ}$ cords, suggesting an alteration in the balance of excitation and inhibition within the null cord. Furthermore, studies of locomotor-like activity in the ERRγ null cord have revealed a motor deficit characterized by (1) abnormal phasic alternation between left and right L2 roots and (2) abnormal synchronization of activity among extensor (L5) and flexor (L2) motor circuits of the ipsilateral cord. This

is the first report of a nuclear hormone receptor influencing the activity of a rhythm generating neural network in the spinal cord. Our findings suggest that ERRγ is essential for the proper development and function of spinal motor circuits. A determination of the exact role of ERRγ-expressing neurons in spinal motor circuits will require further analysis of the anatomical and electrophysiological properties of these cells.

Perinatal Lethality

The observation that significant deviation from a Mendelian ratio of null offspring at P1, in conjunction with reduced feeding, suggested that ERRγ-null mice were not dying of acute organ failure or global metabolic deficiencies immediately after birth, as have been observed in other mouse models (Reichert, 1998; ChAT KO, Zetterstrom, 1997). The finding that body weight was directly proportional to having eaten, not to genotype, further suggested that some null mice are capable of feeding appropriately. In fact, these animals can eat an appropriate amount during the first week of life, and were not significantly different in body weight relative to controls, provided competing littermates were cross-fostered to eliminate competition. Null mice raised in these conditions were not grossly distinguishable, save for behavioral alterations (Supplementary Data). These conditions demonstrate that ERRγ-null mice are severely compromised, relative to controls, in their ability to compete for milk in normal litters. Furthermore, these conditions conclusively demonstrate that ERRγ-null mice are metabolically and behaviorally capable of normal growth, provided care is taken to reduce mechanical obstacles to feeding.

Motor Function

Careful analysis of P0 animals in a simple test of motor functions suited to the limited behavioral repertoire of neonatal mice, demonstrated a reduced capacity by ERRγ-null mice to execute forward movement (Figure 1E; Le Roy, 1999; Crawley, 2000). This analysis reveals that ERRγ-null mice can move all limbs, maintain an upright posture and react appropriately to vestibular cues (data not shown). However, unlike WT and HET mice—which adopt a prone posture and paddling limb movements which are occasionally alternating—null mice instead will extend hindlimbs and arch (kyphosis/ dorsiflex) their backs. The limb movements of nulls were generally inappropriate, disorganized and ineffective.

Under careful breeding conditions, the generation of mice to 10 or more days is possible allowing a larger and more robust behavioral repertoire (Le Roy, 1999; Crowley, 2000). At this age, null mice displayed grossly normal, albeit attenuated behavior, including rooting and locomotion (data not shown). However, righting reflex and the maintenance of posture in the null animals was severely affected and is reflected by their reduced fitness in the presence of WT littermates (Figure 1F). This motor defect is sensitive to gene dosage, as one allele does not completely compensate for two alleles, as demonstrated by the modest, but significant reduction in motor performance on the Rotorod. These Rotorod experiments were performed with animals of a mixed (C57Bl/6J and 129/SVJ) hybrid—strains known to display significantly different behaviors (Crawley, 2000)—requiring a larger cohort to provide statistical power in the face of large strain differences.

ERRγ Defines Novel Classes of Motor and Interneurons

Immunolocalization of ERRγ in the developing spinal cord reveals robust ventral expression that is enriched at limb levels. Within the ventral cord, ERRγ-expressing neurons are largely localized to ventromedial and ventrolateral areas, regions of the cord known to contain neurons of the locomotor CPG (Kiehn, 1996). This expression parallels the expression of the known motor-associated markers Isl1 and 2. However there is only modest colocalization of ERRγ with known MN markers, and very infrequent colocalization with IN markers of V0 (Evx1) V1 (En1), V2 (Chx10 or Lim3), or V3 (Sim1) classes. Interestingly, a small number of ERRγ-expressing neurons in the ventrolateral cord (Rexed lamina IX) also express VAChT, the vesicular transporter for acetylcholine, suggesting that these neurons are cholinergic. Furthermore, ventral root axoplasm, arising entirely from motor neurons, is positive for the ERRγ directed expression of beta-galactosidase. These ERRγ-expressing cholinergic neurons express Isl1/2, but fail to significantly express Hb9, a marker of most somatic motor neurons. These data indicate that a small sub-population of Isl1/2^{+}/Hb9^{-} motor neurons express ERRγ. The precise functional role of these ERRγ-positive motor neurons remains to be identified.

The vast majority of ERRγ-expressing neurons in the ventral cord are interneurons which fail to express any of the genetic markers for the well-described ventral interneuron classes: V0 (Evx1), V1 (En1), V2 (Chx10), and V3 (Sim1). These ERRγ-positive interneurons express the glycine transporter 2 (GlyT2),

suggesting that they are glycinergic inhibitory interneurons. Overall, these findings indicate that ERRγ-expressing interneurons represent a novel class of ventrally-located inhibitory interneurons. These neurons may form a family of commissural interneurons, which project axons across the midline to coordinate activity between the two sides of the cord. Alternatively, these neurons may represent a family of ipsilaterally-projecting interneurons which largely act to coordinate activity along one side of the cord. It is also possible that ERRγ-expressing interneurons form a heterogeneous group of both ipsilaterally- and contralaterally-projecting interneurons. The exact projection pattern for these inhibitory neurons remains to be identified.

Motor Circuits in the ERRγ Null Cord: An Imbalance of Excitation and Inhibition

Spontaneous activity is a characteristic feature of developing circuits in virtually every part of the nervous system that has been examined (Ben-Ari et al, 1989; Christie et al, 1989; Fortin et al., 1995). This type of network-driven embryonic activity is remarkably similar in tissues as diverse as the hippocampus, retina, and spinal cord (O'Donovan, 1999) and is manifest as recurrent depolarizing events, during which cells within the network are synchronously activated. During these events, intracellular calcium is elevated (Garaschuk, 1998; Kulik, 2000; Leinekugel, 1995; O'Donovan, 1994), suggesting a role in developmental or trophic processes.

Recordings from the L2 roots of the ERRγ-null cord reveal an approximately three-fold increase in the frequency of spontaneous bursting, relative to ERRγ$^{+/+}$ and ERRγ$^{+/LacZ}$ control cords, suggesting an imbalance in excitatory and inhibitory neurotransmission in the null cord.. This imbalance could result from: firstly, an increase in excitatory input; secondly, a decrease in inhibitory input; or thirdly, some combination of these events. The expression of ERRγ in a subset of glycinergic neurons suggests that loss of ERRγ may alter the functional contribution of these cells to the CPG. In the ERRγ-null, loss of the glycinergic inhibitory potential of these cells could increase the overall level of network excitability.

Does an increase in the level of network excitability observed during spontaneous bursting explain the abnormal pattern of locomotor activity observed in the ERRγ null cord? This question presumes that the motor circuit that drives the spontaneous rhythm is related in some way to that which drives the locomotor rhythm. It is likely that many of the neurons that participate in spontaneous bursting also

participate in the alternating rhythmic bursting of locomotor activity and vice-versa. For example, motor neurons are obviously the output cells of the motor circuit for both spontaneous and locomotor activity. However, it is not necessarily true that neurons behave the same way when bursting spontaneously as they do when participating in a locomotor rhythm. Recently, a group of glutamatergic descending commissural interneurons (dCINs) has been identified that make polysynaptic GABAergic connections onto motor neurons at rest, but which switch into having monosynaptic glutamatergic connections during locomotion (Kiehn, 2003). Thus, these "switch" cells effectively act as inhibitory neurons at rest via interposed GABAergic connections, but act as excitatory neurons at rest via a monosynpatic connection onto motor neurons. From these findings, one can argue that the behavior of motor circuits during normal, spontaneous activity does not necessarily reflect their behavior during locomotion. The presence of neurons within motor circuits that can effectively switch from excitation at rest to inhibition during locomotion complicates an interpretation of the ERRγ null phenotype.

Loss of ERRγ Alters L2 and L2-L5 Coordinated Firing

Recordings of the locomotor activity of left and right L2 roots of the ERRγ null have revealed a low-frequency superimposed pattern of alternating suppression (SPAS) upon the left-right burst-to-burst alternation that characterizes the wild-type rhythm. The SPAS is defined by alternating 'burst' and 'suppression' phases distinguished by the amplitude and duration of bursting activity. 'Burst' phases are characterized by higher amplitude, shorter duration bursts than those observed for the 'suppression' phases. These phases of activity strictly alternate between left and right roots, such that when the left L2 root is in a 'suppression' phase, the right L2 root is in a 'burst' phase and vice-versa. Two properties of this pattern of activity suggest potential models. Firstly, since the phasic alternation of the ERRγ null cord occurs between left and right L2 roots, it must be mediated, at some level, by commissural neurons. Secondly, the alternating phasic activity of the ERRγ null cord appears to represent oscillations in the level of network excitability. An increase in the level of network excitability at the level of either ipsilaterally- or contralaterally-projecting interneurons could potentially explain this phenomenon. Thirdly, inappropriate cycle period persist in the absence of commissural projections suggesting an inappropriate excitatory tone within either hemicord.

We first consider a model of increased excitatory tone arising within either hemicord. Within a segment, increased excitatory drive would tend to increase the burst rate, and duration ipsilaterally, while suppressing the contralateral cord via increased action of inhibitory commissural interneurons (CINs). This increased ipsilateral excitatory tone may dominate L2 to L5 dCIN signaling and result in inappropriate synchrony of ipsilateral L2 and L5 bursts. Periodically, this ipsilateral tone declines and releases an enhanced excitatory tone contralaterally that then acts reciprocally to further depress the hemicord dominant during the previous phase.

Alternatively, a model of extrinsic projections upon the hemicord could be proposed. However in light of the inappropriate periodicity in the ERRγ-null split-cord preparation, either hemicord maintains an inappropriate tone in the absence of CIN projections. This suggests that excess excitatory drive within either hemicord is the dominant influence in the generation of the SPAS. How this pattern is superimposed without disrupting the normal left-right alternation is not known.

The above models present mechanisms by which either ipsilaterally or contralaterally located inhibitory or excitatory interneurons could generate the abnormal left-right phasic rhythm of the ERRγ null cord. These models suggests that a phasic decrease in inhibitory input from contralaterally located CINs may be all that is necessary to allow for a 'burst' phase to occur on one side of the cord. When one side of the cord enters a 'burst' phase, it activates a robust 'suppression' phase in the contralateral cord via inhibitory CINs. A phasic decrease in the abnormally high level of inhibition mediated by these inhibitory CINs would allow for a switch in the 'burst' and 'suppression' phases from one side of the cord to the other. The mechanism controlling the timing of this abnormal phasic switch remains to be understood, but it likely represents the derangement of a "clock" mechanism that may act normally to control the timing of left-right reciprocal inhibition.

So, where do ERRγ-deficient neurons fit into this mutant model? What does the phenotype tell us about the potential role of ERRγ-expressing neurons in the motor circuit? As described previously, immunostaining analysis of the ERRγ null indicates that most ERRγ-expressing neurons are glycinergic, suggesting that they normally function as inhibitory interneurons in the E18.5 locomotor CPG. However, ERRγ-expressing cells may represent a population of either inhibitory ipsilaterally- or contralaterally-

projecting interneurons. If ERRγ-expressing neurons project ipsilaterally, they could indirectly affect activity across the midline by making inhibitory synapses onto excitatory and/or inhibitory CINs. If ERRγ neurons project across the midline, they would directly affect activity in the contralateral motor circuit. Given the abnormal phasic alternation of the ERRγ null cord; it seems possible that ERRγ-expressing neurons normally play a role in mediating reciprocal inhibition between bilateral motor circuits. A definitive analysis of the role of ERRγ-expressing neurons in the locomotor circuits of the mouse cord will require an understanding of the projection pattern of these cells, the neurons with which they make contact and their electrophysiological behavior during locomotion.

Loss of ERRγ Disrupts the Locomotor CPG Clock Function

These findings suggest that there is an imbalance of excitatory and inhibitory synaptic influences in the motor circuit of the ERRγ null cord. The increase in spontaneous bursting frequency observed in the ERRγ null motor circuit may result from a decrease in the level of inhibition, an increase in the level of excitation, or some combination of these events. Additionally, these findings argue for a role of ERRγ positive neurons in the modulation of spontaneous motor activity. In other words, it is likely that neurons expressing ERRγ are components (or modulators) of the CPG for motor activity.

Following lesion of the ventral commissure, the null hemicord maintains a pace like that of the intact cord, suggesting that a reduced inhibitory contribution to the CPG is found within each null hemicord. In the WT intact cord, either 1) excitatory commissural projections compete with ipsilateral inhibitory interneurons to activate MN firing, or 2) inhibitory commissural projections act upon ipsilateral inhibitory neurons to release inhibition on MN firing. When WT cord is lesioned, the loss of either a competing excitatory drive, or loss of an inhibitor of inhibitory tone results in excess inhibitory tone and resultant decrease in firing and fictitious stepping frequency. In the null animal, loss of contralateral input has a greatly reduced effect due to the reduced inhibitory drive inherent in either hemicord. This suggests that the ERRγ-dependent defect resides within the ERRγ-positive neuron and that this defect is of a metabolic or electrophysiological nature that results in an imbalance in the excitatory tone. This imbalance in excitatory tone is corrected by the application of sarcosine to in vitro spinal cord preparations. A model of reduced inhibitory drive in either hemicord is consistent with the greater spontaneous firing observed

bath conditions without the addition of the drug cocktail. The low-frequency alternating pattern of suppression might result from the altered firing properties of these presumptive inhibitory interneurons dependent on ERRγ.

In conclusion, these studies provide evidence that in addition to the role of nuclear hormone receptors in the treatment of inflammatory processes or traumatic injury to the spinal cord, that this superfamily, in particular ERRγ, may provide therapeutic targets to address conditions where alterations to CPG rhythm production are important, such as sleep apnea or skeletal muscle spasticity following spinal cord injury or in conditions of inappropriate reductions of inhibitory tone, such as stiff-person syndrome and hyperekplexia.

Measures of Whole Heart and Isolated Cardiomyocytes

Studies were performed on E18.5 mice delivered by Caesarean section to allow normalization of caloric parameters in ERRγ-null animals. In the first few hours of life outside the womb, metabolic parameters, as measured in blood, are grossly normal. For example, blood glucose and lactate levels are indistinguishable at four hours post-partum. While the gross metabolic parameters of the ERRγ mice were well controlled at this time, several other parameters were abnormal. Electrocardiographic (ECG) analysis revealed several quantifiable differences that reflect the inability of mice to completely compensate for loss of ERRγ.

Of the several alterations in cardiac physiology that result from loss of ERRγ, we can be certain of the following. Loss of ERRγ alters the electrical depolarization of the ventricular myocardium. This is reflected in the broadened QRS complex. In the strictest sense this broadening may result from: 1) slowed propagation of depolarizing signal through the conduction myocardium (the common bundle, left and right bundles and Purkinje fibers); or 2) depolarization of the working myocardium; or 3) some combination of both properties.

Loss of ERRγ alters the electrical repolarization of the ventricular myocardium. Here the conduction system can be eliminated because the ST interval, which occurs after the depolarization of the ventricle and QRS complex, is prolonged. Traditionally this is expressed at a prolonged QT or corrected QT (QTc). The QT prolongation of 10% ($P<0.001$) observed in ERRγ-null animals indicates a sluggishness

in repolarizing the ventricular myocardium. This delay could be explained by the observation three key potassium channels (Kcne1, Kcne2, Kcnq1) have reduced expression in ventricle. Human mutations in each of these channels have been associated with prolonged QT interval syndromes (LQT5, LQT2, LQT6) like the QT prolongation observed in the ERRγ-null mice—making the assignment of to these channels'

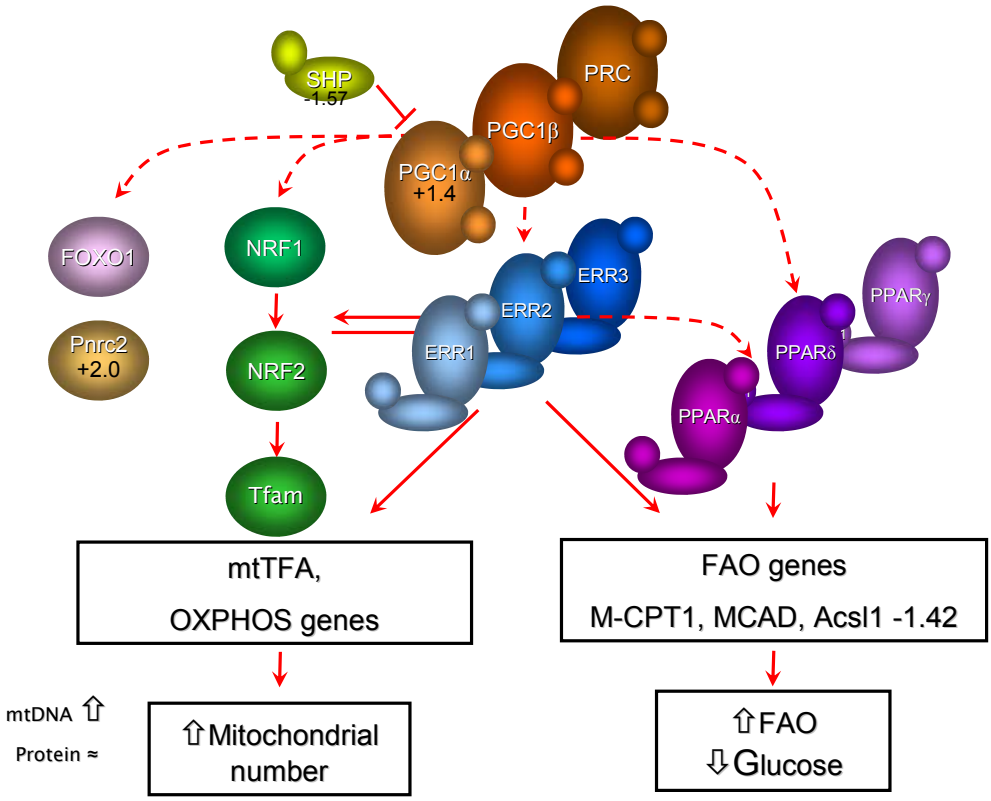

Figure 6.1: Transcription Factors Controlling Mitochondrial Biogenesis

expression plausible. Furthermore, the observation from genomic studies indicates that ERRγ may occupy the promoter region of Kcne1 and Kcne2 allowing direct regulation of these channels. Therefore, ERRγ appears to serve as a regulator of potassium homeostasis in the heart. In addition to the regulation of potassium, and likely other ions, ERRγ is associated with alteration in mitochondrial physiology. The transcription neighborhood that ERRγ occupies is largely associated with metabolic function. ERRα has been demonstrated to 1) influence metabolic function; 2) compete with ERRγ for DNA binding; 3) compete with ERRγ for coactivators, such as PGC-1α. Both ERα and ERβ have also been shown to interact with ERRγ. The PPARs (α, δ, and γ) have all been implicated to interact with PGC-1α and therefore compete

with ERRγ for this coactivator as well. The PPARs have strong metabolic effects and can alter both mitochondrial biogenesis and substrate utilization. Other transcription factors associated with metabolic function that interact with ERRγ include: SHP, PNRC, PGC-1β, and PERC. Removal of ERRγ from this robust, redundant network of several transcription factors and cofactors results in a phenotype that is lethal to the whole animal—revealing that some systems, such as the CNS are less capable of appropriate compensation perhaps due to a smaller 'safety margin. In the heart however, while the loss of ERRγ does cause ECG abnormalities, there appears to be a greater capacity for compensatory responses that allows this tissue to perform its function for several days, if not weeks. The observation of five ERRγ-null weight-matched animals that survived to ten days of age demonstrates that loss of ERRγ is not catastrophic. These mice had gross motor disturbances, but were capable of feeding and incorporating that nutrition in a grossly appropriate manner—provided they were given maternal care, as occurred in these rare cases.

Within the mitochondria, loss of ERRγ results in paradoxical responses. Firstly, mitochondrial volume and morphology appear normal, which is often seen with de facto mitochondrial diseases; however the measure of mitochondrial mass (by citrate synthase activity) suggests that the mitochondria may be 'anemic'. In addition to a significant reduction in citrate synthase (Figure 14.14), there are very likely to be other factors that alter the performance of the mitochondria the complex and dynamic *in vivo* regulatory environment that cannot be detected by the coarse methods of single enzyme biochemistry or dissociated tissue preparations. Altered biochemistries and increased mitochondrial DNA suggest that the mitochondria are under stress. The observation of fasting lactic acidosis indicates that mice deficient in ERRγ have mitochondria with reduced performance under physiologic challenge.

The role of ERRγ is not a simple one. It serves several subtle functions to fine-tune the metabolic and ionic properties of tissues with demanding tasks: cardiac, neural, renal. This dissertation describes in detail how loss of ERRγ in early life results in 1) motor and feeding defects that occur with central pattern generation circuits of the spinal cord; and 2) electrocardiographic defects in the heart. The defects in the heart correlate with gene expression and chromatin immunoprecipitation findings suggesting that the mitochondria and ion channels of the heart are dysregulated. But the specific enumeration of target genes and the mechanisms of their regulation remain to be more fully elucidated.

Appendix I

Appendix I: Cellular Functional Classification of Target Genes Occupied by ERRα, ERRγ or Both in Mouse Heart (p≤ 0.01)

GENE	DESCRIPTION	ERRα	ERRγ
Amino Acid Metabolism			
As3mt	Arsenic (+3 oxidation state) methyltransferase		x
Bhmt	Betaine-homocysteine methyltransferase		x
Cbs	Cystathionine beta-synthase		x
Got1	Glutamate oxaloacetate transaminase 1, soluble	x	x
Got2	Glutamate oxaloacetate transaminase 2, mitochondrial		x
Gpt1	Glutamic pyruvic transaminase 1, soluble		x
Oplah	5-Oxoprolinase (ATP-hydrolysing)	x	x
Pah	Phenylalanine hydroxylase		x
Thnsl1	Threonine synthase-like 1 (bacterial)		x
Apoptosis			
Als2cr2	Amyotrophic lateral sclerosis 2 (juvenile) chromosome region, candidate 2 (human)		x
Aven	Apoptosis, caspase activation inhibitor	x	
Bdnf	Brain derived neurotrophic factor	x	x
Cd59a	CD59a antigen	x	x
Dad1	Defender against cell death 1		x
Eef1a2	Eukaryotic translation elongation factor 1 alpha 2		x
Endog	Endonuclease G		x
Ets1	E26 avian leukemia oncogene 1, 5' domain		x
Fgl2	Fibrinogen-like protein 2	x	x
Mtch2	Mitochondrial carrier homolog 2 (C. elegans)	x	x
Pdcd7	Programmed cell death protein 7	x	
Pdcl3	Phosducin-like 3		x
Rabep1	Rabaptin, RAB GTPase binding effector protein 1		x
Stk2	Serine-threonine kinase 2	x	x
Trp53	Tumor protein p53		x
Carbohydrate Metabolism			
1810014F10Rik	RIKEN cDNA 1810014F10 gene	x	x
2310032D16Rik	RIKEN cDNA 2310032D16 gene	x	
Chst3	Carbohydrate (chondroitin 6/keratan) sulfotransferase 3	x	
Clybl	Citrate lyase beta like	x	x
Fuk	Fucokinase		x
Gnpda2	Glucoseamine-6-phosphate deaminase 2		x
H6pd	Hexose-6-phosphate dehydrogenase (glucose 1-dehydrogenase)	x	x
Hdhd3	Haloacid dehalogenase-like hydrolase domain containing 3		x
Hk2	Hexokinase 2		x
Ldh2	Lactate dehydrogenase 2, B chain	x	x
Man1b	Mannosidase, alpha, class 1A, member 2	x	
Me3	Malic enzyme 3, NADP(+)-dependent, mitochondrial	x	
Muc15	Mucin 15	x	x
Neu3	Neuraminidase 3		x
Ppp1r3a	Protein phosphatase 1, regulatory (inhibitor) subunit 3A		x
Slc2a12	Solute carrier family 2 (facilitated glucose transporter), member 12 (GLUT-12)		x
Stxbp3	Syntaxin binding protein 3	x	x
Cell Adhesion			
Cd6	CD6 antigen		x

GENE	DESCRIPTION	ERRα	ERRγ
Cdh26	Cadherin-like 26	x	x
Nrxn3	Neurexin III		x
Pcdha6	Protocadherin alpha 6		x
Rs1h	Retinoschisis 1 homolog (human)	x	x
Ssx2ip	Synovial sarcoma, X breakpoint 2 interacting protein	x	
Tnr	Tenascin R		x
Cell Cycle			
Spin	Spindlin	x	
Cell Motility			
Dnali1	Dynein, axonemal, light intermediate polypeptide 1	x	
Ferd3l	Fer3-like (Drosophila)		x
Pxn	Paxillin		x
Cell Proliferation			
Commd5	COMM domain containing 5	x	x
Cspg4	Chondroitin sulfate proteoglycan 4		x
Nmyc1	Neuroblastoma myc-related oncogene 1		x
Chromosome Biogenesis			
Cenpa	Centromere autoantigen A	x	x
Cytoskeleton			
FHOS2	Formin-family protein FHOS2		x
Ipp	IAP promoted placental gene		x
Klhl5	Kelch-like 5 (Drosophila)		x
Krtap4-7	Keratin associated protein 4-7	x	
Mtap2	Microtubule-associated protein 2	x	
Ppl	Periplakin		x
Defense Response			
Abhd8	Abhydrolase domain containing 8		x
Ccr3	Chemokine (C-C motif) receptor 3		x
Clecsf12	C-type (calcium dependent, carbohydrate recognition domain) lectin, superfamily member 12	x	
Defb41	Defensin beta 41	x	
Hspa9a	Heat shock protein 9A	x	x
Hus1	Hus1 homolog (S. pombe)	x	
Krt2-8	Keratin complex 2, basic, gene 8		x
Map3k4	Mitogen activated protein kinase kinase kinase 4		x
Ppp1r10	Protein phosphatase 1, regulatory subunit 10		x
Reg3a	Regenerating islet-derived 3 alpha	x	
Ugt2a3	UDP glucuronosyltransferase 2 family, polypeptide A3		x
DNA Repair			
Smc6l1	SMC6 structural maintenance of chromosomes 6-like 1 (yeast)		x
Electron Transport/Oxidative Metabolism			
1110020P15Rik	RIKEN cDNA 1110020P15 gene	x	
Atp5b	ATP synthase, H+ transporting, mitochondrial F1 complex, beta subunit	x	x
Atp5c1	ATP synthase, H+ transporting, mitochondrial F1 complex, gamma polypeptide 1		x
Atp5f1	ATP synthase, H+ transporting, mitochondrial F0 complex, subunit b, isoform 1		x
Atp5g1	ATP synthase, H+ transporting, mitochondrial F0 complex, subunit c, (subunit 9), isoform 1		x
Atp5g3	ATP synthase, H+ transporting, mitochondrial F0 complex, subunit c, (subunit 9), isoform 3	x	x

GENE	DESCRIPTION	ERRα	ERRγ
BC019806	cDNA sequence BC019806	x	x
Coq7	Demethyl-Q-7	x	x
Cox6c	Cytochrome c oxidase, subunit VIc	x	x
Cox8a	Cytochrome c oxidase, subunit VIIIa		x
Cox8b	Cytochrome c oxidase, subunit VIIIb		x
Cybrd1	Cytochrome b reductase 1		x
Cycs	Cytochrome c, somatic	x	x
Cyp27a1	Cytochrome P450, family 27, subfamily a, polypeptide 1		x
Etfb	Electron transferring flavoprotein, beta polypeptide		x
Etfdh	Electron transferring flavoprotein, dehydrogenase		x
Fh1	Fumarate hydratase 1	x	x
Mdh1	Malate dehydrogenase 1, NAD (soluble)		x
Ndufa4	NADH dehydrogenase (ubiquinone) 1 alpha subcomplex, 4		x
Ndufa8	NADH dehydrogenase (ubiquinone) 1 alpha subcomplex, 8		x
Ndufa9	NADH dehydrogenase (ubiquinone) 1 alpha subcomplex, 9	x	x
Ndufb2	NADH dehydrogenase (ubiquinone) 1 beta subcomplex, 2		x
Ndufb4	NADH dehydrogenase (ubiquinone) 1 beta subcomplex, 4	x	x
Ndufb5	NADH dehydrogenase (ubiquinone) 1 beta subcomplex, 5	x	x
Ndufs1	NADH dehydrogenase (ubiquinone) Fe-S protein 1		x
Ndufs2	NADH dehydrogenase (ubiquinone) Fe-S protein 2		x
Ndufs7	NADH dehydrogenase (ubiquinone) Fe-S protein 7	x	x
Ndufv1	NADH dehydrogenase (ubiquinone) flavoprotein 1		x
Sdha	Succinate dehydrogenase complex, subunit A, flavoprotein (Fp)	x	x
Sdhb	Succinate dehydrogenase complex, subunit B, iron sulfur (Ip)	x	x
Sdhd	Succinate dehydrogenase complex, subunit D, integral membrane		x
Txn2	Thioredoxin 2		x
Txnl2	Thioredoxin-like 2	x	x
Energy Transfer			
Ckm	Creatine kinase, muscle		x
Ckmt2	Creatine kinase, mitochondrial 2	x	x
Slc25a4	Solute carrier family 25 (mitochondrial carrier, adenine nucleotide translocator), member 4	x	x
Heart Development			
Casq2	Calsequestrin 2	x	x
Htr2b	5-hydroxytryptamine (serotonin) receptor 2B	x	
Oxt	Oxytocin	x	x
Phc1	Polyhomeotic-like 1 (Drosophila)	x	
Immune Response			
Cd83	CD83 antigen		x
Ctss	Cathepsin S		x
Igj	Immunoglobulin joining chain		x
Lipid Metabolism			
Acadm	Acetyl-Coenzyme A dehydrogenase, medium chain	x	x
Ankrd9	Ankyrin repeat domain 9	x	

GENE	DESCRIPTION	ERRα	ERRγ
Ankrd23	Ankyrin repeat domain 23	x	
Cerk	Ceramide kinase	x	x
Fabp3	Fatty acid binding protein 3, muscle and heart		x
Mir16	Membrane interacting protein of RGS16	x	x
Mttp	Microsomal triglyceride transfer protein	x	
Osbpl3	Oxysterol binding protein-like 3	x	
Pla2g12a	Phospholipase A2, group XIIA	x	
Plscr2	Phospholipid scramblase 2	x	
Pte2a	Peroxisomal acyl-CoA thioesterase 2A	x	
Slc25a29	Solute carrier family 25 (mitochondrial carrier, palmitoylcarnitine transporter), member 29		x
Sptlc2	Serine palmitoyltransferase, long chain base subunit 2		x
Vldlr	Very low density lipoprotein receptor	x	
Muscle Development			
Eno1	Enolase 1, alpha non-neuron	x	x
Myl3	Myosin, light polypeptide 3	x	x
Tcap	Titin-cap		x
Nucleic Acid Metabolism			
Exosc2	Exosome component 2	x	x
Polr3d	Polymerase (RNA) III (DNA directed) polypeptide D	x	
Rbm27	RNA binding motif protein 27	x	
Rbms2	RNA binding motif, single stranded interacting protein 2	x	x
Sart3	Squamous cell carcinoma antigen recognized by T-cells 3	x	
Organogenesis			
Rara	Retinoic acid receptor, alpha		x
Tuft1	Tuftelin 1		x
Vegfc	Vascular endothelial growth factor C		x
Oxidoreductase			
BC034099	cDNA sequence BC034099		x
Zadh1	Zinc binding alcohol dehydrogenase, domain containing 1	x	
Polyamine Biosynthesis			
Oaz1	Ornithine decarboxylase antienzyme		x
Protein Modification/Metabolism			
5330414D10Rik	RIKEN cDNA 5330414D10 gene	x	
Adam3	A disintegrin and metalloprotease domain 3 (cyritestin)	x	
Ahsa1	Activator of heat shock 90kDa protein ATPase homolog 1	x	x
Ap1g2	Adaptor protein complex AP-1, gamma 2 subunit		x
Apoa1bp	Apolipoprotein A-I binding protein	x	x
Arf1	ADP-ribosylation factor 1		x
Arf4	ADP-ribosylation factor 4	x	x
Arih2	Ariadne homolog 2 (Drosophila)		x
Art4	ADP-ribosyltransferase 4		x
D10Ertd322e	NA segment, Chr 10, ERATO Doi 322, expressed		x
Eef1b2	Eukaryotic translation elongation factor 1 beta 2		x
Eif2b4	Eukaryotic translation initiation factor 2B, subunit 4 delta		x
Gtl6	Gene Trap locus 6		x
Grwd1	Glutamate-rich WD repeat containing 1	x	
Gtpbp4	GTP binding protein 4	x	x
Hbs1l	Hbs1-like (S. cerevisiae)	x	
Kin	Kin of IRRE like 2 (Drosophila)		x
Lman2	Lectin, mannose-binding 2	x	x
Lmln	Leishmanolysin-like (metallopeptidase M8 family)	x	
Mmp20	Matrix metalloproteinase 20 (enamelysin)	x	x

GENE	DESCRIPTION	ERRα	ERRγ
Mrpl34	Mitochondrial ribosomal protein L34		x
Mrp147	Mitochondrial ribosomal protein L47	x	x
Mrps18b	Mitochondrial ribosomal protein S18B	x	
Nifun	NifU-like-N-terminal domain containing	x	
Nktr	Natural killer tumor recognition sequence		x
Nmt1	N-myristoyltransferase 1		x
Ormdl1	ORM1-Like 1 (S. cerevisiae)		x
Pdk4	Pyruvate dehydrogenase kinase, isoenzyme 4		x
Phactr1	Phosphatase and actin regulator 1	x	
Pi15	Protease inhibitor 15		x
Plod3	Procollagen-lysine, 2-oxoglutarate 5-dioxygenase 3		x
Ppia	Peptidylprolyl isomerase A		x
Ppif	Peptidylprolyl isomerase F (cyclophilin F)		x
Ptpn18	Protein tyrosine phosphate, non-receptor type 18		x
Qrsl1	Gutaminyl-tRNA synthase (glutamine-hydrolyzing)-like 1		x
Rab21	RAB21, member RAS oncogene family	x	x
Rpl3l	Ribosomal protein L3-like	x	x
Rnf187	Ring finger protein 187	x	
Sec61g	SEC61, gamma subunit	x	
Timm8b	Translocator of inner mitochondrial membrane 8 homolog		x
Timm17a	Translocator of inner mitochondrial membrane 17a		x
Trim39	Tripartite motif protein 39	x	
Usp52	Ubiquitin specific protease 52		x
Zcsl2	Zinc finger, CSL domain containing 2	x	x
Signal Transduction			
2610312B22Rik	RIKEN cDNA 2610312B22 gene	x	
5730466P16Rik	RIKEN cDNA 5730466P16 gene	x	x
9830160G03Rik	RIKEN cDNA 9830160G03 gene	x	
Centd2	Centaurin, delta 2		x
Crtam	Cytotoxic and regulatory T cell molecule	x	x
Dgkθ	Diacylglycerol kinase, theta		x
Gnb2	Guanine nucleotide binding protein, beta 2	x	
Gsbs	G substrate	x	x
Il15ra	Interleukin 15 receptor, alpha chain	x	
Ldb3	LIM domain binding 3		x
Mapk8ip2	Mitogen activated protein kinase 8 interacting protein 2	x	x
Nadk	Nad kinase	x	x
Olfr131	Olfactory receptor 131	x	
Olfr149	Olfactory receptor 149	x	
Olfr460	Olfactory receptor 460	x	
Olfr558	Olfactory receptor 558	x	
Olfr653	Olfactory receptor 653	x	
Olfr667	Olfactory receptor 667	x	
Olfr692	Olfactory receptor 692	x	
Olfr802	Olfactory receptor 802	x	x
Olfr871	Olfactory receptor 871	x	x
Olfr893	Olfactory receptor 893	x	
Olfr895	Olfactory receptor 895	x	x
Olfr1019	Olfactory receptor 1019		x
Olfr1136	Olfactory receptor 1136		x
Olfr1342	Olfactory receptor 1342	x	
Olfr1431	Olfactory receptor 1431	x	
Pde6g	Phosphodiesterase gG, cGMP-specific, rod, gamma	x	

GENE	DESCRIPTION	ERRα	ERRγ
Plpi	Prolactin like protein I	x	x
Rala	V-ral simian leukemia viral oncogene homolog A (ras related)	x	x
Rit1	Ras-like without CAAX 1	x	
Snx3	Sorting nexin 3	x	
Snx17	Sorting nexin 17		x
Tbc1d4	TBC1 domain family, member 4	x	
Tm4sf3	Transmembrane 4 superfamily member 3	x	
Vlrc7	Vomeronasal 1 receptor, C7		x
Vlre1	Vomeronasal 1 receptor, E1		x
Spermatogenesis			
Acrbp	Proacrosin binding protein		x
Spata11	Spermatogenesis associated 11	x	x
Theg	Testicular haploid expressed gene		x
Transcriptional Regulation			
AI591476	Expressed sequence AI591476	x	x
BC034204	cDNA sequence BC034204		x
Crsp3	Cofactor required for Sp1 transcriptional activation, subunit 3	x	x
Esrra	Estrogen related receptor, alpha	x	x
Gabpa	GA repeat binding protein, alpha	x	x
Gsc	Goosecoid		x
Helic1	Helicase, ATP binding 1		x
Mycbp	C-myc binding protein	x	x
Phf5a	PHD finger protein 5A	x	x
Phtf2	Putative homeodomain transcription factor 2		x
Pias3	Protein inhibitor of activated STAT3		x
Rai17	Retinoic acid induced 17	x	
Recc1	Replication factor C1		x
Rpo1-4	RNA polymerase 1-4		x
Skiip	SKI interacting protein	x	
Snip1	Smad nuclear interacting protein 1	x	
Sp2	Sp2 transcription factor		x
Spz1	Spermatogenic Zip 1		x
Tead3	TEA domain family member 3		x
Trrap	Transformation/transcription domain-associated protein		x
V2r16	Vomeronasal 2, receptor, 16		x
Zfp93	Zinc finger protein 93		x
Zfp101	Zinc finger protein 101	x	x
Zfp422	Zinc finger protein 422	x	
Transport			
Abcc6	ATP-binding cassette, sub-family C (CFTR/MRP), member 6		x
Atp9a	ATPase, class II, type 9A		x
Atp10d	ATPase, class V, type 10D		x
Clca6	Chloride channel calcium activated 6		x
Hbb-y	Hemoglobin Y, beta-like embryonic chain	x	
Kcnj16	Potassium inwardly-rectifying channel, subfamily J, member 16		x
Slc35E2	Solute carrier family 35, member E2		x
Slc38a3	Solute carrier family 38, member 3		x
Slc41a3	Solute carrier family 41, member 3	x	x
Slco1b2	Solute carrier organic anion transporter family,		

GENE	DESCRIPTION	ERRα	ERRγ
	member 1		x
Sv2b	Synaptic vesicle glycoprotein 2b	x	x
Tumor Supressor			
Csmd1	CUB and Sushi multiple domains 1		x

Cellular functional classifications were based on GO annotation (http://fatigo.org/) and NCBI gene descriptions. Hypothetical genes and genes without an assigned function are not shown. ERRα and ERRγ columns marked with « x » indicates ERRα or ERRγ targets, respectively. Incidences where individual loci could be assigned to two distinct genes, both genes were included in the functional analysis.

ERRα and/or ERRγ target genes without an assigned function.

GENE	ERRα	ERRγ
0610009O20Rik	x	x
0610011N22Rik	x	x
0610039A15Rik		x
0710005M24Rik	x	
1010001D01Rik	x	x
1110019N10Rik		x
1700010A17Rik		x
1700020B09Rik	x	x
1700040L02Rik	x	
1810031K02Rik	x	
1810049H19Rik	x	
2210020M01Rik		x
2210418O10Rik		x
2310042D19Rik		x
2610044O15Rik		x
2610312E17Rik		x
2610510L01Rik		x
2700038I16Rik		x
2810422B04Rik		x
2810485I05Rik		x
3110002L15Rik		x
3110048E14Rik		x
3830408P04Rik		x
3830422K02Rik	x	
4932435O22Rik	x	x
4933409D10Rik	x	x
5133401N09Rik		x
5730521E12Rik	x	
6330578E17Rik		x
9830130M13		x
A030001H23Rik	x	
A130022J15Rik	x	x
A730055L17Rik	x	x
A930025J12Rik		x
AB124611		x

GENE	ERRα	ERRγ
AI413782	x	x
AI428936	x	
AI839550		x
AU021034	x	
AV249152		x
AV312086		x
BC002059	x	x
BC004004	x	
BC018101	x	
BC021790		x
BC028949	x	
BC034902	x	
BC051227	x	x
BC055791	x	x
BC070434	x	
BC072647	x	
D15Wsu169e		x
D5Ertd593e	x	
D630004N19Rik	x	x
G630055P03Rik	x	x
Gm631	x	x
Gsdm		x
LOC432637		x
MGC6357		x
MGC67181	x	
Mic2l1		x
Pgbpll	x	
Rcl	x	
Rtn4ip1	x	
Sacm1l		x
Schip1	x	
Sepm	x	
Unc50		x
Unc93b1	x	
Znhit1		x

Appendix II

Table 4.2: QPCR Results From Whole E18.5 Heart

Transcript	P-Value	Fold Change
ERR3	9.5E-08	9.99
SHP	0.0003	-1.57
CaCNA1D	0.004	1.60
Cx43	0.005	1.39
KCNE2	0.007	-1.85
CaCNA1c	0.010	1.81
KCNE1	0.013	-2.03
Prkag1	0.009	1.26
KCNH2	0.010	-1.39
SCN1A	0.03	2.12
SCN1B	0.03	-1.40
Cx37	0.04	1.23
Cx45	0.09	2.37
RYR2	0.07	1.36
PLb	0.06	1.13
CaCNA2D	0.07	-1.25
PPARa	0.11	1.47
KCNJ4	0.10	1.39
SCN2A	0.12	1.31
Prkaa2	0.14	1.43
Slc25A4	0.13	-1.30
SCN4A	0.15	-1.29
Cx40	0.14	1.16
SCN5A	0.17	1.18
KCNJ8	0.23	-1.17
SCN3A	0.24	-1.15
NRF1	0.27	-1.14
KCNA4	0.36	1.22
Prkab1	0.34	-1.08
KCNJ11	0.36	-1.12
KCNA1	0.45	-1.29
KCNQ1	0.51	1.16
KCNH8	0.62	-1.36
SCN10A	0.53	-1.10
ATP5F1	0.66	1.32
KCNE4	0.57	1.08
MHCa	0.70	1.21
ATP2A	0.72	1.07
KCNJ2	0.72	-1.07
PPARg	0.75	1.06
CaCNA1G	0.76	1.05
TR a	0.77	1.03
KCN1P4	0.85	1.08
COUP-TFII	0.86	-1.04
SCN7A	0.88	1.03
KCNJ12	0.87	1.02
KCNA2	0.90	-1.05
KCNAB3	0.91	-1.03

Table 4.2: QPCR Results From Whole E18.5 Heart, Continued

Transcript	P-Value	Fold Change
36B4	0.91	1.00
PPARd	0.95	-1.01
KCNJ5	0.96	1.00
NRF2	0.99	1.00